REGULATORY MECHANISMS FOR IMPROVING CEREAL SEED QUALITY

EDITED BY: Vincenzo Rossi and Yingyin Yao

PUBLISHED IN: Frontiers in Plant Science

frontiers Research Topics

ISSN 1664-8714
ISBN 978-2-88976-278-1
DOI 10.3389/978-2-88976-278-1

About Frontiers

Frontiers is more than just an open-access publisher of scholarly articles: it is a pioneering approach to the world of academia, radically improving the way scholarly research is managed. The grand vision of Frontiers is a world where all people have an equal opportunity to seek, share and generate knowledge. Frontiers provides immediate and permanent online open access to all its publications, but this alone is not enough to realize our grand goals.

Frontiers Journal Series

The Frontiers Journal Series is a multi-tier and interdisciplinary set of open-access, online journals, promising a paradigm shift from the current review, selection and dissemination processes in academic publishing. All Frontiers journals are driven by researchers for researchers; therefore, they constitute a service to the scholarly community. At the same time, the Frontiers Journal Series operates on a revolutionary invention, the tiered publishing system, initially addressing specific communities of scholars, and gradually climbing up to broader public understanding, thus serving the interests of the lay society, too.

Dedication to Quality

Each Frontiers article is a landmark of the highest quality, thanks to genuinely collaborative interactions between authors and review editors, who include some of the world's best academicians. Research must be certified by peers before entering a stream of knowledge that may eventually reach the public - and shape society; therefore, Frontiers only applies the most rigorous and unbiased reviews.
Frontiers revolutionizes research publishing by freely delivering the most outstanding research, evaluated with no bias from both the academic and social point of view. By applying the most advanced information technologies, Frontiers is catapulting scholarly publishing into a new generation.

What are Frontiers Research Topics?

Frontiers Research Topics are very popular trademarks of the Frontiers Journals Series: they are collections of at least ten articles, all centered on a particular subject. With their unique mix of varied contributions from Original Research to Review Articles, Frontiers Research Topics unify the most influential researchers, the latest key findings and historical advances in a hot research area! Find out more on how to host your own Frontiers Research Topic or contribute to one as an author by contacting the Frontiers Editorial Office: frontiersin.org/about/contact

REGULATORY MECHANISMS FOR IMPROVING CEREAL SEED QUALITY

Topic Editors:
Vincenzo Rossi, Research Centre for Cereal and Industrial Crops, Council for Agricultural and Economics Research (CREA), Italy
Yingyin Yao, China Agricultural University, China

Citation: Rossi, V., Yao, Y., eds. (2022). Regulatory Mechanisms for Improving Cereal Seed Quality. Lausanne: Frontiers Media SA. doi: 10.3389/978-2-88976-278-1

Table of Contents

frontiers | Frontiers in Plant Science

EDITORIAL
published: 13 May 2022
doi: 10.3389/fpls.2022.924543

Editorial: Regulatory Mechanisms for Improving Cereal Seed Quality

Vincenzo Rossi[1]* *and Yingyin Yao*[2]*

[1] Council for Agricultural Research and Economics, Research Centre for Cereal and Industrial Crops, Bergamo, Italy, [2] State Key Laboratory for Agrobiotechnology, Key Laboratory of Crop Heterosis and Utilization (MOE), Beijing Key Laboratory of Crop Genetic Improvement, China Agricultural University, Beijing, China

Keywords: cereals, seed, quality, nutritional value, end-use, regulatory mechanisms

Editorial on the Research Topic

Regulatory Mechanisms for Improving Cereal Seed Quality

In past years, enormous progress has been made in increasing the cereals yield to cope with the increase in the world population. More recently, with rising of living standard, consumers and industry have also paid great attention to quality improvement. Cereal quality is mainly determined by cereal grain and includes its processing and end-use quality, as well as the health-associated and nutritional value. Cereal quality is a complex trait affected by both genetics and environmental factors. This Research Topic aims to illustrate advances of seed quality improvement in cereals.

Maize and wheat are the most widely grown cereals (FAO, 2021) and two reviews in this Research Topic are focused on their seed quality improvement. Wu et al. wrote a comprehensive review describing the maize endosperm developmental patterns in different tissues and cell types and underlaying molecular regulatory mechanisms. The authors illustrated prospects for how knowledge of endosperm development regulation could be utilized to improve grain quality through the alteration of metabolic pathways and alteration of cellular development. Sweet corn represents one of the more familiar examples of metabolic pathways alteration, as it arises from mutations in enzymes of the starch biosynthetic pathway that impede the incorporation of glucose subunits into starch, resulting in the accumulation of free sugars in the endosperm (Lertrat and Pulam, 2007). Manipulation of basal endosperm transfer layer (BETL) development or function represents an example of cellular developmental manipulation for altering quality. Cells forming BETL are responsible for transporting metabolites from maternal tissues into the endosperm and the modulation of the relative expression levels of various classes of transporters could enhance grain filling or shift grain composition (Dai et al., 2021). This review highlighted the relevance of the gene network analyses as powerful tools to predict central regulators of gene expression modules that can be the targets of modern genetic approaches for modifying endosperm development and improving seed quality. Peng et al. provided a summary about the role of seed storage proteins (SSPs) for conferring wheat dough unique rheological properties required for the production of specific food for human nutrition. They also discussed about the efforts done for reducing specific gliadins epitopes associated with coeliac disease, while maintaining desirable end-use quality. In particular, the authors focused on the relevance of specific agricultural practices, including nitrogen and sulfur fertilization, as well as irrigation strategies, for manipulating yield and seed quality.

Due to climate change, the average global temperature is increasing continuously and is predicted to rise by 2°C until 2100, thus severely affecting crop yield and quality (Porter et al., 2014). In this Research Topic, three articles focused on the association between temperature variation and cereals quality. A slight increase in temperature induces rice chalkiness, which affects not only appearance but also milling and cooking quality (Peng et al., 2018). Wang et al. showed that application of nitrogen fertilizer during agronomical practices increased prolamin accumulation

OPEN ACCESS

Edited and reviewed by:
Raj K. Pasam,
AgriBio, La Trobe University, Australia

***Correspondence:**
Vincenzo Rossi
vincenzo.rossi@crea.gov.it
Yingyin Yao
yingyin@cau.edu.cn

Specialty section:
This article was submitted to Crop and Product Physiology, a section of the journal Frontiers in Plant Science

Received: *20 April 2022*
Accepted: *02 May 2022*
Published: *13 May 2022*

Citation:
Rossi V and Yao Y (2022) Editorial: Regulatory Mechanisms for Improving Cereal Seed Quality. Front. Plant Sci. 13:924543. doi: 10.3389/fpls.2022.924543

in seed, resulting in chalkiness reduction. Fan et al. grew wheat plants under field conditions to show that night-warning treatment applied at the plant vegetative stage during winter or spring significantly reduced the flag leaf senescence induced by increased warming during the post-anthesis period. Liu W. et al. used proteomics to investigate the regulatory effects of high temperature on rice grain metabolic pathways under field conditions. The results supported previous findings about the negative effects of temperature on starch and protein accumulation and composition (Tang et al., 2018). In addition, the authors identified specific molecular chaperone heat shock proteins as potential novel targets for alleviating the impact of increased warming on seed quality.

Products derived from cereals grain are relevant for human food and animal feeding, but the concentration of essential amino acids and micronutrients must reach the thresholds required for providing sufficient nutritional value. Lysine is an essential amino acid and it must be supplied through diet (Hou and Wu, 2018). The high concentration of lysine-poor prolamin storage proteins in cereals is associated with the sub-optimal nutritional quality of cereal grains. For example, barley *lys3* mutants have an increased lysine content but a reduced seed size and yield (Orman-Ligeza et al., 2020). Proteomics approaches were employed by Bose et al. to predict the impact of barley *lys3* mutations to other signaling pathways. In this study the authors provided preliminary indications to understand the nature of the pleiotropic effects associated with *ly3s* mutations, which is an essential step forward to improve lysine content without affecting yield. Even micronutrients, like Zn and Fe, are present in suboptimal levels within cereals grain and their deficiency in human diet has become one of the most common health problems (Vasconcelos et al., 2017). Tong et al. used genome-wide association studies to identify novel quantitative trait loci associated with Zn and Fe concentrations in wheat grain, thus providing essential knowledge required for improving Zn and Fe level though targeted breeding programs.

The Research Topic ends with two articles that investigate the end-use quality of cereals grain by specifically focusing on biscuits derived from the wheat flour. Liu L. et al. tested starch addition to flour of wheat cultivars with different protein content to provide information about how starch affect biscuits quality and showed that this approach can be particularly useful for improving biscuits quality using flour from wheat with low gluten content. Ma et al. focused on wheat SSPs to show that a knock-out mutation in one of the gene of the high molecular weight glutenin subunits family decreased glutenin macropolymers content, thus weakening gluten strength and improving sugar snap cookie processing quality without yield penalty.

AUTHOR CONTRIBUTIONS

All authors listed have made a substantial, direct, and intellectual contribution to the work and approved it for publication.

ACKNOWLEDGMENTS

We are grateful to all authors, journal editors, and peer reviewers who contributed to this Research Topic.

REFERENCES

Dai, D., Ma, Z., and Song, R. (2021). Maize endosperm development. *J. Integr. Plant Biol.* 63, 613–627. doi: 10.1111/jipb.13069

FAO (2021). *World Food and Agriculture—Statistical Yearbook 2021*. Rome: FAO.

Hou, Y., and Wu, G. (2018). Nutritionally essential amino acids. *Adv. Nutr.* 9, 849–851. doi: 10.1093/advances/nmy054

Lertrat, K., and Pulam, T. (2007). Breeding for increased sweetness in sweet corn. *Int. J. Plant Breeding* 1, 27–30. Available online at: http://www.globalsciencebooks.info/Online/GSBOnline/images/0706/IJPB_1(1)/IJPB_1(1)27-30o.pdf

Orman-Ligeza, B., Borrill, P., Chia, T., Chirico, M., Doležel, J., Drea, S., et al. (2020). LYS3 encodes a prolamin-box-binding transcription factor that controls embryo growth in barley and wheat. *J. Cereal Sci.* 93:102965. doi: 10.1016/j.jcs.2020.102965

Peng, B., Kong, D. Y., Nassirou, T. Y., Peng, Y., He, L. L., Sun, Y. F., et al. (2018). The arrangement of endosperm cells and development of starch granules are associated with the occurrence of grain chalkiness in japonica varieties. *J. Agric. Sci.*10, 156–166. doi: 10.5539/jas.v10n7p156

Porter, J. R., Xie, L., Challinor, A. J., Cochrane, K., Howden, S. M., Iqbal, M. M., et al. (2014). "Food security and food production systems," in *Climate Change 2014: Impacts, Adaptation, and Vulnerability. Part A: Global and Sectoral Aspects. Contribution of Working Group II to the Fifth Assessment Report of the Intergovernmental Panel on Climate Change*, eds C. B. Field, V. R. Barros, D. J. Dokken, K. J. Mach, M. D. Mastrandrea, T. E. Bilir (Cambridge: Cambridge University Press), 485–533.

Tang, S., Chen, W., Liu, W., Zhou, Q., Zhang, H., Wang, S., et al. (2018). Open-field warming regulates the morphological structure, protein synthesis of grain and affects the appearance quality of rice. *J. Cereal Sci.* 84, 20–29. doi: 10.1016/j.jcs.2018.09.013

Vasconcelos, M. W., Gruissem, W., and Bhullar, N. K. (2017). Iron biofortification in the 21st century: setting realistic targets, overcoming obstacles, and new strategies for healthy nutrition. *Curr. Opin. Biotechnol.* 44, 8–15. doi: 10.1016/j.copbio.2016.10.001

Conflict of Interest: The authors declare that the research was conducted in the absence of any commercial or financial relationships that could be construed as a potential conflict of interest.

frontiers in Plant Science

ORIGINAL RESEARCH
published: 30 August 2021
doi: 10.3389/fpls.2021.715436

Nitrogen Fertilizer Regulated Grain Storage Protein Synthesis and Reduced Chalkiness of Rice Under Actual Field Warming

Xueqin Wang[1], *Kailu Wang*[1], *Tongyang Yin*[1], *Yufei Zhao*[1], *Wenzhe Liu*[1], *Yingying Shen*[1], *Yanfeng Ding*[1,2] *and She Tang*[1,2]*

[1] College of Agronomy, Nanjing Agricultural University, Nanjing, China, [2] Jiangsu Collaborative Innovation Center for Modern Crop Production, Nanjing, China

Our previous study has shown that nitrogen plays an important role in dealing with significantly increased chalkiness caused by elevated temperature. However, the role of nitrogen metabolites has not been given sufficient attention, and its regulatory mechanism is not clear. This study investigated the effects of high temperature and nitrogen fertilizer on the synthesis of grain storage protein and further explored the quality mechanism under the actual scenario of field warming. Results showed that increased temperature and nitrogen fertilizer could affect the activities of nitrogen metabolism enzymes, namely, glutamate synthetase, glutamine synthetase, glutamic pyruvic transaminase, and glutamic oxaloacetic transaminase, and the expressions of storage protein synthesis factor genes, namely, *GluA* and *GluB*, and subfamily genes, namely, *pro14*, *BiP1*, and *PDIL1*, which co-induced the changes of storage protein synthesis in rice grains. Furthermore, the increased temperature changed the balance of grain storage substances which may lead to the significantly increased chalky rate (197.67%) and chalkiness (532.92%). Moreover, there was a significant negative correlation between prolamin content and chalkiness, indicating that nitrogen fertilizer might regulate the formation of chalkiness by affecting the synthesis of prolamin. Results suggested that nitrogen application could regulate the related core factors involved in nitrogen metabolism pathways, which, in turn, affects the changes in the storage protein components in the grain and further affects quality. Therefore, as a conventional cultivation measure, nitrogen application would have a certain value in future rice production in response to climate warming.

Keywords: rice, actual field warming, nitrogen fertilizer, grain storage protein, quality, chalkiness

OPEN ACCESS

Edited by:
Yingyin Yao,
China Agricultural University, China

Reviewed by:
Yulong Ren,
Institute of Crop Sciences, Chinese Academy of Agricultural Sciences, China
Dongcheng Liu,
Institute of Genetics and Developmental Biology/Innovation Academy of Seed Design, Chinese Academy of Sciences, China

***Correspondence:**
She Tang
tangshe@njau.edu.cn

Specialty section:
This article was submitted to Crop and Product Physiology, a section of the journal Frontiers in Plant Science

Received: *27 May 2021*
Accepted: *05 August 2021*
Published: *30 August 2021*

Citation:
Wang X, Wang K, Yin T, Zhao Y, Liu W, Shen Y, Ding Y and Tang S (2021) Nitrogen Fertilizer Regulated Grain Storage Protein Synthesis and Reduced Chalkiness of Rice Under Actual Field Warming. Front. Plant Sci. 12:715436. doi: 10.3389/fpls.2021.715436

INTRODUCTION

With the improvement of living standards of people, the demand for high-quality rice is increasing. However, rice quality is extremely sensitive to temperature. With the intensification of global warming, the increase of chalkiness in rice quality traits has become a key issue that needs to be focused on. Studies conducted by artificial climate room (Xu et al., 2020) and actual field warming experiments (Rehmani et al., 2014) illustrated that high temperature was

conducive to the occurrence of chalkiness (Mitsui et al., 2013). Increased grain chalkiness affects not only appearance quality but also milling and cooking quality (Cheng et al., 2005; Guo et al., 2011). Based on our previous field trials, a small scale of temperature increase during the rice grain-filling stage can lead to a significant increase in chalkiness, which will bring new challenges to the production of high-quality rice in the future and reasonable cultivation measures that are urgently needed. Nitrogen application is a simple agronomic measure, which has been proved that it can alleviate high-temperature damage through decelerating the early grain-filling rate of rice and could further reduce the occurrence of chalkiness (Dou et al., 2017; Tang et al., 2019). Although the regulatory effect of nitrogen on the physicochemical properties of rice starch had been preliminarily clarified in our previous study, the characteristics of its effects on grain nitrogen metabolism have not yet been investigated.

The formation of grain chalkiness is closely related to carbon and nitrogen metabolism. Previous studies have shown that genes contributed to the formation of chalkiness are all related to the carbon and nitrogen metabolism key enzymes (Kang et al., 2005; Fujita et al., 2007; Wang et al., 2008). Our previous studies showed that nitrogen fertilizer effectively influenced the accumulation and structural characteristics of starch, which further alleviated the rice quality under increased temperature (Tang et al., 2019). The application of nitrogen fertilizer affected the structure of rice starch, which further changed its functional properties and eventually led to the changes in the grain quality (Zhou et al., 2020). Being the second largest storage components in rice grain, rice seed storage protein (SSP) accounts for about 8–10% of grain weight (Kawakatsu and Takaiwa, 2010). The grain protein content has been proved to be significantly negatively correlated with appearance, and increased temperature could regulate the grain protein synthesis, resulting in the changes in balance of storage substance, which could further regulate the formation of grain chalkiness (Tang et al., 2018; Liu et al., 2020). Studies also showed that reasonable nitrogen application could alleviate chalkiness caused by elevated temperature (Wada et al., 2019). Therefore, understanding the mechanisms of nitrogen fertilizer on grain storage protein synthesis and appearance quality under open-field warming condition would be contributed to the establishment of reasonable cultivation measures.

Our previous studies on temperature increase and nitrogen application have clarified the effect of carbon metabolism on quality and chalkiness, but the effect of nitrogen metabolism on the formation of chalkiness is still unclear. As a simple measure suitable for actual field operations, nitrogen fertilizer can alleviate the deterioration of quality caused by climate warming, including reducing chalkiness, but its mechanism has not been fully revealed. Therefore, the purpose of this study was to explore the contribution of nitrogen metabolism to the formation of chalkiness through the application of nitrogen fertilizer under the increased open-air temperature experiment. By clarifying the regulatory effects of nitrogen application on nitrogen metabolism-related enzymes and regulatory factors under increased temperature, the results would help supplement its effect on grain nitrogen metabolites. Based on this, the mechanism of nitrogen fertilizer measures in alleviating the deterioration of rice quality could be further revealed, and this may help systematically assess the potential role of nitrogen in combating the deterioration of rice quality under climate warming.

MATERIALS AND METHODS

Experimental Conditions

The actual field warming scene is located in the middle and lower reaches of the Yangtze River Basin, and the experiments were conducted at the Rice Research Station of Nanjing Agricultural University (31°56′39″N, 118°59′13″E, 80 m altitude). Rice was sowed on May 27, transplanted on June 15, and headed on August 26 in 2019. The experimental site soil type is clay loam, with a pH value of 6.41. The total nitrogen, available nitrogen, total phosphorus, available phosphorus, and available potassium from 0 to 20 cm soil were 1.4 g kg^{-1}, 7.8 mg kg^{-1}, 0.6 g kg^{-1}, 20 mg kg^{-1}, and 91.7 mg kg^{-1}, respectively.

Plant Materials and Treatment

The test material was the conventional *japonica* rice variety Wuyujing 3 (W3), which belongs to the high-quality *japonica* rice variety widely planted in the local area, and its chalkiness is sensitive to external temperature. The cultivation process including artificial transplanting was carried out after the nursery, and field management besides pest control was conducted on the basis of local high-yield and high-quality cultivating measures. The experimental treatments of elevated temperature and nitrogen fertilizer application are as follows: ambient temperature (CK), elevated temperature (ET), application of nitrogen fertilizer under normal temperature (CKN), and application of nitrogen fertilizer under elevated temperature (ETN). Field warming treatment was conducted through the free-air temperature enhancement (FATE) facility (**Supplementary Figures 1, 2**). The infrared ceramic heaters of the FATE system were used to warm the rice plants during day and night after anthesis. The detailed parameters of the system can be retrieved in our previous studies (Rehmani et al., 2014; Tang et al., 2019). A temperature and hygrometer HOBO U23-001 was placed in the rice canopy to record the temperature during grain filling, and HOBOwarePro software (Onset Computer Co., Bourne, MA, USA) was used for data processing. The total nitrogen application of CK and ET was 300 kg·hm^{-2}, and the ratio of basal fertilizer, tiller fertilizer, and panicle fertilizer was 4:2:4. Compared with CK and ET, CKN and ETN with increased nitrogen fertilizer were applied with 60 kg N·hm^{-2} nitrogen at the beginning of temperature increasing treatment.

Determination of Yield and Quality

The effective panicles of dozens of holes were randomly investigated in the no sampling area at the maturity stage, and the spikelets per panicle and seed setting rate were calculated, with three replicates in each group. Panicle samples were threshed at 70°C and dried to constant weight, and the grain weight was

weighed to calculate the theoretical yield of rice. Determinations of grain quality traits were conducted (refer to our previous test procedures) (Dou et al., 2017; Tang et al., 2019), and the brief protocols are as follows: the ratio of grain length to width was measured by using a vernier caliper. The chalkiness degree was calculated by the multiplication of the chalkiness rate and chalkiness area. JLGJ 4.5 shelling machine of Taizhou Grain Industry Instrument Company was used for shelling, and the brown rice rate was calculated. Brown rice was weighed and milled by JNMJ3 rice mill for 90 s to determine the milled rice rate. Samples with integrity >80% were picked from the milled rice and weighed to calculate the head rice rate. Rapid-visco-analyzer (RVA) characteristics of rice were determined by RVA-4500, a rapid viscosity analyzer developed by Newport Scientific Instrument Company in Australia. A total of 3.00 g of rice flour with a moisture content of about 14.0% was added to the aluminum box, with 25 ml of distilled water, and quickly stir it up and down with a stirrer for 10 times to make the rice flour disperse evenly according to the AACC standard (2012). The prepared samples were tested on RVA-4500 according to the set procedure.

Transmission Electron Microscope Observation

The spikelets were obtained from the first branch in the middle of the panicle at 6, 9, 12, 15, and 20 days after anthesis (DAA). Transverse segments (1–2 mm thick) from the same middle of the kernels were obtained to observe the morphological and structural changes and the shape and spatial arrangement of amyloplasts and protein bodies (PBs) according to the JEM-1200EX transmission electron microscope (Tang et al., 2018).

Determination of Grain Storage Material Contents

The polarimetric method was employed to determine the total starch content of rice flour samples after 100 mesh screening. The amylose content was measured according to the standard of the People's Republic of China GB/17891-1999 high-quality rice. The grain storage proteins, namely, albumin, globulin, prolamin, and glutelin, were extracted from distilled water, dilute hydrochloric acid, ethanol, and dilute alkali. Among them, albumin, globulin, and prolamin were determined by Coomassie brilliant blue colorimetry, and glutelin was determined by biuret colorimetry. The content of 17 amino acids in the protein was detected by using the Hitachi L-8900 amino acid analyzer (Hitachi Corp, Japan) according to the hydrochloric acid hydrolysis method.

Analysis of Enzyme Activities Related to Protein Synthesis

The spikelets collected from 6, 9, 12, 15, 20, 25, and 35 DAA were grounded into powder in liquid nitrogen. The glutamine synthetase (GS) and glutamate synthetase (GOGAT) activities were determined by using the protocols described in our previous study by Tang et al. (2018), and the glutamic oxaloacetic transaminase (GOT) and glutamic pyruvic transaminase (GPT) activities were analyzed according to the protocols described by Wu et al. (1998).

RNA Extraction and RT-PCR

Total RNAs of test samples were extracted and purified from shelled grains of 6, 9, 12, 15, and 20 DAA according to the instructions of the RNAprep Pure Plant Kit (TIANGEN, Beijing, https://www.tiangen.com/). After extraction, the concentration and purity of total RNA were analyzed using the NanoDrop One C Ultra-micro spectrophotometer (Thermo Fisher Scientific, USA). Reverse transcription was performed using the Takara's PrimeScript™ RT Kit (Takara Biotechnology, Tokyo, Japan). The real-time quantitative analysis was conducted based on the Biosystems 7300 and StepOnePlus™ real-time PCR system. The cycling parameters were as follows: 30 s at 95°C, 40 cycles of 5 s at 95°C, and 31 s at 65°C. *Actin* was used to calculate the relative expression level of target genes. Primers used in this study are listed in **Supplementary Table 1**.

Data Analysis

Data sorting and analysis were performed using Microsoft Excel 2019 (Microsoft Corporation, WA, USA) and SPSS20.0 statistical software (IBM SPSS® Statistics, NY, USA) statistical software. Origin 8.1 (OriginLab Corporation, MA, USA) was employed for figure preparation. ANOVA was used to analyze data according to a completely random design, and the averages were compared by using the Duncan's multiple range test (DMRT) based on the least significant difference test at the 5% probability level.

RESULTS AND ANALYSIS

Effects of Nitrogen Fertilizer on Yield and Quality of Rice Under Elevated Temperature

The results of actual paddy field warming on rice yield are basically consistent with previous studies on the impact of climate warming on rice yield. Compared with CK, ET had a negative impact on yield with a decrease of 23.72%. In particular, the increase in temperature has led to a significant decrease in the grain weight and the seed setting rate, which is also the main reason for the decrease in yield. Furthermore, in this study, the most prominent results of the effect of increasing temperature on the rice quality were the significantly increased chalky rice rate (197.67%), chalky area (104.62%), and chalkiness (532.92%). This result is also consistent with the results of our warming field trials carried out since 2012. Compared with the ET treatment, the application of nitrogen under ETN alleviated the loss of the grain weight and the seed setting rate to a certain extent and thus reduced the adverse effect of warming on yield (16.09%). Nitrogen fertilizer also had a significant effect on alleviating chalkiness with a decrease of 22.27%. However, nitrogen fertilizer had no significant effect on the chalky rate and chalk area (**Tables 1**, **2** and **Figure 1**). The milled rice rate and head rice rate were decreased by 3.93 and 8.33%, respectively, under elevated temperature, while nitrogen application increased the head rice rate by 4.34% at the significance level. The hot paste viscosity, peak viscosity, breakdown viscosity, and gelatinization temperature were increased by 14.43, 5.56, 23.72, and 5.39%, respectively, and the cool paste viscosity and setback viscosity

TABLE 1 | Effects of warming and nitrogen fertilizer on yield and yield components in rice.

Treatment	Spikelets per panicle (× 10^4 hm^{-2})	Panicles per panicle	1,000 grain weight (g)	Seed setting rate (%)	Yield (t hm^{-2})
CK	401.71a	96.10a	26.80a	95.35a	9.78a
ET	410.26a	86.02a	23.56d	89.70b	7.46c
CKN	418.80a	96.64a	26.03b	92.84a	9.77a
ETN	418.80a	90.77a	24.45c	93.24a	8.66b
T	ns	ns	**	*	**
N	ns	ns	ns	ns	ns
T*N	ns	ns	**	**	ns

*, **, *significant at 0.05 and 0.01 probability levels, respectively, ns means there is no significant difference. Values with different letters in each row represent for the significantly different with $p < 0.05$. T represents temperature, N represents nitrogen fertilizer, CK represents ambient temperature, ET represents elevated temperature, CKN represents application of nitrogen fertilizer under normal temperature, and ETN represents application of nitrogen fertilizer under elevated temperature.*

were decreased by 8.01 and 175.45%, respectively, under elevated temperature. Nitrogen application could alleviate the changes of peak viscosity and breakdown viscosity but had no significant effect on other parameters (**Table 2**). Overall, the increase in temperature during the rice grain-filling stage has a certain negative effect on the yield components and quality indicators, while from the perspective of years of field trials, the application of nitrogen fertilizer has a positive regulatory role on the adverse effects of temperature increase and could be considered as a potential effective cultivation measure to cope with high-quality rice production under climate warming.

Effects of Nitrogen Fertilizer on Endosperm Development and Grain Storage Proteins Under Elevated Temperature

Endosperm Development

The effects of elevated temperature and nitrogen on the development of grain (superior pikelets) endosperm were investigated, and the results showed that there was no amyloplast found in CK and CKN treatments, while a small amount of amyloplasts and PB I and PB II were observed in ETN at 6 DAA. The PBs and amyloplasts in rice endosperm were increased rapidly, and the volume and quantity of PBII were increased significantly at 9 DAA. Results indicated that PBs were closely packed around amyloplasts under elevated temperature, while this phenomenon was not observed under normal temperature treatment in CK and CKN at 15 DAA. At 20 DAA, the endosperm of grain was basically mature, and the PBs of each treatment were closely packed among the amyloplasts. The PBs in ET were increased continuously and were tightly arranged in the endosperm and further connected and squeezed with the starch granules to fill the entire endosperm tissue. Compared with the ET treatment, the compression degree of amyloplasts and PBs under nitrogen treatment was relatively lower, indicating that the development of endosperms was slower than ET (**Figure 2**).

Dynamic Changes of the Protein Content

Results of grain storage protein components showed that when compared with CK, the albumin content of grains was increased at 6, 9, and 12 DAA under elevated temperature, and nitrogen application also had the same regulatory effect, while the difference in the albumin content of ET and ETN was not significant. Compared with CK, ET and ETN treatments increased the globulin content by 11.63 and 7.34%, respectively, at 25 DAA. Compared with CK, the prolamin content under the ET treatment increased after the initial stage of filling and then decreased, resulting in a relatively low prolamin content in the ET treatments. ETN significantly increased the prolamin content by 6.25% compared with ET during the whole grain-filling stage. Changes in the glutelin content indicated that at 15 DAA, elevated temperature obviously increased the glutelin content, while nitrogen application further increased its content. The glutelin content was increased by 10.61%, and the content of prolamin was decreased by 5.73% under elevated temperature at 35 DAA (**Figure 3**). Correlation results showed that the prolamin content was significantly and negatively correlated with chalkiness, hot paste viscosity, peak viscosity, breakdown viscosity, and gelatinization temperature, while it was positively related to head rice rate, amylose content, cool paste viscosity, and setback viscosity. The glutelin content was negatively associated with cool paste viscosity and was positively correlated with gelatinization temperature (**Table 3**).

Effect of Nitrogen Fertilizer on the Protein Activities Related to Synthetase Under Warming Condition

The activity of GOGAT was relatively increased under elevated temperature before 20 DAA and was significantly increased by 39.48% at 15 DAA Compared with ET, the activity of GOGAT was increased in ETN during the whole grain-filling period. GS activity under the ET treatment was lower than that of the CK and was significantly decreased by 43.94 and 12.14% at 9 DAA and 15 DAA, respectively. Compared with the ET treatment, GS activity was significantly increased in the ETN treatment at 6 DAA, 9 DAA, and 12 DAA. However, the difference was not significant in the later stages in both ET and ETN treatments. During the whole grain-filling stage, increased temperature significantly increased the GOT activity, while nitrogen application under elevated temperature could further improve GOT activity until 12 DAA. Compared with CK, GPT was maintained higher activity in elevated temperature treatment, and nitrogen application under

TABLE 2 | Effects of nitrogen fertilizer on appearance, milling quality, and RVA characteristic parameters under elevated temperature in rice.

Treatment	Chalkiness rate (%)	Chalkiness area (%)	Chalkiness (%)	Length (mm)	Width (mm)	Thickness (mm)	Milled rice rate (%)	Head rice rate (%)	Peak viscosity (cP)	Hot paste viscosity (cP)	Breakdown viscosity (cP)	Cool paste viscosity (cP)	Setback viscosity (cP)	Gelatinization temperature (°C)
CK	28.78b	26.40b	7.32c	4.95a	2.93a	1.69ab	76.30a	73.60a	2931.50c	1500.50b	1431.00c	2573.00a	−358.50b	72.40b
ET	85.67a	54.02a	46.33a	4.73c	2.78b	1.71ab	73.3b	67.47c	3354.50a	1584.00a	1770.50a	2367.00b	−987.50c	76.30a
CKN	15.00c	20.12b	2.76d	4.96a	2.98a	1.67b	77.13a	73.83a	2804.50d	1478.50b	1326.00d	2521.00a	−283.50a	72.83b
ETN	82.67a	43.63a	36.01b	4.82b	2.77b	1.74a	73.83b	70.40b	3247.00b	1540.00ab	1707.00b	2293.50b	−953.50c	76.70a
T	**	**	**	**	**	*	**	**	**	**	**	**	**	**
N	**	*	**	*	ns	ns	*	**	**	ns	**	*	**	*
T*N	*	ns	*	ns	ns	ns	ns	**	ns	ns	ns	ns	ns	ns

*, **, *significant at 0.05 and 0.01 probability levels, respectively, ns means there is no significant difference. Values with different letters in each row represent for the significantly different with $p < 0.05$. T represents temperature, N represents nitrogen fertilizer, CK represents ambient temperature, ET represents elevated temperature, CKN represents application of nitrogen fertilizer under normal temperature, and ETN represents application of nitrogen fertilizer under elevated temperature.*

elevated temperature had similar regulatory effects on the activity of GPT (**Figure 4**).

Regulatory Effects of Nitrogen Fertilizer on Main Regulatory Factors Related to Grain Protein Under Warming Conditions

The regulatory effect of elevated temperature and nitrogen application on the currently known regulatory factors related to storage protein synthesis showed that increased temperature had a significant upregulating effect on both *GluA1* and *GluA2*. For example, compared with CK, the expressions of *GluA1* and *GluA2* were increased by 86.01 and 38.32%, respectively, at 15 DAA. The nitrogen application under elevated temperature decreased the relative expression of *GluA1* (except 12 DAA) but significantly increased the relative expression of *GluA2* (except 20 DAA). Under elevated temperature, the expression of *GluB1* at 6 DAA and 9 DAA was decreased and subsequently increased, while nitrogen increased the expression of *GluB1* under both ambient and elevated temperatures. The expression of *GluB5/GluB4* was significantly increased by 50.83% at 15 DAA under elevated temperature. Compared with CK, the relative expression of *pro14* was first increased and then decreased in ET. The application of nitrogen fertilizer effectively increased the relative expression of *pro14* in ETN treatment. The relative expression of *BiP1* was decreased by 30.63% at 9 DAA under elevated temperature. There was no significant difference in the relative expression of *BiP1* between ET and ETN treatments. The relative expression of *PDIL1* was decreased by 39.14% at 9 DAA and increased later by 30.29% at 15 DAA under elevated temperature (**Figure 5**).

DISCUSSION

Free-air Temperature Enhancement (FATE) Facility

With the intensification of climate warming in recent years, the production of high-quality rice is facing new challenges. It is imperative to carry out studies on rice quality and cultivation strategies under this background. Since 2009, the FATE facilities have been introduced and continuously optimized to achieve the stable warming treatment in the actual paddy field with a limited influence on other environmental factors (Rehmani et al., 2014; Tang et al., 2019; Dou et al. 2017). Results of the warming effect of the FATE system indicated that when compared with CK, the average daytime temperature was increased by 2.78°C and the average night temperature was increased by 4.96°C in the ET treatment (**Supplementary Figure 2**). The warming effect of the FATE system was consistent with the IPCC prediction (global surface temperature was estimated to increase by 1.4–5.8°C by 2,100). Furthermore, the results indicated that the increase of night temperature was greater than daytime temperature, which is in line with the current global warming trend (IPCC, AR5, 2014). Therefore, based on the years of actual field test results, the FATE facility could be used to simulate the trend and characteristics of climate warming and that enables us to

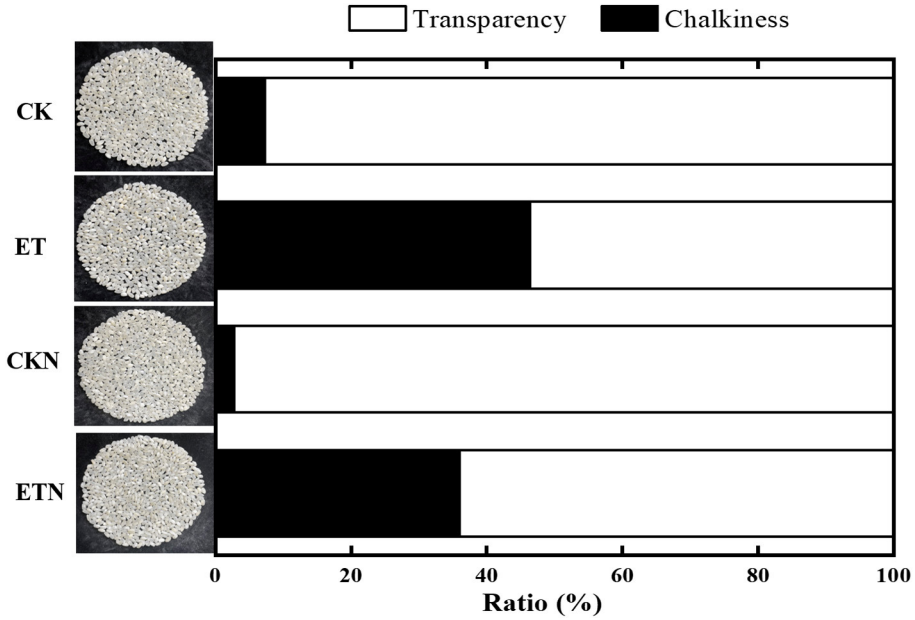

FIGURE 1 | Effects of nitrogen fertilizer on grain chalkiness under elevated temperature. The rice plants were subjected to ambient temperature (CK), elevated temperature (ET), application of nitrogen fertilizer under ambient temperature (CKN), and application of nitrogen fertilizer under elevated temperature (ETN). Vertical bars represent mean ± SE ($n = 3$).

better assess the impact of temperature increase on rice quality and simultaneously evaluate the effects of nitrogen cultivation measures in coping with climate warming.

Nitrogen Fertilizer Regulates Endosperm Development Under Elevated Temperature

When the temperature exceeds a certain limitation in the grain-filling stage, the grain transparency would be adversely affected (Dhatt et al., 2019). Decreased grain length or width could reduce the grain weight (Counce et al., 2005), and chalky grains generally exhibited inferior weight when compared with the CK (Wu et al., 2016; Nakata et al., 2017). Nitrogen application under increased temperature significantly reduced chalkiness, and it also decreased the grain length and weight caused by warming in this study, which is consistent with the abovementioned studies.

Studies had shown that the formation of chalkiness was closely associated with the grain-filling process. The increased temperature led to the obvious acceleration of early grain-filling rate and rapid decline in the mid-late period, resulting in poor filling of starch granules and PBs in the endosperm, which could further induce a large number of gaps, and thus forming chalkiness (Ito et al., 2009; Kobata et al., 2011). Both this study and our previous studies have shown that elevated temperature increased the rate of grain filling and significantly accelerated the development of endosperm (**Figure 2**). Previous studies on heat stress of rice showed that heat would induce a significant increase in protein storage vacuoles and less accumulation of storage protein, which eventually led to more gaps in protein storage vacuoles, thus resulting in chalkiness (Wada et al., 2019). Our results indicated that nitrogen application could effectively increase the protein accumulation in endosperm and that could further fill the gaps in protein storage vacuoles, thereby reducing chalkiness. Furthermore, the results also showed that the application of nitrogen fertilizer under elevated temperature could alleviate grain development, prolong the grain-filling period, and coordinate the development of amyloplasts and PBs (**Figure 2**), and it may be one of the main reasons for the decrease in chalkiness. However, Xi et al. (2021) showed that nitrogen application at the panicle differentiation stage promoted the formation of chalky grains. This may indicate that the mechanism of the formation of chalkiness is relatively complicated, and physiological factors, genetic factors, and ecological factors could co-modulate its formation. Therefore, conduct more in-depth studies, such as the use of transcriptome analysis and the construction of mutants, would be contributed to further revealing its mechanism.

Nitrogen Fertilizer Affected the Grain Storage Protein Accumulation and Reduced the Formation of Grain Chalkiness Under Warming Condition

As the second major component, rice storage proteins are divided into albumin, globulin, prolamin, and glutelin according to the solubility (Shewry and Halford, 2002). Glutelin is the main component of grain storage protein, accounting for about 80% of seed storage proteins. The synthesis of glutelin begins with glutelin precursor subunits, which are then folded by a molecular chaperone, such as lumenal chaperon binding protein (BiP) and protein disulfide isomerase (PDI), transported into protein

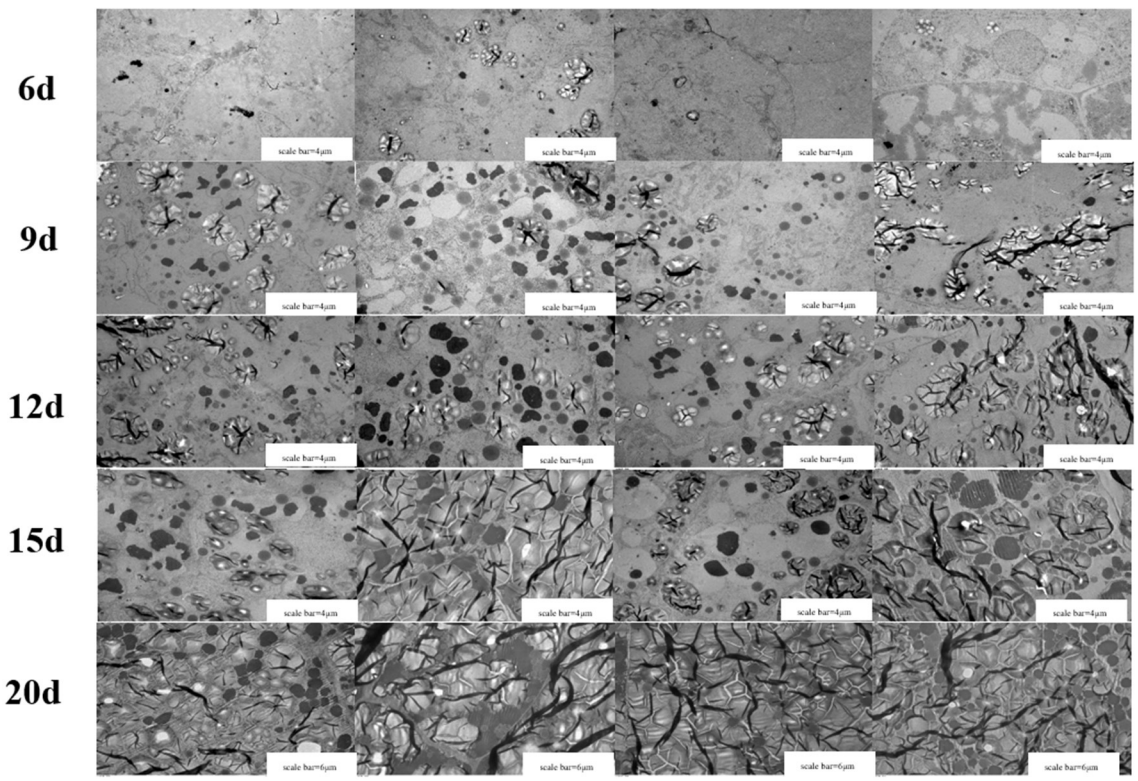

FIGURE 2 | Effects of nitrogen fertilizer on dynamic changes of starch granules and protein bodies under elevated temperature during the grain-filling stage. The order of horizontal arrangement was CK, ET, application of CKN, and application of ETN, and the order of vertical column is 6, 9, 12, 15, and 20 days after anthesis (DAA). Scale bar = 4 μm at 6, 9, 12, and 15 DAA; scale bar = 6 μm at 20 DAA.

storage vacuoles, and formed mature acidic and basic subunits by splicing. Similar to the glutelin synthesis, prolamin consists of 10, 13, and 16 kDa protein subunits (Yamagata et al., 1982). The contents of albumin and globulin are relatively low and mainly distributed in the aleurone layer, pericarp, and embryo (Shewry and Halford, 2002). Storage protein plays an important role in the rice quality and is closely related to the formation of chalkiness (Liu et al., 2020). This study showed that the storage protein accumulated rapidly at 15–20 DAA (**Figure 3**), which was consistent with the study by Ashida et al. (2013), indicating that the storage protein is mainly accumulated in the middle grain-filling stage. Studies had shown that the high temperature decreased the starch content but this is conducive to the amino acids and the protein content accumulate in grains (Wang and Frei, 2011; Beckles and Thitisaksakul, 2014; Chun et al., 2015; Wang et al., 2019), and this feature was also obtained in the results of this study (**Supplementary Tables 2–4**). It is speculated that the increased temperature during the grain-filing stage promoted the activities of related enzymes, and the key regulators encoded the gene expressions, which jointly promoted the protein synthesis, and gradually accumulated the organic matter from source to sink organs, thus promoting the protein contents in rice grains (Lancien et al., 2000; Cao et al., 2017).

Results of the changes of protein components indicated that the total protein and glutelin contents were all increased, but prolamin was decreased under the condition of increased temperature (**Supplementary Table 2**). The influence of temperature on the glutelin content was significant, especially during 11–20 days after heading, which was consistent with the study conducted by Ashida et al. (2013).

The content of prolamin was significantly decreased under the warming condition, indicating that the decrease of the prolamin content may be related to the increase of chalkiness (Lin et al., 2010). This study showed that there was a significantly negative correlation between prolamin content and chalkiness, and Ishimaru et al. (2020) showed that the content of 13 kDa prolamin subunits in grains with more chalkiness was lower than that in transparent grains under field conditions. The transparency of grain was closely related to the physiological process of 13 kDa prolamin subunit synthesis under the high temperature. Previous studies have shown that transgenic lines with reduced 13 kDa gliadin exhibit a relatively transparent phenotype. Kawakatsu et al. (2010) constructed transgenic rice (SSP-less mutant), and the results showed that not only in the Glu-less mutant but also in the Pro-less mutant obtained no opaque phenotype. This may suggest that the formation of

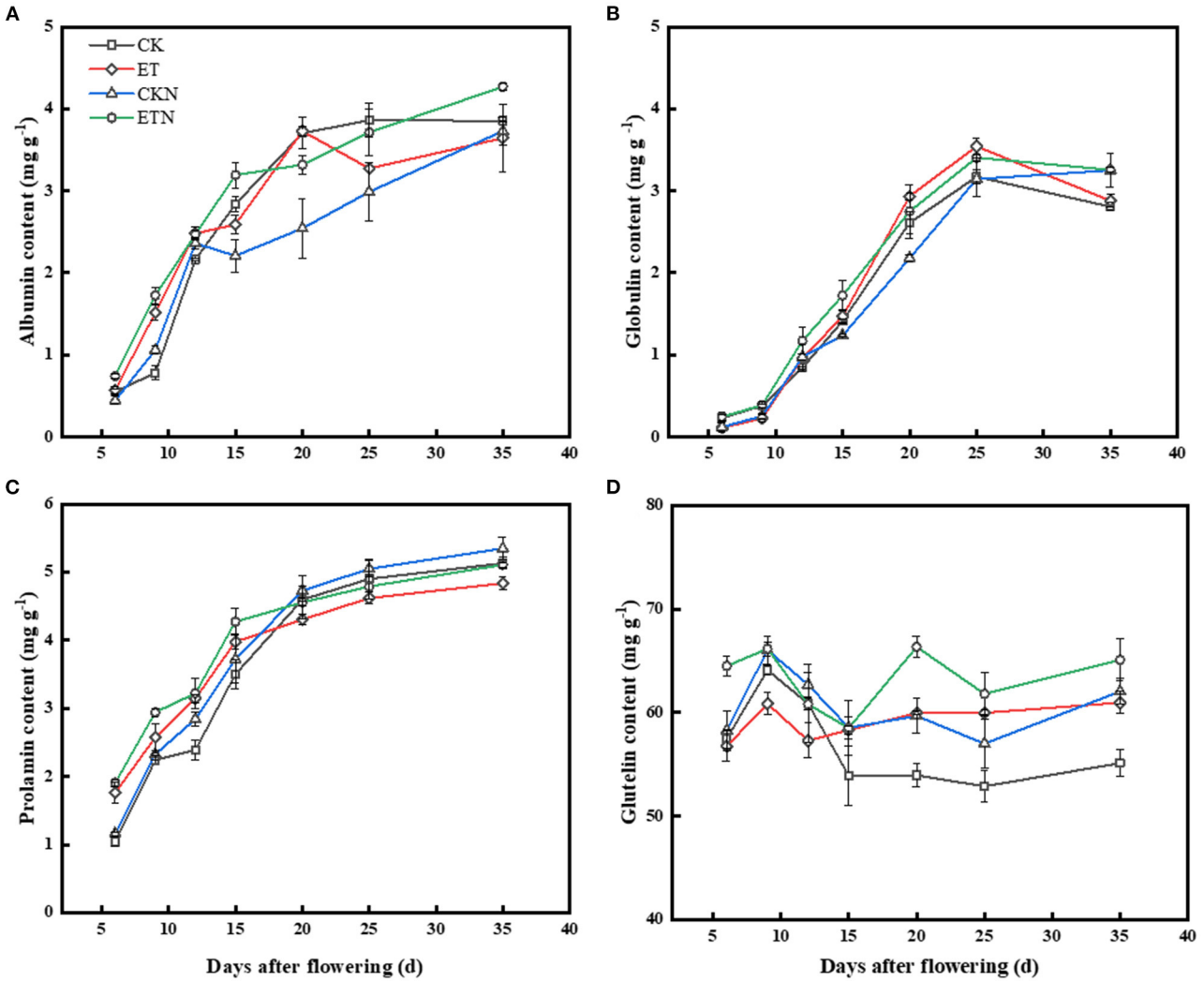

FIGURE 3 | Effects of nitrogen fertilizer on grain dynamic content changes of protein components under elevated temperature during the grain-filling stage in rice. **(A)** Albumin, **(B)** globulin, **(C)** prolamin, and **(D)** glutelin. The rice plants were subjected to CK, ET, application of CKN, and application of ETN. Vertical bars represent mean ± SE ($n = 3$).

TABLE 3 | Correlation coefficients among grain quality and protein components in rice.

Index	Albumin	Globulin	Prolamin	Glutelin	Amylose	Amylopectin
Head rice rate	−0.11	0.09	0.94**	−0.25	0.94**	0.09
Chalkinesss	0.21	0.09	−0.92**	0.41	−0.94**	0.06
Amylose	−0.21	−0.01	0.90**	−0.40	1	0.20
Amylopectin	−0.40	0.27	−0.03	−0.16	0.20	1
Peak viscosity	0.18	0.11	−0.93**	0.37	−0.89**	0.04
Hot paste viscosity	0.06	0.07	−0.75**	0.17	−0.58*	0.00
Breakdown viscosity	0.20	0.16	−0.93**	0.41	−0.93**	0.05
Cool paste viscosity	−0.50	0.46	0.70*	−0.75**	0.86**	0.06
Setback viscosity	−0.31	0.24	0.90**	−0.53	0.93**	−0.01
Gelatinization temperature	0.40	0.34	−0.82**	0.65*	−0.86**	−0.01

**, **, significant at 0.05 and 0.01 probability levels, respectively.*

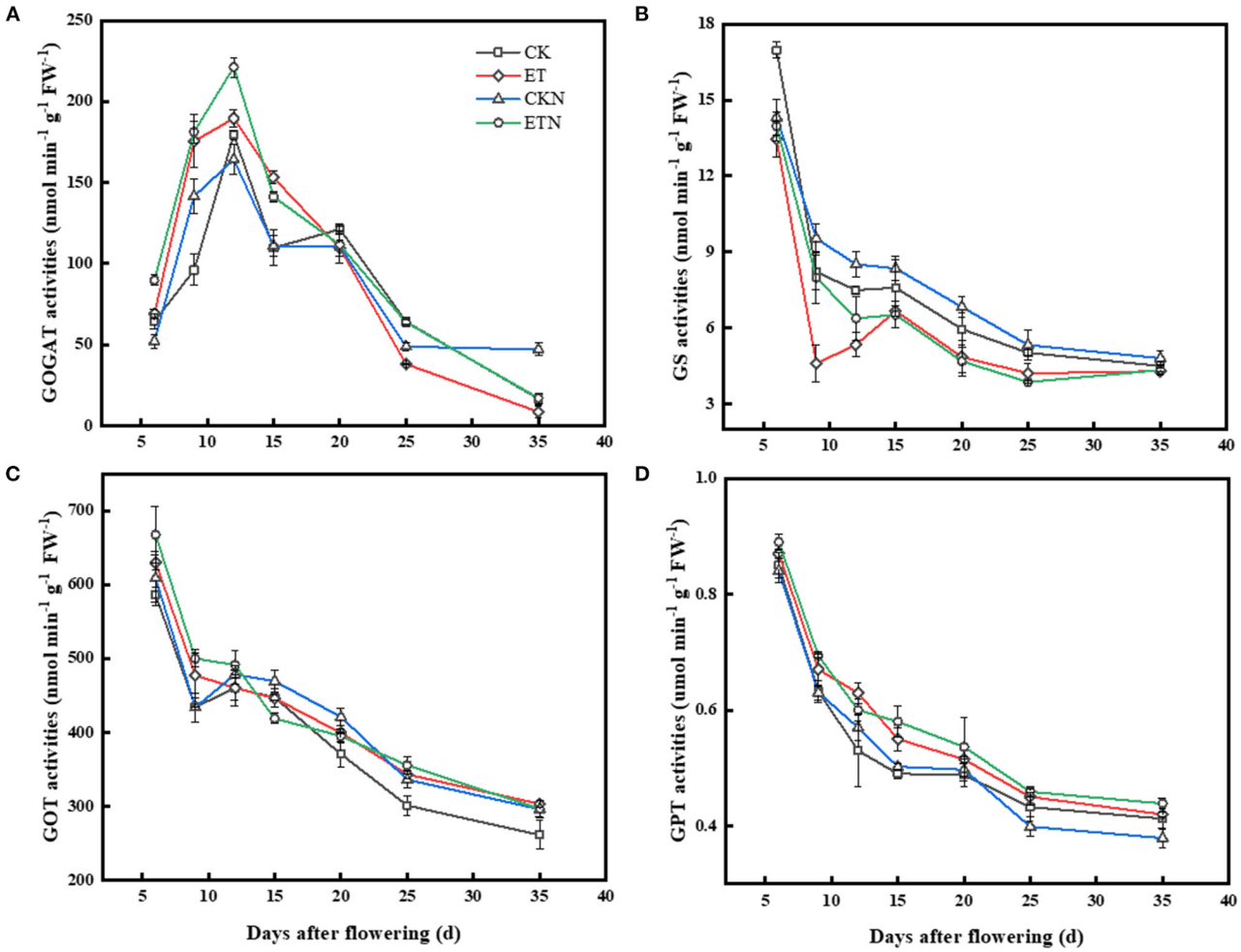

FIGURE 4 | Effects of nitrogen fertilizer on grain nitrogen metabolism key enzyme activities under elevated temperature during the grain-filling stage in rice. **(A)** Glutamine synthetase, **(B)** glutamate synthetase, **(C)** glutamic oxaloacetic transaminase, and **(D)** glutamic pyruvic transaminase. The rice plants were subjected to CK, ET, application of CKN, and application of ETN. Vertical bars represent mean ± SE ($n = 3$).

chalkiness is a complex process, which contains a multi-level of physiological and biochemical reactions. In our previous study, we stated that the balance changes of starch, protein, and other grain storage substances could be the possible reason for inducing the increased grain chalkiness. Therefore, it is, in fact, difficult to fully reveal the mechanism of the formation of grain chalk from only one aspect. Conducting more in-depth studies, such as the use of transcriptome analysis and the construction of mutants, would be contributed in further revealing its mechanism. Studies have shown that the protein and starch components of rice grain have a great influence on RVA characteristics (Champagne et al., 2009; Gu et al., 2015). Our results showed that the RVA parameters were changed under elevated temperature, and were also closely related to the changes of starch and protein contents of rice grains. Results showed that the protein content was significantly related to RVA characteristic parameters, and there was a significant correlation between amylose and RVA parameters. The amylose content was significantly positively associated with cool paste viscosity and setback viscosity and was negatively correlated with hot paste viscosity, peak viscosity, breakdown viscosity, and gelatinization temperature. This result was consistent with studies conducted by Yang et al. (2013), suggesting that the changes in the amylose content caused by warming would obviously change the cooking and eating quality of rice, which is also an important topic worthy of research under the background of climate warming.

Regulatory Effects of Nitrogen Fertilizer on Main Regulatory Factors and Enzyme Activities Related to Nitrogen Metabolism Under Elevated Temperature

Carbon and nitrogen metabolism and its products are important factors that determine the rice quality (Hakata et al., 2012; Tang et al., 2018). Studies have identified the possible key metabolic steps related to starch in rice grains, as well as the role of

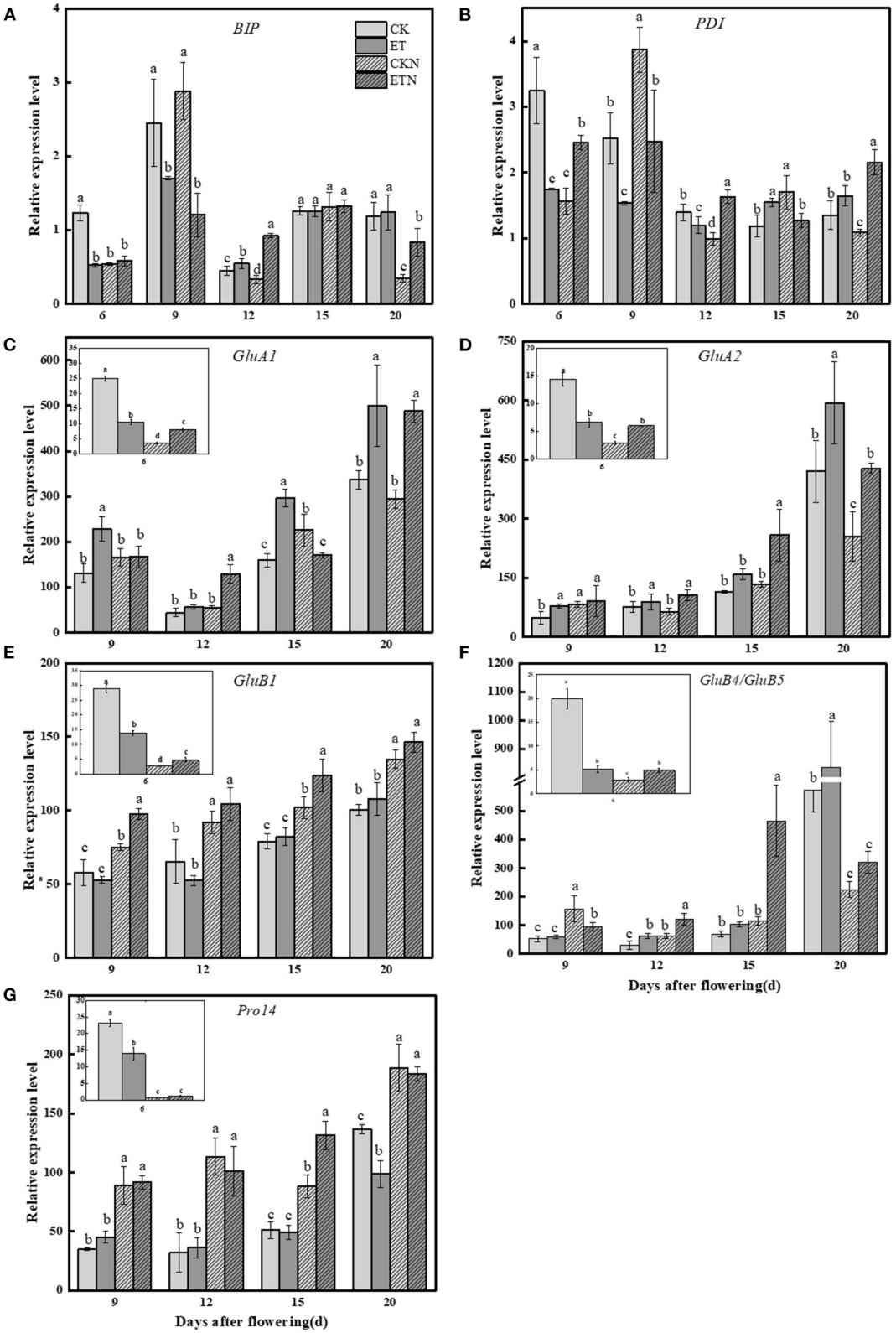

FIGURE 5 | Effects of nitrogen fertilizer on grain nitrogen metabolism main regulatory factor genes under elevated temperature during the grain-filling stage in rice. **(A)** *BiP1*, **(B)** *PDIL1*, **(C)** *GluA1*, **(D)** *GluA2*, **(E)** *GluB1*, **(F)** *GluB5/GluB4*, and **(G)** *pro14*. The rice plants were subjected to CK, ET, application of CKN, and application of ETN. The small picture in the frame showed that the relative expression of each gene at 6 DAA. At the same grain-filling stage, different letters indicate significant differences among different treatments according to the Duncan's multiple range test ($P < 0.05$). Vertical bars represent mean ± SE ($n = 3$).

key enzymes and regulatory factors in starch synthesis, such as granule bound starch synthase and starch branching enzyme (Yamakawa and Hakata, 2010; Yu and Wang, 2016). However, the relationship between nitrogen metabolites and the grain quality has not been given sufficient attention, and the role of activities of main nitrogen metabolism enzymes and regulatory factors is still unclear. More than 95% of inorganic nitrogen in plants is assimilated through the GS/GOGAT cycle (Hirel et al., 2001; Martin et al., 2006). Conversion of glutamic acid to other amino acids was achieved according to the catalysis of GOT and GPT, which provided substrates for protein synthesis. The elevated temperature was conducive to increase the key period activity of GOGAT (Liang et al., 2011). Studies had shown that the increase of GS and GOGAT enzyme activity can promote nitrogen metabolism, protein synthesis, and amino acid transformation (Lancien et al., 2000; Miflin and Habash, 2002). During the grain-filling process, the ammonia transfer process plays an important role in grain nitrogen metabolism. It was generally believed that GOT and GPT activities positively stimulated the protein content (Liang et al., 2011). In this study, the activities of GPT and GOT were increased significantly under increased temperature. Nitrogen application under elevated temperature could improve enzyme activities related to nitrogen metabolism, and the regulation of nitrogen fertilizer on enzyme activity was mainly during the early stage of grain filling (before 15DAA) (**Figure 4**). This may indicate that nitrogen and inorganic nitrogen, which provide substrates for protein synthesis, are assimilated into organic substances, such as proteins and nucleic acids, and participate in the GS/GOGAT cycle, thereby promoting protein synthesis (Yu et al., 2018; Huang et al., 2020).

Rice glutelin encoded by *GluA* and *GluB* subfamily is the important gene family for glutelin synthesis. Our results showed that the glutelin precursor was synthesized and accumulated after 6 DAA, and elevated temperature significantly increased the expression of *GluA1* and *GluA2*, while it decreased the expression of *GluB1* at the early grain-filling stage and increased its expression at the middle grain-filling stage, which was consistent with the changes of the glutelin content. The relative expression of *GluB1* and *GluB5/GluB4* (except 20 DAA) was evidently increased by the nitrogen application under the elevated temperature. The results showed that the expression of prolamin family gene*pro14* is more sensitive to the application of nitrogen during the whole filling stage under the elevated temperature. However, the changes in the expression of *pro14* induced by elevated temperature are not significant compared with normal temperature, which is somewhat different from the results of previous studies (Yamakawa et al., 2007; Cao et al., 2017). Furthermore, the tendency of *pro14* relative expression was consistent with the prolamin content changes under the elevated temperature and nitrogen fertilizer application, and it is speculated that *pro14* can be considered as the main factor in regulating the synthesis of prolamin under the background of warming and nitrogen, and more in-depth mechanism studies could be conducted.

In addition to family coding genes, molecular chaperones, namely, BiP and PDI, are also a kind of key regulators that regulate protein synthesis in rice grains. For example, after the precursor of gluten is transported to the cavity of the endoplasmic reticulum, it folds and assembles with the help of molecular chaperones in the cavity and generates disulfide bonds in the peptide chain (Takemoto et al., 2002; Kawakatsu and Takaiwa, 2010). However, conclusions on the expression pattern of molecular chaperones under the background of increased temperature or heat stress are still not consistent. In this study, elevated temperature significantly increased the relative expression of *PDIL1* in the middle grain-filling period, while *PDIL1* expression was decreased during the early grain-filling stage, and that may be the main reason for the decreased prolamin content detected in the early stage of grain filling. Expression of endoplasmic reticulum chaperone protein, *BiP1*, has been reported to be downregulated in chalky endosperm induced by high temperature (Ishimaru et al., 2009). Although, in this study, it was found that its expression was reduced in the early stage of grain filling, it is still not possible to fully infer the role of *BiP1* in the accumulation of storage proteins under the disposal of this study. Grain protein accumulation is a complex process involving multiple levels of the interaction among gene transcription, translation, protein folding, and degradation. Therefore, it is difficult to fully clarify the influence of temperature increase on protein synthesis and metabolism in rice grain, and more in-depth study, such as the use of transcriptome analysis, would be contributed to further reveal the mechanism.

CONCLUSION

Our previous field study has shown that the application of nitrogen fertilizer can effectively regulate starch synthesis and reduce the appearance of grain chalkiness. In this study, the effects of elevated temperature and nitrogen fertilizer on grain metabolism were further elucidated. Results showed that nitrogen fertilizer could slow down the early grain development, prolong the grain-filling duration, and coordinate the development of PBs and starch bodies under the elevated temperature. Furthermore, nitrogen fertilizer affected the nitrogen metabolism enzyme and the key regulatory factors, which further regulated grain storage protein synthesis under elevated temperature, and this could induce the balance changes of grain storage substances and further regulate the grain quality. These findings would help us to better understand the impacts of global warming on rice quality and provide a theoretical basis for the establishment of high-quality rice cultivation approaches.

DATA AVAILABILITY STATEMENT

The datasets presented in this study can be found in online repositories. The names of the repository/repositories and accession number(s) can be found in the article/**Supplementary Material**.

AUTHOR CONTRIBUTIONS

ST and YD conceived the experiments. ST and XW designed the experiments. XW, KW, and TY performed

the experimental study. XW wrote the manuscript. YZ, WL, and YS edited the manuscript. All authors read and approved the final manuscript.

FUNDING

This study was supported by the National Key R&D Program, Ministry of Science and Technology, China (Grant Nos. 2017YFD0300100 and 2017YFD0300107). This study was also funded by the National Natural Science Foundation of China (Grant Nos. 32071949 and 31701366). We also received funding from the Fundamental Research Funds for the Central Universities, China (Grant No. KJQN201802). We also received support from the Collaborative Innovation Center for Modern Crop Production cosponsored by Province and Ministry (CIC-MCP).

SUPPLEMENTARY MATERIAL

The Supplementary Material for this article can be found online at: https://www.frontiersin.org/articles/10.3389/fpls.2021.715436/full#supplementary-material

REFERENCES

Ashida, K., Araki, E., Maruyama-Funatsuki, W., Fujimoto, H., and Ikegami, M. (2013). Temperature during grain ripening affects the ratio of type-II/type-I protein body and starch pasting properties of rice (*Oryza sativa* L.). *J. Cereal Sci.* 57, 153–159. doi: 10.1016/j.jcs.2012.10.006

Beckles, D. M., and Thitisaksakul, M. (2014). How environmental stress affects starch composition and functionality in cereal endosperm. *Starch-Stärke* 66, 58–71. doi: 10.1002/star.201300212

Cao, Z., Zhao, Q., Pan, G., Wei, K., Zhou, L., and Cheng, F. (2017). Comprehensive expression of various genes involved in storage protein synthesis in filling rice grain as affected by high temperature. *Plant Growth Regul.* 81, 477–488. doi: 10.1007/s10725-016-0225-4

Champagne, E. T., Bett-Garber, K. L., Thomson, J. L., and Fitzgerald, M. A. (2009). Unraveling the impact of nitrogen nutrition on cooked rice flavor and texture. *Cereal Chem.* 86, 274–280. doi: 10.1094/cchem-86-3-0274

Cheng, F. M., Zhong, L. J., Wang, F., and Zhang, G. P. (2005). Differences in cooking and eating properties between chalky and translucent parts in rice grains. *Food Chem.* 90, 39–46. doi: 10.1016/j.foodchem.2004.03.018

Chun, A., Lee, H.-J., Hamaker, B. R., and Janaswamy, S. (2015). Effects of ripening temperature on starch structure and gelatinization, pasting, and cooking properties in rice. *J. Agricult. Food Chem.* 63, 3085–3093. doi: 10.1021/jf504870p

Counce, P. A., Bryant, R. J., Bergman, C. J., Bautista, R. C., Wang, Y. J., Siebenmorgen, T. J., et al. (2005). Rice milling quality, grain dimensions, and starch branching as affected by high night temperatures. *Cereal Chem.* 82, 645–648. doi: 10.1094/cc-82-0645

Dhatt, B. K., Abshire, N., Paul, P., Hasanthika, K., Sandhu, J., Zhang, Q., et al. (2019). Metabolic dynamics of developing rice seeds under high night-time temperature stress. *Front. Plant Sci.* 10:1443. doi: 10.3389/fpls.2019.01443

Dou, Z., Tang, S., Li, G., Liu, Z., Ding, C., Chen, L., et al. (2017). Application of nitrogen fertilizer at heading stage improves rice quality under elevated temperature during grain-filling stage. *Crop Sci.* 57, 2183–2192. doi: 10.2135/cropsci2016.05.0350

Fujita, N., Yoshida, M., Kondo, T., Saito, K., Utsumi, Y., Tokunaga, T., et al. (2007). Characterization of SSIIIa-deficient mutants of rice: the function of SSIIIa and pleiotropic effects by SSIIIa deficiency in the rice endosperm. *Plant Physiol.* 144, 2009–2023. doi: 10.1104/pp.107.102533

Gu, J., Chen, J., Chen, L., Wang, Z., Zhang, H., and Yang, J. (2015). Grain quality changes and responses to nitrogen fertilizer of japonica rice cultivars released in the Yangtze River Basin from the 1950s to 2000s. *Crop J.* 3, 285–297. doi: 10.1016/j.cj.2015.03.007

Guo, T., Liu, X., Wan, X., Weng, J., Liu, S., Liu, X., et al. (2011). Identification of a stable quantitative trait locus for percentage grains with white chalkiness in rice (*Oryza sativa*). *J. Integr. Plant Biol.* 53, 598–607. doi: 10.1111/j.1744-7909.2011.01041.x

Hakata, M., Kuroda, M., Miyashita, T., Yamaguchi, T., Kojima, M., Sakakibara, H., et al. (2012). Suppression of alpha-amylase genes improves quality of rice grain ripened under high temperature. *Plant Biotechnol. J.* 10, 1110–1117. doi: 10.1111/j.1467-7652.2012.00741.x

Hirel, B., Bertin, P., Quillere, I., Bourdoncle, W., Attagnant, C., Dellay, C., et al. (2001). Towards a better understanding of the genetic and physiological basis for nitrogen use efficiency in maize. *Plant Physiol.* 125, 1258–1270. doi: 10.1104/pp.125.3.1258

Huang, S. J., Zhao, C. F., Zhu, Z., Zhou, L. H. E., Zheng, Q. H., and Wang, C. L. (2020). Characterization of eating quality and starch properties of two Wx alleles japonica rice cultivars under different nitrogen treatments. *J. Integr. Agric.* 19, 988–998. doi: 10.1016/s2095-3119(19)62672-9

Ishimaru, T., Horigane, A. K., Ida, M., Iwasawa, N., San-oh, Y. A., Nakazono, M., et al. (2009). Formation of grain chalkiness and changes in water distribution in developing rice caryopses grown under high-temperature stress. *J. Cereal Sci.* 50, 166–174. doi: 10.1016/j.jcs.2009.04.011

Ishimaru, T., Miyazaki, M., Shigemitsu, T., Nakata, M., Kuroda, M., Kondo, M., et al. (2020). Effect of high temperature stress during ripening on the accumulation of key storage compounds among Japanese highly palatable rice cultivars. *J. Cereal Sci.* 95:103018. doi: 10.1016/j.jcs.2020.103018

Ito, S., Hara, T., Kawanami, Y., Watanabe, T., Thiraporn, K., Ohtake, N., et al. (2009). Carbon and nitrogen transport during grain filling in rice under high-temperature conditions. *J. Agronomy Crop Sci.* 195, 368–376. doi: 10.1111/j.1439-037X.2009.00376.x

Kang, H. G., Park, S., Matsuoka, M., and An, G. H. (2005). White-core endosperm floury endosperm-4 in rice is generated by knockout mutations in the C-4-type pyruvate orthophosphate dikinase gene (OsPPDKB). *Plant J.* 42, 901–911. doi: 10.1111/j.1365-313X.2005.02423.x

Kawakatsu, T., Hirose, S., Yasuda, H., and Takaiwa, F. (2010). Reducing rice seed storage protein accumulation leads to changes in nutrient quality and storage organelle formation. *Plant Physiol.* 154, 1842–1854. doi: 10.1104/pp.110.164343

Kawakatsu, T., and Takaiwa, F. (2010). Cereal seed storage protein synthesis: fundamental processes for recombinant protein production in cereal grains. *Plant Biotechnol. J.* 8, 939–953. doi: 10.1111/j.1467-7652.2010.00559.x

Kobata, T., Miya, N., and Nguyen Thi, A. (2011). High risk of the formation of milky white rice kernels in cultivars with higher potential grain growth rate under elevated temperatures. *Plant Prod. Sci.* 14, 359–364. doi: 10.1626/pps.14.359

Lancien, M., Gadal, P., and Hodges, M. (2000). Enzyme redundancy and the importance of 2-oxoglutarate in higher plant ammonium assimilation. *Plant Physiol.* 123, 817–824. doi: 10.1104/pp.123.3.817

Liang, C. G., Chen, L. P., Wang, Y., Liu, J., Xu, G. L., and Tian, L. I. (2011). High temperature at grain-filling stage affects nitrogen metabolism enzyme activities in grains and grain nutritional quality in rice. *Rice Sci.* 18, 210–216. doi: 10.1016/s1672-6308(11)60029-2

Lin, C. J., Li, C. Y., Lin, S. K., Yang, F. H., Huang, J. J., Liu, Y. H., et al. (2010). Influence of high temperature during grain filling on the accumulation of storage proteins and grain quality in rice (*Oryza sativa* L.). *J. Agric. Food Chem.* 58, 10545–10552. doi: 10.1021/jf101575j

Liu, Q., Tao, Y., Cheng, S., Zhou, L., Tian, J., Xing, Z., et al. (2020). Relating amylose and protein contents to eating quality in 105 varieties of Japonicarice. *Cereal Chem.* 97, 1303–1312. doi: 10.1002/cche.10358

Martin, A., Lee, J., Kichey, T., Gerentes, D., Zivy, M., and Tatout, C. (2006). Two cytosolic glutamine synthetase isoforms of maize are specifically involved in the control of grain production. *Plant Cell* 18, 3252–3274. doi: 10.1105/tpc.106.042689

Miflin, B. J., and Habash, D. Z. (2002). The role of glutamine synthetase and glutamate dehydrogenase in nitrogen assimilation and possibilities for

improvement in the nitrogen utilization of crops. *J. Exp. Bot.* 53, 979–987. doi: 10.1093/jexbot/53.370.979

Mitsui, T., Shiraya, T., Kaneko, K., and Wada, K. (2013). Proteonnics of rice grain under high temperature stress. *Front. Plant Sci.* 4:36. doi: 10.3389/fpls.2013.00036

Nakata, M., Fukamatsu, Y., Miyashita, T., Hakata, M., Kimura, R., Nakata, Y., et al. (2017). High temperature-induced expression of rice alpha - amylases in developing endosperm produces chalky grains. *Front. Plant Sci.* 8:2089. doi: 10.3389/fpls.2017.02089

Rehmani, M. I. A., Wei, G., Hussain, N., Ding, C., Li, G., Liu, Z., et al. (2014). Yield and quality responses of two indica rice hybrids to post-anthesis asymmetric day and night open-field warming in lower reaches of Yangtze River delta. *Field Crops Res.* 156, 231–241. doi: 10.1016/j.fcr.2013.09.019

Shewry, P. R., and Halford, N. G. (2002). Cereal seed storage proteins: structures, properties and role in grain utilization. *J. Exp. Bot.* 53, 947–958. doi: 10.1093/jexbot/53.370.947

Takemoto, Y., Coughlan, S. J., Okita, T. W., Satoh, H., Ogawa, M., and Kumamaru, T. (2002). The rice mutant esp2 greatly accumulates the glutelin precursor and deletes the protein disulfide isomerase. *Plant Physiol.* 128, 1212–1222. doi: 10.1104/pp.010624

Tang, S., Chen, W., Liu, W., Zhou, Q., Zhang, H., Wang, S., et al. (2018). Open-field warming regulates the morphological structure, protein synthesis of grain and affects the appearance quality of rice. *J. Cereal Sci.* 84, 20–29. doi: 10.1016/j.jcs.2018.09.013

Tang, S., Zhang, H., Liu, W., Dou, Z., Zhou, Q., Chen, W., et al. (2019). Nitrogen fertilizer at heading stage effectively compensates for the deterioration of rice quality by affecting the starch-related properties under elevated temperatures. *Food Chem.* 277, 455–462. doi: 10.1016/j.foodchem.2018.10.137

Wada, H., Hatakeyama, Y., Onda, Y., Nonami, H., Nakashima, T., Erra-Balsells, R., et al. (2019). Multiple strategies for heat adaptation to prevent chalkiness in the rice endosperm. *J. Exp. Bot.* 70, 1299–1311. doi: 10.1093/jxb/ery427

Wang, E., Wang, J., Zhu, X., Hao, W., Wang, L., Li, Q., et al. (2008). Control of rice grain-filling and yield by a gene with a potential signature of domestication. *Nat. Genet.* 40, 1370–1374. doi: 10.1038/ng.220

Wang, J. Q., Hasegawa, T., Li, L. Q., Lam, S. K., Zhang, X. H., Liu, X. Y., et al. (2019). Changes in grain protein and amino acids composition of wheat and rice under short-term increased CO2 and temperature of canopy air in a paddy from East China. *New Phytol.* 222, 726–734. doi: 10.1111/nph.15661

Wang, Y., and Frei, M. (2011). Stressed food - the impact of abiotic environmental stresses on crop quality. *Agricult. Ecosyst. Environ.* 141, 271–286. doi: 10.1016/j.agee.2011.03.017

Wu, L., Jiang, S., and Tao, Q. (1998). The application of colormetric method on the determination of transaminase activity. *Chin. J. Soil Sci.* 3, 41–43. doi: 10.19336/j.cnki.trtb.1998.03.015

Wu, Y. C., Chang, S. J., and Lur, H. S. (2016). Effects of field high temperature on grain yield and quality of a subtropical type japonica rice-Pon-Lai rice. *Plant Prod. Sci.* 19, 145–153. doi: 10.1080/1343943x.2015.1128091

Xi, M., Wu, W., Xu, Y., Zhou, Y., Chen, G., Ji, Y., et al. (2021). Grain chalkiness traits is affected by the synthesis and dynamic accumulation of the storage protein in rice. *J. Sci. Food Agric.* doi: 10.1002/jsfa.11269

Xu, H., Li, X., Zhang, H., Wang, L., Zhu, Z., Gao, J., et al. (2020). High temperature inhibits the accumulation of storage materials by inducing alternative splicing of OsbZIP58 during filling stage in rice. *Plant Cell Environ.* 43, 1879–1896. doi: 10.1111/pce.13779

Yamagata, H., Sugimoto, T., Tanaka, K., and Kasai, Z. (1982). Biosynthesis of storage proteins in developing rice seeds. *Plant Physiol.* 70, 1094–1100. doi: 10.1104/pp.70.4.1094

Yamakawa, H., and Hakata, M. (2010). Atlas of rice grain filling-related metabolism under high temperature: joint analysis of metabolome and transcriptome demonstrated inhibition of starch accumulation and induction of amino acid accumulation. *Plant Cell Physiol.* 51, 795–809. doi: 10.1093/pcp/pcq034

Yamakawa, H., Hirose, T., Kuroda, M., and Yamaguchi, T. (2007). Comprehensive expression profiling of rice grain filling-related genes under high temperature using DNA microarray. *Plant Physiol.* 144, 258–277. doi: 10.1104/pp.107.098665

Yang, X. Y., Lin, Z. M., Liu, Z. H., Ajim, M. A., Bi, J. G., Li, G. H., et al. (2013). Physicochemical and sensory properties of japonica rice varied with production areas in china. *J. Integr. Agric.* 12, 1748–1756. doi: 10.1016/s2095-3119(13)60338-x

Yu, H., and Wang, T. (2016). Proteomic dissection of endosperm starch granule associated proteins reveals a network coordinating starch biosynthesis and amino acid metabolism and glycolysis in rice endosperms. *Front. Plant Sci.*7:707. doi: 10.3389/fpls.2016.00707

Yu, Z., Juhasz, A., Islam, S., Diepeveen, D., Zhang, J., Wang, P., et al. (2018). Impact of mid-season sulphur deficiency on wheat nitrogen metabolism and biosynthesis of grain protein. *Sci. Rep.* 8:2499. doi: 10.1038/s41598-018-20935-8

Zhou, T., Zhou, Q., Li, E., Yuan, L., Wang, W., Zhang, H., et al. (2020). Effects of nitrogen fertilizer on structure and physicochemical properties of 'super' rice starch. *Carbohydr. Polym.* 239:116237. doi: 10.1016/j.carbpol.2020.116237

Conflict of Interest: The authors declare that the research was conducted in the absence of any commercial or financial relationships that could be construed as a potential conflict of interest.

Publisher's Note: All claims expressed in this article are solely those of the authors and do not necessarily represent those of their affiliated organizations, or those of the publisher, the editors and the reviewers. Any product that may be evaluated in this article, or claim that may be made by its manufacturer, is not guaranteed or endorsed by the publisher.

frontiers in Plant Science

ORIGINAL RESEARCH
published: 09 September 2021
doi: 10.3389/fpls.2021.718504

Proteome and Nutritional Shifts Observed in Hordein Double-Mutant Barley Lines

Utpal Bose[1,2†], Angéla Juhász[2†], Ronald Yu[3], Mahya Bahmani[2], Keren Byrne[1], Malcolm Blundell[3], James A. Broadbent[1], Crispin A. Howitt[3] and Michelle L. Colgrave[1,2]*

[1] CSIRO Agriculture and Food, St Lucia, QLD, Australia, [2] Australian Research Council Centre of Excellence for Innovations in Peptide and Protein Science, School of Science, Edith Cowan University, Joondalup, WA, Australia, [3] CSIRO Agriculture and Food, Canberra, ACT, Australia

Lysine is the most limiting essential amino acid in cereals, and efforts have been made over the decades to improve the nutritional quality of these grains by limiting storage protein accumulation and increasing lysine content, while maintaining desired agronomic traits. The single *lys3* mutation in barley has been shown to significantly increase lysine content but also reduces grain size. Herein, the regulatory effect of the *lys3* mutation that controls storage protein accumulation as well as a plethora of critically important processes in cereal seeds was investigated in double mutant barley lines. This was enabled through the generation of three hordein double-mutants by inter-crossing three single hordein mutants, that had all been backcrossed three times to the malting barley cultivar Sloop. Proteome abundance measurements were integrated with their phenotype measurements; proteins were mapped to chromosomal locations and to their corresponding functional classes. These models enabled the prediction of previously unknown points of crosstalk that connect the impact of *lys3* mutations to other signalling pathways. In combination, these results provide an improved understanding of how the mutation at the *lys3* locus remodels cellular functions and impact phenotype that can be used in selective breeding to generate favourable agronomic traits.

Keywords: barley, *Hordeum vulgare*, *lys3* mutant, omics, hordein, coeliac disease, proteomics, SWATH-MS

OPEN ACCESS

Edited by:
Yingyin Yao,
China Agricultural University, China

Reviewed by:
Ganggang Guo,
Institute of Crop Sciences, Chinese Academy of Agricultural Sciences, China
Dezhi Wu,
Zhejiang University, China

***Correspondence:**
Michelle L. Colgrave
michelle.colgrave@csiro.au

† These authors have contributed equally to this work

Specialty section:
This article was submitted to Crop and Product Physiology, a section of the journal Frontiers in Plant Science

Received: *01 June 2021*
Accepted: *09 August 2021*
Published: *09 September 2021*

Citation:
Bose U, Juhász A, Yu R, Bahmani M, Byrne K, Blundell M, Broadbent JA, Howitt CA and Colgrave ML (2021) Proteome and Nutritional Shifts Observed in Hordein Double-Mutant Barley Lines. Front. Plant Sci. 12:718504. doi: 10.3389/fpls.2021.718504

INTRODUCTION

Barley is an important cereal grown mainly for feed and malting. The major seed storage proteins in barley, the hordeins, are elicitors of coeliac disease (CD) – a condition that adversely affects ∼1% of the world population (∼70 million people). There is no current treatment other than strict adherence to a life-long gluten-free (GF) diet. In the diploid barley genome, there are four types of hordeins present: B-, C-, D- and γ-hordeins. The B- and C-hordeins are the primary classes representing >90% of the hordeins in barley (Kreis et al., 1983; Shewry et al., 1985). The B- and C-hordeins are encoded by the *Hor-2* and *Hor-1* loci, respectively, and both loci are located on the short arm of chromosome 1. The high molecular weight glutenin orthologous D-hordein genes are located at *Hor-3* (1H long arm) and the S-rich γ-hordeins present at *Hor-5* (1H short arm) (Shewry, 1993). The B- and C-hordeins comprise two multigene families consisting

of 13 B-hordein genes (Kreis et al., 1983) and 20–30 C-hordein genes, respectively (Shewry et al., 1985). Attempts have been made to reduce the hordein abundance in barley through mutagenesis, gene technology (antisense or RNAi), or by applying selective breeding techniques. The potential pleiotropic consequences of these mutations on the grain proteome are not well understood.

The high concentration of lysine-poor prolamin storage proteins in cereals are associated with the sub-optimal nutritional quality of cereal grains. Attempts have been made over the decades to increase the lysine content in cereal seeds by using chemical and physical mutagenesis. Early success was reported for two high lysine maize cultivars opaque-2 (Mertz et al., 1964) and floury-2 (Nelson et al., 1965). These two mutants had increased lysine and tryptophan content in the grain resulting from suppression of the lysine-deficient zein fraction without altering the contribution of other protein fractions. Screening efforts to identify similar *lys* mutants in other cereal grains led to the identification of a high-lysine gene in barley cultivars Hiproly (Munck et al., 1970) and Risø (Doll, 1973). Within the series of Risø mutants, Risø 1508 contained 45% more lysine and was shown to improve pig (Batterham, 1992) and rat (Gabert et al., 1995) growth in feeding trials without protein or amino acid supplementation. Although there was a significant down-regulation of hordeins (lysine-poor proteins) and an increase of free lysine, an increase in embryo size (as a proportion of grain size) compared to wild-types was significant (Tallberg, 1981); almost all Risø *lys* mutants had low starch content and shrunken grain size. The shrunken grain size was shown to relate to a set of genes involved in starch biosynthesis pathways (Cook et al., 2018; Moehs et al., 2019), but there is a lack of understanding of how the corresponding genes in the endosperm control starch content and composition. The abnormally large embryos in *lys3* mutants contain increased starch levels, increased starch granule size in the scutellum (Deggerdal et al., 1986) and have reduced dormancy (Howard et al., 2012). Although these mutants offer promise in terms of nutritional quality improvement, the concomitant reduction in seed size leading to lower agronomic yield negatively impacted their suitability for use as commercial crops.

Conventional breeding strategies were used to combine three recessive alleles to further reduce the hordein content in barley lines (Tanner et al., 2015). The high-lysine mutant Risø 56 barley line consists of a large gamma-ray-radiation-induced genomic deletion of at least 85 kb chromosome segment that accommodates the entire B-hordein loci (Kreis et al., 1983) on the short arm of chromosome 1H and does not accumulate the majority of the B-hordeins (Shewry et al., 1979). Another cultivar Risø 1508 contains an ethyl methanesulfonate (EMS)-induced mutation in the Lys3 locus on chromosome 5H (Karlsson, 1977). Risø 1508 has near zero C-hordein levels and significantly decreased B-hordein levels (Doll, 1973; Deggerdal et al., 1986; Hansen et al., 2007), confirmed by the transcription of the B- and C-hordein genes which are significantly down-regulated (Sørensen, 1992). An Ethiopian-derived landrace, R118 contains a single spontaneous mutation that encodes a premature stop codon that prevents expression of the full-length D-hordein (Tanner et al., 2015). Although several approaches have been used over the past decades to reduce hordein abundance in cereal crops, including antisense or RNAi, or selective breeding approaches (Hansen et al., 2007; Lange et al., 2007; Tanner et al., 2015; Moehs et al., 2019), the potential pleiotropic effects on the proteome upon mutation are not well understood.

The mechanisms activated in the grains of these double-mutant lines to compensate for the loss of these major storage proteins and decrease in starch content remain unknown. In the current study, phenotypic characterisation was performed in parallel with data-independent acquisition (DIA) mass spectrometry analyses (Venable et al., 2004), specifically sequential window acquisition of all theoretical spectra (SWATH)-mass spectrometry (Gillet et al., 2012). The aim was to study the large-scale quantitative changes in grain proteins within the hordein DM lines in comparison to their parent lines. Functional annotation and bioinformatic analyses were carried out to uncover the protein classes related to the hordein reduction in the DM lines. Balanced changes in the induced and suppressed protein abundances indicate differences both in the hordein levels and composition as well as in the lysine content of the DMs. This study serves as a framework for future proteomics-assisted crop development to study the pleotropic effects of genetic modification on safety and nutrition quality-related improvements.

MATERIALS AND METHODS

Plant Materials

The hordein null lines used in this study were developed in a previous study (Colgrave et al., 2016). Briefly, the barley varieties Risø 56 (B-hordein null), Risø 1508 (C-hordein null), and Ethiopian R118 (D-hordein null) were each crossed with the standard malting grain cv Sloop four times followed by selfing generations to create hordein single-nulls at backcross 3 (BC3), which theoretically share 93.75% genetic identity with Sloop. One homozygous hordein single-null for each of the three loci was selected and those three lines were intercrossed to create all three possible combinations of the Sloop hordein double-nulls.

The lines have also been assessed by MS to confirm the absence of the hordeins confirming that these mutations have not arisen spontaneously during the crossing programme. A limitation of this experiment is that only one line of each SM was selected for further study, and mutant segregants from each inter-cross of the SM were not examined. Pools of seeds from SM and DM lines were milled separately for obtaining the flour samples for analysis. Milling the individual seed was avoided as this was expected to introduce losses from already limited sample during the milling process.

Embryo Size Measurement

The size of the whole barley caryopsis was observed under stereomicroscopy (MZFIII, Leica Microsystems). The image was then processed by the image processing package Fiji in ImageJ (**Supplementary File 1**) (Schindelin et al., 2012).

Barley β-Glucan Analysis

Barley β-glucan was measured according to AOAC Method 995.16 (McCleary and Draga, 2016). Samples representing 20 mg of barley flour underwent sequential enzymatic digestion with lichenase and β-glucosidase and the glucose released was quantified through the standard glucose oxidase/peroxidase (GOPOD) system (**Supplementary File 1**).

Total Starch Content Analysis

The total starch content was measured using the AOAC Method 996.11 (AOAC, 1995), according to McCleary et al. (1997). The commercial K-TSTA kit (Megazyme) was used under manufacturer's procedures (McCleary et al., 1997). Briefly, starch was hydrolysed by thermostable α-amylase and amyloglucosidase to D-glucose. Glucose was then determined and quantified with glucose oxidase-peroxidise reagent (**Supplementary File 1**).

Total Fatty Acid and Total Triacyl Glycerol (TAG) Content Analysis

The extraction of total lipid, fractionation of neutral lipid (mainly TAG), free fatty acid, and polar lipid (mainly phosphocholine), and the subsequent lipid quantification were conducted according to the methods described by Liu et al. (2017). The quantitation of total lipid content and fatty acid composition were conducted based on the methods described by Vanhercke and co-authors in 2014 (Vanhercke et al., 2014). Detailed protocols have been described in **Supplementary File 1**.

Protein Extraction and Digestion

Proteins were extracted from three biological replicates of wholemeal flour (100 mg) in 1 mL of 8 M urea, 2% (w/v) dithiothreitol (DTT). The solution was thoroughly vortexed and sonicated for 5 min until completely mixed. Protein reduction continued on a thermomixer block, shaking at 1,000 rpm at 22°C for 45 min. The solutions were centrifuged for 15 min at 20,800 × *g* and the supernatants were used for subsequent analysis. Protein estimations were performed using the Bio-Rad microtiter Bradford protein assay (California, United States) following the manufacturer's protocol. The protein extracts were diluted in water over two dilutions (1:20, 1:40) in duplicate and measurements were made at 595 nm using a SpectraMax Plus (Molecular Devices). Bovine serum albumin (BSA) standard was used in the linear range from 0.05 to 0.5 mg/mL. The BSA standard concentration was determined by high sensitivity amino acid analysis at the Australian Proteomics Analysis Facility (Sydney, Australia). Blank-corrected standard curves were run in duplicate. Linear regression was used to fit the standard curve. Protein sample wash and digestion steps were performed as precisely described in Colgrave et al. (2016).

LC-MS/MS Data Acquisition

Protein extracts were reconstituted in 100 μL of aqueous 0.1% formic acid/10.0% acetonitrile. The peptide fractions (5.0 μL) with iRT peptides (0.5 μL; Biognosys, Zurich, Switzerland) were chromatographically separated with an Ekspert nanoLC425 (Eksigent, Dublin, CA, United States) directly coupled to a TripleTOF 6600 MS (SCIEX, Redwood City, CA, United States). The peptides were desalted on an YMC Triart C18 (12 nm, 5.0 mm × 0.5 mm) trap column at a flow rate of 15 μL/min in solvent A and separated on an YMC Triart C18 (3 μm, 120 Å, 5.0 × 0.5 mm) column at a flow rate of 5 μL/min. The injection volume was 5.5 μL for the information-dependant acquisition (IDA). The analysis method and LC-MS/MS parameters were precisely described in Colgrave et al. (2016).

SWATH-MS Data Acquisition and Library Generation

The digested protein extracts (2.5 μL; 2.0 μL of sample plus 0.5 μL of iRT peptide standard, Biognosys) were chromatographically separated as described for IDA. The MS source conditions were also identical. The TOF-MS survey scan was collected over the mass range of *m/z* 360-2000 with a 150 ms accumulation time and the product ion mass spectra were acquired over the mass range *m/z* 110-2000 with 30 ms accumulation time. Variable window SWATH ranges were determined using the SWATH variable window calculator 1.0 (SCIEX) to identify 30 optimal ranges (including 1 Da overlap) spanning *m/z* 360-2000 and resulting in a 1.1 s cycle time. Collision energy (CE) was determined using each window centre as the input *m/z* for CE equations and a CE spread of 5 eV used to allow for *m/z* variance across each SWATH window.

SWATH-MS Data Processing for Peptide Quantitation

Targeted data extraction of SWATH files was performed using the MS/MS^{ALL} with SWATH Acquisition MicroApp v2.0 plug-in for PeakView v2.2 software (SCIEX). Retention time alignment was achieved using the iRT peptides. The peptide ion library was generated by searching IDA data against the Poaceae subset of the UniProt-KB database (2017/05; appended with a custom gluten database and the iRT peptides; 1,437,912 sequences). Protein and peptide identifications were filtered at a 1% false discovery rate (FDR) during input of the search result to PeakView. The processing settings were a maximum of 100 peptides per protein with 6 transitions per peptide. The peptide confidence was set to 91% (corresponding to <1% FDR by database search), and the SWATH peak group FDR threshold was set to 1%. Subsequently, peptides were selected manually to ensure that all peptides were fully tryptic (no missed cleavages) and contained no unusual modifications (oxidation of Met and pyroglutamination of N-terminal Gln were allowed). The fragment ions used for peak area extraction were manually curated to eliminate potential interferences and ensure the correct peak was selected. A retention time width of 5 min was used with a 75 ppm extracted ion chromatogram (XIC) width. The peak areas were exported to MarkerView software (version 1.3.1) for preliminary data quality checks and exported as a data frame for further statistical analysis.

Statistical Analyses

Total fatty acids, starch, β-glucan, and triacylglycerol (TAG) content were examined to test the hypothesis that the nutrient content of BC-, CD-, and BD-mutant lines was different from

wild-type (WT) with the null hypothesis as no difference. This was tested using ANOVA followed by Tukey's test using the R statistical computing environment with differences with a corresponding $p < 0.05$ reported as significant.

Proteome analytics were performed with SIMCA (Sartorius Stedim Biotech; version 15.0), MetaboAnalyst (Xia et al., 2009), using the set of Poaceae proteins downloaded from the UniProt database (2018/03; 1,605,728 sequences). Data were pre-treated by log10 transformation and mean centring prior to analysis. Unsupervised analysis using Principal Component Analysis (PCA) was initially performed on SIMCA software to reveal any outliers and to assess any groupings or trends in the dataset. The pathway enrichment analysis was calculated using the Benjamini-Hochberg false discovery rate-adjusted p-value < 0.05 and fold change >2. Mean log2 ratios of biological triplicates and the corresponding p-values ($p \leq 0.05$) were visualised using volcano plots. One-way ANOVA with multiple comparisons correction was used to compare the median of five experimental groups depicted as violin plots using Biovinci v 1.1.4) (BioTutoring Inc., San Diego, California, United States). Gene Ontology (GO) analysis was performed in BLAST2GO (OmicsBox, Biobam) (Conesa et al., 2005).

Amino Acid Composition Change Estimation

The overall bound amino acid composition in DM lines were estimated by using the Biopython collection of tools. In this regard, sets of proteins with significantly higher or lower abundance in the mutant lines (*cf* WT lines) were provided to the ProtParam (Gasteiger et al., 2005) tool to determine percent amino acid composition for each protein within a set. The mean percent of each amino acid was then determined, and the composition of higher abundance proteins divided by the composition of lower abundance proteins. This measure is intended to provide an indication of the amino acid compositional change induced by gene knockout but does not account for protein abundance.

To investigate changes in the protein-bound amino acid composition at a protein level the individual amino acid contents were normalised against the Viridiplantae protein dataset using the Protein Report tool in CLC Genomics Workbench v12.1 (Qiagen, Aarhus, Denmark). Proteins with a lysine content of at least 1.5 times higher than the plant background data set were considered as lysine-rich proteins.

Chromosome Mapping of the Identified Proteins to the Barley Reference Genome

UniProtKB annotation of proteins with significant fold change values in any of the wild type – DM or DM – DM comparisons were reference against the barley reference genome protein IDs retrieved from EnsemblPlants (International Barley Genome Sequencing Consortium, Mayer et al., 2012). Proteins without a barley reference genome protein ID were mapped to the translated and annotated barley gene models (Hordeum_vulgare_IBSC_v2_pepall) using BLASTp (International Barley Genome Sequencing Consortium, Mayer et al., 2012). Chromosomal location and exact position of the mapped hits were collected and used to annotate the Circos plots (Yiming et al., 2018). Detailed methods for chromosomal mapping and protein-protein interaction maps were given in **Supplementary File 1**.

Ternary Plot Analysis

Protein abundance patterns in the three DMs compared to the parent lines (single-SMs and wild-type) were plotted using Ternary plot.[1] Normalised peak abundance values were used to calculate the plot parameters. Rdist was used to calculate Euclidean distances of proteins from protein abundance bias categories as described by Ramírez-González et al. (2018).

Protein-Protein Co-abundance Network Analysis

The combined set of proteins showing significant changes in any of the WT-DM or DM-DM comparisons were used to build a protein-protein interaction network in Cytoscape v 3.7.2 (Shannon et al., 2003). The network was built using the ExpressionCorrelation plugin with a 0.95 correlation value cut off. The cluster ID for proteins showing similar abundance values as defined in the hierarchical clustering was used to annotate the network and to reveal relationships between the different protein groups. NetworkAnalyzer was used to define the network measures (Assenov et al., 2008).

Promoter Motif Analysis

Non-coding sequences (1,000 base pairs long 5'-end) were extracted from the barley reference genome assembly and used for a promoter motif search analysis of BPBF transcription factor binding sites (International Barley Genome Sequencing Consortium, Mayer et al., 2012). Prolamin box (TGTAAAG and TGTAAAGT), Pyrimidine box (CTTTT), GA-MYB (AACA), GA (TAACAAA) motifs have been annotated with 100% sequence identity using CLC Genomics Workbench v12.1. The obtained annotation pattern was visualised using UpsetR in R/Shiny package Intervene (Khan and Mathelier, 2017).

RESULTS

Phenotype Measurements Across Hordein-Mutant Lines

Previous studies have shown that lines containing the Lys3 locus have larger embryos (Tallberg, 1977; Deggerdal et al., 1986; Cook et al., 2018). The embryo in the CD-mutant was the largest (65.6% increase), followed by BC-mutant (53.6% increase), while the BD-mutant was not significantly different from WT (**Figure 1**).

To measure the nutritional changes across the mutants, total fatty acid, TAG, starch content, and β-glucan were studied in detail. The CD-mutant line showed the substantial increase in total fatty acid, with an 82.2% increase as compared to the

[1] https://www.ternaryplot.com

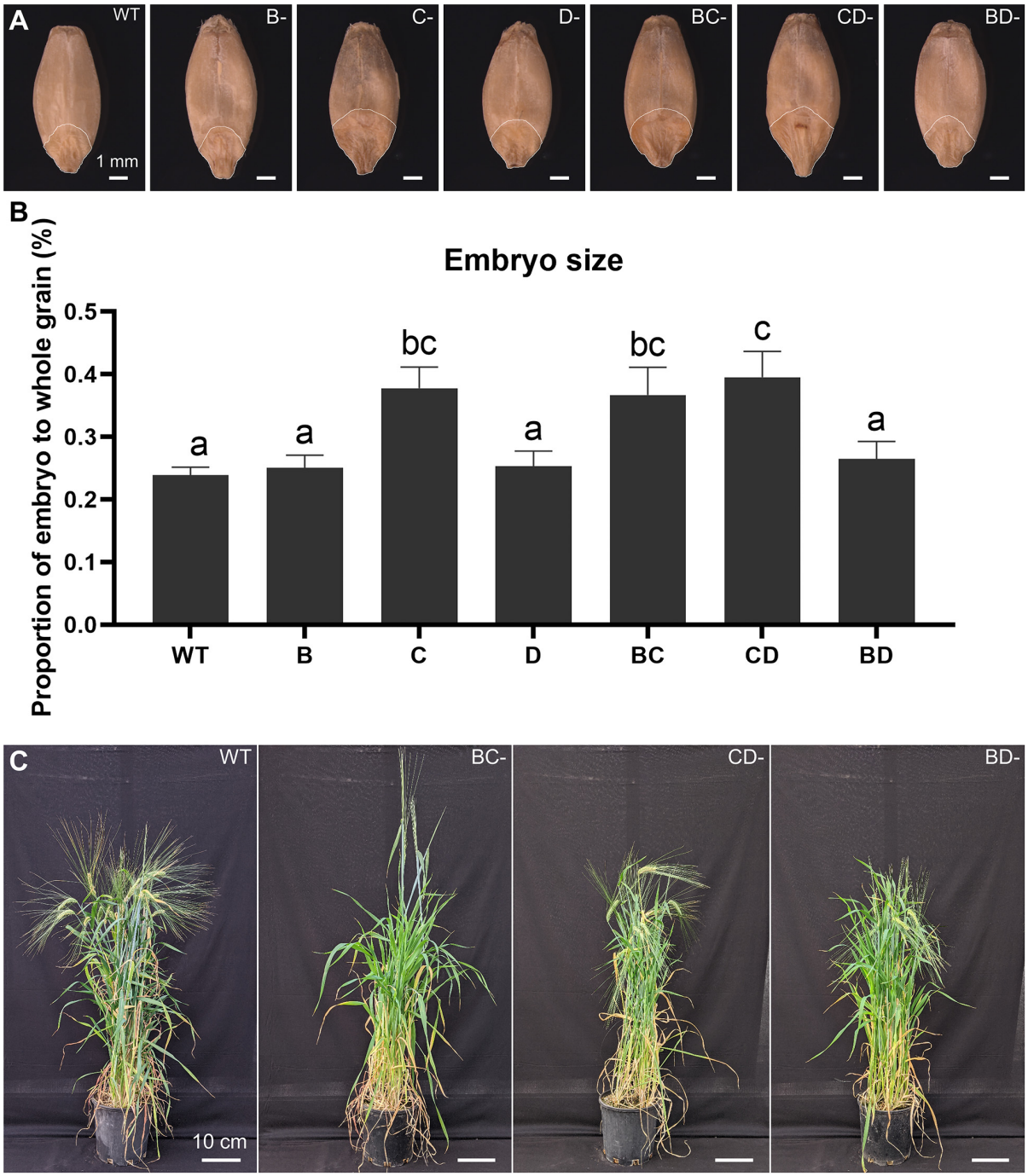

FIGURE 1 | Plant phenotypes and embryo size measurement across the WT, single- and double-mutant lines. **(A)** Grain morphologies of WT, B-, C-, D-hordein single-mutant lines and BC-, CD-, and BD-hordein double-mutant lines. The region on the grain outlined with a white line represents the embryo. Scale bar = 1 mm. **(B)** Embryo size comparison presented as mean ± standard deviation. Different letters indicate that the mean in each bar is significantly different ($p < 0.05$) using ANOVA, Tukey's HSD. **(C)** Plant morphologies of WT, BC-, CD-, and BD-hordein double-mutant lines. Scale bar = 10 cm.

WT, followed by the BC-mutant with 67.6% increase and no significant change in the BD-mutant (**Table 1**). Triacylglycerol is one of the major components in the total lipid of barley caryopsis. To investigate how the change in total fatty acid content can affect the lipid composition in the DM lines, the total TAG level was measured across all lines. The highest increase in total TAG content was observed in the CD-mutant (127.3% increase), followed by the BC-mutant (110.1% increase); however, no significant change was observed in the BD-mutant (**Table 1**).

TABLE 1 | Total content of fatty acid, TAG, starch and β-glucan of WT- and double-mutant lines.

Sample	Total fatty acid	Total TAG	Total starch content	Total β-glucan
WT	3.15(± 0.07)	1.39(± 0.20)	51.65(± 0.96)	3.29(± 0.04)
B-mutant	3.12(± 0.04)	1.47(± 0.27)	45.02(± 2.20)**	2.54(± 0.05)**
C-mutant	5.76(± 0.38)**	3.22(± 0.32)**	38.82(± 0.83)**	1.20(± 0.04)**
D-mutant	2.76(± 0.07)	1.26(± 0.18)	49.16(± 2.84)	3.36(± 0.07)
BC-mutant	5.28(± 0.04)**	2.92(± 0.35)**	38.42(± 2.60)**	1.40(± 0.10)**
CD-mutant	5.74(± 0.53)**	3.16(± 0.15)**	35.64(± 0.90)**	1.24(± 0.11)**
BD-mutant	3.47(± 0.23)	1.57(± 0.12)	42.95(± 0.90)**	2.09(± 0.07)**

*All the measurement unit for fatty acid, TAG, total starch and beta-glucan is in g/100g (Dry Weight). Mean value (n = 3); ** double asterisks represent significant difference ($p < 0.05$) with wild-type by one-way ANOVA and Tukey's HSD test. Tukey's HSD (honestly significant difference) test was used to test the hypothesis that the nutrient content of null barley line was different from wild-type with the null hypothesis as no difference (Kirk, 1969; Tukey, unpublished). Statistical analyses were conducted using R and all the results reported as significant were those with significance level of $p < 0.05$ (R Core Team, 2013).*

All three DM lines showed significant decreases in total starch content. The CD-mutant had a 31.0% reduction in total starch content, which was the highest among the three DM lines, followed by BC-mutant with a 25.6% reduction and a 16.9% reduction of total starch content in the BD-mutant (**Table 1**). The β-glucan content analysis was reduced in all three double-mutant lines. The highest reduction in β-glucan content was observed in the CD-mutant with a 61.3% reduction, followed by the BC-mutant with a 56.3% reduction and the BD-mutant with a 34.7% reduction (**Table 1**).

Establishing a Proteomic Map of the Hordein Double-Mutant Lines

To investigate the extent to which the combination of two single hordein mutants altered the proteome of the three barley DM lines, DIA-based proteome measurement was used to detect and quantify proteins across the barley lines. To this end, information-dependent acquisition enabled the identification of 2,446 proteins, which were used in the construction of a peptide ion library. The ion library was manually curated at the peptide level to remove sequences with missed cleavages and/or variable modifications such as deamidation to improve quantitative accuracy in the resultant data frame. A total of 6,138 unique peptide sequences were quantified (representing 1,907 unique proteoforms). Subsequently, the resultant data (ion, peptide and protein) were exported to MarkerView software (SCIEX) to perform an initial quality check. No unexpected outliers or stratification was observed between samples at ion, peptide and protein resolutions. As a result, the protein level data matrix was selected for further statistical and functional analyses.

A high-level assessment of proteomic similarities and differences across the barley lines was accomplished using principal component analysis (**Figure 2A**). The WT replicates clustered together in principal component 1 (PC1) and explain the largest variation of the *x*-dimension. Overall, the three-component PCA model explains ∼72% of the total variance within the dataset where 54% and 13% of the variance were modelled to PC1 and PC2, respectively.

Violin plots were generated using the protein measurements for the three biological replicates originating from individual experimental groups to evaluate the overall variation (**Figure 2B**). No significant differences were observed between WT and the BD-mutant line. However, significant protein abundance variation was observed between WT and the BC-mutant ($p < 0.009$) and the CD-mutant ($p < 0.02$) lines. Protein quantitation using the Bradford protein assay supports the variations observed in the SWATH-MS data across the experimental groups. The Bradford protein estimates the wild-type as 4.2 mg/mL of protein in extracts from a 100 mg flour equivalent (per mL of solvent). In the DM samples, the total amount of proteins presents 3.7, 2.5 and 2.7 mg/mL of proteins in the BC-, CD-, and BD-mutant lines, respectively. Notably, the protein content in the DM lines were >1.5 fold increased in comparison to SM lines (**Supplementary Table 1**). For instance, the protein content in the B- and C-mutants were 2.1 and 1.4 mg/mL, respectively; whilst upon combining the two recessive lines the protein content was 3.7 mg/mL.

Altered Proteome in DMs With *lys3*-Mutant Background Reveals Repression and Compensation Mechanisms

To further explore the proteome measurements, a volcano plot was generated to compare the protein abundance differences between WT and BC-mutant lines. The results indicate that there was alteration in 296 (15.5%) proteins wherein 151 (7.9%) proteins were more abundant in the BC-mutant line whilst 145 (7.6%) proteins were less abundant within the BC-mutant line (**Figure 3A**).

To obtain functional insights into the BC-mutant line proteome changes, the protein accessions that yielded identifications to non-barley Poaceae proteins, due to the incomplete nature of the public barley protein databases, were subjected to homology searching using BLASTp to find *H. vulgare* orthologs. The GO-based analysis revealed that molecular functions including metal ion binding, oxidoreductase activity, and enzymatic activities were increased in the BC-mutant lines (**Figure 3B**). The molecular functions associated with the down regulated proteins from the BC-mutant lines included oxidoreductase activities, enzyme activities and nutrient reservoir activity (**Figure 3B**).

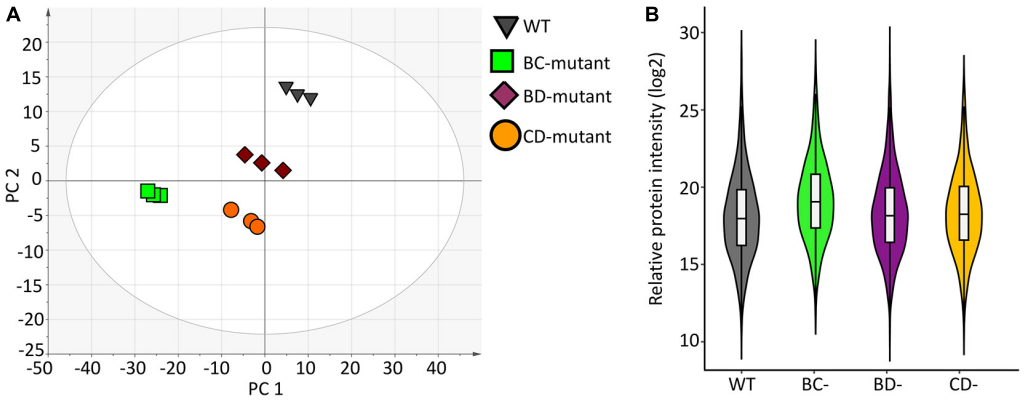

FIGURE 2 | Data structure and variance within the proteome measurement of WT and double-mutant lines. **(A)** PCA scores plot shows separation due to protein abundance variation for WT and double-mutant lines. Each symbol represents one replicate from a barley line. **(B)** Violin plot depicting protein variance from wild-type (WT) and three double mutant lines (n = 3).

The comparison between the BD-mutant line with the WT identified the perturbation of 200 (10.5%) proteins. Within these proteins, 113 (5.9%) were significantly more abundant in the BD-mutant lines whilst 87 (4.6%) proteins were less abundant (**Figure 3C**). Proteins involved in catalytic activities such as transferase, hydrolase and oxidoreductase molecular functions were more abundant (**Figure 3D**). As expected, proteins involved in nutrient reservoir activities were less abundant along with the serine-endopeptidase inhibitor activity (**Figure 3D**).

The comparison between WT and CD-mutant lines reveals the alteration of 274 (14.4%) proteins; wherein 138 (7.2%) proteins were more abundant and 136 (7.1%) proteins were less abundant (**Figure 3E**). In accordance with the other DM lines, enzymatic activities such as oxidoreductase, hydrolase, transferase, lyase and peptidase activities were more abundant along with metal ion and nucleic acid-binding (**Figure 3F**). On the other hand, proteins involved in nutrient reservoir function and serine endopeptidase inhibitors, primary metabolic pathways and enzymatic activities were less abundant (**Figure 3F**).

Pairwise Comparison Between WT and DM Lines Reveals the Link Between Parent and DM Lines

A heatmap was generated from the differentially abundant proteins identified from pairwise comparisons between WT and DM lines to visualise the link between single and DM lines. The SM proteome abundance profiles were also included in the heatmap to allow contrast to the parent lines (**Figure 4**) (Bose et al., 2020). Hierarchical clustering shows the grouping of the biological replicates and that the D-hordein mutant line is closely linked to the WT, as D-hordein proportionately represents just 1–2% of total hordein content resulting in a minimal perturbation to the proteome.

To further explore proteome, co-regulation and phenotype perturbation, the differentially abundant proteins were functionally annotated and plotted as heatmaps (**Figure 4** and **Supplementary Table 3**). The comparison between the WT and BC-mutant line was used as an example as B- and C-hordeins represent >95% of total hordein content in barley grain and thus the BC-mutant is expected to have substantial impact on the proteome compared to the remaining DM lines. **Figure 4** highlights the abundance of hordeins, fatty acid metabolism and starch metabolism-associated proteins along with lysine, methionine and tryptophan-rich proteins. The abundance of lysine-rich proteins was increased in the BC-mutant line whilst the proteins associated with nutrient reservoir functions were decreased. Proteins associated with fatty acid synthesis were more abundant (**Figure 4**). The final column illustrates the relative changes in protein abundance between the WT and BC-mutant lines, thereby revealing that the nutrient reservoir activity-related proteins were less abundant in the BC-mutant line (**Figure 4**). Proteins sharing similar abundance profiles among the DMs and their parents clustered into 12 modules (**Supplementary File 1**). Module 1 is composed of 13 proteins and is enriched in C- and γ-hordeins and avenin-like proteins (ALPs). Additionally, B-hordeins are clustered in module 4 along with 12S seed storage globulin while D-hordein are in module 12. Module 4 includes 24 proteins that are either BD-dominant or balanced when comparing the three DMs. Proteins involved in starch and carbohydrate metabolism are clustered in module 4, 5, and 6 encompassing 24, 24, and 51 proteins, respectively. The largest module, module 9 is composed of 161 proteins that are enriched under energy and carbohydrate metabolism functions. Module 11 is enriched in proteins related to protein processing in the endoplasmic reticulum with the abundance of these proteins mostly balanced between the DM and WT.

A supervised Orthogonal Projections to Latent Structures Discriminant Analysis (OPLS-DA) model was built to identify how the SM parent lines contribute to the alteration of DM lines. Therein, the WT, B-, and C-mutant lines stratified in class 1 space while the BC-mutant line stratified in the class 2 space. Next, the analysis of VIP (Variable Importance in Projection) plot allowed the identification of the top 100 most influential proteins (VIP > 1.2), which were altered in their abundance in the BC-mutant line when compared to WT, B-, and C-mutant lines (**Supplementary Figure 1** and **Supplementary Table 3**). To determine the magnitude of proteome perturbation, the mutant

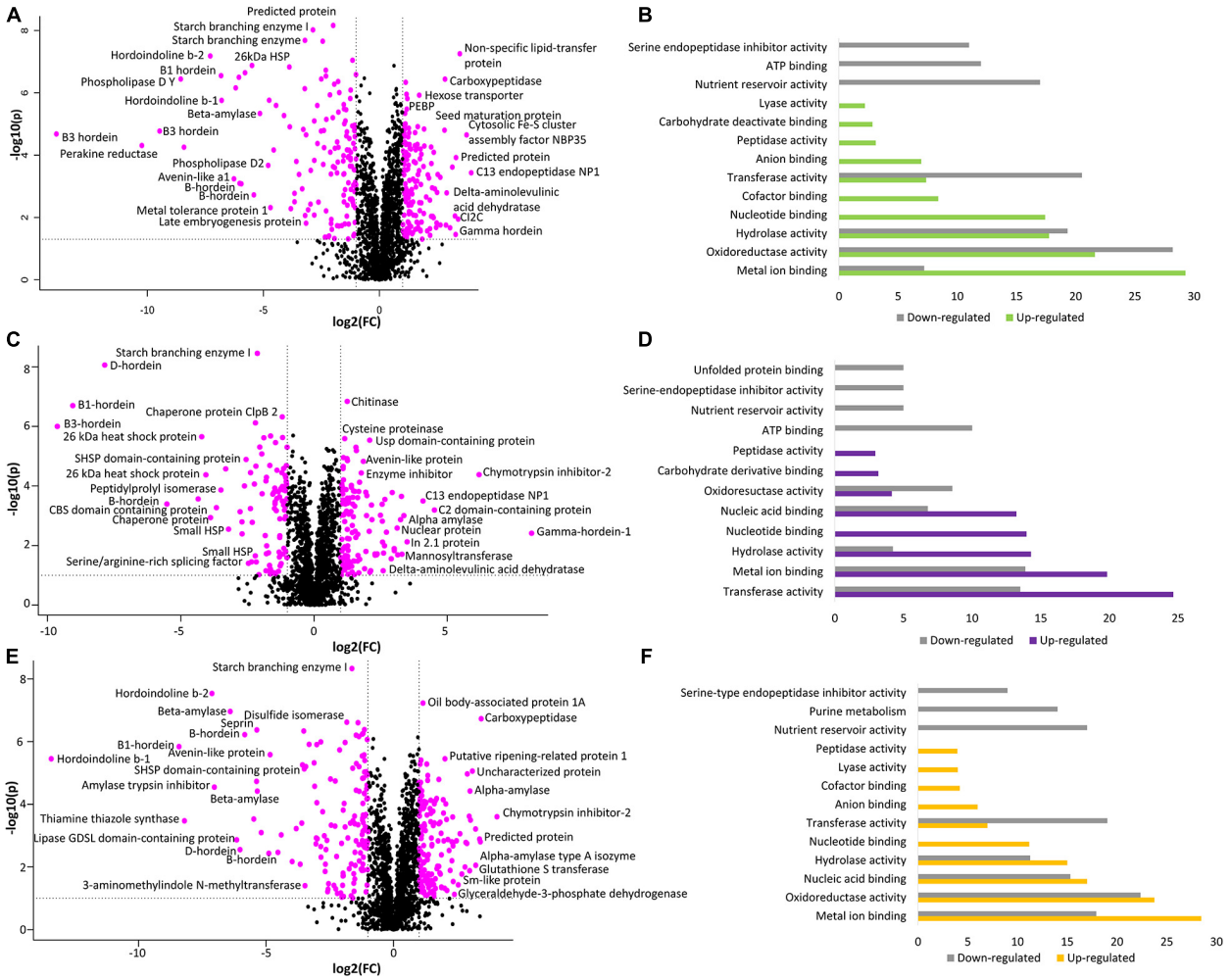

FIGURE 3 | The comparison between WT and double-mutant lines illustrates the alteration of protein abundances and their associated functional classes. **(A)** Volcano plot of fold-change vs. p-value for comparison of BC-mutant and WT lines. **(B)** GO analyses (molecular function) performed on perturbed proteins: increased (green) or decreased (grey) in the BC-mutant line relative to WT. **(C)** Volcano plot of fold-change vs. p-value for comparison of BD-mutant and WT lines. **(D)** GO analyses (molecular function) performed on perturbed proteins: increased (purple) or decreased (grey) in the BD-mutant line relative to WT. **(E)** Volcano plot of fold-change vs. p-value for comparison of CD-mutant and WT lines. **(F)** GO analyses (molecular function) performed on perturbed proteins: increased (orange) or decreased (grey) in the CD-mutant line relative to WT. The pink points in the volcano plots represent proteins with significant perturbation ($p < 0.05$; FC < 0.5 or FC > 2.0).

lines were compared with the WT (**Supplementary Figure 1**). The proteins with perturbed abundance in the BC-mutant line was highly concordant with the changes observed in the parent B- and C-hordein mutant lines (Bose et al., 2020). Additionally, the *lys3* mutant, *i.e.,* removal of C-hordein, had a dominant influence on the proteome in the BC-mutant line (**Supplementary Figure 1**).

Alteration of Amino Acid Compositions in Barley DM Lines

To measure the amino acid composition changes between WT and DM lines, the lists of differentially abundant proteins were collected from the pairwise comparative analysis (**Supplementary Table 3**). One essential (His) and three non-essential amino acids (Ala, Gly, and Tyr) were significantly increased in the DM lines. As expected, glutamine and proline were significantly decreased by up to 47% and 15% in the prolamin-depleted BC- and CD-mutant lines, respectively, but not in the BD-mutant line. Interestingly, essential amino acids such as lysine were found to be most abundant in the BC-mutant line, while proline was significantly decreased (**Supplementary Figure 2**). In accordance with the current finding, previous study has also shown that the incorporation of mutant lines significantly increased the free amino acids (Tanner et al., 2015).

Ternary plots were used to explore the abundance patterns of proteins in the DMs and their relationship with each other or their parent mutant lines across the three double-mutant lines (**Figure 5** and **Supplementary Figure 3**). Two of the B-hordeins (I6TMW0 and A0A0K2GRQ1) have a balanced abundance when

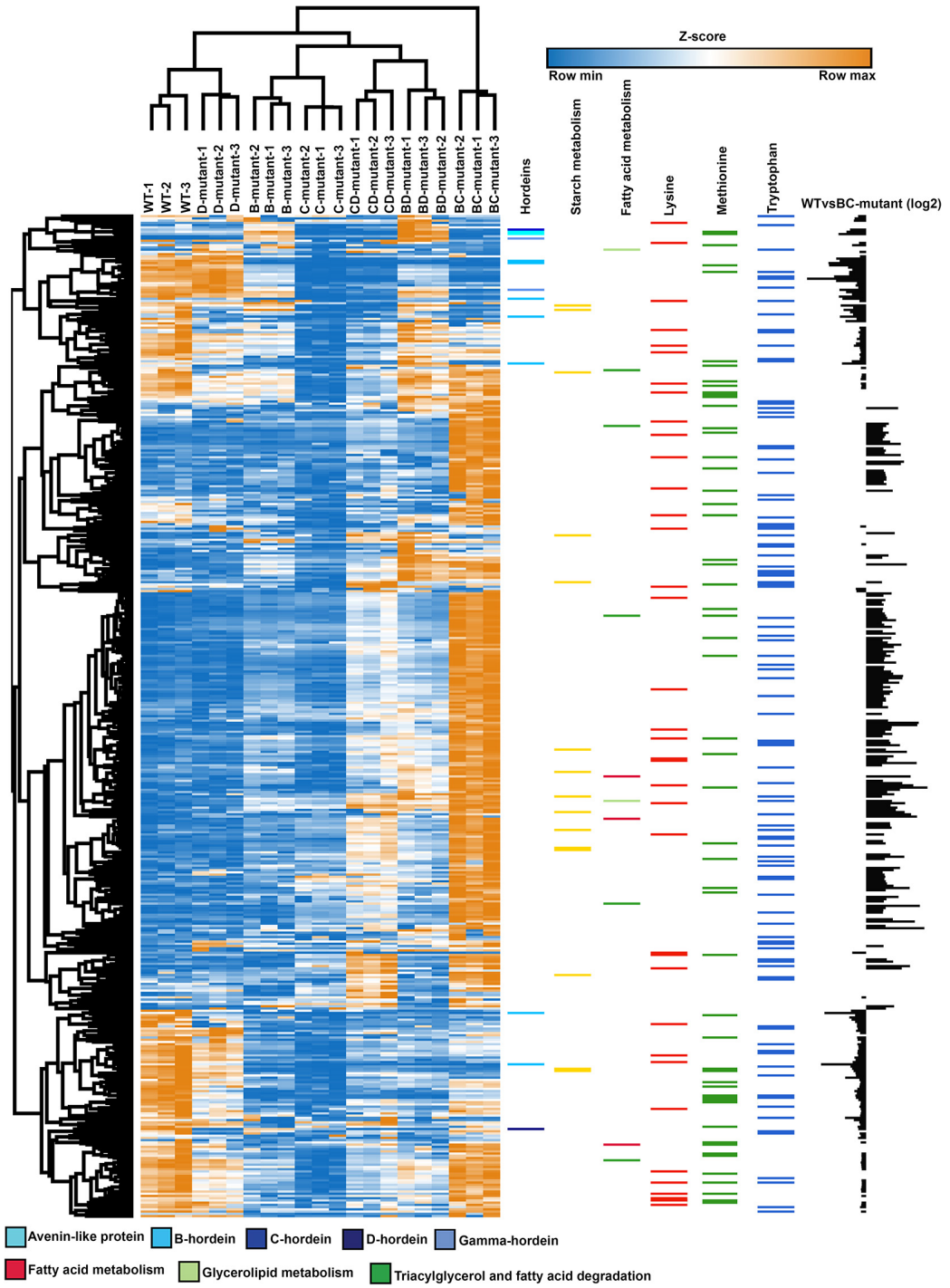

FIGURE 4 | Abundance profile of the chromosome mapped and differentially abundant proteins across the WT, single- and double-mutant lines. Heatmap showing the relative abundance levels (Z-scored) of proteins across the single and double-mutant barley lines in comparison to WT. Colour bars represent the abundance of hordeins, starch and fatty acid metabolism, lysine, methionine, and tryptophan-rich proteins. The individual amino acid contents were calculated using the Protein Report tool in CLC Genomics Workbench. The bar chart (last column) illustrates the log2 abundance of differentially abundant proteins in the WT and BC-mutant lines.

the three DMs are compared (**Supplementary Figure 3A**), while other B-hordeins as well as gamma- and C-hordeins show a relative enrichment in the BD-mutant compared to the BC- and CD-mutant lines. However, these proteins show a balanced abundance when BD- is compared to D- and WT indicating that B-hordeins with a higher abundance value in the

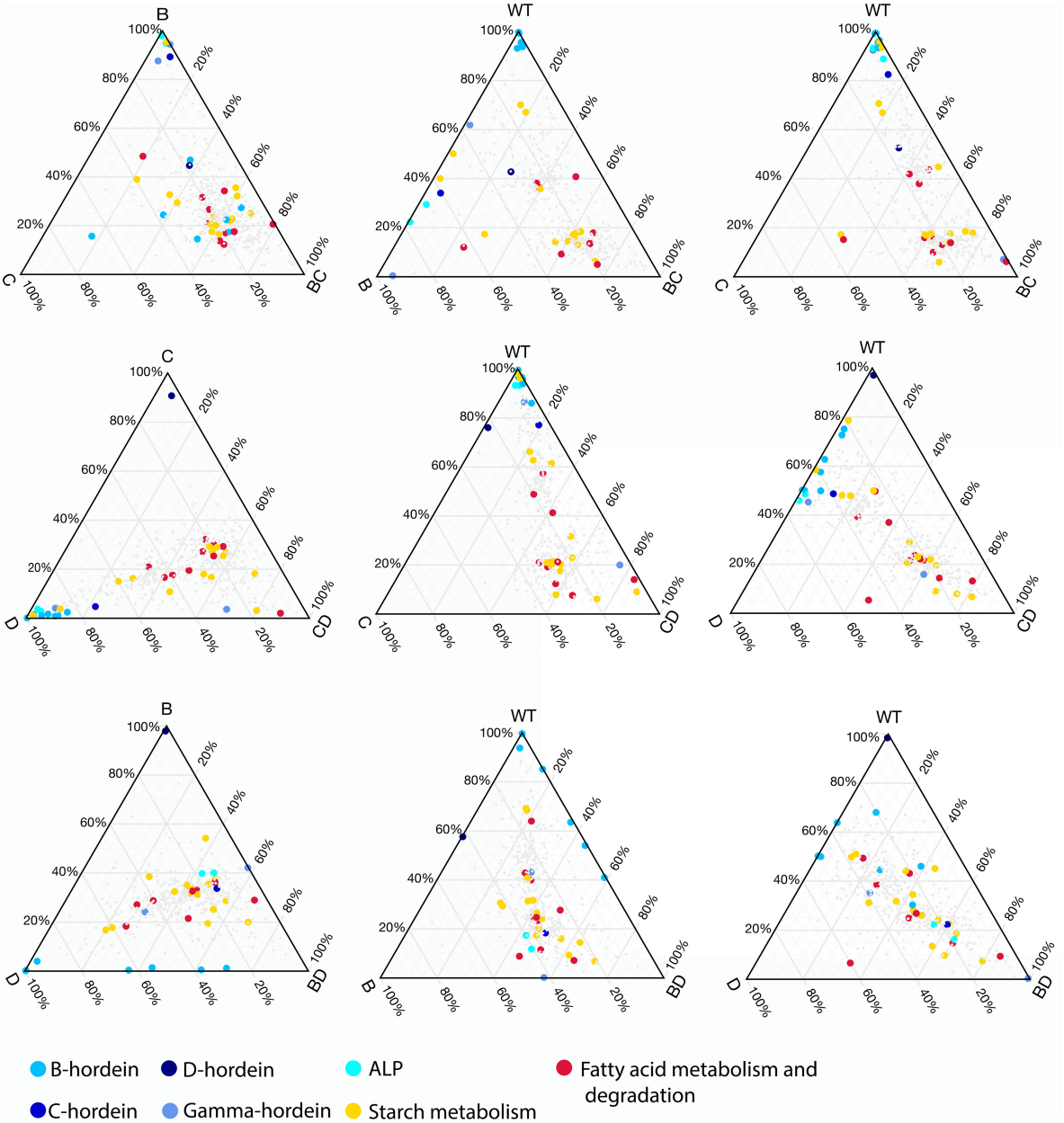

FIGURE 5 | Changes in relative abundance patterns in the double-mutant and parent lines. Ternary plots were constructed to highlight relative abundance differences between DMs, SMs, and WT. For each DM three plots are presented representing DM and SM relationships followed by DM, WT relationships combined with the presence of one of the SM parents. The colours highlight the different hordeins, starch metabolism, fatty acid metabolism and degradation associated proteins.

BD-mutant line might be inherited from the D-hordein mutant parent (**Figure 5**). Comparing the relative distribution of the fatty acid metabolism-related proteins in the three DMs compared to their parents, most of the fatty acid metabolism-related proteins show a balanced abundance in the DMs with a D-hordein mutant in the background. However, these proteins are relatively enriched in the BC-mutant when compared to the WT or any of the single mutant parents. Comparing the relative abundance of starch metabolism related proteins, they are depleted in the DMs with the C-hordein mutant parent in the background; however, they show a balanced abundance if B- or D-hordein mutant lines are present.

Altered Proteins From the Double-Mutant Lines Indicate Orchestrated Changes in Nutrient, Starch, and Fatty Acid Metabolism

To elucidate the effect of protein alteration at the chromosome level, hordeins and proteins showing significant changes in

abundance were mapped to the Morex barley reference genome (International Barley Genome Sequencing Consortium, Mayer et al., 2012). Gamma-, B-, and C-hordein sequences were mapped to the short arm of chromosome 1H and clustered in five loci, representing two B-hordein, two C-hordein and a gamma-hordein loci (**Supplementary Figures 3B,C**). Detailed annotation of mapped protein sequences including their chromosomal position is presented in **Supplementary Table 2**.

B-hordeins located in the B hordein locus 1 (**Supplementary Figures 3B,C** and **Supplementary Table 2**) share similar abundance patterns with starch branching enzyme I mapped to the unassigned chromosome (Chr Un), protein folding-related heat-shock proteins and chaperones from chromosomes 1H, 5H, 4H, and 6H (**Figure 6**). Two of the B-hordeins, R9XWE6 and C7FB16 were found in higher amounts in the D-hordein mutant compared to the B- and C-hordein mutant lines, and were enriched in the BD-mutant compared to the BC- and CD-mutants, sharing opposite abundance patterns to energy metabolism proteins (e.g., M0WGK7, M8C3P1, M0Y565). The C-hordein I6TEV8 shared highly similar abundance patterns to ALPs from chromosome 7H and the gamma-hordein in 1H. The C-hordein was higher in abundance in the BD-mutant line when compared to the other DMs and was a dominant protein in the WT (**Figure 6**).

Proteins with functions in fatty acid degradation shared similar abundance trends with many of the lysine-rich proteins such as LEA proteins (C9ELM9, B5TWD1, F2DZK3) from chromosomes 7H, 1H and 6H. Proteins linked to fatty acid metabolism (F2CWX3 and W5BXE7) were associated with proteins enriched in lysine, methionine or threonine, such as disease defence proteins and seed maturation-related proteins mainly located at chromosomes 1H, 3H and 5H.

Starch metabolism associated links have been identified between chromosomes 3H, 4H, 6H and 7H. Among the proteins with highly similar abundance patterns there were 25 lysine-rich proteins. Some of these, like a seed maturation-related dehydrin (Q40043), an energy metabolism related glyceraldehyde-3-phosphate dehydrogenase (M0Y565) and a protein with unknown function (M0YTG0) show a strong negative correlation with the B-hordeins enriched in DMs with a D-hordein mutant origin, while a calreticulin (M0V198), a HSP90 protein (M0 × 173), a chaperone and a calcium-binding protein were positively correlated.

To further investigate the co-abundance relationships between lysine-rich proteins and hordeins and other cysteine-rich prolamin superfamily members, 1,000 bp non-coding promoter regions of the coding genes of mapped proteins were searched for transcription factor binding sites characteristic of BPBF (Prolamin-box with a DOF core motif, Pyrimidine-box and GAMyb motif). Twenty-three of the mapped lysine-rich protein coding genes contain both the pyrimidine box and a DOF core motif in their sequence within the first 1,000 nucleotide upstream of the start codon (**Supplementary Figure 4** and **Supplementary Table 2**). Comparing the promoter motif composition of proteins from the various modules shows potential negative interactions between proteins with Pyr-GAMyb and Pyr-Pbox or Pyr-Pbox and Pyr-Pbox-GAMyb TFBS containing promoter regions. While interacting partners from the energy, fatty acid and carbohydrate metabolism module 6, 9 and 10 that show similar positive abundance trends mostly have Pyr-GAMyb and Pyr-GAMyb or Pyr-Pbox-GAMyb TFBSs. Modules enriched in storage proteins (module 1, 3, and 4) and ER-acting, folding and ripening-related proteins are characterised with the presence of Pbox motifs either in a combination with Pyr-box or with Pyr-box and GAMyb motifs (**Supplementary Table 2**).

DISCUSSION

The temporal and spatial regulation of cereal storage protein synthesis is orchestrated by precise mechanisms primarily at the transcription level. High resolution genome sequences and gene model annotations help to understand, utilise and process the genomic information characteristic of seed development and maturation programmes. The suppression of three hordein subclasses B, C, and D within the barley SM lines led to multiple repression and compensation events. These events are further evident in the double-recessive lines where the compensation events more clearly depend on their parent lines (**Figures 5**, **6** and **Supplementary Figure 1**). Additionally, the incorporation of mutant lines significantly affects the free amino acids (Tanner et al., 2015) and bound amino acids analysed in the present study (**Supplementary Figure 2**).

The positions of the hordein coding genes in chromosome 1H were determined using the available barley hordein sequences. In the Morex reference genome both the B-hordeins and the C-hordeins are clustered into two separate loci (**Supplementary Figure 3B**). Most of the B-hordein coding proteins are located in the B-hordein locus 1 (2.43 – 3.30 Mb), while some additional B-hordein coding genes were mapped to the 11.86 – 11.96 Mb region. In the B-hordein mutant line the γ-ray induced mutation deleted ∼85 kb of the storage protein enriched distal 1H end and eventually caused the depression in hordein accumulation (∼75%) in the grain endosperm (Shewry et al., 1980; Kreis et al., 1983). The B-hordeins from both B-hordein loci are significantly less abundant in the BC-mutant line compared to the WT while a slight compensation can be seen in some of the B-hordein abundance values both in the BC- and BD-mutant lines (**Supplementary Figures 3A,B**). This provides evidence that the proteins I6TMW0 and Q40022 might be inherited from the C and D single mutant parent in the BC- and BD-double mutant lines. Due to incomplete deletion of B-hordein locus, and the existence of a variety of hordein gene models mapped to the chromosome 1H (**Supplementary Figure 3B**), it is possible that the B-mutant line, Risø 56, carries additional hordein coding regions of which gene products were not detected herein. The remaining B-hordein-type proteins are evident in the B-mutant parent line where a hordein closely related to B-hordein subclasses was increased up to ∼8 fold (Bose et al., 2020) as well as two low molecular weight B-hordeins (C7FB16, R9XWE6) from the B-hordein locus 2 in the BD-double mutant line (**Figure 5** and **Supplementary Figure 3B**). Notably, the deletion of the major B-hordein locus did not affect the C-hordein locus. As a result of B-hordein removal, the total

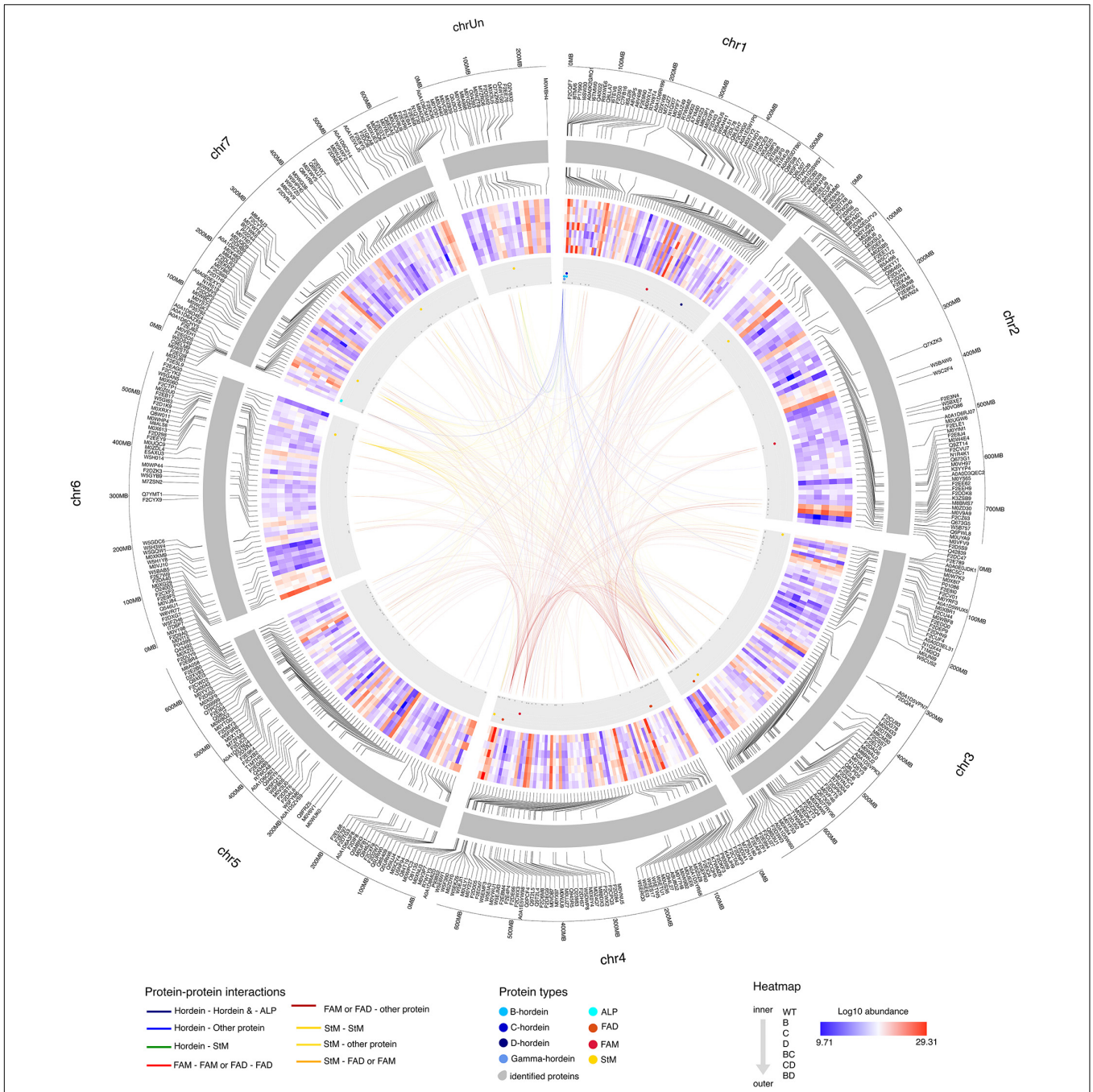

FIGURE 6 | Protein-protein interaction patterns of highlighted hordeins, fatty acid metabolism and degradation and starch metabolism associated proteins. Chromosomes are visualised in the outer circle as grey bands. Mapped proteins showing significant fold-changes compared to the WT are labelled with accession numbers. Log2 protein abundance values are presented in the heat map section. The direction of samples indicated from the inner to the outer circle as WT, single mutants B-, C-, and D-, double-mutants BC-, CD-, and BD-, respectively. The position of hordeins and the highly related avenin-like proteins are shown as blue dots in the grey annotation band, fatty acid metabolism and fatty acid degradation associated proteins are highlighted in red and deep red colours, while orange dots represent proteins related to starch metabolism. Links between chromosome regions represent potential interactions. Only correlations above 0.95 (strong positive) and below -0.95 (strong negative) are highlighted. Interactions are coloured to indicate the interactor types.

abundance of C-hordein and γ-hordein were shown to increase, possibly to compensate for the loss of B-hordeins. Interestingly a clear positive interaction was detected between the abundance patterns of C-hordeins, γ-hordeins and some ALPs encoded on the short arm end of chromosome 7H (**Supplementary Figure 3C**). ALPs represent a protein subgroup within the prolamin superfamily that, similarly to gliadins, possess gliadin Pfam domains (PF13016) (Juhász et al., 2018). These proteins

were reported to have both storage protein functions and are also involved in stress defence mechanisms (Zhang et al., 2018a,b).

In cereals, *lys3* encodes a transcription factor known as prolamin binding factor (PBF), located on the long arm of chromosome group 5 in wheat and 5H in barley, which express in the starchy endosperm, embryo and the aleurone during seed development and germination (Marzábal et al., 2008; Moehs et al., 2019). PBF acts as an activator or repressor through some known transcription factor binding site domains like the TGTAAG (Prolamin box and Pyrimidine-box (CCTTTT) (Shewry et al., 1995; Marzábal et al., 2008). In the developing seed PBF negatively regulates the GA-responsive production of thiol proteases, α-amylases, proteases, hydrolases and acts as an activator for the prolamin genes as well as genes involved in starch accumulation. PBF triggers storage protein and starch accumulation primarily by activating genes through the Prolamin-box, while in embryo-related genes and especially during germination it relates to gibberellic acid (GA) signalling and acts through the Pyrimidine box. The Pyrimidine box is usually part of the GARC triad (GA responsive complex of GAMyb + PBF + GA response factors) and is enriched in aleurone- and endosperm-related genes (Mena et al., 2002). The *lys3* mutant Risø 1508 has regulatory impact on a wider range of biochemical processes in addition to hordein synthesis (Orman-Ligeza et al., 2020). Indeed, the decrease in lysine-poor storage protein accumulation and starch content in the grains of *lys3* mutant plants lead to more lysine-rich proteins and free lysine (Ingversen et al., 1973). Generally, this loss of PBF TF activity is concomitant with an above average embryo size (Cook et al., 2018). Herein, stereomicroscope measurements show a significantly higher embryo size in the BC- and CD-double mutants providing evidence for the presence of an active PBF gene in the BD-mutant line that show similar embryo size to the WT (**Figure 1**).

Notably, an impact on embryo size was previously observed for the parental hordein SM lines used in this study (Bose et al., 2020). Herein, the double-mutant lines display repression of B- and C-hordeins resulting in a shift to an increased proportion of lysine-rich proteins such as seed folding and maturation related proteins, including 60S ribosomal proteins, LEA proteins, chymotrypsin inhibitors and serpins (**Figure 3** and **Supplementary Figure 1**). In maize, the overexpression of elongation factor 1α (EF 1α) in the endosperm regulates the higher production of lysine-rich proteins (Habben et al., 1995). Similarly, here, a 60S acidic ribosomal protein with a translation elongation activity (M0XWV5) was measured to be >5-fold higher in the BC-mutant line in comparison to WT (**Supplementary Table 3**). This protein co-clustered with the energy metabolism and fatty acid metabolism associated proteins in module 9. In the endosperm, EF 1α can be found in the protein bodies where they have been associated with the cytoskeleton, bind to the endoplasmic reticulum, couple with the mitotic apparatus and several microtubules (Durso and Cyr, 1994). The cytoskeleton plays a key role in storage protein synthesis in cereal grains through their association with the rough endoplasmic reticulum membrane surrounding the protein bodies (Shewry et al., 1995; Bose et al., 2020). Thus, it is possible that the EF 1α concentration provides an index of a complex group of proteins making up the cytoskeleton that helps to redistribute nitrogen away from the normal sink in order to increase non-storage proteins.

Previous morphological and phenological studies have shown that the *lys3* mutation influences aleurone cell size, starch granule formations, β-glucan content, seed germination rate and fatty acid content (Arruda et al., 1978; Deggerdal et al., 1986; Christensen and Scheller, 2012; Moehs et al., 2019; Orman-Ligeza et al., 2020). In this study, all DM lines displayed a reduced total starch content. In the BC- and CD-mutant lines, the large embryo phenotype results in a corresponding reduction of starchy endosperm. As this is the major storage tissue for starch in seed (Duffus and Cochrane, 1993; Radchuk et al., 2009), the reduction in this compartment likely corresponds to the reduced total starch content of the seed. However, the embryo size of the BD-mutant line is unchanged, therefore, the total starch content may be affected by factors other than the embryo starchy endosperm proportion. Therefore, it is highly likely that the combination of D-hordein mutant with the B- and C-hordein mutant lines activates the starch and storage protein accumulation or regulates the starch and B- and C-hordein contents.

In barley *lys5* mutants, the starch synthesis was reduced due to the lesions of *Hv.Nst1* genes located on chromosome 6, which encodes a plastidial ADP-Glc transporter (Patron et al., 2004). Herein, an ADP-Glc transporter protein (Q6E5A5) located in chromosome 7H was shown to have no significant changes in the single- and double-mutant lines (**Supplementary Table 2**). Although *lys5* mutants have decreased starch content, the major component of cell wall (1,3;1,4)-β-D-glucan was increased due to higher concentration of cytosolic UDP-Glc (Rudi et al., 2006; Christensen and Scheller, 2012). Yet, in the *lys3* mutants the (1,3;1,4)-β-D-glucan content was reduced 1,000-fold due to the repression of *Cellulose Synthase-Like* (CSL) *F6* transcript throughout the endosperm development period (Christensen and Scheller, 2012). In this study, the β-glucan [(1,3;1,4)-β-D-glucan] content in BC- and CD-mutant lines was reduced. This indicates that *lys3* transcriptional regulation from C-hordein mutant lines can regulate *CSLF6* expression in double mutant lines to reduce the β-glucan content. Although CSLF6 was not detected herein, other genes related to β-glucan metabolism were perturbed. Q8S3U1 is a β-1,3-glucanase II and Q9XEI3 a β-D-glucan exohydrolase isoenzyme, both functioning in β-glucan degradation, were significantly increased in all three double-mutants. These β-glucan-related proteins show negative concordance with a range of fatty acid metabolism and lysine-rich proteins in the DMs with a *lys3* mutant parent. Of interest, the abundance pattern of these β-glucan metabolism-associated proteins is similar in all three double-mutants with the highest abundance in the BD-mutant line, which cannot be explained by the mutation in the PBF gene. Quantitative trait loci linked to β-glucan content in wheat were found on chromosomes 1A, 2A, 2B, 5B, and 7A (Marcotuli et al., 2016). Among these, a glycosyl transferase is located in the short arm end of chromosome 1H in a relatively close proximity to the hordein loci. It is therefore possible that this protein is inactive or suppressed in the mutant lines with B-mutant in the background resulting in a decrease

of β-glucan content. Additionally, it may also possible that the *CSLF6* repression results from the hypermethylation of the upstream promoter region of the *lys3* mutants, as this promoter is shared among these genes.

Unlike starch, the total fatty acid (FA) and TAG content was increased in the BC- and CD-mutant lines and their abundance can be directly linked to the *lys3* mutant, *i.e.,* C-hordein-mutant line (**Figure 1**). In this barley *lys3* mutant, three intermediates of lipid metabolism, including 2-hydroxyheptanoate, 9,10-dihydroxy-octadecanoic acid methyl ester and dimethyl ester of threo-9,10-dihydroxy-octadecanedioic acid, were found to be more abundant (Khakimov et al., 2017). This mutant may use excess lysine to convert to acetyl-CoA and thus provide more precursors for fatty acid synthesis leading to increased abundance of FA and TAG. Additionally, seeds may use these excess reserves as an energy supply to exit dormancy and initiate germination. The *Lys* mutation also influences the accumulation of Lys-rich proteins in the BC and CD DMs; abundant protein functions were associated with protein translation, folding and seed maturation. The abundance of the *Lys*-rich *late* embryogenesis abundant (LEA) protein in the *Lys* mutants are known to provide desiccation tolerance and co-regulated with abscisic acid to extend the dormancy period (Tan and Irish, 2006; Angelovici et al., 2009). The higher abundance of lysine-rich LEA proteins and dehydrins combined with reduced TCA cycle metabolism offers some explanation regarding the low germination success and reduced growth vigour for *lys3* mutants.

CONCLUSION

Cereals are lower in grain protein content and essential amino acids such as lysine compared to legumes and oilseeds. Selectively breeding cultivars with more desirable amino acid composition has been attempted in cereal grains to improve the nutritional quality for human and livestock consumption. Yet, the low agronomic yield, germination defects and technological challenges for cereals have presented barriers for the commercial uptake of these crops. Within the DM lines measured herein, the BC-mutant lines are more suitable for those suffering with celiac disease. The D-hordeins, homologs of the wheat high molecular weight glutenins, have only shown a mild immune response for the patients with HLA-DQ8 (Molberg et al., 2003) and even less immune-reactivity for patients with HLA-DQ2 alleles. The accumulation of HMW glutenins are not affected in wheat PBF mutant lines (Moehs et al., 2019), and similar results were obtained in the present study for D-hordeins. Therefore, the reduction in hordein content, improvement in amino acid composition, while concomitantly maintaining desirable agronomic and functional characteristics through this DM line, offers a promising step toward production of a grain with desirable health and commercial traits.

DATA AVAILABILITY STATEMENT

The original contributions presented in the study are publicly available. This data can be found here: The mass spectrometric DDA and DIA raw data and result files have been uploaded to the CSIRO public data access portal. Data can be accessed through: https://doi.org/10.25919/5d5c83eb2e6dc.

AUTHOR CONTRIBUTIONS

UB and AJ analysed the dataset and prepared the first draft. RY performed phenotype analysis. MBa annotated the proteomics dataset. KB prepared proteomics samples and reviewed the manuscript. MBl performed the plant breeding and flour sample preparation. JB analysed the amino acid profiles and reviewed the manuscript. MC acquired the LC-MS dataset. MC and CH conceived the project idea and critically reviewed the manuscript. All authors contributed to the article and approved the submitted version.

FUNDING

UB was supported by a Research Plus Postdoctoral Fellowship from CSIRO. MBa was supported the Australian Government Research Training Program (RTP) Scholarship.

SUPPLEMENTARY MATERIAL

The Supplementary Material for this article can be found online at: https://www.frontiersin.org/articles/10.3389/fpls.2021.718504/full#supplementary-material

Supplementary Figure 1 | Abundance profile of the 100 differentially abundant proteins across the WT, B-, C-, and BC-mutant lines. Heatmap showing the relative abundance levels (Z-scored) of significant altered proteins across the lines. Colour bars represent the abundance of proteins associated with GO functions such as fatty acid synthesis, nutrient reservoir and inhibitory activity. The bar charts (last three column) shows the log2 abundance of differentially abundant proteins in the WT and B-, C-, and BC-mutant lines.

Supplementary Figure 2 | Protein bound amino acid composition changes between double-mutant and WT lines. Amino acid composition was determined for proteins significantly perturbed by hordein deletion and expressed as a fold-change for the composition of proteins that are more abundant in mutant lines divided by the composition of proteins that are more abundant in the WT. These fold change values were log2 transformed for symmetry in the heat map where darker red indicates higher abundance in the mutant line and darker blue indicates higher abundance in the WT. Essential amino acids are indicated by black row side colouring.

Supplementary Figure 3 | (A) Ternary plot representing relative abundance comparison of the three DMs. Abundance bias categories highlighting DM dominant, DM suppressed and balanced abundance are presented. **(B)** Ternary plot highlighting relative abundance values of the analysed hordeins. Mapped hordein locus positions are also labelled. **(C)** Genomic location of barley hordeins indicate the presence of multiple B- and C- hordein loci on the short arm of chromosome 1H as identified using publicly available hordein sequences mapped to the barley reference genome. The position of identified genes is labeled by circles and is differentiated for each hordein type using the colours presented in the colour legend. The first C-hordein locus is located at 1.45 Mb and is composed of at two C-hordein genes. This locus is followed by the gamma-hordein locus at 1.75 Mb and is composed of at least of three gamma-hordein genes. The B hordein locus 1 spans between 2.52 and 3.25 Mb and includes 11 gene models. The second C-hordein locus covers a 200 kb

region between 11 and 11.2 Mb and includes nine C-hordein gene models. This gene cluster is followed by further two B-hordein genes at 11.95 Mb. In the proteomic analyses of the double-mutants we have identified two hordein sequences from the gamma hordein locus, six hordein sequences in B-hordein locus 1, two sequences in the C-hordein locus 2 and two sequences in the B-hordein locus 2. The position of identified proteins were labelled in coloured dots.

Supplementary Figure 4 | Enrichment of Prolamin box variants (TGTAAAGT, TGTAAAGG, TGAAAAGT, TGAAAAGG, TGTAAAG), DOF-core motif (A/TAAG) and Pyrimidine-box (CCTTTT) motifs.

Supplementary Table 1 | Hordein content of WT and hordein-single and DM lines.

Supplementary Table 2 | Detailed annotation of mapped protein sequences including their chromosomal position.

Supplementary Table 3 | Differentially abundant proteins were functionally annotated and plotted as heatmaps.

Supplementary File 1 | Detailed materials and methods for embryo size measurement, barley β-glucan analysis, total starch content analysis, total fatty acid, and total TAG content analysis and circus plot.

REFERENCES

Angelovici, R., Fait, A., Zhu, X., Szymanski, J., Feldmesser, E., Fernie, A. R., et al. (2009). Deciphering transcriptional and metabolic networks associated with lysine metabolism during *Arabidopsis* seed development. *Plant Physiol.* 151, 2058–2072. doi: 10.1104/pp.109.145631

AOAC (1995). Starch (total) in cereal products, amyloglucosidase—α—amylase method 996.11. *J. Assoc. Off. Anal. Chem.* 55–58.

Arruda, P., Da Silva, W., and Teixeira, J. (1978). Protein and free amino acids in a high lysine maize double mutant. *Phytochemistry* 17, 1217–1218. doi: 10.1016/s0031-9422(00)94558-8

Assenov, Y., Ramírez, F., Schelhorn, S.-E., Lengauer, T., and Albrecht, M. (2008). Computing topological parameters of biological networks. *Bioinformatics* 24, 282–284. doi: 10.1093/bioinformatics/btm554

Batterham, E. S. (1992). Availability and utilization of amino acids for growing pigs. *Nutr. Res. Rev.* 5, 1–18. doi: 10.1079/nrr19920004

Bose, U., Broadbent, J. A., Byrne, K., Blundell, M., Howit, C. A., and Colgrave, M. L. (2020). Proteome analysis of hordein-null barley lines reveals storage protein synthesis and compensation mechanisms. *J. Agric. Food Chem.* 68, 5763–5775.

Christensen, U., and Scheller, H. V. (2012). Regulation of (1, 3; 1, 4)-β-d-glucan synthesis in developing endosperm of barley lys mutants. *J. Cereal Sci.* 55, 69–76.

Colgrave, M. L., Byrne, K., Blundell, M., Heidelberger, S., Lane, C. S., Tanner, G. J., et al., (2016). Comparing multiple reaction monitoring and sequential window acquisition of all theoretical mass spectra for the relative quantification of barley gluten in selectively bred barley lines. *Anal. Chem.* 88, 9127–9135. doi: 10.1021/acs.analchem.6b02108

Conesa, A., Götz, S., García-Gómez, J. M., Terol, J., Talón, M., and Robles, M. (2005). Blast2GO: a universal tool for annotation, visualization and analysis in functional genomics research. *Bioinformatics* 21, 3674–3676. doi: 10.1093/bioinformatics/bti610

Cook, F., Hughes, N., Nibau, C., Orman-Ligeza, B., Schatlowski, N., Uauy, C., et al. (2018). Barley lys3 mutants are unique amongst shrunken-endosperm mutants in having abnormally large embryos. *J. Cereal Sci.* 82, 16–24. doi: 10.1016/j.jcs.2018.04.013

Deggerdal, A., Klemsdal, S., and Olsen, O. A. (1986). The effect of the high lysine genes of the barley mutants Risø 1508 and 527 on embryo development. *Physiol. Plant* 68, 410–418. doi: 10.1111/j.1399-3054.1986.tb03374.x

Doll, H. (1973). Inheritance of the high-lysine character of a barley mutant. *Hereditas* 74, 293–294. doi: 10.1111/j.1601-5223.1973.tb01131.x

Duffus, C., and Cochrane, M. (1993). "Formation of the barley grain-morphology, physiology, and biochemistry," in *Barley: Chemistry and Technology*, eds A. W. Macgregor and R. S. Bhatty (Madison, WI: American Association of Cereal Chemists), 31–72.

Durso, N. A., and Cyr, R. J. (1994). A calmodulin-sensitive interaction between microtubules and a higher plant homolog of elongation factor-1 alpha. *Plant Cell* 6, 893–905. doi: 10.1105/tpc.6.6.893

Gabert, V. M., Brunsgaard, G., Eggum, B. O., and Jensen, J. (1995). Protein quality and digestibility of new high-lysine barley varieties in growing rats. *Plant Foods Hum. Nutr.* 48, 169–179. doi: 10.1007/bf01088313

Gasteiger, E., Hoogland, C., Gattiker, A., Wilkins, M. R., Appel, R. D., and Bairoch, A. (2005). "Protein identification and analysis tools on the ExPASy server," in *The Proteomics Protocols Handbook*, ed. J. M. Walker (Totowa, NJ: Humana Press), 571–607. doi: 10.1385/1-59259-890-0:571

Gillet, L. C., Navarro, P., Tate, S., Röst, H., Selevsek, N., Reiter, L., et al. (2012). Targeted data extraction of the MS/MS spectra generated by data-independent acquisition: a new concept for consistent and accurate proteome analysis. *Mol. Cell. Proteomics* 11, O111.016717.

Habben, J. E., Moro, G. L., Hunter, B. G., Hamaker, B. R., and Larkins, B. A. (1995). Elongation factor 1 alpha concentration is highly correlated with the lysine content of maize endosperm. *Proc. Natl. Acad. Sci. U.S.A.* 92, 8640–8644. doi: 10.1073/pnas.92.19.8640

Hansen, M., Lange, M., Friis, C., Dionisio, G., Holm, P. B., and Vincze, E. (2007). Antisense-mediated suppression of C-hordein biosynthesis in the barley grain results in correlated changes in the transcriptome, protein profile, and amino acid composition. *J. Exp. Bot.* 58, 3987–3995. doi: 10.1093/jxb/erm254

Howard, T. P., Fahy, B., Craggs, A., Mumford, R., Leigh, F., Howell, P., et al. (2012). Barley mutants with low rates of endosperm starch synthesis have low grain dormancy and high susceptibility to preharvest sprouting. *New Phytol.* 194, 158–167. doi: 10.1111/j.1469-8137.2011.04040.x

Ingversen, J., Køie, B., and Doll, H. (1973). Induced seed protein mutant of barley. *Cell. Mol. Life Sci.* 29, 1151–1152. doi: 10.1007/bf01946777

International Barley Genome Sequencing Consortium, Mayer, K. F., Waugh, R., Brown, J. W., Schulman, A., Langridge, P., et al. (2012). A physical, genetic and functional sequence assembly of the barley genome. *Nature* 491, 711–716. doi: 10.1038/nature11543

Juhász, A., Belova, T., Florides, C. G., Maulis, C., Fischer, I., Gell, G., et al. (2018). Genome mapping of seed-borne allergens and immunoresponsive proteins in wheat. *Sci. Adv.* 4:eaar8602. doi: 10.1126/sciadv.aar8602

Karlsson, K. (1977). Linkage studies in a gene for high lysine content in Riso barley mutant 1508. *Barley Genet. Newslett.* 7, 40–43.

Khakimov, B., Rasmussen, M. A., Kannangara, R. M., Jespersen, B. M., Munck, L., and Engelsen, S. B. (2017). From metabolome to phenotype: GC-MS metabolomics of developing mutant barley seeds reveals effects of growth, temperature and genotype. *Sci. Rep.* 7:8195.

Khan, A., and Mathelier, A. (2017). Intervene: a tool for intersection and visualization of multiple gene or genomic region sets. *BMC Bioinformatics* 18:287. doi: 10.1186/s12859-017-1708-7

Kirk, R. E. (1969). *Experimental Design: Procedures for the Behavioral Sciences. (Second Printing.).* Pacific Grove, CA: Brooks/Cole Publishing Company.

Kreis, M., Shewry, P., Forde, B., Rahman, S., and Miflin, B. (1983). Molecular analysis of a mutation conferring the high-lysine phenotype on the grain of barley (*Hordeum vulgare*). *Cell* 34, 161–167. doi: 10.1016/0092-8674(83)90146-0

Lange, M., Vincze, E., Wieser, H., Schjoerring, J. K., and Holm, P. B. (2007). Suppression of C-hordein synthesis in barley by antisense constructs results in a more balanced amino acid composition. *J. Agric. Food Chem.* 55, 6074–6081. doi: 10.1021/jf0709505

Liu, Q., Guo, Q., Akbar, S., Zhi, Y., El Tahchy, A., Mitchell, M., et al. (2017). Genetic enhancement of oil content in potato tuber (*Solanum tuberosum* L.) through an integrated metabolic engineering strategy. *Plant Biotechnol. J.* 15, 56–67. doi: 10.1111/pbi.12590

Marcotuli, I., Houston, K., Schwerdt, J. G., Waugh, R., Fincher, G. B., Burton, R. A., et al. (2016). Genetic diversity and genome wide association study of β-glucan content in tetraploid wheat grains. *PLoS One* 11:e0152590. doi: 10.1371/journal.pone.0152590

Marzábal, P., Gas, E., Fontanet, P., Vicente-Carbajosa, J., Torrent, M., and Ludevid, M. D. (2008). The maize Dof protein PBF activates transcription of γ-zein

during maize seed development. *Plant Mol. Biol.* 67, 441–454. doi: 10.1007/s11103-008-9325-5

McCleary, B. V., and Draga, A. (2016). Measurement of β-glucan in mushrooms and mycelial products. *J. AOAC Int.* 99, 364–373. doi: 10.5740/jaoacint.15-0289

McCleary, B. V., Gibson, T. S., and Mugford, D. C. (1997). Measurement of total starch in cereal products by amyloglucosidase-α-amylase method: collaborative study. *J. AOAC Int.* 80, 571–579. doi: 10.1093/jaoac/80.3.571

Mena, M., Cejudo, F. J., Isabel-Lamoneda, I., and Carbonero, P. (2002). A role for the DOF transcription factor BPBF in the regulation of gibberellin-responsive genes in barley aleurone. *Plant Physiol.* 130, 111–119. doi: 10.1104/pp.005561

Mertz, E. T., Bates, L. S., and Nelson, O. E. (1964). Mutant gene that changes protein composition and increases lysine content of maize endosperm. *Science* 145, 279–280. doi: 10.1126/science.145.3629.279

Moehs, C. P., Austill, W. J., Holm, A., Large, T. A., Loeffler, D., Mullenberg, J., et al. (2019). Development of reduced gluten wheat enabled by determination of the genetic basis of the lys3a low hordein barley mutant. *Plant Physiol.* 179, 1692–1703. doi: 10.1104/pp.18.00771

Molberg, Ø, Solheim flÆte, N., Jensen, T., Lundin, K. E., Arentz-Hansen, H., Anderson, O. D., et al. (2003). Intestinal T-cell responses to high-molecular-weight glutenins in celiac disease. *Gastroenterology* 125, 337–344. doi: 10.1016/s0016-5085(03)00890-4

Munck, L., Karlsson, K., Hagberg, A., and Eggum, B. O. (1970). Gene for improved nutritional value in barley seed protein. *Science* 168, 985–987. doi: 10.1126/science.168.3934.985

Nelson, O. E., Mertz, E. T., and Bates, L. S. (1965). Second mutant gene affecting the amino acid pattern of maize endosperm proteins. *Science* 150, 1469–1470. doi: 10.1126/science.150.3702.1469

Orman-Ligeza, B., Borrill, P., Chia, T., Chirico, M., Doležel, J., Drea, S., et al. (2020). LYS3 encodes a prolamin-box-binding transcription factor that controls embryo growth in barley and wheat. *J. Cereal Sci.* 93:102965. doi: 10.1016/j.jcs.2020.102965

Patron, N. J., Greber, B., Fahy, B. F., Laurie, D. A., Parker, M. L., and Denyer, K. (2004). The lys5 mutations of barley reveal the nature and importance of plastidial ADP-Glc transporters for starch synthesis in cereal endosperm. *Plant Physiol.* 135, 2088–2097. doi: 10.1104/pp.104.045203

R Core Team (2013). *R: A Language and Environment for Statistical Computing*. Vienna: R Foundation for Statistical Computing. Available online at: http://www.R-project.org/

Radchuk, V. V., Borisjuk, L., Sreenivasulu, N., Merx, K., Mock, H.-P., Rolletschek, H., et al. (2009). Spatiotemporal profiling of starch biosynthesis and degradation in the developing barley grain. *Plant Physiol.* 150, 190–204. doi: 10.1104/pp.108.133520

Ramírez-González, R., Borrill, P., Lang, D., Harrington, S., Brinton, J., Venturini, L., et al. (2018). The transcriptional landscape of polyploid wheat. *Science* 361:eaar6089.

Rudi, H., Uhlen, A. K., Harstad, O. M., and Munck, L. (2006). Genetic variability in cereal carbohydrate compositions and potentials for improving nutritional value. *Anim. Feed Sci. Technol.* 130, 55–65. doi: 10.1016/j.anifeedsci.2006.01.017

Schindelin, J., Arganda-Carreras, I., Frise, E., Kaynig, V., Longair, M., Pietzsch, T., et al. (2012). Fiji: an open-source platform for biological-image analysis. *Nat. Methods* 9, 676–682. doi: 10.1038/nmeth.2019

Shannon, P., Markiel, A., Ozier, O., Baliga, N. S., Wang, J. T., Ramage, D., et al. (2003). Cytoscape: a software environment for integrated models of biomolecular interaction networks. *Genome Res.* 13, 2498–2504. doi: 10.1101/gr.1239303

Shewry, P., Bunce, N., Kreis, M., and Forde, B. (1985). Polymorphism at the Hor 1 locus of barley (*Hordeum vulgare* L.). *Biochem. Genet.* 23, 391–404. doi: 10.1007/bf00499082

Shewry, P., Faulks, A. J., and Miflin, B. (1980). Effect of high-lysine mutations on the protein fractions of barley grain. *Biochem. Genet.* 18, 133–151. doi: 10.1007/bf00504365

Shewry, P., Hm, P., Mm, L., and Gj, M. (1979). Protein metabolism in developing endosperms of high-lysine and normal barley. *Cereal Chem* 56, 110–117.

Shewry, P. R. (1993). *Barley: Chemistry and Technology*, eds A. W. Macgregor and R. S. Bhatty (St Paul, MN: American Association of Cereal Chemists), 131–197.

Shewry, P. R., Napier, J. A., and Tatham, A. S. (1995). Seed storage proteins: structures and biosynthesis. *Plant Cell* 7:945. doi: 10.2307/3870049

Sørensen, M. (1992). Methylation of B-hordein genes in barley endosperm is inversely correlated with gene activity and affected by the regulatory gene Lys3. *Proc. Natl. Acad. Sci. U.S.A.* 89, 4119–4123. doi: 10.1073/pnas.89.9.4119

Tallberg, A. (1977). The amino-acid composition in endosperm and embryo of a barley variety and its high lysine mutant. *Hereditas* 87, 43–46. doi: 10.1111/j.1601-5223.1977.tb01243.x

Tallberg, A. (1981). Protein and lysine content in high-lysine double-recessives of barley II. Combinations between mutant 7 and a Hiproly back-cross. *Hereditas* 94, 261–268. doi: 10.1111/j.1601-5223.1981.tb01763.x

Tan, Q. K.-G., and Irish, V. F. (2006). The Arabidopsis zinc finger-homeodomain genes encode proteins with unique biochemical properties that are coordinately expressed during floral development. *Plant Physiol.* 140, 1095–1108. doi: 10.1104/pp.105.070565

Tanner, G. J., Blundell, M. J., Colgrave, M. L., and Howitt, C. A. (2015). Creation of the first ultra-low gluten barley (*Hordeum vulgare* L.) for coeliac and gluten-intolerant populations. *Plant Biotechnol. J.* 14, 1139–1150. doi: 10.1111/pbi.12482

Vanhercke, T., El Tahchy, A., Liu, Q., Zhou, X. R., Shrestha, P., Divi, U. K., et al. (2014). Metabolic engineering of biomass for high energy density: oilseed-like triacylglycerol yields from plant leaves. *Plant Biotechnol. J.* 12, 231–239. doi: 10.1111/pbi.12131

Venable, J. D., Dong, M.-Q., Wohlschlegel, J., Dillin, A., and Yates, J. R. (2004). Automated approach for quantitative analysis of complex peptide mixtures from tandem mass spectra. *Nat. Methods* 1:39. doi: 10.1038/nmeth705

Xia, J., Psychogios, N., Young, N., and Wishart, D. S. (2009). MetaboAnalyst: a web server for metabolomic data analysis and interpretation. *Nucleic Acids Res.* 37, W652–W660.

Yiming, Y., Yidan, O., and Wen, Y. (2018). shinyCircos: an R/Shiny application for interactive creation of Circos plot. *Bioinformatics* 34, 1229–1231. doi: 10.1093/bioinformatics/btx763

Zhang, Y., Cao, X., Juhasz, A., Islam, S., Qi, P., She, M., et al. (2018a). Wheat avenin-like protein and its significant Fusarium Head Blight resistant functions. *bioRxiv* [Preprint]. bioRxiv: 406694,

Zhang, Y., Hu, X., Islam, S., She, M., Peng, Y., Yu, Z., et al. (2018b). New insights into the evolution of wheat avenin-like proteins in wild emmer wheat (*Triticum dicoccoides*). *Proc. Natl. Acad. Sci. U.S.A.* 115, 13312–13317. doi: 10.1073/pnas.1812855115

Conflict of Interest: The authors declare that the research was conducted in the absence of any commercial or financial relationships that could be construed as a potential conflict of interest.

Publisher's Note: All claims expressed in this article are solely those of the authors and do not necessarily represent those of their affiliated organizations, or those of the publisher, the editors and the reviewers. Any product that may be evaluated in this article, or claim that may be made by its manufacturer, is not guaranteed or endorsed by the publisher.

frontiers in Plant Science

ORIGINAL RESEARCH
published: 06 October 2021
doi: 10.3389/fpls.2021.706567

Night-Warming Priming at the Vegetative Stage Alleviates Damage to the Flag Leaf Caused by Post-anthesis Warming in Winter Wheat (*Triticum aestivum* L.)

Yonghui Fan[1†], Zhaoyan Lv[2†], Ting Ge[1], Yuxing Li[1], Wei Yang[1], Wenjing Zhang[1], Shangyu Ma[1], Tingbo Dai[3] and Zhenglai Huang[1*]*

[1] College of Agronomy, Anhui Agricultural University/Key Laboratory of Wheat Biology and Genetic Improvement on South Yellow and Huai River Valley, Ministry of Agriculture, Hefei, China, [2] College of Horticulture, Anhui Agricultural University, Hefei, China, [3] Key Laboratory of Crop Physiology, Ecology and Production Management, Nanjing Agricultural University, Nanjing, China

The asymmetric warming in diurnal and seasonal temperature patterns plays an important role in crop distribution and productivity. Asymmetric warming during the early growth periods of winter wheat profoundly affects its vegetative growth and post-anthesis grain productivity. Field experiments were conducted on winter wheat to explore the impact of night warming treatment in winter (Winter warming treatment, WT) or spring (Spring warming treatment, ST) on the senescence of flag leaves and yield of wheat plants later treated with night warming during grain filling (Warming treatment during grain filling, FT). The results showed that FT decreased wheat yield by reducing the number of grains per panicle and per 1,000-grain weight and that the yield of wheat plants treated with FT declined to a greater extent than that of wheat plants treated with WT + FT or ST + FT. The net photosynthetic rate, chlorophyll content, and chlorophyll fluorescence parameters of the flag leaves of wheat plants treated with WT + FT or ST + FT were higher than those under the control treatment from 0 to 7 days after anthesis (DAA) but were lower than those under the control treatment and higher than those of wheat plants treated with FT alone from 14 to 28 DAA. The soluble protein and Rubisco contents in the flag leaves of wheat plants treated with WT + FT or ST + FT were high in the early grain-filling period and then gradually decreased to below those of the control treatment. These contents were greater in wheat plants treated with WT + FT than in wheat plants treated with ST + FT from 0 to 14 DAA, whereas the opposite was true from 21 to 28 DAA. Furthermore, WT + FT and ST + FT inhibited membrane lipid peroxidation by increasing superoxide dismutase and peroxidase activities and lowering phospholipase D (PLD), phosphatidic acid (PA), lipoxygenase (LOX), and free fatty acid levels in the early grain-filling period, but their inhibitory effects on membrane lipid peroxidation gradually weakened during the late grain-filling period. Night-warming priming alleviated the adverse effect of post-anthesis warming on yield by delaying the post-anthesis senescence of flag leaves.

Keywords: grain-filling stage, night warming, wheat, senescence, yield

OPEN ACCESS

Edited by:
Vincenzo Rossi, Council for Agricultural and Economics Research (CREA), Italy

Reviewed by:
Andrea Brandolini, Council for Agricultural and Economics Research (CREA), Italy
Xiaoyan Wang, Yangtze University, China
Md Alamgir Hossain, Bangladesh Agricultural University, Bangladesh

***Correspondence:**
Zhenglai Huang
xdnyyjs@163.com
Tingbo Dai
tingbod@njau.edu.cn

[†]These authors have contributed equally to this work

Specialty section:
This article was submitted to Crop and Product Physiology, a section of the journal Frontiers in Plant Science

Received: *07 May 2021*
Accepted: *02 September 2021*
Published: *06 October 2021*

Citation:
Fan Y, Lv Z, Ge T, Li Y, Yang W, Zhang W, Ma S, Dai T and Huang Z (2021) Night-Warming Priming at the Vegetative Stage Alleviates Damage to the Flag Leaf Caused by Post-anthesis Warming in Winter Wheat (Triticum aestivum L.). Front. Plant Sci. 12:706567. doi: 10.3389/fpls.2021.706567

INTRODUCTION

In the twentieth century, the annual mean temperature in China increased from 0.4 to 0.8°C, and the mean temperature increases in spring, summer, fall, and winter were 0.33, 0.40, 0.73, and 1.37°C, respectively. China experienced 17 consecutive warm winters beginning in 1990, and the mean temperature increase in winter was more than two times the average annual increase in global temperature (0.6°C) (Qin et al., 2010; Gao et al., 2011; Hatfield et al., 2011). According to the prediction by the Intergovernmental Panel on Climate Change (Haines, 2003), climate warming in China will continue in the twenty-first century, especially in the winter half-year in northern China. Increasingly drastic climate change will greatly affect atmospheric circulation and cause more extreme weather events (Zhao et al., 2010; You et al., 2011). It is expected that these extreme weather events will occur to a greater extent and at higher frequencies in East China because the warming rate in this region is higher than the global average (Ren et al., 2008).

Wheat is one of the three major crops in the world and the leading food crop in China, and its yield plays a key role in the food security and socioeconomic development of China (Slafer, 2003). High temperature in the post-anthesis period often accelerates wheat maturation and, thus, severely reduces wheat yield and quality (Riaz et al., 2021). Grain number is mainly determined during the period immediately preceding anthesis, and individual grain weight is defined during the grain-filling period (Karim et al., 2020). Temperature is an important environmental factor affecting grain filling during grain formation (Hütsch et al., 2018; Osman et al., 2020). Shirdelmoghanloo et al. (2016) found that warming in the early post-anthesis period significantly reduces photosynthesis and the antioxidant capacity of flag leaves in wheat, resulting in smaller grain size and weight but barely affecting grain yield. Bian et al. (2012) found that a temperature increase of approximately 1.8°C after anthesis, with an average daily temperature of approximately 20.8°C and an average daytime temperature of approximately 23.1°C, was conducive to protein accumulation, with the highest increase coming in grain albumins, while a temperature increase of <1.8°C barely affected the starch content. Huebner and Bietz (1988) reported that, during wheat grain filling, the most suitable ambient temperature is 20–24°C. An ambient temperature higher than 25°C shortens the grain-filling period, thus affecting grain weight, while an ambient temperature lower than 12°C causes chilling injuries in wheat.

Crop yield is closely related to the net photosynthetic assimilation process during the grain-filling period in wheat. The photosynthesis of flag leaves contributes the most to the final grain dry weight in winter wheat. Hence, the study of flag leaves in response to climate warming occurring during the winter and spring seasons is crucial. The main source of mass accumulation in wheat grain is the photosynthetic products of flag leaves during the grain-filling period, and the physiological activities of these leaves directly affect dry matter accumulation and transport (Feng et al., 2014). Grain filling is also affected by the photosynthetic characteristics of flag leaves, which, in turn, affects grain weight and yield (Prieto et al., 2009). The soluble protein content in plant leaves reflected the nitrogen content, and the nitrogen content in leaves had a positive relation with photosynthetic capacity. Most of the nitrogen in plants is stored in enzymes participating in photosynthesis, especially in Rubisco, which is a major source of nitrogen recycling (Makino et al., 1997; Masclaux-Daubresse et al., 2008). However, in the middle and late grain-filling periods of wheat, flag leaf senescence often occurs. During the grain-filling stage, programmed leaf senescence occurs, accompanied by a burst of excessive reactive oxygen species (ROS), such as superoxide and hydroxyl radicals (Kong et al., 2015, 2017). The significant declines in chlorophyll content (Lee et al., 2001), protein content, and the activities of various antioxidant enzymes in wheat during senescence break the dynamic balance between the generation and elimination of ROS in plants, causing the accumulation of large amounts of ROS, damage to biological macromolecules, and the destruction of membrane lipid structures, thus hindering the normal operation of photosynthesis (Huffaker, 1990).

A high temperature in the late growth stage reduces the photosynthetic capacity of wheat leaves, intensifies membrane lipid peroxidation, accelerates plant senescence, and leads to lower wheat yield (Savin and Nicolas, 1996). Suitable stress stimuli during the early reproductive period can increase the resistance of crops to the same or other stresses (Bruce et al., 2007). Li et al. (2011) reported that a pre-anthesis waterlogging pretreatment improved the resistance of wheat plants to post-anthesis waterlogging, thereby significantly increasing yield. Another study exposed wheat seedlings at 21 days after sowing to moderate drought for 9 days and then allowed them to recover for 1 day. These drought-adapted seedlings showed a stronger drought resistance than non-drought-adapted seedlings when they were later exposed to severe drought stress for 9 days (Selote and Khanna-Chopra, 2006).

There is a lack of relevant research on whether warming in the early reproductive period can improve the viability of wheat in the late reproductive period. In the present study, field experiments were conducted to investigate the impact of a moderate night-warming treatment in winter (WT) or spring (ST) on the senescence of flag leaves and the yield of wheat plants that were later treated with night warming during the grain-filling period (FT). The mechanism underlying these effects was investigated by determining the photosynthetic and oxidative metabolism characteristics of flag leaves and their yield output.

MATERIALS AND METHODS

Experimental Design

The field experiments were conducted at the Jiangpu Experimental Station of Nanjing Agricultural University from 2013 to 2014. Two local cultivars, vernal type Yangmai 13 (YM13) and facultative type Yannong 19 (YN19), were used. The soil in the test plots before sowing contained 21.62 g kg^{-1} of organic matter, 1.12 g kg^{-1} of total nitrogen, 14.39 mg kg^{-1} of available nitrogen, 17.4 mg kg^{-1} of available phosphorus, and 115.52 mg kg^{-1} of available potassium. The plot size was 8 m^2 (2 m × 4 m) with a row spacing of 25 cm. The randomized block design was adopted for field experiments with three

TABLE 1 | Phenophase of the two wheat cultivars.

Cultivar	Phenophase date (day/month)				
	Sowing	Stem-elongation	Booting	Anthesis	Maturity
Yangmai 18	26th October 2013	21st February 2014	22nd March 2014	13rd April 2014	20th May 2014
Yannong 19	26th October 2013	28th February 2014	28th March 2014	19th April 2014	24th May 2014

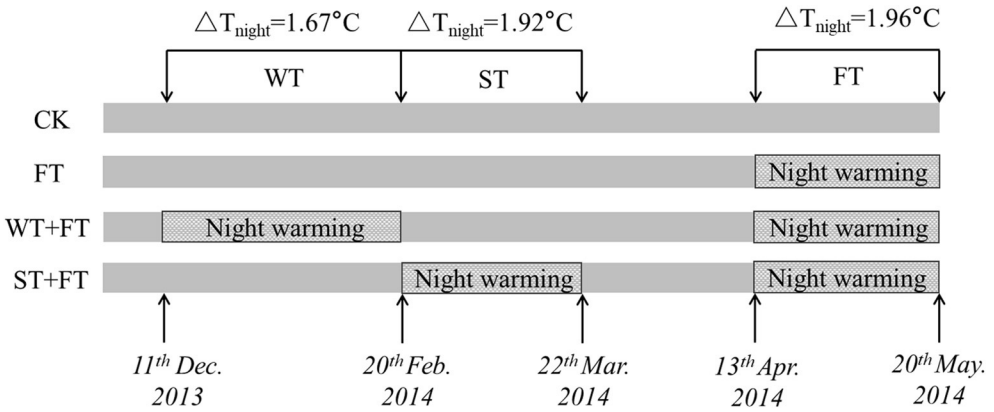

FIGURE 1 | Schematic of the setup of different warming treatments. CK: control; FT: night warming treatment during the grain-filling period; WT + FT: night warming treatment during winter and the grain-filling period; ST + FT: night warming treatment during spring and the grain-filling period. NW: night warming. ΔT_{night} refers to the increase of mean night temperature between treatments and the control. Mean night temperature is the mean of all temperature data on a 10 min interval from 19:00 p.m. to 07:00 a.m.

replications. A total of 240 kg ha^{-1} of nitrogen was applied in three applications over the whole growth period. The basal: topdressing ratio (basal fertilizer:jointing fertilizer:booting fertilizer) was 5:3:2. Superphosphate (P_2O_5) and potassium oxide (K_2O) fertilizers were applied together as the basal fertilizers at 100 and 150 kg ha^{-1}, respectively, during the wheat growth period. The seeds were sown on October 26, 2013. The seedlings were then thinned to a density of 180 m^{-2} when they sprouted three leaves. Plants were carefully noted to have reached a particular growth stage when more than 50% of the wheat plants reached that stage (tillering: Zadoks growth stage 21, main shoot and one tiller; jointing: Zadoks growth stage 31, the first node was detectable; booting: Zadoks growth stage 41, flag leaf sheath-extending stage; anthesis: Zadoks growth stage 60, the beginning of pollination). The stages were determined according to Zadoks et al. (1974). The phenophases of the two wheat cultivars are provided in **Table 1**. The days taken from flowering to grain formation were recorded when more than 50% of the plants completed their flowering to the physiological maturity of the crop. Uniform tillers flowering on the same day were tagged for sampling and measurements. The rest of the management measures were the same as those used for the high-yield cultivation of field crops.

Passive night warming (Shaver et al., 1998; Beier et al., 2004; DeMarco et al., 2014; Deslippe et al., 2015) was adopted in this study using a warming facility (length: 3 m, width: 5 m, and height: 2 m) with a removable plastic membrane. Designated personnel rolled down the plastic membrane at sunset to cover the warmed plots and rolled it up at sunrise to expose the warmed plots to the natural environment (from around 19:00 p.m. to 07:00 a.m. of the next day). The facility was equipped with a ventilation system to ensure the normal respiration and ventilation of the crops at night. To ensure that each plot received the same precipitation, the plastic membrane was rolled up at night when it rained or snowed. A dual-channel thermometer (NZ-LBR-F, Nanjing Nengzhao Electronic Instrument Co., Ltd., China) was used to record the canopy night temperature of warmed plots once every 10 min during the wheat growth period. **Figure 1** shows the setup of the different warming treatments. The four treatments included non-warming (CK), night-warming treatment during the grain-filling period only (FT: anthesis to maturity), night-warming treatment during winter (WT: tillering to jointing) and the grain-filling period (WT + FT), and night-warming treatment during spring (ST: jointing to booting) and the grain-filling period (ST + FT). The mean nighttime temperatures of the winter wheat canopy increased by 1.67 (WT) and 1.92°C (ST), respectively. FT increased the mean nighttime temperature of the winter wheat canopy by 1.96°C. The temperature and humidity data during the warming period are shown in **Figure 2**.

Measures and Methods

Yield and Yield Components

Two plants of 2 m long rows (1 m^2) were marked at anthesis in the center of the plots to measure grain yield at maturity. Spike number per m^2 was counted at physiological maturity, and the

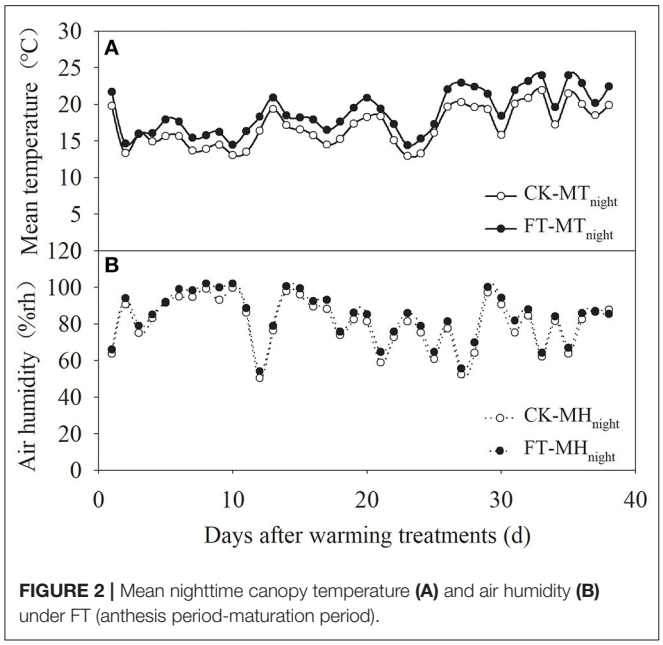

FIGURE 2 | Mean nighttime canopy temperature **(A)** and air humidity **(B)** under FT (anthesis period-maturation period).

plants were cut with a sickle at the soil level. Harvested plants were carefully threshed, dried, and weighed to measure grain yield in kg ha^{-1} at 14% moisture. A total of 50 culms from the four rows in the middle of each plot were sampled at the soil level to measure grain number, grain weight per spike, and 1,000-grain weight.

The Net Photosynthetic Rate (Pn)

The net photosynthetic rate of flag leaves was measured at 0, 7, 14, 21, 28, and 35 days after anthesis (DAA). Four flag leaves with uniform growth and similar light-incidence directions were measured for each treatment with three replications. The *Pn* of wheat leaves was measured using an LI-6400 portable photosynthesis system (Li-Cor Inc., Lincoln, NE, USA). The chamber had an opening for air and a red/blue light source. The photosynthetically active radiation (PAR) was set to 1,200 $\mu mol\ m^{-2}\ s^{-1}$, and the CO_2 concentration was approximately 380 $\mu mol\ L^{-1}$.

Chlorophyll Content

One gram of leaves was cut into several sections and placed in 50 ml of acetone:ethanol (v:v = 1:1) extracting solution in the dark at 25°C for 24 h, and the optical density (OD) of the extracts was measured at 470, 663, and 645 nm. The chlorophyll content was calculated according to the formula of Zheng et al. (2009).

Chlorophyll Fluorescence Kinetics Parameters

The chlorophyll fluorescence kinetics parameters of the same flag leaves used in the photosynthesis measurements were measured with a chlorophyll fluorometer (PAM-2500, Heinz Walz GmbH, Effeltrich, Germany). The minimum and maximum chlorophyll fluorescence (F_0 and F_m, respectively) were measured after dark adaptation for 30 min. Steady-state fluorescence (F_s) was measured after irradiation with 1,200 $\mu mol\ m^{-2}\ s^{-1}$ for 10 min and a strong flash. The maximum fluorescence under light adaptation (F_m') was recorded. After dark adaptation for 3 s, the far-red light was turned on, and the initial fluorescence F_0' under light adaptation was measured to calculate the effective quantum yield of photosystem II (PSII) photochemistry (Φ_{PSII}). Parameters were calculated referring to the maximum efficiency of PSII photochemistry under dark-adapted (F_v/F_m), $F_v/F_m = (F_m\text{-}F_0)/F_m$, where F_v is the variable chlorophyll fluorescence and $\Phi_{PSII} = (F_m'\text{-}F_0')/F_m'$ (Genty et al., 1989).

Soluble Protein and Rubisco Content

Soluble protein content measurement followed the procedure of Lowry et al. (1951) with little change. Frozen samples (0.5 g) were extracted in a sodium phosphate buffer (50 mM, pH 7). The extracts were centrifuged (4,000 × *g*, 10 min, and 4°C). Soluble proteins were quantified using the supernatants of the samples, with bovine serum albumin as a standard. Rubisco was analyzed using sodium dodecyl sulfate-polyacrylamide gel electrophoresis (SDS-PAGE) as described previously (Makino et al., 1986), with few changes. Frozen tissue was homogenized in 50 mM of a Tris–HCl buffer (pH 8) containing 5 mM of β-mercaptoethanol and 12.5% of (v/v) glycerol and then centrifuged at 15,000× *g* for 15 min. To the supernatant, we added SDS, β-mercaptoethanol, and glycerol to final concentrations of 1% (w/v), 2% (v/v), and 5% (v/v), respectively, and then boiled the mixture for 5 min. A sample of this preparation was used for electrophoresis. For protein visualization, the gels were stained with 0.1% (w/v) Coomassie Brilliant Blue R-250. The stained bands were excised from the gels with a razor blade and eluted in 1 ml of formamide in a stoppered amber test tube at 50°C for 8 h with no stained gel as a standard. The absorbance of the resultant solution was read at 595 nm with a spectrophotometer (UV-4806S, Unico Instrument, Shanghai, China). This part has been revised accordingly.

Antioxidant Capacity of the Leaves

The rate of superoxide anion radical (O_2^-) production was measured according to Sui et al. (2007). Superoxide dismutase (SOD, EC 1.15.1.1) activity was measured according to Yang et al. (2007), and peroxidase (POD, EC 1.11.1.7) activity was determined according to Zheng et al. (2009). Malondialdehyde (MDA) content was measured according to Zheng et al. (2009). The above measurements were carried out in three biological replicates (leaves).

Membrane Phospholipid Metabolism

The phospholipase D, PA, LOX, and FFA concentrations were determined using the double-antibody sandwich ELISA using the reagent kit DRE97194 (Fengxiang Biotech, Shanghai, China).

Data Processing

All data are expressed as the means of three replicates. A one-way ANOVA was performed for the PLD, PA, LOX, and FFA contents to assess the significant differences between temperature treatments. A two-way ANOVA was performed on grain yield and its components, *Pn*, chlorophyll content,

TABLE 2 | Impact of a night warming treatment in winter (WT) or spring (ST) on the grain yield and yield components of wheat later treated with night warming treatment during the grain-filling period (FT).

Cultivar	Treatment	Spikes ($\times 10^4$ hm^{-2})	Grain number (spike^{-1})	1000-grain weight (g)	Grain yield (kg hm^{-2})
YM13	CK	450.33 a	47.56 a	41.54 a	7297.80 a
	FT	446.00 a	44.86 b	38.77 c	6079.67 d
	WT+FT	428.00 a	47.81 a	40.18 b	6536.13 c
	ST+FT	438.67 a	48.19 a	40.96 ab	6790.66 b
YN19	CK	497.67 a	44.40 a	39.08 a	6832.73 a
	FT	492.00 a	41.56 b	36.64 b	5645.86 c
	WT+FT	473.33 abc	43.26 ab	37.95 ab	5789.74 c
	ST+FT	479.67 ab	43.72 a	38.34 ab	6175.65 b
F-value	F_{Cultivar}	43.013**	127.864**	69.469**	104.551**
	$F_{\text{Treatment}}$	2.247	14.935**	15.627**	86.315**
	$F_{C\times T}$	0.036	1.158	0.152	1.697

*Different letters in the same column indicate the differences between treatments at $p < 0.05$. F_{Cultivar} and $F_{\text{Treatment}}$ represent the F value of the cultivar and the warming treatment, respectively; $F_{C\times T}$ represents the F value of the interaction between the cultivar and temperature. ** represent significance at the 0.01 level.*

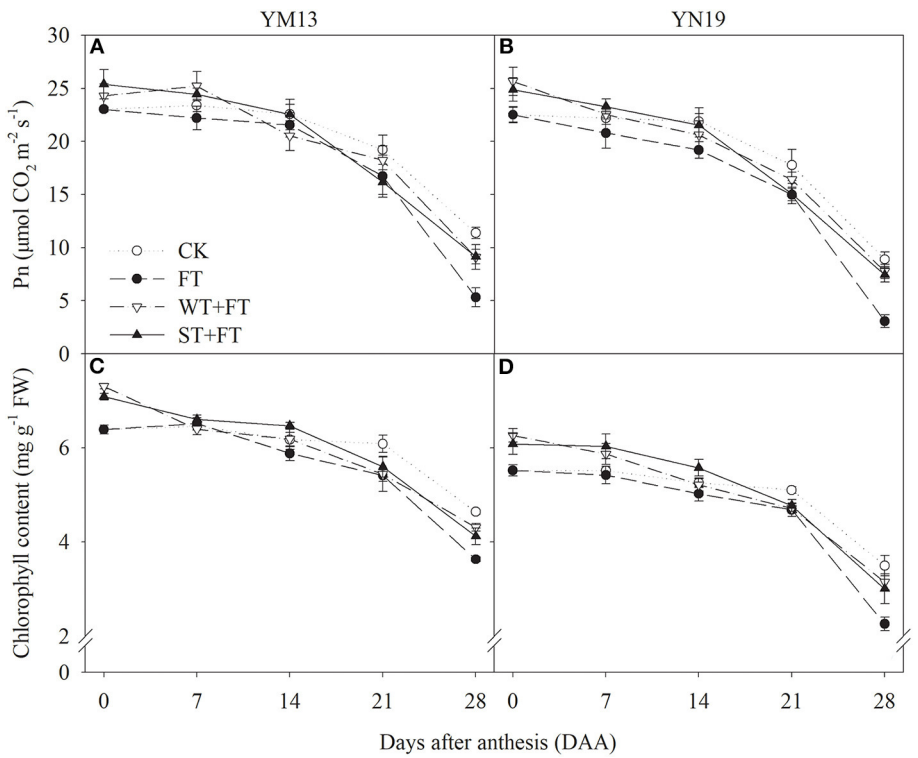

FIGURE 3 | Impact of night warming treatment in winter or spring on the net photosynthetic rate *(Pn)* **(A,B)** and chlorophyll content **(C,D)** of wheat flag leaves later treated with night warming during the grain-filling period.

Fv/Fm, Φ_{PSII}, soluble protein content, Rubisco content, O_2^- production rate, malondialdehyde (MDA) content, SOD activity, and POD activity to identify the significant differences between the cultivars and temperature treatments. Statistical analyses were conducted using the Statistical Package for the Social Sciences (SPSS) software (SPSS ver. 10, SPSS, Chicago, IL, USA). The results were plotted in SigmaPlot 10.0.

RESULTS

Yield and Yield Components

Table 2 shows that the three warming treatments reduced the yields of the two wheat cultivars, and in terms of yield, the treatments followed the descending order of CK > WT + FT > ST + FT > FT, indicating that FT was not conducive to yield.

In particular, the WT and ST priming treatments reduced the inhibitory effect of FT on grain yield. Compared with control, FT had a similar spike number but significantly lower grain number, 1,000-grain weight, and, therefore, yield (minus 17%). On the other hand, the spike number, grain number, and 1,000-kernel weight in primed plants were like those of the control, and yield losses, especially in the ST samples, were limited.

Pn and Chlorophyll Content

Figures 3A,B shows the *Pn* values of wheat flag leaves under WT + FT and ST + FT were higher than those under the control treatment from 0 to 7 DAA and were lower than those under the control treatment, but still higher than those under FT from 14 to 28 DAA. At 28 DAA, the *Pn* values of the flag leaves in primed plants were significantly higher than those under the FT of the two cultivars. There was a significant difference in the flag leaf *Pn* between warming treatments at 0–7 and 21–28 DAA ($p < 0.01$; **Table 3**). **Figures 3C,D** shows that the flag leaf chlorophyll content in the two cultivars was higher under WT + FT and ST + FT than under the control treatment from 0 to 7 DAA and was lower than the control from 21 to 28 DAA. Night-warming priming increased the post-anthesis chlorophyll content in flag leaves than that under FT. There was a significant difference in the flag leaf chlorophyll contents between warming treatments and cultivars at 0–28 DAA ($p < 0.01$; **Table 3**).

Chlorophyll Fluorescence Parameters

Figures 4A,B shows that the F_v/F_m of the flag leaves was higher under WT + FT and ST + FT than under the control treatment from 0 to 7 DAA, lower under WT + FT and ST + FT than under the control treatment from 14 to 28 DAA (this difference increased over time during the grain-filling period), and always higher under WT + FT and ST + FT than under FT. There was a significant difference in the flag leaf F_v/F_m between warming treatments at 0–28 DAA ($p < 0.01$; **Table 3**). **Figures 4C,D** shows that the Φ_{PSII} of flag leaves was higher under WT + FT and ST + FT than under the control treatment from 0 to 7 DAA and higher under WT + FT and ST + FT than under FT from 0 to 21 DAA.

Soluble Protein and Rubisco Content

Figures 5A,B shows that FT reduced the soluble protein content of flag leaves after anthesis, and this reduction gradually increased over time in the grain-filling period. The soluble protein contents of flag leaves were higher under WT + FT and ST + FT than under the control treatment from 0 to 7 DAA and lower under WT + FT and ST + FT than under the control treatment from 21 to 28 DAA. Night-warming priming alleviated the FT-induced reduction in soluble protein content in flag leaves during the grain-filling period. **Figures 5C,D** shows that the differences in the post-anthesis Rubisco contents between treatments followed a trend similar to that of the soluble protein contents, suggesting that a primed plant resulted in stronger photosynthetic carbon assimilation in flag leaves in the early grain-filling period and alleviated the FT-induced damage to the photosynthetic system during the middle to late grain-filling period.

TABLE 3 | Two-way ANOVA analysis for *Pn*, chlorophyll content, Fv/Fm, Φ_{PSII}, soluble protein content, Rubisco content, O_2^- production rate, MDA content, SOD activity, and POD activity of the two cultivars as affected by a night warming treatment and the interactive effect.

Time	*Pn*			Chlorophyll content			F_v/F_m			Φ_{PSII}			Soluble protein			Rubisco content			O_2^- production rate			MDA content			SOD activity			POD activity		
	C	T	C×T	C	T	C×T	C	T	C×T	C	T	C×T	C	T	C×T	C	T	C×T	C	T	C×T	C	T	C×T	C	T	C×T	C	T	C×T
0 DAA	ns	**	ns	**	**	ns		ns	**	*	ns	**	*	**	ns	**	**	ns	ns	**	ns		ns	*	ns	**	ns	**	**	*
7 DAA	**	**	ns	**	**	*		ns	**	ns	*	*	ns	**	ns	**	**	ns	**	*	ns		ns	*	ns	*	ns	ns	**	ns
14 DAA	*	*	ns	**	**	ns		**	**	**	*	ns	*	**	ns	**	*	**	**	**	ns		ns	*	ns	ns	ns	**	**	**
21 DAA	*	**	ns	**	**	ns		**	**	**	**	*	**	**	ns	ns	**	**	**	**	**		**	**	*	ns	**	ns	**	**	ns
28 DAA	**	**	ns	**	**	ns		ns	**	**	**	**	**	**	**	ns	**	**	ns	**	ns		**	**	**	ns	**	*	**	**	**

*Pn, F_v/F_m, Φ_{PSII}, $O_2^{\bullet-}$, MDA, SOD, and POD refer to net photosynthetic rate, maximum efficiency of photosystem II (PS II) photochemistry under dark adapted, the effective quantum yield of PS II photochemistry, superoxide anion radical, malondialdehyde, superoxide dismutase, and peroxidase, respectively. DAA refers to days after anthesis. *, **, and ns indicate being significant at 0. 05, 0.01 levels, and no significant difference, respectively. C, T, and C × T refer to cultivar, treatment, and the interaction of cultivar with treatment, respectively.*

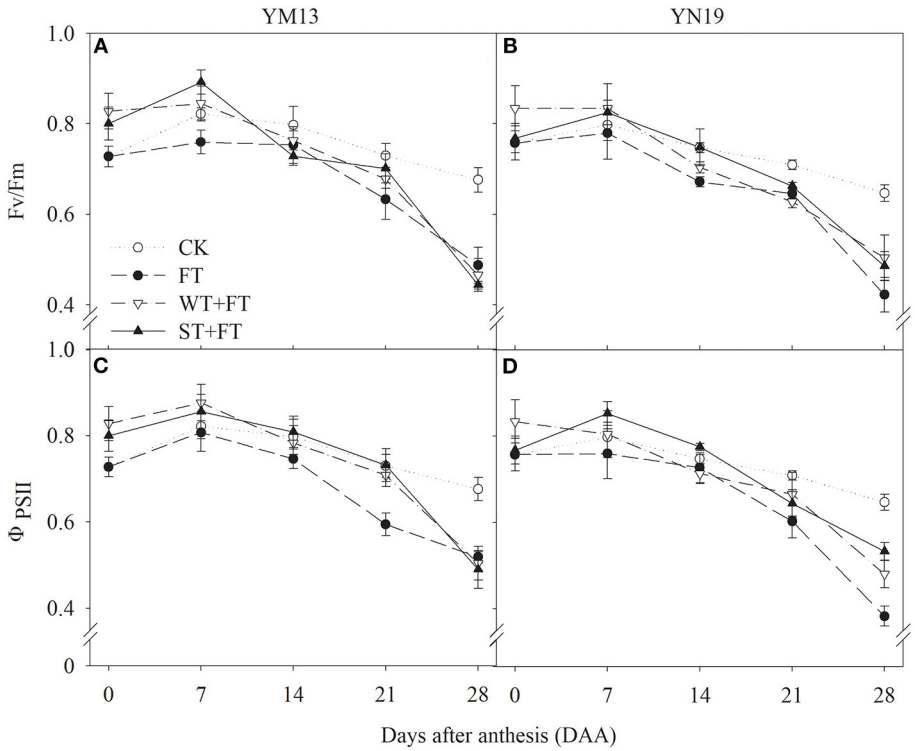

FIGURE 4 | Effect of a night warming treatment in winter or spring on maximum efficiency of photosystem II (PS II) photochemistry under dark-adapted (Fv/Fm) **(A,B)** and the effective quantum yield of PS II photochemistry (ΦPSII) **(C,D)** in wheat flag leaves later treated with night warming during the grain-filling period.

Degree of Oxidative Metabolism

Figures 6A,B shows that FT increased the production rate of O_2^- in the post-anthesis flag leaves, indicating that FT accelerated the senescence of flag leaves. The production rates of O_2^- in flag leaves were lower under WT + FT and ST + FT than under the control treatment during the anthesis period. This was accompanied by increasingly higher rates of senescence after anthesis, which was significantly higher under WT + FT and ST + FT than under the control treatment at 28 DAA, and always lower under WT + FT and ST + FT than FT at 0–14 DAA. **Figures 6C,D** shows that the MDA concentrations in flag leaves under WT + FT and ST + FT were lower than those under the control treatment during the anthesis period, and they were also lower under WT + FT and ST + FT than under FT at 0–21 DAA. There was a significant difference in the flag leaf production rate of O_2^- and MDA content between warming treatments at 0, 21–28 DAA ($p < 0.01$; **Table 3**). These results indicate that night-warming priming alleviated the ROS-induced damage caused by FT.

Membrane Phospholipid Metabolism

Figures 7A,B shows that the PLD in flag leaves at 14 DAA was higher under FT than under the control treatment, but not significantly different among WT + FT, ST + FT, and the control. The PLD in flag leaves at 28 DAA was significantly higher under all the warming treatments than under the control treatment, and FT had the highest PLD. **Figures 7C,D** shows that, in YM13, the PA in flag leaves was significantly lower under WT + FT and ST + FT than FT at 14 DAA, and significantly higher under the three warming treatments than under the control treatment at 28 DAA. In YN19, the PA contents in flag leaves were significantly lower under ST + FT than under the control and FT treatment at 14 DAA, were significantly higher under FT and WT + FT than under the control treatment at 28 DAA, and were not significantly different between ST + FT and the control treatment at 28 DAA.

Figures 8A,B shows that the LOX in flag leaves at 14 and 28 DAA was higher under the three warming treatments than under the control treatment, which was the highest under FT. **Figures 8C,D** shows that the FFA in YM13 and YN19 at 28 DAA was significantly higher under the three warming treatments than under the control treatment, following the ranking FT > WT + FT > ST + FT > CK. Thus, FT promoted the degradation of membrane phospholipids by LOX in flag leaves and accelerated the senescence of flag leaves. Night-warming priming alleviated the post-florescence degradation of membrane phospholipids in the flag leaves of wheat plants treated with FT.

Activities of Antioxidant Enzymes

Figures 9A,B shows that the SOD activity in flag leaves of YM13 and YN19 was higher under WT + FT and ST + FT from 0 to 7 DAA and lower from 21 to 28 DAA than under the control treatment. In particular, WT + FT and ST + FT increased the post-anthesis SOD activity in flag leaves than that under FT. **Figures 9C,D** shows that FT gradually decreased post-anthesis

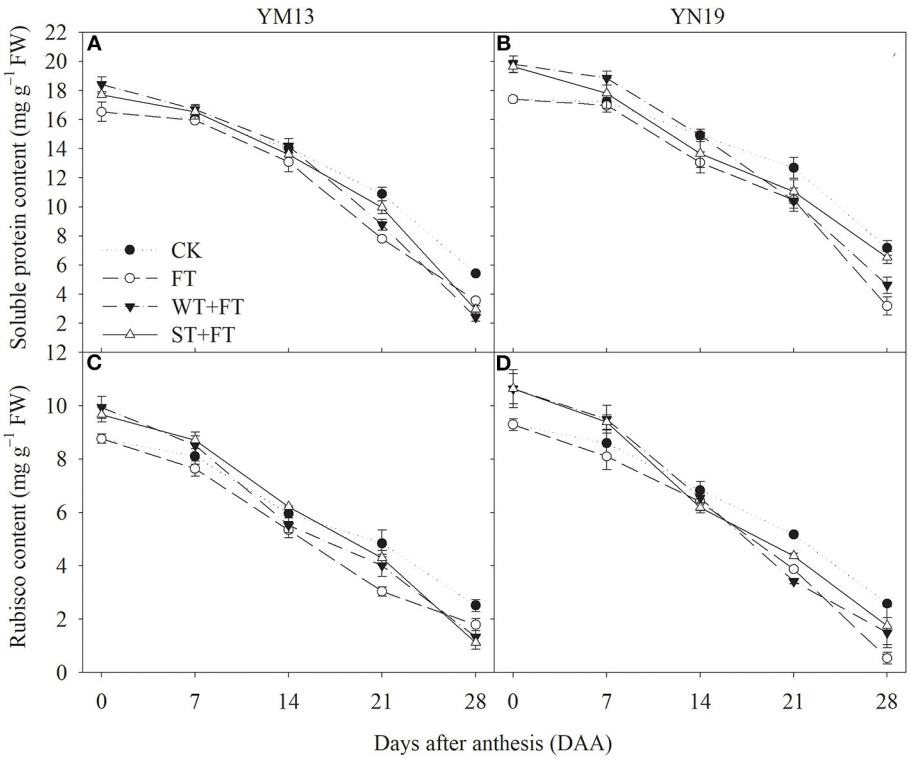

FIGURE 5 | Impact of night warming treatment in winter or spring on the soluble protein content **(A,B)** and Rubisco content **(C,D)** in wheat flag leaves later treated with night warming during the grain-filling period.

POD activity during the grain-filling period, while the POD activity in flag leaves of wheat plants treated with WT + FT and ST + FT remained high during the early grain-filling period but gradually decreased and became lower than under the control treatment in the late grain-filling period, but still higher than that under FT from 0 to 21 DAA. There was a significant difference in the flag leaf POD activity between warming treatments at 0–28 DAA ($p < 0.01$; **Table 3**).

DISCUSSION

The yields of both wheat cultivars were significantly lower under the three warming treatments than under the control treatment, with the treatments following descending order of CK > WT + FT > ST + FT > FT. In other words, FT resulted in the greatest reduction in wheat grain yield, while WT and ST alleviated the adverse effect of FT on grain yield mainly by increasing the number of grains per panicle and 1,000-grain weight. Heat stress can a?ect the yield components by shortening the grain filling duration due to an accelerated rate of development, accelerated leaf senescence, and the inhibition of photosynthesis and carbohydrate synthesis (Asseng et al., 2011). Pre-stress treatments during vegetative stages (priming) have been shown to increase stress tolerance in plants and alleviate abiotic stress in grasses (Wang et al., 2017; Thayna et al., 2018). Our previous study showed that, compared with the damage observed in non-primed plants, heat priming during the stem-elongation stage and booting significantly prevented the grain-yield damage caused by heat stress during grain-filling (Fan et al., 2018). Tian et al. (2012) indicated that an increased night temperature can increase cell metabolism, the nighttime respiration rate of leaves, and the growth rate of leaves. Under night-warming conditions, the number of leaf cells and the plant metabolism become more vigorous. The above evidence suggests that night-warming priming at the vegetative stage proved to contribute to grain yield sustainability by enhancing the ability of plants to mitigate the effects of warming during the grain-filling stage.

Photosynthesis is the most sensitive physiological process to high temperatures. Depressed photosynthesis under heat stress often negatively affects the growth and grain yield of wheat. Many studies have demonstrated that most plant species can adapt to alterations in growth temperature by adjusting their photosynthetic system to optimize performance in a new temperature environment (Martinez et al., 2014; Liu et al., 2016). In the present study, the flag leaves of primed plants maintained a high *Pn* and chlorophyll content in the early grain-filling period, and their photosynthetic capacity gradually became lower than the capacity of the control group but still higher than that under FT. Lobell et al. (2012) found that a high temperature in the late growth period decreases the photosynthetic capacity of wheat

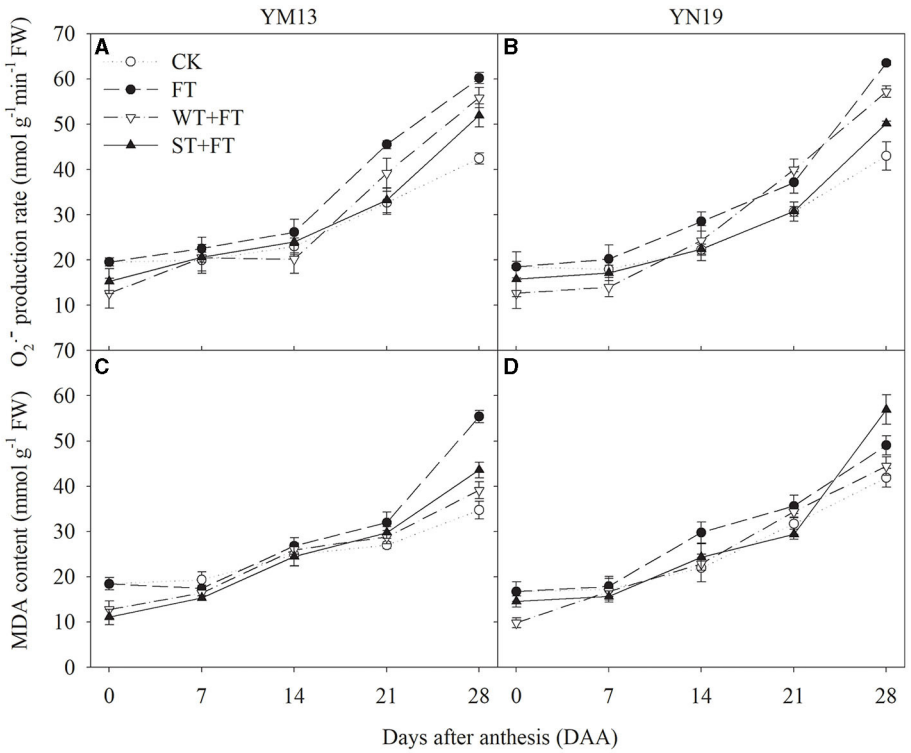

FIGURE 6 | Impact of a night warming treatment in winter or spring on the rate of superoxide anion generation ($O_2^{\bullet -}$) **(A,B)** and the malondialdehyde level (MAD) **(C,D)** in wheat flag leaves later treated with night warming during the grain-filling period.

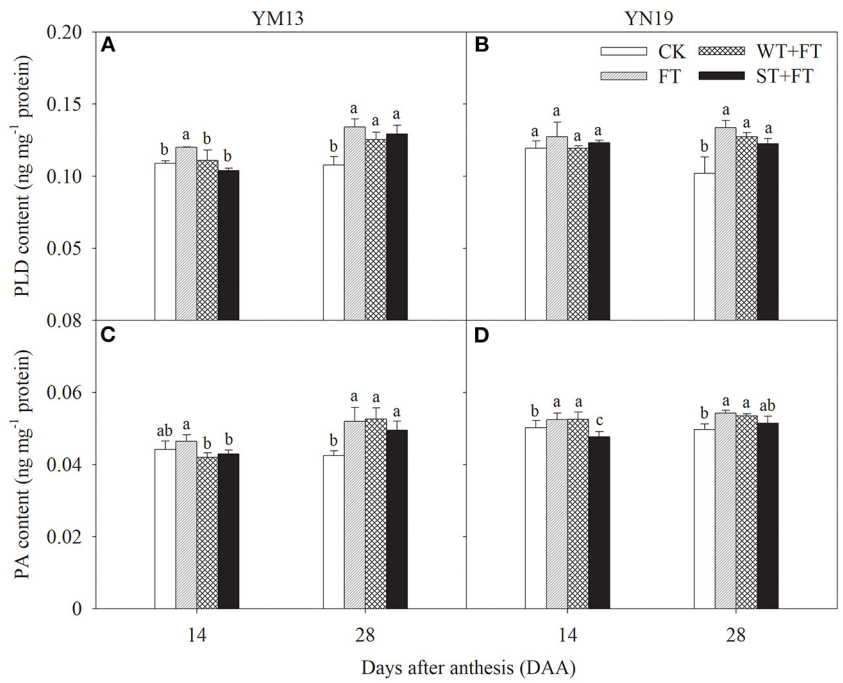

FIGURE 7 | Impact of a night warming treatment in winter or spring on the phospholipase D (PLD) **(A,B)** and phosphatidic acid (PA) contents **(C,D)** in wheat plants later treated with night warming during the grain-filling period. Different lowercase letters indicate significant differences between treatments ($p < 0.05$) hereinafter.

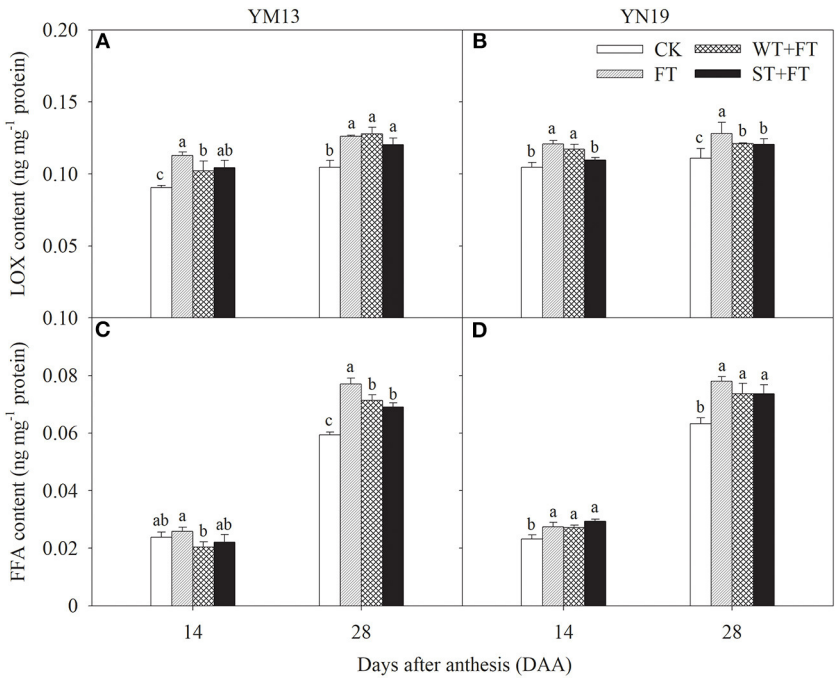

FIGURE 8 | Impact of a night warming treatment in winter or spring on the lipoxygenase (LOX) **(A,B)** and free fatty acid concentrations (FFA) **(C,D)** in flag leaves of wheat plants later treated with night warming during the grain-filling period. Different lowercase letters indicate significant differences between treatments ($P < 0.05$) hereinafter.

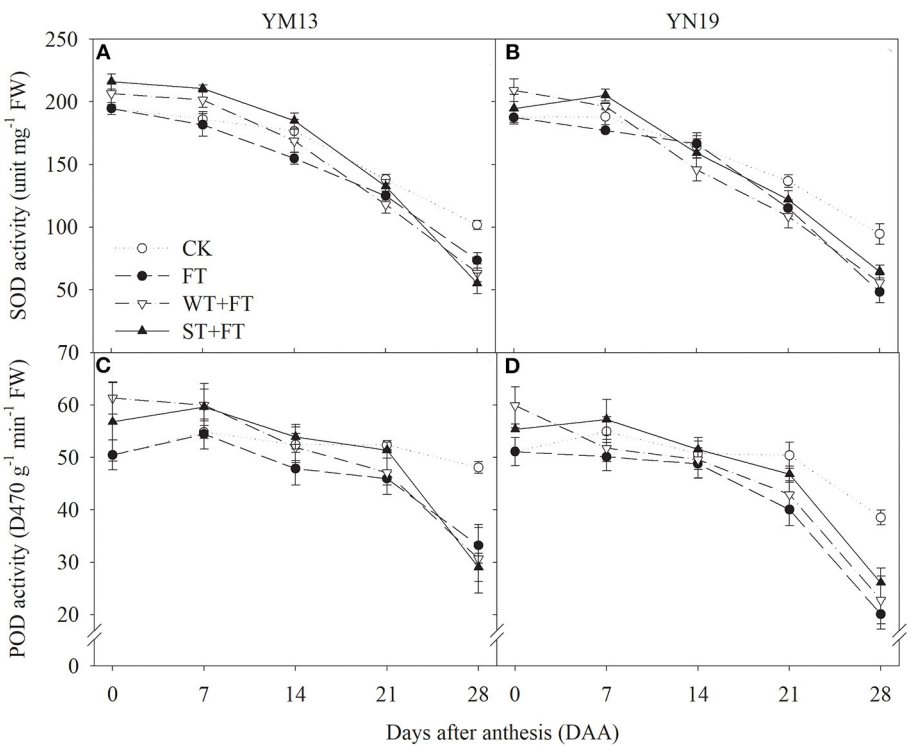

FIGURE 9 | Impact of a night warming treatment in winter or spring on the superoxide dismutase (SOD) **(A,B)** and antioxidant enzyme activities **(C,D)** in the flag leaves of wheat plants later treated with night warming during the grain-filling period.

leaves, exacerbates membrane lipid peroxidation, accelerates plant senescence, and reduces wheat yield. Li et al. (2011) showed that the pre-anthesis waterlogging of wheat plants improved their resistance to post-anthesis waterlogging. Liu et al. (2016) reported that post-anthesis heat stress and its combination with drought significantly decreased *Pn*, and the primed plants showed a significantly higher *Pn* than the non-primed plants under post-anthesis drought and heat stress, suggesting that drought priming enhanced the capacity of the plants to protect photosynthetic activity from exposure to a later stress event. These findings suggest that warming and stresses in an early stage can induce the partial memory of stress-response signals in plants through self-regulation, thereby improving their stress tolerance. The chlorophyll fluorescence parameters of plants change significantly under stress, such as high temperature, and are closely related to the heat resistance of plants (Allakhverdiev et al., 2008). In this study, FT reduced the chlorophyll fluorescence parameters of flag leaves, making them unconducive to the electron transfer needed for photosynthesis. The night-warming priming treatment reduced the negative impact of post-anthesis warming on the chlorophyll fluorescence parameters of wheat flag leaves, thereby maintaining the electron transfer in photosynthesis and the high light use efficiency in flag leaves of wheat plants. This finding indicates that, compared with the non-primed treatment, night-warming priming at the vegetative stage enhanced the photosynthetic capacity and stress tolerance in the flag leaves of winter wheat, which benefited the grain-filling process.

The enzyme Rubisco catalyzes the assimilation of CO_2 by the carboxylation of ribulose diphosphate carboxylase (RuBP) in the Calvin cycle. Rubisco accounts for 50% of the leaf's total soluble protein content and is, therefore, the most obvious target for improving the photosynthetic capacity of crops (Galmés et al., 2014). In this study, the soluble protein and Rubisco contents in post-anthesis flag leaves of the primed plants were higher than those in post-anthesis flag leaves treated with post-anthesis warming. This means that night-warming priming at the vegetative stage could improve flag leaf's photosynthetic carbon assimilation ability and be conducive to the accumulation of photosynthetic products. The response mechanism that resisted the high-temperature stress could have been generated in wheat plants after the night-warming adaptation during winter and spring, which could have prompted a stress-induced tolerance of the wheat plants to post-anthesis warming. The soluble protein content in plant leaves reflected the nitrogen content, and the nitrogen content in the leaves had a positive relation with photosynthetic capacity. Most of the nitrogen in plants is stored in the enzymes that participated in the photosynthesis, especially in Rubisco, which is a major source of nitrogen recycle (Masclaux-Daubresse et al., 2008). The above evidence suggests that the Rubisco and soluble protein contents were relatively high at the post-anthesis stage in the primed plants, which was conducive to increasing photosynthetic capacity and grain yield.

Leaf senescence is associated with increased cellular ROS and increased membrane lipid peroxidation (Lu et al., 2001). Pre- and post-anthesis heat stress has already been shown to reduce photosynthetic rates in wheat through oxidative damage, which accelerates leaf senescence (Wang et al., 2011, 2012). Under heat-stress conditions, higher photosystem efficiency also prevents ROS generation and assists rapid and complete photosystem recovery at normal temperatures (Li et al., 2014). The results of this study showed that, under pre-anthesis night warming, the O_2^- production rate and MDA content in post-anthesis leaves were lower under WT + FT and ST + FT than under FT, indicating that night-warming priming reduced membrane lipid peroxidation in the flag leaves of wheat plants treated with post-anthesis warming. In this study, the behavior of phospholipid metabolism in flag leaves indicated that FT aggravated membrane lipid peroxidation in flag leaves and increased the PLD and LOX contents and PA and FFA production. This result indicates that night-warming priming effectively alleviated the FT-induced degradation of membrane phospholipids in wheat flag leaves, thus alleviating senescence. Wang et al. (2011) reported that pre-anthesis heat priming increases grain yield against subsequent high temperatures during the grain-filling stage, and their finding was attributed to the improved photosynthetic and antioxidative activity in the acclimated plants. Furthermore, SOD and POD, as endogenous protective enzymes, can remove toxic substances, such as ROS, produced during metabolic processes, thereby reducing membrane lipid peroxidation, maintaining normal cellular metabolism, and delaying leaf senescence (Noodén et al., 1997; Zhang et al., 2015). Jing et al. (2020) found that warming in late winter and early spring significantly increased the SOD and POD activities of flag leaves and effectively alleviated their senescence. The results of our study indicate that FT impairs the maintenance of the activity of the antioxidative protection system in post-anthesis flag leaves and that night-warming priming can alleviate the inhibitory effects of FT on the activities of antioxidant enzymes, thus alleviating peroxidative stress. This result indicated that night-warming priming at the vegetative stage increased the antioxidant capacity of flag leaves treated with FT, helped maintain higher cell membrane thermostability (an essential trait related to heat stress tolerance) and the balance between the generation and elimination of ROS, and thereby improved the high-temperature tolerance of post-anthesis wheat plants.

CONCLUSIONS

In summary, the wheat plants treated with winter and spring night warming maintained a high photosynthetic capacity and strong ROS scavenging ability in flag leaves, thus reducing membrane lipid peroxidation and improving plant tolerance, which then contributed to yield formation. Night-warming priming at the vegetative stage proved to be a valuable strategy for triggering plants to initialize an efficient tolerance mechanism, which, in turn, permitted the plants to tolerate post-anthesis warming conditions. Thus, knowledge of the mechanisms underlying temperature adaptation and acclimation in wheat cultivars offers another perspective for understanding how crop performance can be improved under changing climate conditions.

DATA AVAILABILITY STATEMENT

The original contributions presented in the study are included in the article/supplementary material, further inquiries can be directed to the corresponding authors.

AUTHOR CONTRIBUTIONS

YF, ZL, ZH, and TD designed the experiment. YF and ZL conducted the study, collected and analyzed the data, and prepared the draft. TG, YL, and WY helped in sampling and measuring physiological parameters. WZ and SM helped draft the manuscript and interpret the results. All authors contributed to the article and approved the submitted version.

FUNDING

This work was supported by the National Natural Science Foundation of China (U19A2021), the Project of Natural Science Foundation of Anhui Province (2008085qc118), and the Major Science and Technology Special Project of Anhui Province (S202003a06020035). We also acknowledge the support from the Jiangsu Collaborative Innovation Center for Modern Crop Production (JCIC-MCP).

REFERENCES

Allakhverdiev, S. I., Kreslavski, V. D., Klimov, V. V., Los, D. A., Carpentier, R., and Mohanty, P. (2008). Heat stress: an overview of molecular responses in photosynthesis. *Photosynth. Res.* 98, 541–550. doi: 10.1007/s11120-008-9331-0

Asseng, S., Foster, I., and Turner, N. C. (2011). The impact of temperature variability on wheat yields. *Glob. Change Biol.* 17, 997–1012. doi: 10.1111/j.1365-2486.2010.02262.x

Beier, C., Emmett, B., Gundersen, P., Tietema, A., Peñuelas, J., Estiarte, M., et al. (2004). Novel approaches to study climate change effects on terrestrial ecosystems in the field: drought and passive nighttime warming. *Ecosystem* 7, 583–597. doi: 10.1007/s10021-004-0178-8

Bian, X. B., Chen, D. D., Wang, Q. S., and Wang, S. H. (2012). Effects of different day and night temperature enhancements on wheat grain yield and quality after anthesis underfree air controlled condition. *Sci. Agric. Sin.* 8, 1489–1498. doi: 10.3864/j.issn.0578-1752.2012.08.004

Bruce, T. J. A., Matthes, M. C., Napier, J. A., and Pickett, J. A. (2007). Stressful "memories" of plants: Evidence and possible mechanisms. *Plant Sci.* 173, 603–608. doi: 10.1016/j.plantsci.2007.09.002

DeMarco, J., Mack, M. C., Bret-Harte, M. S., Burton, M., and Shaver, G. R. (2014). Long-term experimental warming and nutrient additions increase productivity in tall deciduous shrub tundra. *Ecosphere* 5:72. doi: 10.1890/ES13-00281.1

Deslippe, J. R., Hartmann, M., Mohn, W. W., and Simard, S. W. (2015). Long-term experimental manipulation of climate alters the ectomycorrhizal community of *Betula nana* in Arctic tundra. *Glob. Change Biol.* 17, 1625–1636. doi: 10.1111/j.1365-2486.2010.02318.x

Fan, Y. H., Ma, C. H., Huang, Z. L., Abid, M., Jiang, S. Y., Dai, T. B., et al. (2018). Heat priming during early reproductive stages enhances thermotolerance to post-anthesis heat stress *via* improving photosynthesis and plant productivity in winter wheat (*Triticum aestivum* L.). *Front. Plant Sci.* 9:805. doi: 10.3389/fpls.2018.00805

Feng, B., Liu, P., Li, G., Dong, S. T., Wang, F. H., Kong, L. A., et al. (2014). Effect of heat stress on the photosynthetic characteristics in flag leaves at the grain-filling stage of different heat-resistant winter wheat varieties. *J. Agro. Crop Sci.* 200, 143–155. doi: 10.1111/jac.12045

Galmés, J., Conesa, M. À., Díaz-Espejo, A., Mir, A., Perdomo, J. A., Niinemets, Ü., et al. (2014). Rubisco catalytic properties optimised for present and future climatic conditions. *Plant Sci.* 226, 61–70. doi: 10.1016/j.plantsci.2014.01.008

Gao, X. J., Shi, Y., and Giorgi, F. (2011). A high resolution simulation of climate change over China. *Sci. China Earth Sci.* 54, 462–472. doi: 10.1007/s11430-010-4035-7

Genty, B., Briantais, J. M., and Baker, N. R. (1989). The relationship between the quantum yield of photosynthetic electron transport and quenching of chlorophyll fluorescence. *Biochim. Biophys. Acta Gen Subj.* 990, 87–92. doi: 10.1016/S0304-4165(89)80016-9

Haines, A. (2003). Climate change 2001: the scientific basis. Contribution of Working Group 1 to the Third Assessment report of the Intergovernmental Panel on Climate Change. *Int. J. Epidemiol.* 32:321. doi: 10.1093/ije/dyg059

Hatfield, J. L., Boote, K. J., Kimball, B. A., Ziska, L. H., Izaurralde, R. C., Ort, D., et al. (2011). Climate impacts on agriculture: implications for crop production. *Agron. J.* 103, 351–370. doi: 10.2134/agronj2010.0303

Huebner, F. R., and Bietz, J. A. (1988). Quantitative variation among gliadins of wheats grown in different environments. *Cereal Chem.* 65, 362–366.

Huffaker, R. C. (1990). Tansley review No. 25 proteolytic activity during senescence of plants. *New phytol.* 116, 199–231. doi: 10.1111/j.1469-8137.1990.tb04710.x

Hütsch, B. W., Jahn, D., and Schubert, S. (2018). Grain yield of wheat (*Triticum aestivum* L.) under long-term heat stress is sink-limited with stronger inhibition of kernel setting than grain filling. *J. Agro. Crop Sci.* 205, 22–32. doi: 10.1111/jac.12298

Jing, J. G., Guo, S. Y., Li, Y. F., and Li, W. H. (2020). The alleviating effect of exogenous polyamines on heat stress susceptibility of different heat resistant wheat (*Triticum aestivum* L.) varieties. *Sci. Rep.* 10, 7467. doi: 10.1038/s41598-020-64468-5

Karim, M. R., Islam, M. A., Hossain, M. A., Ahmed, M. K., and Haque, M. S. (2020). Heat stress differentially regulates wheat genotypes in respect of the contribution of culm reserves to grain yield. *J. Bangl. Agric. Univ.* 18, 894–900. doi: 10.5455/JBAU.127741

Kong, L. A., Sun, M. Z., Xie, Y., Wang, F. H., and Zhao, Z. D. (2015). Photochemical and antioxidative responses of the glume and flag leaf to seasonal senescence in wheat. *Front. Plant Sci.* 6:358. doi: 10.3389/fpls.2015.00358

Kong, L. A., Xie, Y., Hu, L., Si, J. S., and Wang, Z. S. (2017). Excessive nitrogen application dampens antioxidant capacity and grain filling in wheat as revealed by metabolic and physiological analyses. *Sci. Rep.* 7:43363. doi: 10.1038/srep43363

Lee, R. H., Wang, C. H., Huang, L. T., and Chen, S. C. G. (2001). Leaf senescence in rice plants: cloning and characterization of senescence up-regulated genes. *J. Exp. Bot.* 52, 1117–1121. doi: 10.1093/jexbot/52.358.1117

Li, C. Y., Jiang, D., Wollenweber, B., Li, Y., Dai, T. B., and Cao, W. X. (2011). Waterlogging pretreatment during vegetative growth improves tolerance to waterlogging after anthesis in wheat. *Plant Sci.* 180, 672–678. doi: 10.1016/j.plantsci.2011.01.009

Li, X. N., Cai, J., Liu, F. L., Dai, T. B., Cao, W. X., and Dong, J. (2014). Cold priming drives the sub-cellular antioxidant systems to protect photosynthetic electron transport against subsequent low temperature stress in winter wheat. *Plant Physiol. Biochem.* 82, 34–43. doi: 10.1016/j.plaphy.2014.05.005

Liu, S., Li, X., Larsen, D. H., Zhu, X., Song, F., and Liu, F. (2016). drought priming at vegetative growth stage enhances nitrogen-use efficiency under post-anthesis drought and heat stress in wheat. *J. Agro. Crop Sci.* 203, 29–40. doi: 10.1111/jac.12190

Lobell, D. B., Sibley, A., and Ortiz-Monasterio, J. I. (2012). Extreme heat effects on wheat senescence in India. *Nat. Clim. Chang.* 2, 186–189. doi: 10.1038/nclimate1356

Lowry, O. H., Rosebrough, N. J., Farr, A. L., and Randall, R. J. (1951). Protein measurement with the Folin phenol reagent. *J. Biol Chem.* 193, 256–275. doi: 10.1016/S0021-9258(19)52451-6

Lu, C. M., Lu, Q. T., Zhang, J. H., and Kuang, T. Y. (2001). Characterization of photosynthetic pigment composition, photosystem II photochemistry and

thermal energy dissipation during leaf senescence of wheat plants grown in the field. *J. Exp. bot*. 52, 1805–1810. doi: 10.1093/jexbot/52.362.1805

Makino, A., Mae, T., and Ohira, K. (1986). Colorimetric measurement of protein stained with coomassie brilliant blue R on sodium dodecyl sulfate-polyacrylamide gel electrophoresis by eluting with formamide. *Agric. Biol. Chem*. 50, 1911–1912. doi: 10.1271/bbb1961.50.1911

Makino, A., Shimada, T., Takumi, S., Kaneko, K., Matsuoka, M., Shimamoto, K., et al. (1997). Does decrease in ribulose-1,5-bisphosphate carboxylase by antisense *Rbc*S lead to a higher N-use efficiency of photosynthesis under conditions of saturating CO_2 and light in rice plants? *Plant Physiol*. 114, 483–491. doi: 10.1104/pp.114.2.483

Martinez, C. A., Bianconi, M., Silva, L., Approbato, A., Lemos, M., Santos, L., et al. (2014). Moderate warming increases PSII performance, antioxidant scavenging systems and biomass production in *Stylosanthes capitata* Vogel. *Environ. Exp. Bot*. 102, 58–67. doi: 10.1016/j.envexpbot.2014.02.001

Masclaux-Daubresse, C., Reisdorf-Cren, M., and Orsel, M. (2008). Leaf nitrogen remobilisation for plant development and grain filling. *Plant Biol*. 10, 23–36. doi: 10.1111/j.1438-8677.2008.00097.x

Noodén, L. D., Guiamét, J. J., and John, I. (1997). Senescence mechanisms. *Physiol. Plant*. 101, 746–753. doi: 10.1034/j.1399-3054.1997.1010410.x

Osman, R., Zhu, Y., Cao, W. X., Ding, Z. F., Wang, M., Liu, L. L., et al. (2020). Modeling the effects of extreme high-temperature stress at anthesis and grain filling on grain protein in winter wheat. *Crop J*. 9, 889–900. doi: 10.1016/j.cj.2020.10.001

Prieto, P., Peñuelas, J., Llusi,à, J., Asensio, D., and Estiarte, M. (2009). Effects of long-term experimental night-time warming and drought on photosynthesis, *Fv*/*Fm* and stomatal conductance in the dominant species of a Mediterranean shrubland. *Acta Physiol. Plant* 31, 729–739. doi: 10.1007/s11738-009-0285-4

Qin, N. X., Chen, X., Fu, G., Zhai, J. Q., and Xue, X. W. (2010). Precipitation and temperature trends for the Southwest China: 1960–2007. *Hydrol. Process.* 24, 3733–3744. doi: 10.1002/hyp.7792

Ren, G. Y., Zhou, Y. Q., Chu, Z. Y., Zhou, J. X., Zhang, A. Y., Guo, J., et al. (2008). Urbanization effects on observed surface air temperature trends in North China. *J. Clim.* 21, 1333–1348. doi: 10.1175/2007JCLI1348.1

Riaz, M. W., Yang, L., Yousaf, M. I., Sami, A., Mei, X. D., Shah, L., et al. (2021). Effects of heat stress on growth, physiology of plants, yield and grain quality of different spring wheat (*Triticum aestivum* L.) genotypes. *Sustainability* 13, 1–18. doi: 10.3390/su13052972

Savin, R., and Nicolas, M. E. (1996). Effects of short periods of drought and high temperature on grain growth and starch accumulation of two malting barley cultivars. *Funct. Plant Biol.* 23, 201–210. doi: 10.1071/PP9960201

Selote, D. S., and Khanna-Chopra, R. (2006). Drought acclimation confers oxidative stress tolerance by inducing co-ordinated antioxidant defense at cellular and subcellular level in leaves of wheat seedlings. *Physiol. Plant* 127, 494–506. doi: 10.1111/j.1399-3054.2006.00678.x

Shaver, G. R., Johnson, L. C., Cades, D. H., Murray, G., Laundre, J. A., Rastetter, E. B., et al. (1998). Biomass and CO_2 flux in wet sedge tundrss: responses to nutrients, temperature, and light. *Ecol. Monogr*. 68, 75–97. doi: 10.1890/0012-9615(1998)0680075:BACFIW2.0.CO;2

Shirdelmoghanloo, H., Cozzolino, D., Lohraseb, I., and Collins, N. C. (2016). Truncation of grain filling in wheat (*Triticum aestivum*) triggered by brief heat stress during early grain filling: association with senescence responses and reductions in stem reserves. *Funct. Plant Biol.* 43, 919–930. doi: 10.1071/FP15384

Slafer, G. A. (2003). Genetic basis of yield as viewed from a crop physiologist's perspective. *Ann. Appl. Biol*. 142, 117–128. doi: 10.1111/j.1744-7348.2003.tb00237.x

Sui, N., Li, M., Liu, X. Y., Wang, N., Fang, W., and Meng, Q. W. (2007). Response of xanthophyll cycle and chloroplastic antioxidant enzymes to chilling stress in tomato over-expressing glycerol-3-phosphate acyltransferase gene. *Photosynthetica* 45, 447–454. doi: 10.1007/s11099-007-0074-5

Thayna, M., Eva, R., Benita, H., and CarlOtto, O. (2018). Heat priming effects on anthesis heat stress in wheat cultivars (*Triticum aestivum* L.) with contrasting tolerance to heat stress. *Plant Physiol. Biochem.* 132, 213–221 doi: 10.1016/j.plaphy.2018.09.002

Tian, Y. L., Chen, J., Chen, C. Q., Deng, A. X., Song, Z. W., Zheng, C. Y., et al. (2012). Warming impacts on winter wheat phenophase and grain yield under field conditions in Yangtze Delta Plain, China. *Field Crop. Res*. 134, 193–199. doi: 10.1016/j.fcr.2012.05.013

Wang, X., Cai, J., Jiang, D., Liu, F. L., Dai, T. B., and Cao, W. X. (2011). Pre-anthesis high-temperature acclimation alleviates damage to the flag leaf caused by post-anthesis heat stress in wheat. *J. Plant Physiol*. 168, 585–593. doi: 10.1016/j.jplph.2010.09.016

Wang, X., Cai, J., Liu, F. L., Jin, M., Yu, H. X., Jiang, D., et al. (2012). Pre-anthesis high temperature acclimation alleviates the negative effects of post-anthesis heat stress on stem stored carbohydrates remobilization and grain starch accumulation in wheat. *J. Cereal Sci.* 55, 331–336. doi: 10.1016/j.jcs.2012.01.004

Wang, X., Liu, F. L., and Jiang, D. (2017). Priming: a promising strategy for crop production in response to future climate. *J. Integr. Agric.* 16, 2709–2716. doi: 10.1016/S2095-3119(17)61786-6

Yang, S. H., Wang, L. J., and Li, S. H. (2007). Ultraviolet-B irradiation-induced freezing tolerance in relation to antioxidant system in winter wheat (*Triticum aestivum* L.) leaves. *Environ. Exp. Bot*. 60, 300–307. doi: 10.1016/j.envexpbot.2006.12.03

You, Q. L., Kang, S. C., Aguilar, E., Pepin, N., Flügel, W., Yan, Y. P., et al. (2011). Changes in daily climate extremes in China and their connection to the large scale atmospheric circulation during 1961–2003. *Clim. Dyn*. 36, 2399–2417. doi: 10.1007/s00382-009-0735-0

Zadoks, J. C., Chang, T. T., and Konzak, C. F. (1974). A decimal code for the growth stages of cereals. *Weed Res.* 14, 415–421. doi: 10.1111/j.1365-3180.1974.tb01084.x

Zhang, Y. H., Yang, Y. M., Cao, L., Hao, Y. F., Huang, J., Li, J. P., et al. (2015). Effect of high temperature on photosynthetic capability and antioxidant enzyme activity of flag leaf and non-leaf organs in wheat. *Acta Agron. Sin*. 41, 36–144. doi: 10.3724/SP.J.1006.2015.00136

Zhao, P., Yang, S., and Yu, R. C. (2010). Long-term changes in rainfall over eastern china and large-scale atmospheric circulation associated with recent global warming. *J. Clim.* 23, 1544–1562. doi: 10.1175/2009JCLI2660.1

Zheng, C. F., Jiang, D., Liu, F. L., Dai, T. B., Jing, Q., and Cao, W. X. (2009). Effects of salt and waterlogging stresses and their combination on leaf photosynthesis, chloroplast ATP synthesis, and antioxidant capacity in wheat. *Plant Sci*. 176, 575–582. doi: 10.1016/j.plantsci.2009.01.015

Conflict of Interest: The authors declare that the research was conducted in the absence of any commercial or financial relationships that could be construed as a potential conflict of interest.

Publisher's Note: All claims expressed in this article are solely those of the authors and do not necessarily represent those of their affiliated organizations, or those of the publisher, the editors and the reviewers. Any product that may be evaluated in this article, or claim that may be made by its manufacturer, is not guaranteed or endorsed by the publisher.

frontiers in Plant Science

ORIGINAL RESEARCH
published: 21 October 2021
doi: 10.3389/fpls.2021.746180

Effects of High Temperature on Rice Grain Development and Quality Formation Based on Proteomics Comparative Analysis Under Field Warming

Wenzhe Liu[1], *Tongyang Yin*[1], *Yufei Zhao*[1], *Xueqin Wang*[1], *Kailu Wang*[1], *Yingying Shen*[1], *Yanfeng Ding*[1,2] *and She Tang*[1,2*]

[1] College of Agronomy, Nanjing Agricultural University, Nanjing, China, [2] Jiangsu Collaborative Innovation Center for Modern Crop Production, Nanjing, China

OPEN ACCESS

Edited by:
Yingyin Yao,
China Agricultural University, China

Reviewed by:
Kaushal Kumar Bhati,
Catholic University of Louvain, Belgium
Mohamed Sheteiwy,
Mansoura University, Egypt
Shuwei Liu,
Shandong University, China

***Correspondence:**
She Tang
tangshe@njau.edu.cn

Specialty section:
This article was submitted to Crop and Product Physiology, a section of the journal Frontiers in Plant Science

Received: 23 July 2021
Accepted: 23 September 2021
Published: 21 October 2021

Citation:
Liu W, Yin T, Zhao Y, Wang X, Wang K, Shen Y, Ding Y and Tang S (2021) Effects of High Temperature on Rice Grain Development and Quality Formation Based on Proteomics Comparative Analysis Under Field Warming. Front. Plant Sci. 12:746180. doi: 10.3389/fpls.2021.746180

With the intensification of global warming, rice production is facing new challenges. Field evidence indicates that elevated temperature during rice grain-filling leads to the further deterioration of grain quality. In order to clarify the potential regulatory mechanism of elevated temperature on the formation of rice quality, the DIA mass spectrometry method under the background of field warming was conducted to investigate the regulatory effects of high temperature on grain development and material accumulation pathways. The results showed that a total of 840 differentially expressed proteins were identified during the grain-filling process under elevated temperature. These differentially expressed proteins participated in carbon metabolism, amino acid biosynthesis, signal transduction, protein synthesis, and alternately affected the material accumulation of rice grains. The significant up-regulation of PPROL 14E, PSB28, granule-bound starch synthase I, and the significant down-regulation of 26.7 kDa heat shock protein would lead to the component difference in grain starch and storage proteins, and that could be responsible for the degradation of rice quality under elevated temperature. Results suggested that proteins specifically expressed under elevated temperature could be the key candidates for elucidating the potential regulatory mechanism of warming on rice development and quality formation. In-depth study on the metabolism of storage compounds would be contributed in further proposing high-quality cultivation control measures suitable for climate warming.

Keywords: rice, global warming, proteomics, data-independent acquisition, grain quality

INTRODUCTION

With the improvement of people's living standards, high-quality rice is more preferred by the rice production and consumption market. However, with the rapid development of industrialization, human activities are estimated to have caused ~1.0°C of global warming above pre-industrial levels (IPCC, 2018). According to the fifth assessment report (AR5) completed by the IPCC

(Intergovernmental Panel on Climate Change), it is estimated that the global temperature is expected to be raised by 1.4–5.8°C in 2100 (IPCC, 2014). The abnormal high temperature would seriously affect the normal growth and development rhythm of rice, and ultimately affect the yield and quality of rice (Jagadish, 2020; Xu et al., 2020). The results of our 10-year field trials showed that rice quality formation generally exhibited negative response characteristics when exposed to elevated temperature. Among them, the increase in temperature have led to the significant increase in chalkiness and the decrease in milling quality of rice, which extremely reduces the purchase expectations and market value of rice (Dou et al., 2017). Therefore, exploring the response mechanism of rice quality under climate change is of great significance for guiding the production of high-quality rice in the future.

As the decisive stage of rice quality formation, grain-filling is the most sensitive period to external temperature. Grain development is accompanied by filling and accumulation of storage substances such as starch, storage protein and lipids, which ultimately determine the relevant indicators of rice quality. As the most abundant components in rice grain, starch had been proved to be sensitive to elevated temperature. Our previous study showed that the accumulation of total starch and amylose in early grain-filling stage was accelerated under the condition of elevated temperature, but the accumulation speed in later stage was significantly decreased, which resulted in the lower content of amylose and total starch in mature grain compared to normal temperature treatment (Tang et al., 2019). In addition, elevated temperature during grain-filling increased the contents of grain storage proteins, with a significantly increased composition of glutelin and decreased prolamin. However, rice with high protein content is more prone to spoilage during storage, and the appearance and eating quality of rice could be further declined (Cao et al., 2017). Furthermore, the activity of protease was enhanced under elevated temperature, and further accelerated the protein transformation into soluble nitrogen compounds, which would significantly increase the total amount of amino acids in rice grains. Overall, elevated temperature mainly accelerated the rate of grain-filling and shortened its active duration, resulting in insufficient accumulation of photosynthetic substances in rice grains (Wahid et al., 2007; Kim et al., 2011). In our previous studies, temperature changes were mainly manifested as abnormal grain development and changes in the accumulation and balance of starch and storage proteins, which synergistically determine the formation of grain quality (Dou et al., 2017; Tang et al., 2018). Although we have obtained the physiological and biochemical evidence of high temperature in regulating grain storage material accumulation through field trials, the regulation mechanism remains to be further elucidated. The synthesis and anabolism of rice starch and proteins is a relatively complex process, including a series of metabolic processes such as synthesis, transport, modification, and accumulation, and it is still difficult to fully grasp the mechanism. Therefore, the main purpose of this study is to further clarify the key regulatory factors involved in grain quality formation under actual paddy field warming scenarios based on the high-throughput proteomics analysis method. An in-depth understanding of the regulation mechanism of climate warming on the synthesis and metabolism of grain storage materials has important practical significance for further establishing high-quality rice cultivation methods under climate warming.

RESULTS

Effects of Elevated Temperature on Rice Quality and Accumulation of Grain Storage Materials

An increase of 1.6°-3.1°C in temperature during grain-filling stage induced various changes in the accumulation of storage materials during grain development, and that further affected the rice yield and quality indicators. Results showed that tested rice yield in warming treatment was 21% lower than that of the normal temperature treatment (**Table 1**). Meanwhile, the elevated temperature increased grain thickness and decreased grain length, and there was no significant change in grain width and aspect ratio of grain shape. Compared with normal temperature, rice chalky rate (36.5%), chalky area (103.3%), and chalkiness (176.4%) were significantly increased under the field warming. Compared with normal temperature, the milled rice rate and head rice rate were significantly reduced by 3.9 and 5.5%. Therefore, based on the field evidence, warming during grain-filling stage led to the overall deterioration in the appearance quality of rice and elevated temperature also had a significant negative effect on rice milling quality.

Starch and storage proteins are the main substances that constitute the grain storage material. Under elevated temperature conditions, grain total starches were increased significantly, of which amylopectin was significant increased when responded to high temperature, while amylose was decreased significantly compared with normal temperature treatment. These changes further induced the changes in the proportion of amylopectin/amylose in rice grains. The response of grain storage protein components to elevated temperature showed a significant increase in glutelin and a significant decrease in prolamin. Elevated temperature also induced significant changes in rice cooking quality indicators. Results indicated that the gelatinization characteristics peak viscosity (PKV), hot-paste viscosity (HPV), and gelatinization temperature (GT) were significant increased and the final viscosity was decreased (**Table 1**). These results suggested that elevated temperature during grain-filling stage have a general negative impact on rice quality parameters.

Quantitative Expression of Rice Grain Proteins Under Elevated Temperature

In order to further explore the regulation mechanism of elevated temperature on rice quality formation, A quantitative proteomics method was used and results showed that a total of 23,968 unique peptides and 5,872 unique proteins were identified (**Supplementary Tables 1–6**). The expression and annotation proteins identified in each period were listed and Pearson correlation analysis showed the repeatability of these protein samples was above 97% (**Figure 1**). Furthermore, proteins were

TABLE 1 | Effects of temperature on grain yield and quality traits of rice.

Treatment	Length (mm)	Width (mm)	Thickness (mm)	Length/Width	Chalky rate (%)	Chalky area (%)	Chalkiness (%)	
CK	4.53a	2.30a	2.07b	1.98a	48.67b	19.43b	9.51b	
ET	4.33b	2.37a	2.13a	1.84a	66.42a	39.50a	26.29a	
Treatment	**Total starch (%)**	**Amylopectin (%)**	**Amylose (%)**	**Amylopectin/Amylose**	**Albumin (μg/g)**	**Globulin (μg/g)**	**Prolamin (μg/g)**	**Glutelin (μg/g)**
CK	66.38b	54.95b	11.43a	4.81b	69.7a	65.4a	128.5a	836.3b
ET	70.17a	60.03a	10.14b	5.92a	68.2a	63.8a	113.4b	1092.7a
Treatment	**Spikelets per panicle ($\times 10^4 \cdot hm^{-2}$)**	**Panicles per panicle**	**1,000-grain weight (g)**	**Seed setting rate (%)**	**Yield (*t*)**	**Brown rice rate (%)**	**Milled rice rate (%)**	**Head rice rate (%)**
CK	471.13a	114.17a	25.03a	95.45a	12.85a	85.90a	76.30a	75.61a
ET	457.11b	104.53b	23.22b	91.47b	10.15b	83.41b	73.31b	71.47b
Treatment	**Peak viscosity**	**Hot paste viscosity**	**Breakdown**	**Final viscosity**	**Setback**	**Peak time (min)**	**Pasting temperature (°C)**	
CK	2881b	1573.5b	1498.5b	2466a	−337a	6.1a	73.3b	
ET	3264.5a	1602.5a	1726a	2351b	−924.5b	5.8b	76.7a	

Values with different letters in the same column are significantly different with $p < 0.05$; CK, normal temperature; ET, elevated temperature.

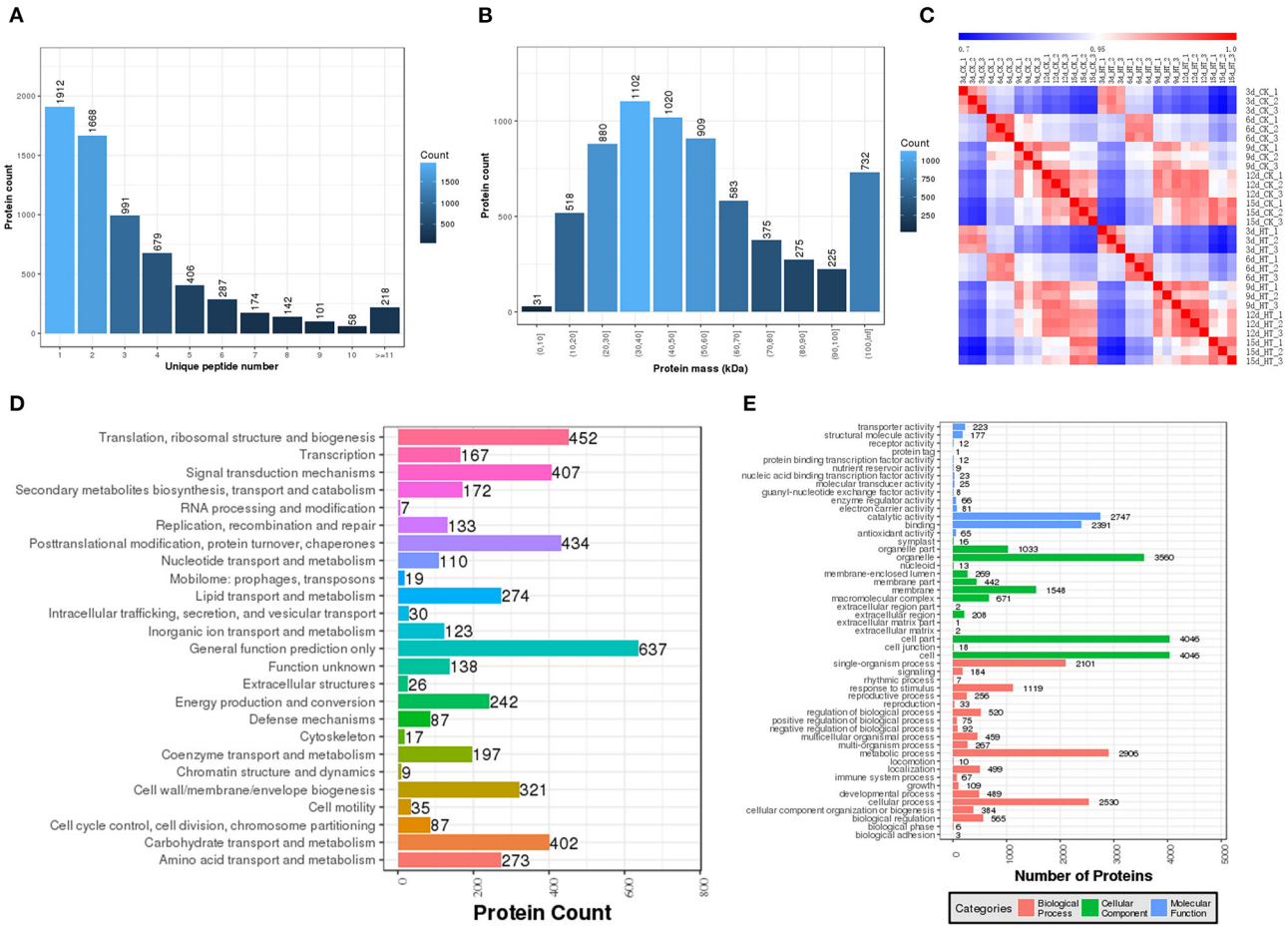

FIGURE 1 | Proteins identified to be responsive to elevated temperature treatment. **(A)** Proteins distributed on the basis of their mass; **(B)** Numbers of unique peptides that were matched to proteins; **(C)** Pearson correlation coefficient; **(D)** GO function classification; **(E)** COG function classification.

enriched with COG and GO to perform functional analysis, and results showed that the effect of elevated temperature was mainly in regulating the translation, post-translational modification, protein conversion, and signal transduction during the grain-filling stage.

Differentially expressed proteins (DEPs) (Fold change $\geq$2 and $P < 0.05$) were identified with three biological replicates. Results showed that 112 DEPs were identified in ET-3d (3d after flowering under elevated temperature treatment) and CK-3d (3d after flowering under normal temperature treatment) groups, of which 66 were upregulated and 46 were downregulated. In ET-6d and CK-6d treatments, 118 DEPs were identified, of which 51 were up-regulated and 67 were down-regulated. Comparing to the CK-9d, 65 proteins were up-regulated and 201 proteins were down-regulated in the ET-9d. In ET-12d and CK-12d treatments, 144 DEPs were identified, of which 59 were up-regulated and 85 were down-regulated. In addition, 200 DEPs were found during the 15d after flowering, including 30 up-regulated and 170 down-regulated proteins. The volcano plots and protein annotation of DEPs in ET and CK (3d, 6d, 9d, 12d, and 15d) treatments are shown in **Figure 2** and **Supplementary Table 2**. GO enrichment analysis showed that the prominent GO terms for cellular component enriched by five stages were the vesicle, nucleus, macromolecular complex, non-membrane-bounded organelle, and protein complex. Based on the molecular function, the DEPs were mainly classified into pyrophosphatase activity, hydrolase activity and nucleoside-triphosphatase activity. The top GO molecular function categories were enriched by ET-12d and CK-12d DEPs, including the response to stress, nucleic acid metabolic process and DNA metabolic process (**Figure 3**).

Differentially expressed proteins were further classified into five stages through KEGG pathway ($P < 0.05$). Metabolic pathways affected under elevated temperature in ET-3d and CK-3d were photosynthesis-antenna proteins, metabolism of xenobiotics by cytochrome P450, photosynthesis, axon guidance, retinol metabolism (**Figure 4**). In ET-6d and CK-6d, the main pathways were homologous recombination, AMPK signaling pathway, inositol phosphate metabolism, plant hormone signal transduction, ether lipid metabolism, MAPK signaling pathway-plant. Among these, the metabolic pathways enriched in

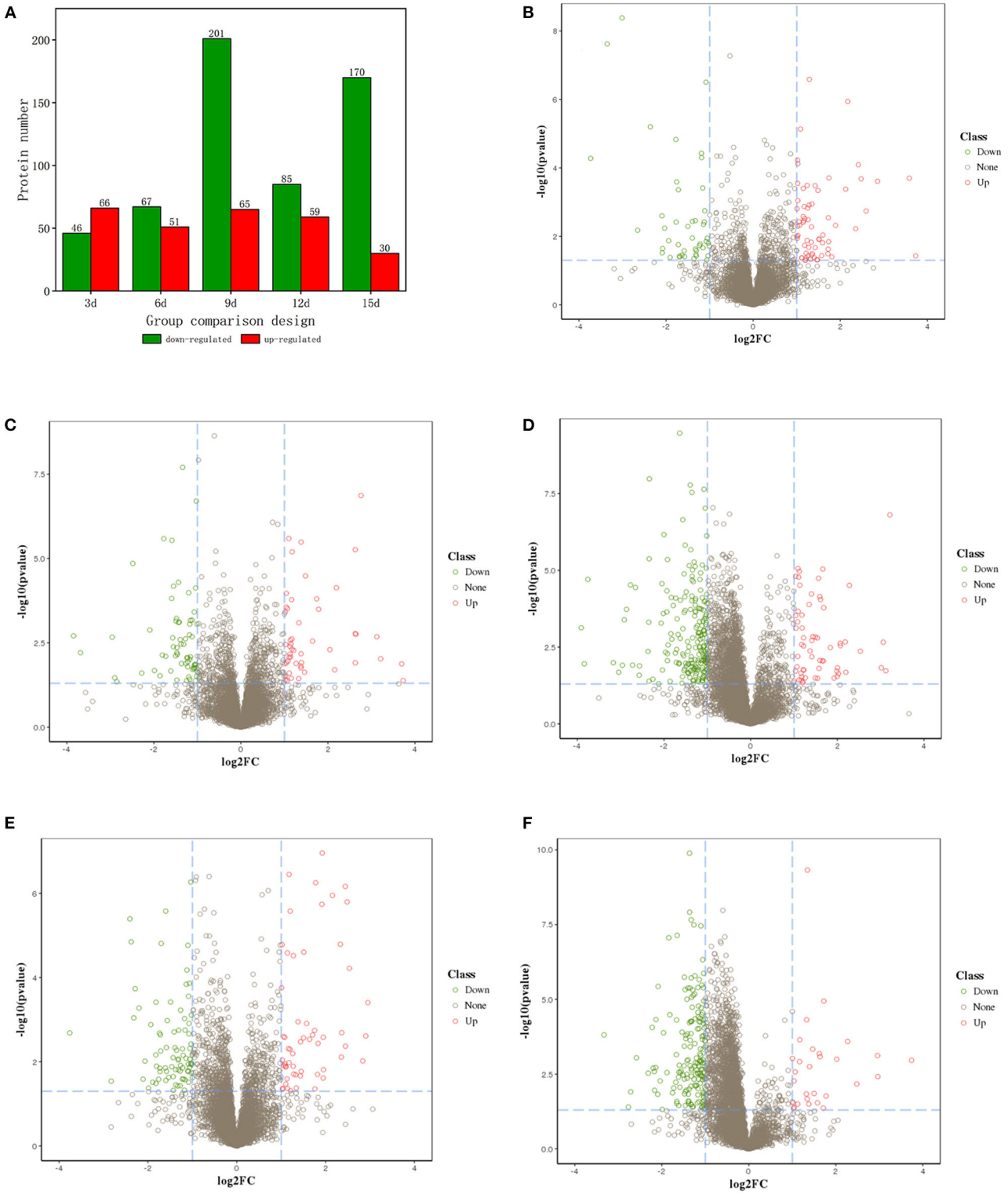

FIGURE 2 | Volcano plots of proteins with differential expression under elevated temperature. **(A)** Number of DEPs in different stages. **(B–F)** Are volcano plots of different expressed proteins on the 3rd, 6th, 9th, 12th, and 15th days after flowering, respectively.

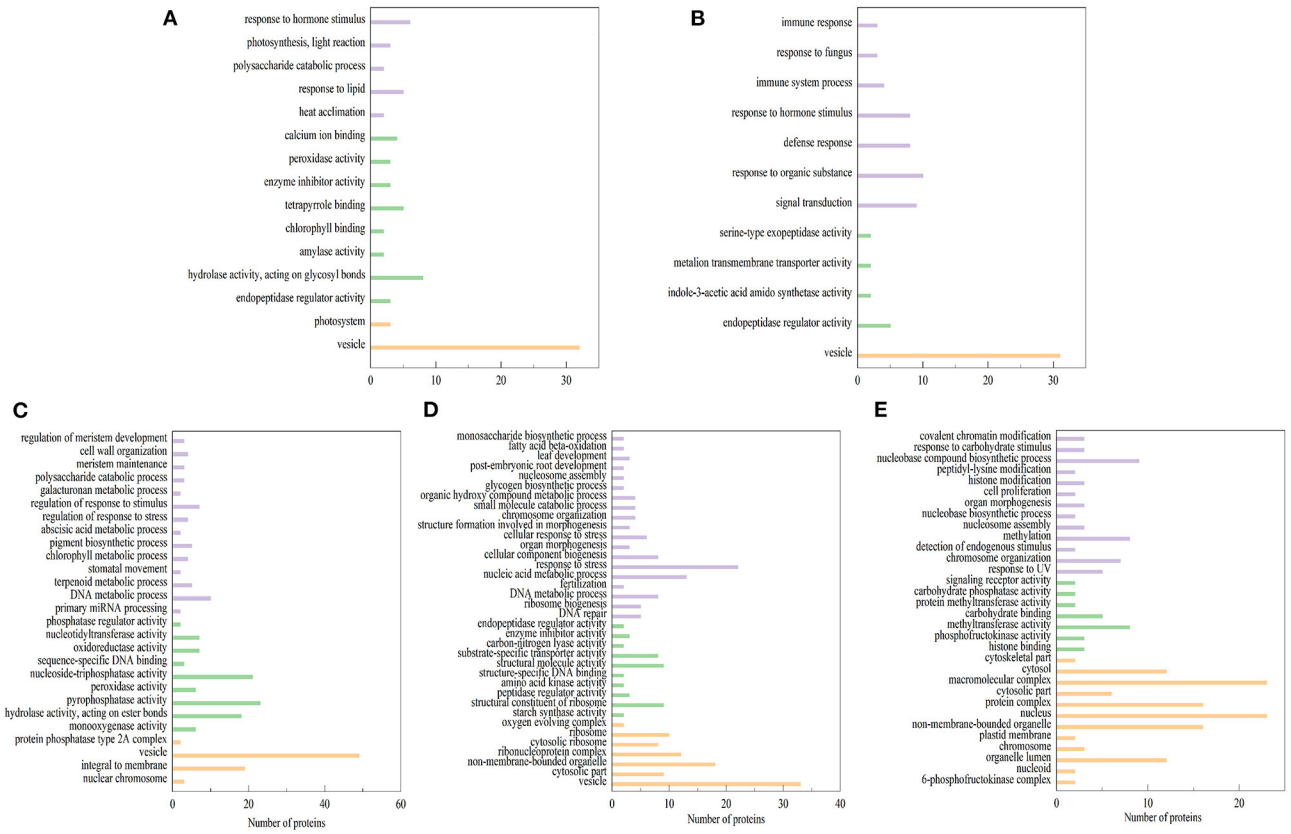

FIGURE 3 | Gene ontology (GO) term enrichment for differentially expressed proteins under elevated temperature. **(A–E)** GO terms (biological process: purple, cellular component: yellow, and molecular function: green) enriched by proteins with differential expression in ET-3d VS CK-3d **(A)**, ET-6d VS CK-6d **(B)**, ET-9d VS CK-9d **(C)**, ET-12d VS CK-12d **(D)**, and ET-15d VS CK-15d **(E)** groups, respectively.

ET-9d and CK-9d mainly include mannose type O-glycan biosynthesis, porphyrin and chlorophyll metabolism, tryptophan metabolism, ABC transporters, phenylpropanoid biosynthesis, isoflavonoid biosynthesis, other types of O-glycan biosynthesis, limonene, and pinene degradation. DEPs identified through pathway enrichment analysis of ET-12d and CK-12d were mainly enriched in ribosome, homologous recombination, C5-Branched dibasic acid metabolism. Furthermore, fructose and mannose metabolism, adipocytokine signaling and indole alkaloid biosynthesis metabolic pathways were found to be more sensitive to elevated temperature at the 15d after flowering, and that indicated the temperature had significantly different regulating effects on different stages of grain development.

Identification of Differentially Expressed Proteins Related to Rice Development and Quality Formation

A total of 748 unique proteins were identified based on their specific expressions when exposed to elevated temperature. After removing 302 proteins with lower scores and unknown functional classification, 39 proteins related to rice development and quality formation were distinguished (**Table 2**, **Figure 5**). In this study, the expression of 16.9 kDa class I heat shock protein in rice grains was significantly reduced at the 3d after heating, with a down-regulation of 84% compared with CK treatment. However, the expression of heat shock factor binding protein 1 involved in heat shock protein synthesis was significantly increased. Furthermore, at the early stage of grain filling, the expression of HSP70 decreased significantly, and the expression on the 3rd, 6th, and 9th day after flowering was only 0.47, 0.5, and 0.43 folds that of normal temperature treatment, respectively. Results showed the most significant change was the 26.7 kDa heat shock protein of the sHSPs family, and its expression was increased significantly at 6, 9, and 12 days after flowering, with 6.78, 3.06, and 5.44 folds compared to the CK treatment. Expressions of 18.0 kda class II heat shock protein, 24.1 kda heat shock protein and heat shock protein 82 were up-regulated at the 12d after flowering (2.26, 2.01, 3.63 folds, respectively) when subjected to elevated temperatures.

Proteins involved in the accumulation of storage protein and starch in rice grains were also significantly affected by the elevated temperature. For example, the glutelin type-A 3, glutelin type-B 1, glutelin type-B 5-like expression levels of rice grains were significantly up-regulated by 2.79, 2.49, and 3.3 folds, respectively. At the same time, the expression levels

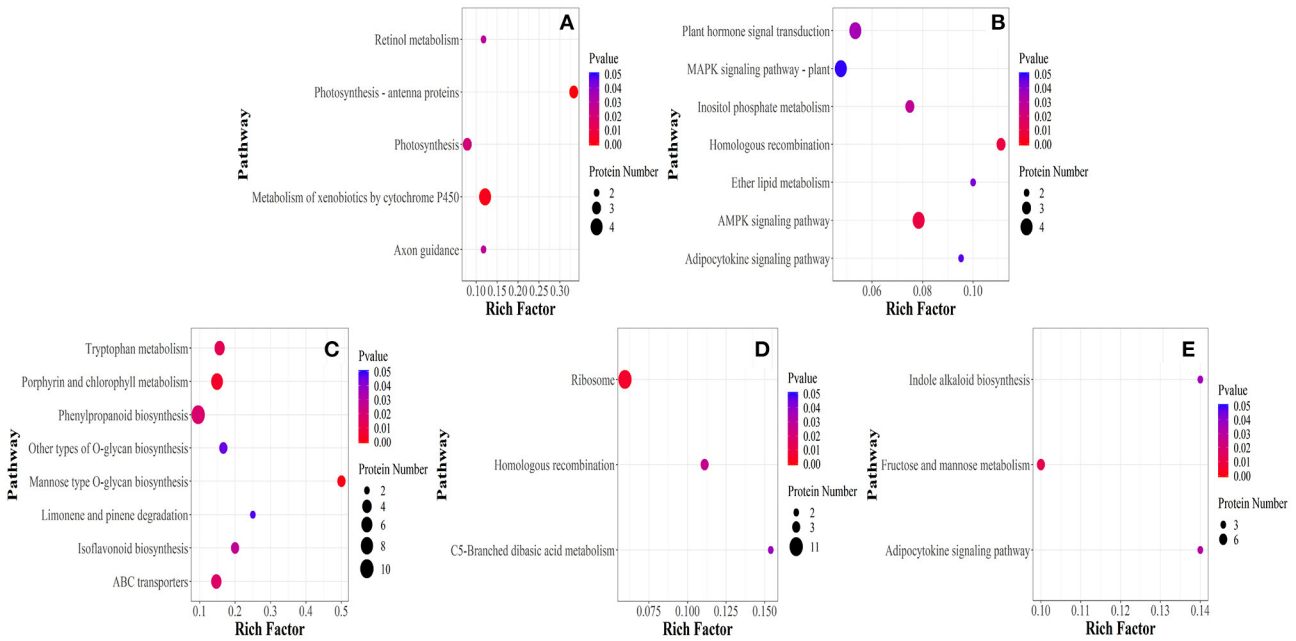

FIGURE 4 | Enrichment of differentially expressed proteins in KEGG pathway under elevated temperature. **(A–E)** Represent the 3rd, 6th, 9th, 12th, and 15th day of samples selected after flowering, respectively.

of glutelin type-B 1-like and glutelin type-B 2-like proteins were decreased significantly. Furthermore, the expression levels of globulin 19 kDa globulin, globulin 1S allele and basic 7S globulin were increased significantly, and that was consistent with the increased content of globulin measured in mature grains. In this study, the significant decrease in prolamin under warming conditions was mainly at the 12d after flowering and expression analysis of prolamin PPROL 14E and prolamin PPROL 14E-like proteins showed that they were both decreased significantly (0.33, 0.38 folds) at this stage when comparted to the normal temperature treatment. As the main component of rice grains, the accumulation of starch has been proved to be sensitive to elevated temperature. Results indicated that enzyme related to starch synthesis during rice starch synthesis were also affected by temperature. In this study, the core starch synthesis-related enzyme GBSS (granule-bound starch synthase) was down-regulated at the 6d after flowering under elevated temperature. While proteins related to amylopectin synthesis obtained no significant changes when compared to the CK. The expression levels of GBSS at 6d, 9d, and 12d after flowering were significantly lower than that of the control and the expression levels of soluble starch synthase responsible for the synthesis of amylopectin SS-IVand SSSII-III were also decreased under the elevated temperature.

Photosynthesis is the process by which light energy is converted into chemical energy and stored, and thus it is essential for the accumulation of rice grain assimilation. Results showed that elevated temperature during the grain filling period had a significant impact on the rice photosynthetic system of rice, which could further affect the formation of the final quality. In this study, the expression levels of the chlorophyll a-b binding protein 1B-21, chlorophyll a-b binding protein P4, and chlorophyll a-b binding protein 7 in chlorophyll ab binding protein were significantly up-regulated at the beginning of grain-filling (2.22, 2.03, 3.3 folds), when compared to the CK. However, the expression of PSB28, which is responsible for water splitting, had a downward trend through the grain-filling stage, and reaching a significant level at 12 days after flowering. Furthermore, TIC 62 (translocon at the inner envelope membrane of chloroplasts) was significantly down-regulated at 9d after flowering, and that may negatively affect the dynamic balance of the proteome in rice grains.

DISCUSSION

Assessment of Field Warming and the Impact on Rice Quality Formation

In order to realistically simulate the characteristics of global warming, the free-air temperature enhancement (FATE) facility was installed in the actual paddy field to perform the warming scenarios during the rice grain-filling process. The FATE device was suspended above the field and 12 sets of ceramic infrared heaters were used to perform uniform heating in an area of 7.1 m^2. The daytime canopy temperature of rice could be increased by FATE with 2.4°C when fully activated on the basis of normal temperature, and the nighttime temperature of canopy could be increased by 5.4°C. This warming range was within the prediction of possible temperature increased by 1.4–5.8°C at the end of the twenty first century by IPCC (2014). Furthermore, field warming effects showed that the increase in night temperature was significantly higher than that during the daytime and that

TABLE 2 | Differentially expressed proteins under elevated temperature.

	Protein_ID	PG_Cscore	Description	Days after flowering	Fold change
Molecular chaperone	1002227700	5.589271	16.9 kDa class I heat shock protein 3	3	0.16
	1002274378	5.026661	Heat shock factor-binding protein 1	3	2.04
	1002249168	5.638757	26.7 kDa heat shock protein, chloroplastic	6; 9; 12	6.78; 3.06; 5.44
	1002279871	5.834035	Heat shock 70 kDa protein 16 isoform X1	9	0.47
	1002296675	5.888584	Heat shock 70 kDa protein, mitochondrial	9	0.5
	1002244395	5.738268	Heat shock 70 kDa protein 17	9; 12	0.43; 0.44
	1002231095	5.419388	18.0 kDa class II heat shock protein	12	2.26
	1002244087	5.593509	24.1 kDa heat shock protein, mitochondrial	12	2.01
	1002259909	5.077947	Heat shock protein 82	12	3.43
Storage protein	1002256234	5.534615	Glutelin type-A 3	3	2.79
	1002242479	5.804829	Glutelin type-B 1	3	2.49
	1002269601	5.323533	19 kDa globulin	3	2.32
	1002238885	5.933567	Glutelin type-B 5-like	3	3.3
	1002239810	5.454091	Glutelin type-B 1-like	3; 6	0.08; 6.19
	1002245900	5.419344	Glutelin type-B 2-like	3; 6	0.38; 0.44
	1002239619	5.638689	Glutelin type-B 2-like	6	0.46
	1002248312	5.772556	Globulin-1 S allele	9	3.17
	1002288955	5.518718	Glutelin type-A 1-like	9	9.27
	1002268046	5.309461	Prolamin PPROL 14E	12	0.38
	1002268263	5.446809	Prolamin PPROL 14E-like	12	0.33
	1002266396	4.918256	Basic 7S globulin	12	2.42
Starch synthesis	1002273855	4.53732	Alpha-amylase isozyme 2A	3	2.25
	1002296409	5.016673	Beta-amylase 2, chloroplastic isoform X1	3	0.48
	1002280365	5.764317	Granule-bound starch synthase 1	6	0.29
	1002230293	4.951311	Probable starch synthase 4	6	0.36
	1002282772	5.383006	Alpha-amylase/trypsin inhibitor	6	0.33
	1002282035	5.501471	Alpha-amylase/trypsin inhibitor	6	0.48
	1002284731	5.634974	Alpha-amylase inhibitor 5	6; 9	0.33; 2.05
	1002292698	5.531977	Alpha-amylase isozyme 3E	9	3.02
	1002285817	5.765962	Granule-bound starch synthase 1b	9; 12	0.5; 0.49
	1002279853	5.673613	Soluble starch synthase 2-3	12	0.47
Photosynthesis	1002280024	5.588999	Chlorophyll a-b binding protein 1B-21	3	2.22
	1002272608	5.337404	Photosystem I reaction center subunit VI	3	2.03
	1002284550	5.787986	Oxygen-evolving enhancer protein 3	3	2.53
	1002290793	4.661148	Chlorophyll a-b binding protein P4	3	2.21
	1002286185	4.714122	Chlorophyll a-b binding protein 7	3; 9	3.3; 0.36
	1002298841	5.009246	Protein TIC 62	9	0.39
	1002224946	4.238946	Photosystem II reaction center PSB28 protein	12	0.4
	1002303125	5.539293	Protochlorophyllide reductase B	15	0.48

is also consistent with the asymmetric trend of climate warming (Pachauri et al., 2014). Compared with closed or semi-closed warming scenario, the warming method and effect adopted in this study could more authentically simulate climate warming characteristics and that provided a more reliable platform for us to conduct related experiments in the actual field.

Grain filling is the key period for grain quality formation, and it is also the period most sensitive to external temperature. Our field evidence indicated that the increase in temperature generally had the relatively negative impact on rice quality, including the significantly increased chalky rate, chalky area and chalkiness. Meanwhile, the milled rice rate and head rice rate were decreased significantly, and that exceedingly reduced the grain milling quality and the market acceptance of rice. To our knowledge, the changes of external temperature inevitably affected the morphological composition and structure of the grain storage material, and that further induced the changes of related quality traits (Dou et al., 2017, 2018; Tang et al., 2018, 2019). Among these attributes, eating and cooking quality (ECQ) is one of the most important indicators, especially from the consumer's perspective. The eating quality refers to the sensory perception of consumers on rice, and that is related to the gloss,

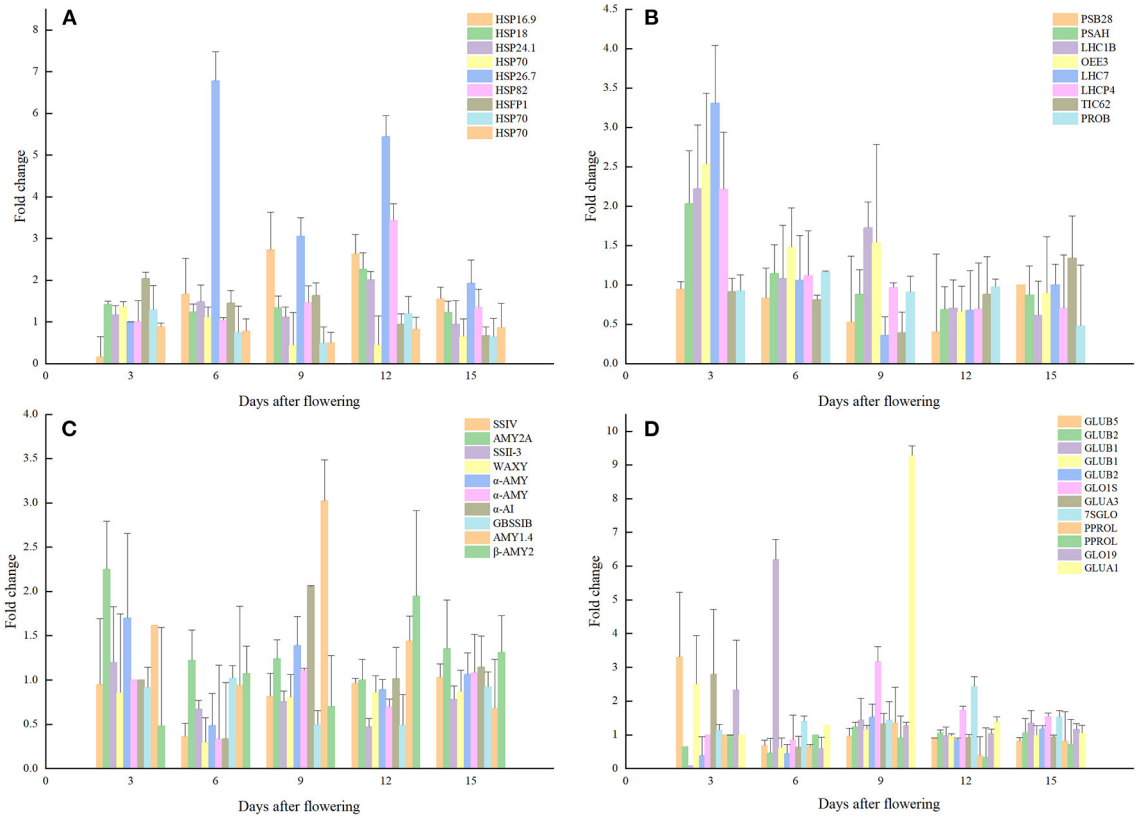

FIGURE 5 | Expression analysis of proteins related to quality formation pathways. **(A)** Storage proteins; **(B)** Molecular chaperone; **(C)** Photosynthesis; **(D)** Starch synthesis.

flavor, and viscosity of rice. Although the physical and chemical properties of starch in rice endosperm can be used as an indirect indicator of ECQ, it is still difficult to assess ECQ through these traits. At the same time, the increase of glutelin content in rice grain is particularly obvious under the condition of elevated temperature, and that could further induce the overall balance change of grain storage materials and negatively affect the taste and appearance quality of the rice.

Overview of DIA Quantitative Proteomics Analysis

In recent years, proteomics-based mass spectrometry has made significant progress from sample preparation to liquid chromatography and instrument detection, making it possible to identify more specific expressed proteins in cells or tissues with excellent accuracy and repeatability (Tsou et al., 2015). Data independent acquisition (DIA) is widely used in proteomics analysis due to its higher protein coverage rate and reliable data acquisition ability (Searle et al., 2015; Renaud and Sumarah, 2016). Compared with iTRAQ, the advantage of DIA technology can effectively measure protein molecules with extremely low-abundance protein molecules in complex samples, which greatly improves the reliability and accuracy of quantitative analysis a. In this study, MaxQuant was used to perform the database search and identification process, and obtained all detectable non-redundant high-quality MS/MS spectral information as DIA spectral library, which contains the fragment ion intensity and retention time describing the peak characteristics of the peptides. We identified 23,968 unique peptides and 5,872 unique proteins, including 840 differential expressed proteins under warming environment. These identified specifically expressed proteins have significant differences in temporal and spatial expression characteristics, which provided the obstacles for us to further identify and screen key regulatory factors. Therefore, this research mainly focused on the essential relationship between grain filling and quality formation, and we further screened the key proteins which were specifically affected by warming during the quality formation process from the perspectives of plant photosynthesis, grain starch, and storage protein accumulations. The results further indicated that induction of the key proteins could lead to the changes in grain storage materials and that could be one of the main reasons for the deterioration of quality under elevated temperature.

Key Regulatory Factors Contributed to Rice Quality Formation Under Elevated Temperature

Photosynthesis is the process by which light energy is converted into chemical energy and stored, and it is also the source of accumulation of rice grain assimilation. Chlorophyll content and

metabolic enzyme activity are closely related to the strength of photosynthesis. In our case, chlorophyll a-b binding protein 1B-21, chlorophyll a-b binding protein P4, and chlorophyll a-b binding protein 7 were significantly up-regulated, which induced the acceleration of the synthesis and binding of chlorophyll (Ballottari et al., 2012). Meanwhile, the expression levels of photosystem I reaction center subunit VI and oxygen-evolving enhancer protein 3 involved in the photosystem I were also increased significantly under warming conditions, and that may explain the accelerated grain filling rate and the significant increase in the accumulation rate of grain materials during the early grain-filling stage under elevated temperature. However, the expression of PSB28, which is responsible for water splitting, had a downward trend throughout the period, obtaining a significant low level at 12d after heading under elevated temperature (0.4 folds). That may inhibit the electron transfer and weaken signal transmission, thereby weakening photochemical reactions and resulting in decreased cell chlorophyll and photosynthesis (Wada et al., 2019). Previous studies have shown that the optical system II (PS II) is the most temperature-sensitive element in the electron transmission chain (Zhou et al., 2013). It would be interesting to further investigate whether PSB28 could be the most critical component affected by elevated temperature during the photosynthesis process.

Photosynthesis is the source of grain assimilate accumulation, and the influence of elevated on photosynthesis will directly lead to changes in the structure and composition of storage materials such as starch in grains. To our knowledge, the contents and ratio of starch and storage protein in rice grains are the decisive factors that determine the final rice quality. Rice starch synthesis is regulated by various proteins and enzymes, including SSS, SBE, DBE, and GBSS. Wx protein encoded by the Waxy gene GBSS-I can tightly bind to the starch granules and promote the synthesis of amylose. Elevated temperatures may induce the down-regulation of gene expression that regulates GBSS synthesis, resulting in decreased amylose content and increased amylopectin content, and the changes of the physical and chemical properties of rice starches have been verified in previous studies (Dian et al., 2005; Fujita et al., 2006; Tang et al., 2019). However, the mechanism of GBSS on the extension of normal starch granules is still unclear. Our results indicated that the GBSS enzyme was down-regulated at 6d after flowering under elevated temperature. However, enzymes related to amylopectin synthesis did not change significantly. From 6d to 12d after flowering, the expression level of granule-bound starch synthase was significantly lower than that of the control. Under warming conditions, the amylose content of mature rice grains was significantly lower compared to the CK, while the amylopectin content was significantly increased. Expression levels of the soluble starch synthase SSIV and SSSII-III, responsible for the synthesis of amylopectin, were also decreased under high temperatures. This change may reduce the activities of granular starch synthase and soluble starch synthase, and lead to change in the ratio of amylose and amylopectin, which eventually affected the physical and chemical properties of starches in rice grain (Hakata et al., 2012; Ahmed et al., 2015; Tang et al., 2019).

Storage proteins are the second largest storage substance in rice grains, accounting for about 8% of the grain dry weight. Rice storage proteins are composed of albumin, globulin, glutelin, and prolamin. Prolamin is directly deposited in the endoplasmic reticulum cavity in the form of intracellular protein particles, and finally buds from the endoplasmic reticulum in the form of spherical protein bodies (PBs). While glutelin is efficiently converted into mature form by vacuolar processing enzymes and forms irregular protein bodies II (PBII) together with α-globulin (Krishnan et al., 1992; Kumamaru et al., 2010). The results of this study showed that warming had significant up or down regulation effects on the expression of storage protein family-related regulatory factors at different stages of grain development. For example, the expression of glutelin type-A and type-B proteins were either significantly up-regulated or down-regulated at 3d and 6d after flowering, and there is no obvious rule for the regulation mode of these regulatory factors under warming conditions. Based on our understanding, the presence of many unknown genes involved in the glutelin synthesis pathway increases the difficulty of understanding expression patterns under warming conditions. Therefore, this study has not been able to essentially identify the regulation mechanism of the changes in the protein content of the final grain storage.

Ribosomes are the primary sites for protein synthesis, and different species of ribosomal proteins play an essential role in translation, ribosome structure, and biogenesis in protein anabolism (Moin et al., 2016a). In this study, the ribosomal protein species (25S, 30S, 40S, 50S, and 60S) exhibited significant decreases during the middle stage of grain-filling, which may cause the reduction in the protein biosynthesis and maintain the balance between synthesis and degradation of proteins (Moin et al., 2016b). The reduction in protein content related to translation, such as RNA recognition motif (RRM) domains, eukaryotic initiation factors (eIFs) and elongation factors (EFs), indicated the adverse effects of elevated temperature on rice protein synthesis. Furthermore, a series of molecular chaperone heat shock proteins (Hsps) were identified to be significantly up-regulated when exposed to elevated temperature. Heat shock proteins are a class of highly conserved peptides in structure and could be activated and produced in large quantities when plants are subjected to abiotic stress (Timperio et al., 2008). In this study, the two most sensitive heat shock proteins are HSP70 and 26.7 kDa heat shock protein from the sHsps (small heat shock proteins) family. Wang et al. (2014) found that overexpression of Hsp70 encoded gene could positively improve the tolerance of plants when subjected to heat stress. In our results, the expression level of HSP70 was decreased sharply at 9d, which in turn led to its inability to participate in the import and translocation of precursor proteins, and that further induced the disorders of rice protein synthesis in rice grains. Li et al. (2019) found that overexpression of Hsf5 could significantly increase the basic heat tolerance of plants in Arabidopsis. The function of sHSP is similar to other ATP-dependent members such as Hsp70, thereby assisting the correct folding and configuration of the protein for further processing (Tabassum et al., 2020). Grain storage protein precursors such as glutelin precursors are synthesized in the endoplasmic reticulum, and then folded

and modified with the help of a series of molecular chaperones to form trimers. These trimers are then transported out of the endoplasmic reticulum through vesicles, and eventually transported to protein storage vacuoles to form protein bodies (PB II) (Ren et al., 2020). During this process, the molecular chaperone heat shock protein family such as Hsp70/BiP located at the endoplasmic reticulum can promote the correct folding of glutelin and keeps the protein stable during the folding and assembly process. In this study, HSP70 and HSPS were significantly expressed under elevated temperature and that could promote the correct protein folding during rice grain filling and further contribute to the accumulation of storage proteins in rice grain.

MATERIALS AND METHODS

Experimental Site Description

The experiment was conducted at the Danyang Experimental Base of Nanjing Agricultural University (31°56′39″N, 118°59′13″E, 80 m). The experiment site belongs to the main high-yield rice cultivation area in the lower reaches of the Yangtze River in China. The climate belongs to the subtropical monsoon climate and the soil condition is loam with a pH value of 6.04. The total soil nitrogen was 1.4 g·kg^{-1}, the available nitrogen was 7.8 mg·kg^{-1}, the available phosphorus was 20.1 mg·kg^{-1} and the available potassium was 91.7 mg·kg^{-1}. The temperature and precipitation in the experiment are shown in the **Supplementary Figure 1**.

Plant Materials and Temperature Treatment

Wuyujing 3 (W3), a high-quality variety that is widely planted locally, was selected as the rice material for this study. Temperature treatments (normal temperature and elevated temperature) were conducted with 3 replicates for each treatment. An interval of 80 cm, and a protection line were set between the treatment blocks to ensure the independence of the experiment. Field cultivation management was conducted according to the local high-yield cultivation measures. The free air warming system (FATE) was used to increase the rice canopy temperature from the rice flowering stage. Twelve ceramic infrared radiator heaters (FTE-1000-240-0-L10-Y; 1000W, 240V) were installed 1.2 m above the rice canopy in each block (length 245 mm × width 60 mm). The heaters were in the horizontal direction and the vertical angles were 45° and 30° to ensure continuous and stable heating. The effective area of infrared radiation was $1.5 \times 1.5 \times 3.1416 = 7.1$ m^2 (**Figure 6**). Two sensors were installed at the height of the canopy (HOBO U23-001) to record the temperature and humidity of rice canopy. The field meteorological data during the test was collected from a weather station (WatchDog 550) located at ∼100 m away from the test site (Rehmani et al., 2011, 2014; Dou et al., 2018; Tang et al., 2019). According to the meteorological data, rice canopy temperature was increased by 1.568° and 3.089°C during the day and night, respectively (**Supplementary Figure 1**). The temperature increase range and trend were in line with the characteristics of global warming.

Sampling

Rice superior spikelets (located at the upper 1/3 of the rice panicle) flowering on the same day were tagged and were collected at 9:00 am on the 3rd, 6th, 9th, 12th, and 15th day after flowering. Thirty marked and representative spikelets were randomly selected and every 10 spikelets were divided into a replicate. Spikelets located at the upper third of the panicle were cut and quickly stored in liquid nitrogen. Glumes of the grains were carefully peeled off using tweezers, and for each replicate about 0.5 g of the grains were used for proteome determination. All samples collected from the ET treatment were within the effective warming area (**Figure 6**). At the mature stage, 10 holes were randomly selected from each treatment and the number of panicles per hole, spikelets per panicle, 1,000-grain weight, seed setting rate were investigated to calculate the final yield. Starch and protein content were determined using the spikelets air dried under natural conditions.

Measurement of Starch and Storage Protein Composition

Refined rice samples were milled into flour in the liquid nitrogen, and the starch was purified according to the instructions of Tran et al. (2011). The starch molecules were completely dissolved by the protease, sodium bisulfate, DMSO/LiBr (0.5%) ethanol solution, and the proteins, fats, and non-starch polymers were removed without starch degradation. Starches were further debranched with isoamylase and dissolved in DMSO/LiBr solution and physicochemical properties of starch were identified from the milled rice. The total starches were determined by using the protocols described in our previous study by Yang et al. (2016).

According to the solubility of protein components in different solvents, albumin, globulin, prolamin, and glutelin were extracted with distilled water, dilute hydrochloric acid, ethanol, and dilute alkali in sequence. The biuret colorimetric method was used to determine the remaining species using the Coomassie brilliant blue colorimetric method.

Determination of Rice Appearance, Milling, Cooking, and Eating Quality

For rice appearance quality, chalk characteristics of brown rice were observed by the cleanliness test-bed according to our previous studies (Tang et al., 2019). Rice grains were milled using a mini universal grinder and dried over a 200-mesh sieve. The length, width, and thickness of brown rice were determined by vernier caliper, and the ratio of length to width were calculate. Three hundred grains of brown rice were randomly selected to detect chalky rice grains and calculate chalky rice rate based on the percentage of chalky rice in the total number. Chalkiness area was determined by the proportion of chalky grain area to total grain area.

Rice milling quality including brown rice rate, milled rice rate, and head rice rate were investigated. During the maturity period, 30 rice panicles with uniform maturity were randomly harvested. After threshing, the grains were naturally dried to the moisture content of 15%. Brown rice percentage (BRP) and milled rice

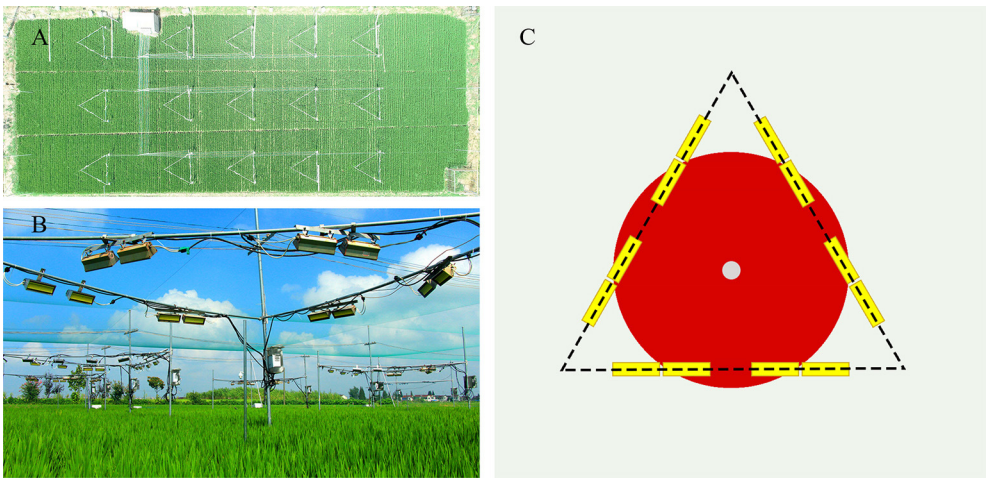

FIGURE 6 | Actual field warming scene based on Free-air temperature enhancement (FATE) system. **(A)** Aerial image of test field block **(B)** Real scene of warming community **(C)** System configuration diagram (The yellow rectangle is an infrared heating device; The white circle is HOBO; The red area is the warming range).

percentage (MRP) were determined by the processing machinery SY88-TH & SY88-TRF (Wuxi Shanglong Grain Equipment Co., Ltd., China), respectively.

Rice cooking and eating quality was determined by the RVA-4500 (a rapid viscometer developed by Newport scientific instruments, Australia). Weigh 3.00 g rice flour with moisture content of about 14.0% into aluminum box, add 25 ml distilled water, and stir it up and down rapidly for 10 times with an agitator to make the rice flour disperse evenly. The determination of RVA characteristic parameters for rice flour was programed as follows: the rice flour solution sample was heated at 50°C for 1 min, then heated to 95°C within 3.8 min, heated at 95°C for 2.5 min, then cooled to 50°C within 3.8 min, and finally heated at 50°C for 1.4 min. The characteristic parameters of RVA spectrum include peak viscosity (PKV), hot paste viscosity (HPV), cooling paste viscosity (CPV), breakdown viscosity (BDV), and depletion value (setback viscosity, SBV) were measured by the viscometer.

Protein Extraction and Enzymatic Hydrolysis

Lysis buffer (8 M Urea, 40 mM Tris–HCl or tetraethylammonium bromide (TEAB) with 1 mM Phenylmethanesulfonyl fluoride (PMSF), 2 mM Ethylene Diamine Tetraacetic Acid (EDTA) and 10 mM dithiothreitol (DTT), pH 8.5), and two magnetic beads (diameter 5 mm) were used to extract the proteins. The mixtures were placed into a Tissue Lyser for 2 min at 50 Hz to release proteins. After centrifugation at 25,000 g at 4°C for 20 min, the supernatant was transferred into a new tube, reduced with 10 mM DTT at 56°C for 1 h and alkylated by 55 mM iodoacetamide (IAM) in the dark at room temperature for 45 min. Following centrifugation (25,000 g, 4°C, 20 min), the supernatant containing proteins was quantified by Bradford and sodium dodecyl sulfate polyacrylamide gel electrophoresis (SDS-PAGE) 0.100 μg of protein solution per sample and dilute with 50 mM NH_4HCO_3 by 4 times volumes. Add 2.5 μg of Trypsin enzyme in the ratio of protein: enzyme = 40:1, and digest for 4 h at 37°C. Add Trypsin once more in the above ratio and continue to digest for 8 h at 37°C. Enzymatic peptides were desalted using a Strata X column and vacuumed to dryness (Gillet et al., 2012; Roest et al., 2014).

High pH RP Separation

200 ug sample mixtures were diluted with 2 mL of mobile phase A (5% ACN pH 9.8) and injected. The Shimadzu LC-20AB HPLC system coupled with a Gemini high pH C18 column (5 um, 4.6 × 250 mm) was used. Samples were subjected to the column and then eluted at a flow rate of 1 mL/min by gradient: 5% mobile phase B (95% CAN, pH 9.8) for 10 min, 5–35% mobile phase B for 40 min, 35% to 95% mobile phase B for 1 min, flow Phase B lasted 3 min, and 5% mobile phase B equilibrated for 10 min. The elution peak was monitored at a wavelength of 214 nm and component was collected every minute. Components were combined into a total of 10 fractions, which were then freeze-dried.

DDA Spectral Library and DIA Analysis by Nano-LC-MS/MS

The peptides separated in liquid phase were ionized by a NanoESI source and then placed on the Q-Exactive HF (Thermo Fisher Scientific, San Jose, CA) for DDA and DIA mode detection. The main parameters of DDA were as follows: the ion source voltage was 1.6 kV; the first-order mass spectrum scanning range was 350–1,500 m/z; the resolution was 6,000, the initial m/z of the secondary mass spectrum is fixed at 100; and the resolution is 15,000. The screening conditions for the precursor ions of the secondary fragmentation are the charge 2^+ to 7^+, and the peak intensity of more than 10,000 is ranked in the top 20 precursor ions. The fragment ions were detected in an Orbitrap. The dynamic exclusion time was 30 s. The main parameters of DIA were as follows: the ion source voltage was 1.6 kV; the first-order mass spectrum scanning range was 350–1,500 m/z; the resolution

was 120,000; and 350–1,500 Da was divided into 40 windows for fragmentation and signal collection. The fragment ions were detected in an Orbitrap. The dynamic exclusion time was 30 s.

Peptide Detection and Annotation

MaxQuant software was used to complete the identification of DDA for the Mass spectrum RAW data. DIA data was analyzed using Spectronaut, which uses iRT peptides to complete the retention time correction. Then, based on the Target-decoy model applicable to SWATH-MS, the false positive control was completed with FDR 1% to obtain significant quantitative results. data was preprocessed using the MS stats to the, and then the significance test was performed based on the model. Screening was performed according to the Fold change ≥ 2 and $P < 0.05$ as the criteria for determining differentially expressed proteins. The mass spectrometry proteomics data has been deposited to the ProteomeXchange Consortium (http://proteomecentral.proteomexchange.org) via the iProX partner repository with the dataset identifier PXD028032.

Data Analysis

The identified proteins were classified into three categories (biological process, cellular compartment and molecular function) based on the gene ontology annotation derived from the NCBI database (http://www.ebi.ac.uk/GOA/). Kyoto Encyclopedia of Genes and Genomes (KEGG) database was used to annotate protein pathway (https://www.kegg.jp/). Gene Ontology was used for functional annotation of proteins (http://www.geneontology.org). Data sorting and analysis were performed using Microsoft Excel 2019 and SPSS22 statistical software. Origin 8.1 was employed for figure preparation. Data analysis of variance was analyzed according to a completely random design, and the averages were compared by Duncan's multiple range test (DMRT) based on the least significant difference test at the 5% probability level.

CONCLUSIONS

Our previous studies have shown that elevated temperatures could deteriorate the rice quality through inducing the imbalance ratio of starch and protein components in rice grains. However, due to the complexity of the accumulation process of storage materials, which involves multi-level interactions between gene transcription, translation, protein folding and degradation, thus it is difficult to fully elucidate the mechanism of the effect of elevated temperature on rice quality formation. In this study, we identified a certain number of key proteins (PPROL 14E, PSB28, granule-bound starch synthase I, and 26.7 kda heat shock protein) and metabolic pathways that were sensitive to elevated temperature through DIA quantitative proteomics analysis. The identified differentially expressed proteins were participated in the accumulation of starch and storage protein in the grains, which may be responsible for the deterioration of rice quality under elevated temperature. The results could help to further clarify the potential regulatory mechanism of global warming on rice development and quality formation.

DATA AVAILABILITY STATEMENT

The original contributions presented in the study are publicly available. This data can be found here: http://proteomecentral.proteomexchange.org/cgi/GetDataset?ID=PXD028032 or https://www.iprox.cn/page/project.html?id=IPX0003400000.

AUTHOR CONTRIBUTIONS

ST and YD conceived the experiments. ST designed the experiments. WL performed the experimental work and carried out the proteomics data analysis. XW and KW did the sampling and data analysis. TY and YZ helped in protein isolation. YS provided plant materials. ST and WL wrote the paper. All authors read and approved the final manuscript.

FUNDING

This work was supported by the National Key R&D Program, Ministry of Science and Technology, China (Grant No. 2017YFD0300100, 2017YFD0300103 & 2017YFD0300107). This work was also funded by the National Natural Science Foundation of China (Grant No. 32071949 & 31701366). We also received support from the Jiangsu Collaborative Innovation Center for Modern Crop Production (JCIC-MCP) and the Fundamental Research Funds for the Central Universities, China (Grant No. KJQN201802).

ACKNOWLEDGMENTS

The authors thank Prof. Shaohua Wang for providing the seeds used in this study, and for growing and maintaining the plants.

SUPPLEMENTARY MATERIAL

The Supplementary Material for this article can be found online at: https://www.frontiersin.org/articles/10.3389/fpls.2021.746180/full#supplementary-material

REFERENCES

Ahmed, N., Tetlow, I. J., Nawaz, S., Iqbal, A., Mubin, M., ul Rehman, M. S. N., et al. (2015). Effect of high temperature on grain filling period, yield, amylose content and activity of starch biosynthesis enzymes in endosperm of basmati rice. *J. Sci. Food Agric.* 95, 2237–2243. doi: 10.1002/jsfa.6941

Ballottari, M., Girardon, J., Dall'Osto, L., and Bassi, R. (2012). Evolution and functional properties of Photosystem II light harvesting complexes in eukaryotes. *Biochim. Et Biophys. Acta-Bioenerget.* 1817, 143–157. doi: 10.1016/j.bbabio.2011.06.005

Cao, Z., Zhao, Q., Pan, G., Wei, K., Zhou, L., and Cheng, F. (2017). Comprehensive expression of various genes involved in storage protein synthesis in filling rice grain as affected by high temperature. *Plant Growth Regul.* 81, 477–488. doi: 10.1007/s10725-016-0225-4

Dian, W. M., Jiang, H. W., and Wu, P. (2005). Evolution and expression analysis of starch synthase III and IV in rice. *J. Exp. Bot.* 56, 623–632. doi: 10.1093/jxb/eri065

Dou, Z., Tang, S., Chen, W., Zhang, H., Li, G., Liu, Z., et al. (2018). Effects of open-field warming during grain-filling stage on grain quality of two japonica rice cultivars in lower reaches of Yangtze River delta. *J. Cereal Sci.* 81, 118–126. doi: 10.1016/j.jcs.2018.04.004

Dou, Z., Tang, S., Li, G., Liu, Z., Ding, C., Chen, L., et al. (2017). Application of nitrogen fertilizer at heading stage improves rice quality under elevated temperature during grain-filling stage. *Crop Sci.* 57, 2183–2192. doi: 10.2135/cropsci2016.05.0350

Fujita, N., Yoshida, M., Asakura, N., Ohdan, T., Miyao, A., Hirochika, H., et al. (2006). Function and characterization of starch synthase I using mutants in rice. *Plant Physiol.* 140, 1070–1084. doi: 10.1104/pp.105.071845

Gillet, L. C., Navarro, P., Tate, S., Roest, H., Selevsek, N., Reiter, L., et al. (2012). Targeted data extraction of the MS/MS spectra generated by data-independent acquisition: a new concept for consistent and accurate proteome analysis. *Mol. Cell. Proteomics* 11:O111.016717. doi: 10.1074/mcp.O111.016717

Hakata, M., Kuroda, M., Miyashita, T., Yamaguchi, T., Kojima, M., Sakakibara, H., et al. (2012). Suppression of alpha-amylase genes improves quality of rice grain ripened under high temperature. *Plant Biotechnol. J.* 10:1110–1117. doi: 10.1111/j.1467-7652.2012.00741.x

IPCC (2014). AR5 Synthesis Report: Climate Change 2014. IPCC.

IPCC (2018). Global Warming of 1.5°C. IPCC.

Jagadish, S. V. K. (2020). Heat stress during flowering in cereals - effects and adaptation strategies. *N. Phytol.* 226, 1567–1572. doi: 10.1111/nph.16429

Kim, J., Shon, J., Lee, C.-K., Yang, W., Yoon, Y., Yang, W.-H., et al. (2011). Relationship between grain filling duration and leaf senescence of temperate rice under high temperature. *Field Crops Res.* 122, 207–213. doi: 10.1016/j.fcr.2011.03.014

Krishnan, H. B., White, J. A., and Pueppke, S. G. (1992). Characterization and localization of rice (*Oryza-sativa* L) seed globulins. *Plant Sci.* 81, 1–11. doi: 10.1016/0168-9452(92)90018-H

Kumamaru, T., Uemura, Y., Inoue, Y., Takemoto, Y., Siddiqui, S. U., Ogawa, M., et al. (2010). Vacuolar processing enzyme plays an essential role in the crystalline structure of glutelin in rice seed. *Plant Cell Physiol.* 51, 38–46. doi: 10.1093/pcp/pcp165

Li, G. L., Zhang, H. N., Shao, H., Wang, G. Y., Zhang, Y. Y., Zhang, Y. J., et al. (2019). ZmHsf05, a new heat shock transcription factor from Zea mays L. improves thermotolerance in Arabidopsis thaliana and rescues thermotolerance defects of the athsfa2 mutant. *Plant Sci.* 283, 375–384. doi: 10.1016/j.plantsci.2019.03.002

Moin, M., Bakshi, A., Saha, A., Dutta, M., Madhav, S. M., and Kirti, P. B. (2016a). Rice ribosomal protein large subunit genes and their spatio-temporal and stress regulation. *Front. Plant Sci.* 7:1284. doi: 10.3389/fpls.2016.01284

Moin, M., Bakshi, A., Saha, A., Kumar, M. U., Reddy, A. R., Rao, K. V., et al. (2016b). Activation tagging in indica rice identifies ribosomal proteins as potential targets for manipulation of water-use efficiency and abiotic stress tolerance in plants. *Plant Cell Environ.* 39, 2440–2459. doi: 10.1111/pce.12796

Pachauri, R. K., Allen, M. R., Barros, V. R., Broome, J., Cramer, W., Christ, R., et al. (2014). *Climate Change 2014: Synthesis Report.* Contribution of Working Groups I, II and III to the fifth assessment report of the Intergovernmental Panel on Climate Change. IPCC.

Rehmani, M. I. A., Wei, G., Hussain, N., Ding, C., Li, G., Liu, Z., et al. (2014). Yield and quality responses of two indica rice hybrids to post-anthesis asymmetric day and night open-field warming in lower reaches of Yangtze River delta. *Field Crops Res.* 156, 231–241. doi: 10.1016/j.fcr.2013.09.019

Rehmani, M. I. A., Zhang, J., Li, G., Ata-Ul-Karim, S. T., Wang, S., Kimball, B. A., et al. (2011). Simulation of future global warming scenarios in rice paddies with an open-field warming facility. *Plant Methods* 7:41. doi: 10.1186/1746-4811-7-41

Ren, Y., Wang, Y., Pan, T., Wang, Y., Wang, Y., Gan, L., et al. (2020). GPA5 encodes a Rab5a effector required for post-golgi trafficking of rice storage proteins. *Plant Cell* 32, 758–777. doi: 10.1105/tpc.19.00863

Renaud, J. B., and Sumarah, M. W. (2016). Data independent acquisition-digital archiving mass spectrometry: application to single kernel mycotoxin analysis of Fusarium graminearum infected maize. *Anal. Bioanal. Chem.* 408, 3083–3091. doi: 10.1007/s00216-016-9391-5

Roest, H. L., Rosenberger, G., Navarro, P., Gillet, L., Miladinovic, S. M., Schubert, O. T., et al. (2014). OpenSWATH enables automated, targeted analysis of data-independent acquisition MS data. *Nat. Biotechnol.* 32, 219–223. doi: 10.1038/nbt.2841

Searle, B. C., Egertson, J. D., Bollinger, J. G., Stergachis, A. B., and MacCoss, M. J. (2015). Using Data Independent Acquisition (DIA) to model high-responding peptides for targeted proteomics experiments. *Mol. Cell. Proteomics* 14, 2331–2340. doi: 10.1074/mcp.M115.051300

Tabassum, R., Dosaka, T., Ichida, H., Morita, R., Ding, Y., Abe, T., et al. (2020). FLOURY ENDOSPERM11-2 encodes plastid HSP70-2 involved with the temperature-dependent chalkiness of rice (*Oryza sativa* L.) grains. *Plant J.* 103, 604–616. doi: 10.1111/tpj.14752

Tang, S., Chen, W., Liu, W., Zhou, Q., Zhang, H., Wang, S., et al. (2018). Open-field warming regulates the morphological structure, protein synthesis of grain and affects the appearance quality of rice. *J. Cereal Sci.* 84, 20–29. doi: 10.1016/j.jcs.2018.09.013

Tang, S., Zhang, H., Liu, W., Dou, Z., Zhou, Q., Chen, W., et al. (2019). Nitrogen fertilizer at heading stage effectively compensates for the deterioration of rice quality by affecting the starch-related properties under elevated temperatures. *Food Chem.* 277, 455–462. doi: 10.1016/j.foodchem.2018.10.137

Timperio, A. M., Egidi, M. G., and Zolla, L. (2008). Proteomics applied on plant abiotic stresses: role of heat shock proteins (HSP). *J. Proteomics* 71, 391–411. doi: 10.1016/j.jprot.2008.07.005

Tran, T. T. B., Shelat, K. J., Tang, D., Li, E., Gilbert, R. G., and Hasjim, J. (2011). Milling of rice grains. The degradation on three structural levels of starch in rice flour can be independently controlled during grinding. *J. Agric. Food Chem.* 59, 3964–3973. doi: 10.1021/jf105021r

Tsou, C.-C., Avtonomov, D., Larsen, B., Tucholska, M., Choi, H., Gingras, A.-C., et al. (2015). DIA-Umpire: comprehensive computational framework for data-independent acquisition proteomics. *Nat. Methods* 12, 258–264. doi: 10.1038/nmeth.3255

Wada, S., Takagi, D., Miyake, C., Makino, A., and Suzuki, Y. (2019). Responses of the photosynthetic electron transport reactions stimulate the oxidation of the reaction center chlorophyll of photosystem I, P700, under drought and high temperatures in rice. *Int. J. Mol. Sci.* 20:2068. doi: 10.3390/ijms20092068

Wahid, A., Gelani, S., Ashraf, M., and Foolad, M. R. (2007). Heat tolerance in plants: an overview. *Environ. Exp. Bot.* 61, 199–223. doi: 10.1016/j.envexpbot.2007.05.011

Wang, Y., Lin, S., Song, Q., Li, K., Tao, H., Huang, J., et al. (2014). Genome-wide identification of heat shock proteins (Hsps) and Hsp interactors in rice: Hsp70s as a case study. *BMC Genomics* 15:344. doi: 10.1186/1471-2164-15-344

Xu, J., Henry, A., and Sreenivasulu, N. (2020). Rice yield formation under high day and night temperatures-A prerequisite to ensure future food security. *Plant Cell Environ.* 43, 1595–1608. doi: 10.1111/pce.13748

Yang, X., Bi, J., Gilbert, R. G., Li, G., Liu, Z., Wang, S., et al. (2016). Amylopectin chain length distribution in grains of japonica rice as affected by nitrogen fertilizer and genotype. *J. Cereal Sci.* 71, 230–238. doi: 10.1016/j.jcs.2016.09.003

Zhou, K., Ren, Y., Lv, J., Wang, Y., Liu, F., Zhou, F., et al. (2013). Young Leaf Chlorosis 1, a chloroplast-localized gene required for chlorophyll and lutein accumulation during early leaf development in rice. *Planta* 237, 279–292. doi: 10.1007/s00425-012-1756-1

Conflict of Interest: The authors declare that the research was conducted in the absence of any commercial or financial relationships that could be construed as a potential conflict of interest.

Publisher's Note: All claims expressed in this article are solely those of the authors and do not necessarily represent those of their affiliated organizations, or those of the publisher, the editors and the reviewers. Any product that may be evaluated in this article, or claim that may be made by its manufacturer, is not guaranteed or endorsed by the publisher.

frontiers in Plant Science

REVIEW
published: 07 March 2022
doi: 10.3389/fpls.2022.852082

Maize Endosperm Development: Tissues, Cells, Molecular Regulation and Grain Quality Improvement

Hao Wu[1], Philip W. Becraft[1] and Joanne M. Dannenhoffer[2]*

[1] Genetics, Development, and Cell Biology, Iowa State University, Ames, IA, United States, [2] Department of Biology, Central Michigan University, Mount Pleasant, MI, United States

Maize endosperm plays important roles in human diet, animal feed and industrial applications. Knowing the mechanisms that regulate maize endosperm development could facilitate the improvement of grain quality. This review provides a detailed account of maize endosperm development at the cellular and histological levels. It features the stages of early development as well as developmental patterns of the various individual tissues and cell types. It then covers molecular genetics, gene expression networks, and current understanding of key regulators as they affect the development of each tissue. The article then briefly considers key changes that have occurred in endosperm development during maize domestication. Finally, it considers prospects for how knowledge of the regulation of endosperm development could be utilized to enhance maize grain quality to improve agronomic performance, nutrition and economic value.

Keywords: kernel, differentiation, cell fate, genetics, seed physiology

OPEN ACCESS

Edited by:
Yingyin Yao,
China Agricultural University, China

Reviewed by:
Yuhai Cui,
Agriculture and Agri-Food Canada (AAFC), Canada
Margaret Woodhouse,
Agricultural Research Service, United States Department of Agriculture (USDA), United States

****Correspondence:***
Philip W. Becraft
becraft@iastate.edu

Specialty section:
This article was submitted to Crop and Product Physiology, a section of the journal Frontiers in Plant Science

Received: *10 January 2022*
Accepted: *11 February 2022*
Published: *07 March 2022*

Citation:
Wu H, Becraft PW and Dannenhoffer JM (2022) Maize Endosperm Development: Tissues, Cells, Molecular Regulation and Grain Quality Improvement. Front. Plant Sci. 13:852082. doi: 10.3389/fpls.2022.852082

INTRODUCTION

Cereal grains represent one of the key agricultural innovations upon which human civilization is founded. A distinguishing feature of cereal grains is their large, persistent, starch-filled endosperm that can be used directly as food or feed, ground to flour for many varied uses such as bread or pasta, malted and fermented for beverages or biofuel, or used as feedstock for industrial processes. Early peoples recognized particular grass seeds for their food value and began the process of domestication by selecting for traits that improved their value as crops. Grain size was an obvious trait that enhanced the caloric reward and ease of harvesting, and since endosperm constitutes the bulk of the grain, selection for larger grains inevitably increased endosperm size (Flint-Garcia, 2017).

From a developmental perspective, increasing grain size is a complex problem. From first principles, an increase in grain or endosperm size must entail either an increase in cell number or an increase in average cell size (or both). However, either of these changes could be accomplished by a variety of means: various alterations to the cell cycle or prolonged duration of active cell division. Any such changes require coordination amongst different tissues and cell types, as well as integration with the complex biochemical and physiological processes that occur during grain filling and seed maturation. Hence, selection pressure for grain traits during domestication and continued improvement either acts directly at the level of kernel and endosperm development, or affects changes in processes that then must be integrated into the developmental programs.

Understanding changes that occurred during domestication and improvement at the developmental and genetic level will greatly aid our ability to direct continued improvement and trait development. Methods are now available for identifying loci that were targets of selection as well as for introducing precise changes in the genome. Thus, it should now be possible to use genomic methods to help elucidate the developmental processes that were manipulated to provide the maize grains we have today, and to extend that knowledge into the future for continued improvement. Here we first describe the process of endosperm development from a kernel and cellular perspective, then review what is known of the molecular regulation of endosperm development, and finally we consider how this knowledge can be used for grain improvement.

KERNEL AND CELLULAR ENDOSPERM DEVELOPMENT

Endosperm Development in the Context of Whole Grain Development

The maize grain develops from a fertilized ovule to a mature kernel over the course of 50–60 days (**Figure 1**). The developing kernel contains tissues of maternal origin, the pericarp and nucellus, as well as those produced by double fertilization, the diploid embryo and the triploid endosperm. Agronomically, kernel development is described from the R1 silking stage to R6 physiological maturity but physiologically, kernel development is divided into the lag, grain-filling, and maturation phases (Egli, 2006; Abendroth et al., 2011). During the lag phase of growth, from 0 days after pollination (DAP) to as late as 15+ DAP, kernel dry weight gain is minimal as the endosperm and embryo develop, differentiate and increase in size. During the lag phase, the endosperm first undergoes free nuclear development, which involves mitotic divisions without cytokinesis, creating a multinucleate coenocyte (Olsen et al., 1995). Subsequent wall formation yields a completely cellular endosperm that further develops by an endosperm-wide proliferation of cells. By the end of the lag phase, mitotic activity becomes restricted to the peripheral layers of the endosperm (Sabelli and Larkins, 2009). Coincident with cell proliferation, four major cell types with specific functions differentiate within the endosperm: aleurone, basal endosperm transfer layer (BETL), embryo surrounding region (ESR) and starchy endosperm (SE) (Randolph, 1936; Kiesselbach, 1949; Leroux et al., 2014; Olsen, 2020). An additional 3–4 cell types develop later (Leroux et al., 2014). By the end of the lag phase, the endosperm accounts for about 60% of the kernel volume. During this phase, the embryo undergoes a formative division to produce the suspensor and embryo proper, then grows and transitions to a bilateral axis, and further develops to the coleoptile stage including establishment of shoot and root apical meristems (Sheridan and Clark, 2017). Also, during the early lag phase, the maternal nucellus tissue at first expands and accounts for a significant portion of the kernel but by ∼12 DAP it degenerates and remains only as the nucellar membrane (Randolph, 1936; Leroux et al., 2014). The exterior pericarp is also expanding and starts to develop thickened walls.

During the linear or grain-filling phase of seed development, (∼12–40 DAP), as endosperm cell proliferation slows, there is rapid water and weight gain as the SE cells expand with deposition of storage compounds and multiple rounds of endoreduplication (Sabelli and Larkins, 2009) (**Figure 1**). SE cells accumulate carbohydrates in the form of starch and seed storage proteins accumulate in protein bodies. Fully differentiated SE cells begin the process of programed cell death (PCD) (Young and Gallie, 2000; Dominguez and Cejudo, 2014). In the linear phase, the embryo continues growth and development and the pericarp cells begin to die. The final maturation stage of seed development involves PCD of all endosperm cells except the aleurone, final development of the embryo, and kernel desiccation and quiescence.

Initial Endosperm Development and Cellularization

The development of the maize coenocyte begins with the first mitosis 2–5 h after fertilization and within 29 h of pollination (Randolph, 1936; Lowe and Nelson, 1946; Kiesselbach, 1949; Mol et al., 1994). The coenocyte is characterized by a large central vacuole surrounded by a thin layer of parietal cytoplasm. The duration of the coenocyte stage varies in maize lines and under different growth conditions but typically lasts for 2–3 days after pollination during which time nuclear divisions are synchronous (Randolph, 1936; Cooper, 1951; Kowles and Phillips, 1988; Leroux et al., 2014). Studies of genetic sectors indicate the first division identifies the sagittal left and right halves of the endosperm (McClintock, 1978) and this was later captured within a serially-sectioned endosperm (Monjardino et al., 2007). The second division occurs in the perpendicular plane specifying endosperm quarters, the third division specifies 8 longitudinal portions that describe conical sections of the endosperm. When there are only a few nuclei, they are located near the endosperm base but after several more rounds of division they migrate to occupy its full longitudinal extent (Randolph, 1936; Monjardino et al., 2007; Leroux et al., 2014). While no study has been undertaken to fully describe the cytoskeleton and its association with migrating nuclei, images of the maize coenocyte show nuclear cytoplasmic domains with radiating microtubules (Brown and Lemmon, 2007) reminiscent of those described for other cereals (Brown et al., 1996). The number of nuclei achieved during the coenocyte stage is 128–512 and it has been suggested that mitotic arrest at 256 or 512 nuclei is associated with commencement of cellularization (Olsen, 2001); however, Leroux et al. (2014) noted endosperm size not number of nuclei is coincident with cellularization.

Cellularization, which begins ∼ 3 days after pollination (DAP) and proceeds rapidly often being completed as early as 4 DAP, is coincident with the first size increase of the endosperm (Randolph, 1936; Cooper, 1951; Monjardino et al., 2007; Leroux et al., 2014). Anticlinal walls that are perpendicular to the outer endosperm wall form without mitosis to encase each parietal nucleus in a structure called an alveolus. Alveoli have

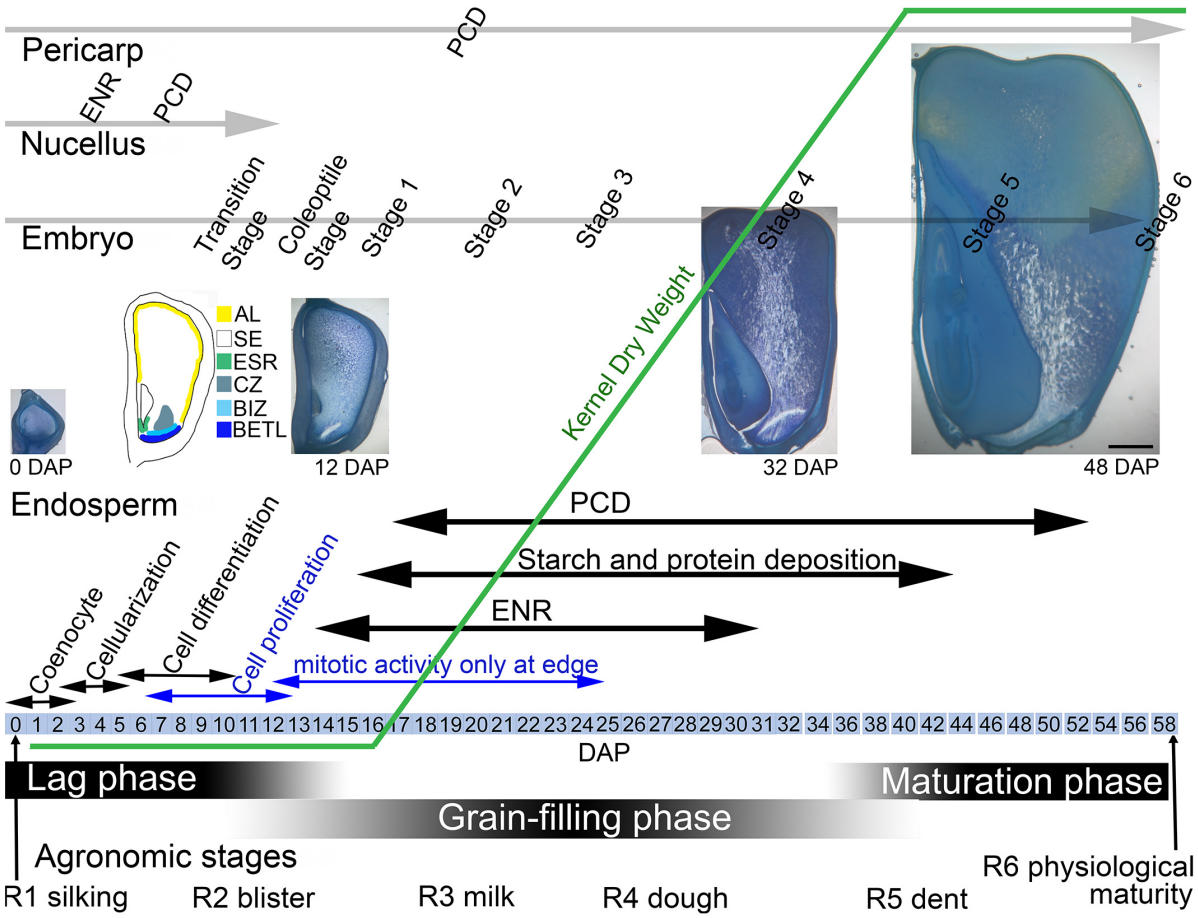

FIGURE 1 | Maize kernel development from pollination to maturity highlighting endosperm growth and development in concert with phases of seed development and development of the embryo. AL, aleurone; BETL, basal endosperm transfer layer; BIZ, basal intermediate zone; CZ, conducting zone; DAP, days after pollination; ENR, endoreduplication; ESR, embryo surrounding region; PC, placenta-chalazal region; PCD, programed cell death; SA, subaleurone; SE, starchy endosperm.

walls on all sides of each nucleus except the face adjacent to the central vacuole. The first alveoli are formed at the base of the endosperm near the embryo, the region of future ESR (Randolph, 1936; Kiesselbach, 1949; Monjardino et al., 2007; Leroux et al., 2014). Within each alveolus, a mitotic division yields sister nuclei and a periclinal wall is deposited between them to produce an outer layer of cells and an inner layer of alveoli. Each alveolus has a successive series of anticlinal wall extension, nuclear mitosis, and periclinal wall deposition forming an externally positioned cell and an internally positioned new alveolus. Although cellularization is completed by successive alveolation in other cereals, maize appears to have a more random final partitioning of the central vacuole in the bulbous base of the endosperm, which may be related to the much larger size and unique shape of the maize endosperm (Leroux et al., 2014).

Cell Proliferation and Cell Type Differentiation

Coenocyte development and cellularization sets up the basic body plan of the endosperm that then increases rapidly in size by cell proliferation and differentiates specialized cell types. During proliferation, endosperm growth occurs throughout the endosperm and is primarily associated with mitotic activity and increase in cell number generating the bulk of the endosperm (Kiesselbach, 1949; Kowles and Phillips, 1985). This contrasts with later stages when mitotic activity slows and becomes restricted to the kernel edge and endosperm growth is predominantly driven by cell and nuclear enlargement associated with storage deposition and endoreduplication (Randolph, 1936; Kiesselbach, 1949; Kowles and Phillips, 1985). Cell proliferation and cell type differentiation occur simultaneously and mitotic activity peaks ∼10 DAP (Kowles and Phillips, 1985). During the cell proliferation and differentiation period, the endosperm grows to exceed 60% of the kernel area (Leroux et al., 2014) and its shape has inverted with a large distal portion where cell divisions are still occurring and a narrower base where divisions have ceased, a shape which it will maintain for the rest of kernel development.

The larger maize endosperm differs from wheat, rice, and barley in that it develops a greater repertoire of specialized cell types (Olsen and Becraft, 2013). It is likely that breeding has impacted the development and functions of each of

these cell types. The cell types are identified and described by a combination of their location, cell shape and contents, nuclear division patterns, wall elaborations, gene expression, and function (**Table 1**). The first cell types to become cytologically identifiable at 4-5 DAP are aleurone, BETL, ESR, and SE (Leroux et al., 2014). Several days later subaleurone (SA), conducting zone (CZ), and basal intermediate zone (BIZ) cells become distinguishable although some authors regard these as subtypes of SE and BETL (Becraft et al., 2001; Chourey and Hueros, 2017) (**Figure 2**). A last possible cell type, described as an endosperm region, is the endosperm adjacent to scutellum (EAS), only identifiable by location and transcriptome analysis because the cells have no identifiable cytological features that separate them from SE (Doll et al., 2020). Of these cell types, only AL and SE remain prominent at seed maturity.

Aleurone and BETL are a single cell layer that is initiated by the first periclinal wall deposition at the beginning of the cellularization process and are in essence the epidermal layer of the endosperm tissue (**Figure 1**). Aleurone cells cover the surface except for at the base of the endosperm adjacent to the maternal placenta-chalazal region (PC) where the BETL and ESR cells are located. After the first division, the nascent aleurone cells have microtubular preprophase bands that mark the future plane of cell division whereas the underlying cells do not (Brown and Lemmon, 2007). At first, cell divisions are at right angles to each other to maintain a cuboid shape, but later divisions occur predominantly in anticlinal planes so surface expansion can keep pace with increasing kernel volume. When periclinal divisions occur, the inner cell switches from aleurone into SE and positioning rather than lineage has been shown to be important for aleurone cell specification (Becraft and Asuncion-Crabb, 2000; Gruis et al., 2006). Cytologically, aleurone cells become apparent by 5 DAP with development of multiple large vacuoles (Kyle and Styles, 1977). Between 10–15 DAP the cells become more distinct as aleurone by beginning to accumulate protein and membranes within smaller vacuoles, forming abundant lipid bodies, and developing a thickened wall (Kyle and Styles, 1977; Reyes et al., 2011). Protein eventually occupies a large proportion of the vacuoles and they develop the characteristic ultrastructure of aleurone bodies or protein storage vacuoles (PSV). These PSV contain many internal structures including a large protein inclusion containing zeins, α-globulin and legumin-1. The zeins in the vacuole apparently transport from the ER to prevacuolar compartments then to PSVs by an atypical autophagic process (Reyes et al., 2011). PSVs also contain phytic acid crystals, a glycoprotein containing matrix, and intravacuolar membranes (Reyes et al., 2011). Late in development, abundant lipid bodies surround the PSVs and the aleurone cell wall thickens considerably (Kyle and Styles, 1977). The colorful kernels that characterize many maize genotypes are produced

TABLE 1 | Maize endosperm cell type location, characteristics and function.

	Aleurone	BETL	ESR	SE	SA	CZ	BIZ	EAS
Location	Epidermal	Epidermal adjacent to placento-chalaza pad	Surrounds embryo early, later restricted to base near suspensor	The bulk of the endosperm tissue	Cell layer internal to aleurone, subtype of SE	In lower central portion of kernel, subtype SE	Between BETL and CZ, subtype BETL or SE	Adjacent to scutellum
Existence	4 DAP – seed maturity	4 DAP – completion grain fill	4–16 DAP	4 DAP – seed maturity	10 – ∼25 DAP cell division, seen at seed maturity	10–24 DAP	10- ? DAP	9–20 DAP
Size and shape	Small, cuboid	Elongate	Small, isodiametric	Irregular shape, very large	Small, cambial-like, wider than long	Very elongate, tapering ends	Elongate, prismatic	NA
Cytoplasm and wall	Prominent protein storage vacuoles, lipid bodies, thickened wall, in some genotypes anthocyanin	Apical end densely cytoplasmic, many mitochondria, Golgi extensive wall ingrowths, lignified wall	Densely cytoplasmic later becoming vacuolated; mitochondria, abundant rER	Vacuolated becoming filled with starch and protein bodies, enlarged up to 192C nuclei	Develop large protein bodies and small starch grains, high concentration of protein in this layer at seed maturity	Granular, non-distinct vacuoles, very large nuclei	Multiple vacuoles, moderately dense cytoplasm, wall ingrowths of flange type only	NA
Function	Storage lipids, proteins, minerals; remobilization of reserves for seedling growth	Transfer of solutes	Evidence for nutrient transfer, defense and signaling	Storage starch and proteins	Meristematic adding cells to edge, protein storage	Transport?	Radial distribution of solutes?	Transport between endosperm and embryo
Select references	Kyle and Styles, 1977; Reyes et al., 2011	Davis et al., 1990; Kang et al., 2009	Schel et al., 1984; Opsahl-Ferstad et al., 1997	Woo et al., 2001; Vilhar et al., 2002	Khoo and Wolf, 1970; Lending and Larkins, 1989	Zheng et al., 2014	Davis et al., 1990; Monjardino et al., 2013	Doll et al., 2020

by anthocyanin deposition in aleurone cells (or sometimes the pericarp). Aleurone cells typically do not endoreduplicate and they are the only endosperm cells that do not enter PCD during development (Burton and Fincher, 2014); thus, they are the only living endosperm cells at seed maturity. Aleurone cells function in mineral, lipid, and protein storage. At germination the aleurone secretes hydrolytic enzymes that digest the starches and proteins stored in the SE and release sugars and amino acids for use by the growing seedling.

Basal endosperm transfer layer cells are epidermal cells that form an interface between the basal filial tissues and the maternal pedicel tissue (**Figure 2**). With elaborate wall ingrowths that increase the surface area of the plasma membrane, they typify transfer cells that are important in solute movement across the apoplastic interface from the maternal tissues into the growing grain where they can be used for growth or assimilated into storage compounds (Zheng and Wang, 2010; McCurdy, 2015). Various authors describe the inner several (2–3) cell layers with similar but distinct cytological features as an extension or inner part of the BETL (Kiesselbach and Walker, 1952; Davis et al., 1990; Gao et al., 1998; Monjardino et al., 2013). However, the distinct cytological characteristics and specific gene expression within these inner cells (Leroux et al., 2014; Li et al., 2014) was used to segregate them from the BETL as the basal intermediate zone (BIZ). Future work is needed to fully describe the characteristics and occurrence of the BIZ and CZ cells to understand their identities, locations, and relationships to the well-known adjacent BETL and SE. Here we will describe the BETL using the features of the most basal cell layer.

BETL cells begin elongation and wall ingrowth deposition ~6 DAP (Kiesselbach and Walker, 1952; Charlton et al., 1995; Kang et al., 2009; Monjardino et al., 2013; Leroux et al., 2014). Before basal wall ingrowth begins there is already a polarized distribution of mitochondria with many of them located adjacent

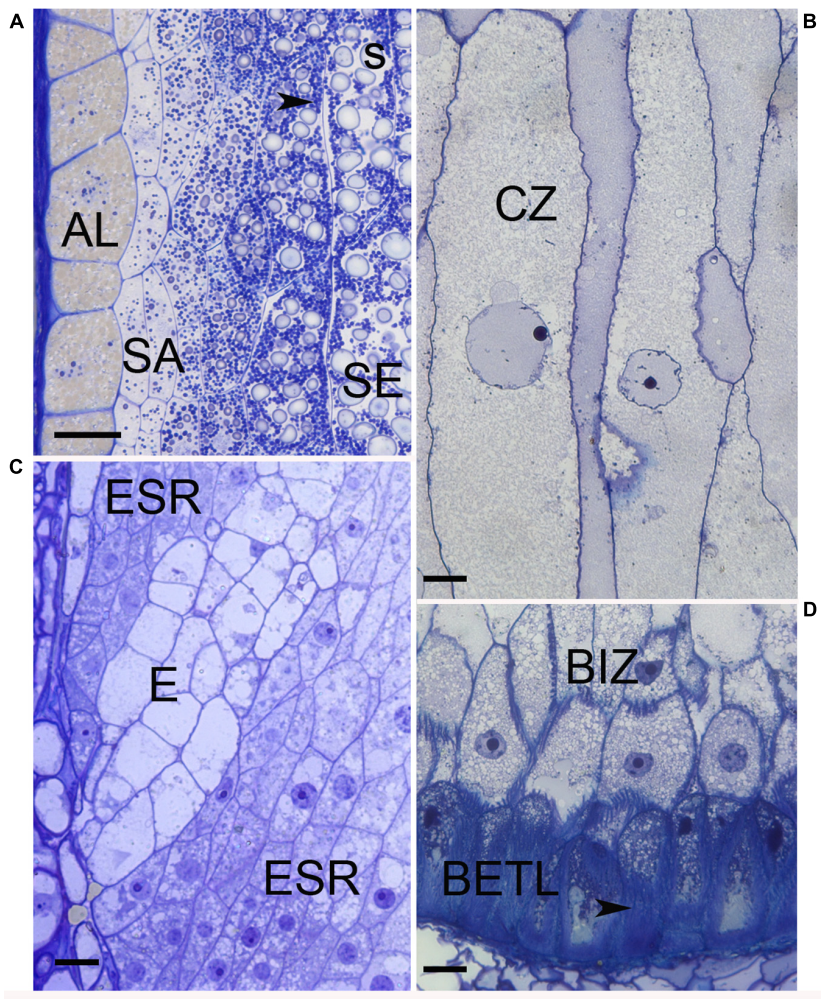

FIGURE 2 | Light micrographs of maize cell types. **(A)** Edge of 20 DAP endosperm with aleurone (AL), subaleurone (SA), and starchy endosperm (SE). Within the SE abundant starch (s) and protein bodies (arrowhead) are present. **(B)** Conducting zone cells when first apparent, about 10 DAP. **(C)** Embryo surrounding region (ESR) cells at 8 DAP are restricted to surrounding the embryo suspensor (E). **(D)** Base of endosperm at 10 DAP when BETL cells have developed wall ingrowths (arrowhead) and adjacent basal intermediate zone cells (BIZ) are visible. Bars = 20 μm.

to the lower wall (Kang et al., 2009). As the plasma membrane invaginates and ingrowths begin to form, there is an increase in mitochondria, Golgi, and *trans*-Golgi-network vesicles indicating high secretory activity (Davis et al., 1990; Charlton et al., 1995; Kang et al., 2009; Monjardino et al., 2013). Within the kernel, there is a gradient of development of BETL cells from near the embryo to the abgerminal side of the endosperm (Hueros et al., 1999).

Developing cells take on the full complement of cytological features after ∼12–16 DAP with an asymmetric distribution of nucleus and dense cytoplasm at the distal end above prominent wall ingrowths adjacent to the PC (Kiesselbach and Walker, 1952; Davis et al., 1990; Kang et al., 2009). The cytoplasm contains variously shaped nuclei, numerous mitochondria, Golgi, and enlarged vesicles; whereas, cytoplasm interstices among the wall ingrowths are packed with ER and abundant mitochondria (Davis et al., 1990; Kang et al., 2009). Plasmodesmata are located in the primary cell wall in between ingrowths and interconnect BETL cells but are absent between BETL cells and the underlying PC (Davis et al., 1990; Monjardino et al., 2013). The wall ingrowths have a complex architecture with abundant parallel, rib-like projections called flange ingrowths that anastomose along their length (Davis et al., 1990; Talbot et al., 2002; Monjardino et al., 2013; McCurdy, 2015). In the lower region of the cells, these flange wall ingrowths are interconnected by lateral extensions so wall material more or less fills the cell volume (Davis et al., 1990; Talbot et al., 2002; Kang et al., 2009). The interconnecting wall architecture is equated to reticulate wall ingrowths (Monjardino et al., 2013); although others view them as an elaboration of the flange outgrowth (Talbot et al., 2002; McCurdy, 2015). Regardless of their origin, this secondary interconnection of flange ingrowths only exists in the first cell layer BETL and not BIZ cells. Using a variety of detection methods, lignin was found in BETL cell walls within both types of wall ingrowth (Rocha et al., 2014).

Basal intermediate zone cells become apparent later than the BETL about the same time as the adjacent CZ, around 8–10 DAP (Kiesselbach and Walker, 1952; Leroux et al., 2014). Cells are more elongate than the adjacent BETL and have oblique ends, sometimes being described as prismatic (**Figure 2**). They have moderately dense cytoplasm, abundant vesicles, and nuclei slightly larger than the adjacent BETL (Kiesselbach and Walker, 1952; Davis et al., 1990; Leroux et al., 2014). Flange wall ingrowths get progressively shorter and fewer in number within the cells adjacent to the CZ (Davis et al., 1990; Kang et al., 2009; Monjardino et al., 2013). Adjacent cells often have the wall ingrowths at the same location giving cross sections of the cells a distinctive appearance. The walls in between the ingrowths have many plasmodesmata these being most abundant in cells near the CZ, (Davis et al., 1990; Gao et al., 1998; Monjardino et al., 2013). It has been suggested that cell wall features, ingrowths and abundant plasmodesmata, might serve the function of radial distribution of solutes (Davis et al., 1990).

Embryo surrounding region cells are the earliest endosperm cells to differentiate, as early as 4 DAP and can even be apparent as the last of the central vacuole becomes cellular. They are located adjacent to the embryo and completely encircle the embryo at first but by 7 DAP they only form a semi-circle of cells located around the suspensor of the embryo (**Figure 2**) (Schel et al., 1984; Opsahl-Ferstad et al., 1997). ESR cells are small, isodiametric, and have dense cytoplasm with small vacuoles. Cytoplasmic characteristics that suggest high metabolic activity include: large nuclear to cell volume, prominent mitochondria, an abundant network of rER with large intracisternal spaces and Golgi associated with many vesicles. Around 15 DAP, ESR cells are the first cells in the endosperm to undergo PCD as the embryo expands (Dominguez and Cejudo, 2014). Proposed functions of the poorly understood ESR include, pathogen defense, embryo/endosperm signaling, nutrient transport from endosperm to embryo and perhaps protecting the embryo from fluxes of auxin (Cossegal et al., 2007; Chen et al., 2014).

Starchy endosperm functions as the major nutrient storage site in the endosperm and occupies the greatest portion (by volume or weight) of the kernel. SE cells differentiate from the inner cells produced by the cellularization process and new cells formed by peripheral divisions in the aleurone/subaleurone layers (**Figure 2**). Accordingly, cell differentiation, endoreduplication and storage deposition within them occurs in a developmental pattern from the kernel crown to base and the center to the edge with the oldest, largest, and most developed SE cells in the endosperm center (Kiesselbach, 1949; Kowles and Phillips, 1988). Beginning ∼10 DAP as SE cells enlarge, they cease mitosis and undergo multiple rounds of endoreduplication that increase the DNA content and nuclear size (Kowles and Phillips, 1985). It is at this time that the cells begin to accumulate starch and storage proteins. Endoreduplication, characterized by DNA replication without chromatid separation, yields multiple copies of the nuclear DNA and 4–5 cycles of endoreduplication (up to 192C) is common (Sabelli and Larkins, 2009; Dante et al., 2014). There is a positive relationship between *C*-value, nuclear size and cell size and in 16 DAP endosperm, the centrally-located largest cells, with the highest *C*-values, were fewest in number (less than 7% of the total cells) but accounted for 60% of the endosperm volume (Vilhar et al., 2002). Starch granules that account for ∼70% of the final kernel dry weight are semi-crystalline structures synthesized from densely-packed amylose and amylopectin (Hannah, 2007). Protein storage in the SE cell involves both the prolamin zeins, which are synthesized and accumulate in rER derived protein bodies, and globulins that accumulate in PSV (Khoo and Wolf, 1970; Lending and Larkins, 1989; Woo et al., 2001; Arcalis et al., 2010). Zeins account for over 60% of the kernel protein and are high in proline and glutamine but low in several essential amino acids (lysine, methionine, and tryptophan) significantly affecting the nutritional value of seeds. Zeins fall within 4 classes and the presence and abundance of different classes within protein bodies affects protein body size and association with the starch granules affecting physical characteristics of kernel (Holding, 2014). The nascent protein body forms with deposition of γ-zeins within small protein bodies. In larger, more mature protein bodies, γ- and β-zeins localize to a peripheral position after abundant α-zein and δ-zein is deposited in the internal portion (Lending and Larkins, 1989; Woo et al., 2001; Guo et al., 2013). Gene expression patterns of developing endosperm shows γ- and β-zeins transcripts occur throughout the endosperm at 10 DAP

whereas α-zein transcripts are confined to the germinal edge reiterating the central to edge pattern of kernel development (Woo et al., 2001). Endoreduplication and storage deposition continue until the cells undergo PCD, which begins in central SE cells about 16 DAP (Young et al., 1997).

Subaleurone cells are located just inside the aleurone in all portions of the endosperm except the base near the BETL. Early workers described the area as cambial-like because periclinal divisions generate linear files of cells that contribute the last cells to the edge of the SE (Randolph, 1936; Kiesselbach, 1949; Cooper, 1951). Subaleurone cells are small in size and the cytoplasm is characterized by numerous mitochondria, proplastids, some aleurone-like lipid bodies and ER but little starch and few protein bodies are present (Khoo and Wolf, 1970; Lending and Larkins, 1989). In mature kernels, the subaleurone is still distinct from the adjacent SE as the cells are smaller, the protein bodies are larger, and the cells lack large starch grains (Duvick, 1961; Khoo and Wolf, 1970).

Endosperm adjacent to scutellum may be a new cell type defined by location and transcriptome but the cells are cytologically indistinguishable from the adjacent SE (Doll et al., 2020). EAS is first detectable at 9 DAP as 2–3 layers of cells whose transcriptome has an enrichment of transporter genes compared to the rest of the endosperm. This area is identifiable until about 20 DAP and presumably facilitates nutrient supply or communication across the endosperm-embryo interface.

Conducting zone cells have received little cytological study and descriptions are all very brief and appear to include BIZ, BETL, and/or SE (Kiesselbach and Walker, 1952; Davis et al., 1990; Monjardino et al., 2013). Several authors have noted a core of elongate cells within the base of the endosperm extending above the BETL and suggested they were vascular-like and had a conducting function (Brink and Cooper, 1947; Cooper, 1951; Charlton et al., 1995). Recently, several studies have more completely described the CZ as a distinct cell type apart from BETL and BIZ cells (Leroux et al., 2014; Zheng et al., 2014). The cells are extremely elongate with tapering end walls and are distinct from neighboring cells by their much larger size, granular cytoplasm, prominent enlarged nuclei, few starch grains, lack of wall ingrowths, and gene expression profiles. At ∼ 24 DAP, these cells are thought to begin to degenerate.

MOLECULAR AND GENETIC REGULATION OF ENDOSPERM DEVELOPMENT

Although the endosperm is composed of several distinct tissues and multiple cell types, each of which contributes uniquely to the biology of the grain, the majority of molecular work has focused on understanding the BETL, aleurone, SE and the ESR, which will each be considered here.

Regulation of Basal Endosperm Transfer Layer Cell Development

The first cells to form during endosperm cellularization give rise to the BETL and aleurone, however, evidence suggests that BETL specification may begin earlier, perhaps in the megagametophyte (Gutierrez-Marcos et al., 2006). The *baseless1* (*bsl1*) mutant causes patterning defects in the embryo sac, which subsequently manifest during endosperm development as disorganized BETL, including mispatterned basal gene expression. Furthermore, several gene transcripts show basal-specific accumulation beginning in coenocytic endosperm prior to cellularization. This suggests that BETL specification begins prior to endosperm cellularization and maybe in the embryo sac before fertilization. Following cellularization, the transfer cells differentiate and form a morphological gradient along the basal-apical axis, grading into the BIZ and CZ, and along the germinal-abgerminal axis (Gómez et al., 2009). As discussed below, this pattern might be associated with concentration gradients of inducing factors such as hormones or sugars.

Myb Related Protein1 Is a Central Regulator of Basal Endosperm Transfer Layer Cell Fate

MRP1 is a transcription factor (TF) and a determinant of BETL cell fate because ectopic expression of *MRP1* was sufficient to cause early aleurone cells to acquire BETL identity (Gómez et al., 2009). MRP1 is specifically expressed in the BETL and directly activates expression of several other BETL-specific genes, collectively known as *basal endosperm transfer layer* (*betl*) genes (Gómez et al., 2002; Barrero et al., 2006). Several *betl* genes encode peptides that are secreted into surrounding pedicel tissue and have antifungal properties suggesting they are protective for the seed (Cai et al., 2002).

A transcriptomic analysis identified *MRP1* as a hub gene for the BETL compartment and among the genes in the expression module were six additional BETL-specific TFs, which may in turn regulate additional downstream BETL-specific genes (Zhan et al., 2015). Other MRP1 targets of particular note include *maternally expressed gene-1* (*meg1*) and two cytokinin response regulator (RR) genes, *ZmTCRR1* and *ZmTCRR2* (Gutiérrez-Marcos et al., 2004; Muniz et al., 2006, 2010; Gómez et al., 2009).

MEG1 and Imprinting Control Basal Endosperm Transfer Layer Development

MEG1 is expressed specifically in the BETL and encodes a small cysteine-rich secreted peptide proposed to function as a developmental signaling molecule (Gutiérrez-Marcos et al., 2004; Costa et al., 2012). Indeed, *meg1* RNAi caused a severe reduction in BETL development in the basal endosperm, while ectopic expression of *MEG1* also caused ectopic BETL formation; hence, MEG1 is necessary and sufficient for BETL differentiation (Costa et al., 2012). These treatments were accompanied with a corresponding reduced expression, or ectopic expression of *MRP1*, respectively. Thus, *MEG1* and *MRP1* both act as determinants of BETL fate and their expression is regulated by a feedback loop of mutual reinforcement.

MEG1 is an imprinted gene where maternally inherited copies are expressed while the paternal allele is silenced by DNA methylation (Gutiérrez-Marcos et al., 2004). Imprinting is often hypothesized as being involved in controlling resource allocation (Rodrigues and Zilberman, 2015). To test this hypothesis, a synthetic *Meg1* gene (*synMeg1*) was constructed where codon replacement produced a coding region with little nucleotide

sequence similarity to the endogenous gene. This was then placed under the control of the *bet9* promoter, which is BETL-specific but is not imprinted. Transgenic maize showed a dosage dependent increase in the extent of BETL cell differentiation and a concomitant increase in kernel size and weight, whereas, *synMeg1* under the control of the native (imprinted) *Meg1* promoter did not produce this effect (Costa et al., 2012). These results are consistent with imprinting of *Meg1* regulating resource acquisition in the kernel by limiting BETL development.

Hormone Signaling and Basal Endosperm Transfer Layer Development

Several lines of evidence suggest that cytokinin (CK) phytohormone may be important for BETL development and/or function. CKs are often associated with sink formation and they accumulate in developing maize kernels, peaking during the period of maximum grain filling. The accumulation pattern mirrors expression of *ZmIPT2*, which encodes isopentenyltransferase, a CK biosynthetic enzyme. *ZmIPT2* is most strongly expressed in the BETL, where the highest CK levels occur (Brugiere et al., 2008).

The CKs signal *via* a pathway where histidine kinase (HK) receptors signal *via* histidine phospho-transfer protein (HP) to regulate the activity of response regulators (RRs) that control expression of downstream factors (To et al., 2008). There are two types of RRs; type-B RRs are MYB family TFs that function as positive effectors of CK signaling, whereas, type-A RRs are negative regulators of CK signaling. In response to CK, HPs phosphorylate type–B RRs, which activates them and allows them to control CK-regulated gene expression. One type–B RR target is activation of type-A RR expression. A pair of type-A RR genes, *ZmTCRR1* (*Zea mays Transfer Cell Response Regulator1*) and *ZmTCRR2*, are specifically expressed in the BETL (Muniz et al., 2006, 2010). Gene expression is highest during the period of maximum BETL differentiation suggesting a possible role in directing BETL development. The protein products of these genes are not restricted to BETL cells but accumulate along a concentration gradient into the CZ, coincident with the gradient in cell morphology.

It remains unclear whether these RR-like genes are in fact involved with CK signaling. There is no experimental evidence for CK regulation and the TCRRs contain some sequence features not found in bona fide RRs (Muniz et al., 2010). As mentioned, *ZmTCRR1* and *ZmTCRR2* are direct targets of regulation by MRP1. Intriguingly, MRP1 contains a motif similar to the GARP motif found in type-B RRs, suggesting either that MRP1 is a type-B RR performing an as yet undiscovered role in CK signaling, or that this represents a regulatory system descended from canonical RRs but no longer connected to hormone signaling.

Sugar Induction of Basal Endosperm Transfer Layer Differentiation

One of the major functions of the BETL is sugar transport and interestingly, several studies have revealed that sugar plays an essential role in promoting BETL differentiation. Proteins involved in sugar import include SWEET sugar transporters and invertase, which cleaves sucrose to glucose and fructose. The *miniature1* (*mn1*) gene is a BETL-specific gene that encodes a cell wall invertase, and *ZmSWEET4c* is also a BETL-specific gene encoding a plasma membrane hexose transporter (Sosso et al., 2015). Mutations in both genes impair sugar transport into developing kernels causing substantial decreases in grain size (Miller and Chourey, 1992; Cheng et al., 1996; Kang et al., 2009; Sosso et al., 2015). Notably, mutants in both genes show dramatically decreased BETL formation showing that sugar flux is required to promote BETL cell differentiation. Furthermore, the expression of *ZmSWEET4c* and *mn1*, as well as *MRP1*, are all sugar inducible, particularly with glucose, and expression of all these genes is decreased in the *zmsweet4c* mutant (Barrero et al., 2009; Sosso et al., 2015). What emerges is a feed-forward model where sugar induces the expression of sugar transport machinery as well as BETL differentiation, which then facilitates increased sugar transport into the endosperm and further reinforces this system (Sosso et al., 2015).

Transport of other classes of molecules is also critical; the choline transporter-like protein1 (ZmCTLP1) is encoded by the *small kernel 10* (*smk10*) gene. Mutations of *smk10* disrupt BETL differentiation, decrease kernel size, and cause extensive alterations in endosperm lipid composition and content (Hu et al., 2021).

Regulation of Aleurone Development

Aleurone is a metastable cell type requiring continuous positional cues to establish and perpetuate aleurone identity (Becraft and Asuncion-Crabb, 2000). Genetic studies identified several factors that are likely involved in signaling aleurone fate. Mutants of *defective kernel 1* (*dek1*) lack aleurone, showing it is essential for aleurone development (Becraft and Asuncion-Crabb, 2000; Becraft et al., 2002; Lid et al., 2002). DEK1 is a plasma membrane-localized protein consisting of several domains. An intracellular region includes a calpain-family proteinase domain whose cysteine protease activity is stimulated by Ca^{++} (Wang et al., 2003; Tian et al., 2007). A transmembrane domain contains a series of 21–24 membrane-spanning helices, depending on the molecular prediction, interrupted by a "loop" that is either cytoplasmic or extracellular, depending on the model (Lid et al., 2002; Kumar et al., 2010). This transmembrane domain is required for mechanosensitive Ca^{++} channel activity, leading to the hypothesis that tension on epidermal (aleurone) cells may trigger Ca^{++} (Tran et al., 2017). This in turn would activate the proteinase and regulate aleurone cell fate through cleavage of yet unidentified signal transduction substrates.

CRINKLY4 (CR4) is a plasma membrane receptor-like kinase that is likewise involved in promoting aleurone fate through an unknown signaling mechanism (Becraft et al., 1996; Jin et al., 2000). Mutants of *cr4* impair aleurone development often producing mosaic kernels partially lacking aleurone (Becraft et al., 1996; Becraft and Asuncion-Crabb, 2000). Genetic evidence suggests that the DEK1 and CR4 signaling pathways converge although the molecular details remain obscure (Becraft et al., 2002).

Whereas most wild type maize lines contain just a single layer of aleurone cells, mutants in the *supernumerary aleurone*

1 (*sal1*) gene produce multiple aleurone layers, indicating SAL1 is normally required to restrict aleurone formation (Shen et al., 2003). SAL1 is a class E vacuolar sorting protein, related to human CHMP1, involved in internalization and sorting of plasma membrane proteins into multivesicular bodies for degradation (Spitzer et al., 2009). The SAL1, DEK1 and CR4 proteins colocalized in endosomes suggesting that SAL1 may limit DEK1 and CR4 levels by protein degradation (Tian et al., 2007). This was hypothesized to limit levels of DEK1 and CR4 signaling and thus restrict the number of aleurone layers.

The *thick aleurone1* (*thk1*) mutation also causes multiple aleurone cell layers indicating THK1 is another negative regulator of maize aleurone cell fate (Becraft and Yi, 2011). The *thk1* gene encodes a homolog of NEGATIVE ON TATA-LESS1 (NOT1), a protein that acts as a scaffold for the CARBON CATABOLITE REPRESSION4-NEGATIVE ON TATA-LESS (CCR4-NOT) complex that mediates many mRNA-related processes, including RNA-turnover, transcription initiation and elongation, translation, and RNA quality control (Wu et al., 2020). The mutant of *thk1* alters expression of genes associated with cell division, cell communication, hormone response, and plant epidermis development, which may contribute to generating multiple aleurone cell layers (Wu et al., 2020). Interestingly, the *thk1* mutant is epistatic to *dek1*; double mutants showed multiple aleurone layers like *thk1*, even though *dek1* mutants are unable to form aleurone, indicating THK1 is a likely component of the signaling system downstream of DEK1 (Becraft and Yi, 2011).

The *naked endosperm* (*nkd*) mutant is a duplicate factor that disrupts aleurone differentiation, producing endosperm with multiple layers of peripheral cells only partially differentiated as aleurone (Becraft and Asuncion-Crabb, 2000). The corresponding genes, *nkd1* and *nkd2*, encode INDETERMINATE DOMAIN (IDD) family C2H2 zinc finger TFs, ZmIDDveg9 (NKD1) and ZmIDD9 (NKD2), respectively (Colasanti et al., 2006; Yi et al., 2015). The NKD1,2 TFs regulate genes important for several aspects of aleurone function including, cell growth and division, anthocyanin accumulation, lipid storage, pathogen defense and abscisic acid (ABA) response (Gontarek et al., 2016; Gontarek and Becraft, 2017).

NKD1,2 and THK1 may co-regulate aleurone cell development. Triple mutants of *nkd1;nkd2;thk1* reveal an additive relationship between *nkd1,2* and *thk1* on controlling the number of aleurone cell layers, and an epistatic relationship on aleurone cell differentiation (*nkd1,2* is epistatic to *thk1*); triple mutants have many layers of partially differentiated aleurone (Becraft and Yi, 2011). This indicates that NKD1,2 and THK1 may negatively regulate aleurone cell fate through independent pathways, and that NKD1,2 is required for aleurone cell differentiation downstream of THK1. A co-expression network analysis between *nkd1,2* and *thk1* mutants suggests that NKD1,2 and THK1 may co-regulate cell cycle and division to restrict aleurone development to a single cell layer, whereas NKD1,2, but not THK1, may regulate auxin signaling to maintain normal aleurone differentiation (Wu and Becraft, 2021).

A recent study suggests that adequate iron content is critical for proper aleurone development (He et al., 2021). The *shrunken4* (*sh4*) gene of maize encodes a YELLOW STRIPE-LIKE2 (ZmYSL2) metal transporter that controls iron abundance in aleurone cells. The *sh4* mutant causes loss of aleurone cell identity accompanied with decreased iron accumulation. The basis for this requirement is unknown but it seems likely that iron may be an essential cofactor for one or more components of the aleurone cell fate machinery. Interestingly, the GO term "iron ion binding" was over-represented among DEGs of *nkd* mutant aleurone (Gontarek et al., 2016).

Regulation of the Embryo Surrounding Region

The ESR is a poorly understood tissue and little is known about how its development is regulated. Weighted gene coexpression network analysis (WGCNA) identified an ESR-specific gene coexpression module, which was enriched for genes involved in cell–cell signaling, consistent with the proposed function of these cells in signaling between the endosperm and embryo (Zhan et al., 2015). ESR-specific promoters were identified and several putative *cis* elements were identified, but most appear to be shared amongst other endosperm cell types (Bonello et al., 2000; Zhan et al., 2015). Several TFs were identified with high module membership scores for the ESR-specific module, which are good candidates for testing experimentally (Zhan et al., 2015).

No bona fide ESR mutant has yet been reported. This could be because disruption of the ESR is lethal, because such mutants are too subtle, or because of genetic redundancy. The *shohai* (*shai*) mutant disrupts the formation of the embryo pocket, a cavity in the endosperm that is normally filled by the embryo (Mimura et al., 2018). In non-concordant kernels, a *Shai* wildtype endosperm rescued the development of mutant embryos whereas, wildtype embryos caused the formation of a normal embryo pocket in mutant endosperms. Thus, SHAI is involved in signaling between the endosperm and embryo, and as a TF of the RWP-RK family, is a good candidate for controlling ESR development. To date, a detailed analysis of the ESR has not been reported for this mutant.

Molecular Regulation of Starchy Endosperm Development

The SE is the most economically valuable part of a grain and, as such, considerable effort has been expended to understand the molecular and biochemical regulation of SE development, particularly as it pertains to protein and starch accumulation. Yet, despite this attention, little is known about the regulation of SE cell fate. Among TFs that regulate SE development, OPAQUE-2 (O2) is a basic leucine zipper (bZIP) TF that has long been recognized as key to regulating the biosynthesis and accumulation of nutrient materials in SE. First shown to activate the expression of the 22-kD α-zein gene (Schmidt et al., 1990, 1992), a genome-wide transcriptional regulatory network study showed that O2 also regulates several additional zein storage protein genes, genes for carbon fixation (PPDK1 and PPDK2), and additional downstream transcription factors (GBF and Myb-like TFs) (Li et al., 2015). Further, proteomic studies showed that protein levels of Granule-Bound Starch Synthase I (GBSSI),

Starch Synthase IIa (SSIIa), and Starch Branching Enzyme I (SBEI) were reduced in *o2* mutants, indicating that O2 may also play an important role in starch biosynthesis, albeit indirectly (Jia et al., 2013; Zhang et al., 2016).

PROLAMIN-BOX BINDING FACTOR1 (PBF1) is a TF that can bind to the *prolamin-box* in promoters of the 27-, 22, and 19-kD zein genes (Wang et al., 1998). Moreover, starch content was reduced in *pbf1* RNAi knockdown mutants, suggesting that PBF1 also affects starch accumulation (Zhang et al., 2016; Qi et al., 2017). Compared with the *o2* or *pbfRNAi* single mutants, the *o2*; *pbfRNAi* double mutant caused further reduction of zein protein and starch content suggesting that O2 and PBF function additively and synergistically to regulate gene networks in SE development (Zhang et al., 2015, 2016).

In addition to O2-PBF1 interactions, O2 also interacts with other TFs, including O2 HETERODIMERIZING PROTEINS (OHPs), ZmbZIP22 and ZmMADS47, forming a complex that regulates expression of zein genes (Li and Song, 2020; Dai et al., 2021). Two NAC transcription factors, ZmNAC128 and 130, are also involved in regulating zein and starch biosynthetic genes (Zhang et al., 2019).

NKD1,2 are involved in SE development in addition to their roles in aleurone formation. Laser-capture microdissection RNA sequencing (LCM RNAseq) showed the *nkd1,2* genes are expressed in both aleurone and SE. The *nkd1,2* mutants have an opaque, floury endosperm phenotype accompanied by widespread changes in expression of genes regulating starch biosynthesis, storage proteins or other cellular components (Yi et al., 2015; Gontarek et al., 2016).

In addition to nutrient biosynthesis and accumulation, endoreduplication and PCD are important features of SE development. As the endosperm transitions from the cell division to nutrient accumulation phases, the cell cycle transitions from mitotic cell division to endoreduplication (Larkins et al., 2001). Cyclin-dependent Kinases (CDKs) are key regulatory factors affecting endoreduplication, among which A-type CDK (CDKA) functions in S-phase and B-type CDK (CDKB) functions to promote G2 to M phase transition. Endoreduplication may be triggered by induction of CDKA and inhibition of CDKB (Grafi and Larkins, 1995; Sabelli, 2012). RETINOBLASTOMA-RELATED (RBR) proteins and CDK inhibitor (CKI) proteins are additional cell cycle regulators that may control the transition to endoreduplication. An *rbr1* mutant with decreased expression resulted in enhanced endoreduplication suggesting RBR1 is a negative regulator (Sabelli et al., 2013). Two different families of CKIs have been implicated to regulate endoreduplication, Kip-related proteins (KRPs) and SIAMESE (SIA) proteins (Coelho et al., 2005; Zhang et al., 2020). Members of both families are expressed at appropriate times in SE and overexpression of KRP1 in maize callus promoted endoreduplication. Hormones also appear to influence endoreduplication, with auxin promoting the initiation and maintenance of endoreduplication, whereas, cytokinin inhibited proliferating cells from entering the endoreduplication cycle (Sabelli, 2012).

Beginning at around 12-16 DAP, SE cells undergo PCD (Young and Gallie, 2000) with the initiation of PCD promoted by ethylene and sugar accumulation (Bhave et al., 1990; Young et al., 1997). The maize ABA-insensitive *viviparous1* (*vp1*) mutant showed increased levels of ethylene and accelerated progression of PCD, indicating that ABA might inhibit PCD *via* negatively regulating ethylene synthesis (Young and Gallie, 2000). Cell cycle regulation also interfaces with PCD as the *rbr1* mutant enhanced PCD, suggesting negative effects of RBR1 on both PCD and endoreduplication in maize SE (Sabelli, 2012). The details of the connections among hormones, cell cycle control factors, endoreduplication, and PCD are still unclear and require further characterization.

Transcription Networks and Endosperm Development

Different endosperm cell types have distinct transcriptomes and recent studies have begun to unravel the gene regulatory networks (GRNs) that underlie endosperm development and function (Zhan et al., 2015; Gontarek et al., 2016; Zhang et al., 2016; Feng et al., 2018; Ji et al., 2021; Wu and Becraft, 2021). Some of the key TFs known to regulate specific processes during endosperm development were discussed above. In addition, there are extensive inter-regulatory relationships among many of these TFs. These involve direct regulation of target genes as well as indirect regulation *via* downstream TFs. NKD1 and NKD2 directly regulate each other's expression as well as directly promote expression of other important TFs including O2 and PBF1 (Gontarek et al., 2016). The DOF3 TF gene is also regulated by NKD1 and NKD2 but most likely indirectly. DOF3 in turn directly regulates the expression of NKD1 and NKD2 (Qi et al., 2017) while O2 promotes expression of NKD2 (Zhan et al., 2018). NKD2 is also regulated by OPAQUE11 (O11, a bHLH TF), which also regulates the expression of DOF3, O2, and PBF (Feng et al., 2018). O2 also transactivates ZmGRAS11, a GRAS-family transcription factor without a DELLA domain, which then directly regulates the expression of ZmEXPB12, a cell wall loosening protein important for cell expansion (Ji et al., 2021). This suggests that O2 not only regulates grain filling, but also controls cell expansion in developing endosperm. ZmABI19 is a B3 domain TF that regulates expression of multiple key TF genes, including O2, PBF1, ZmbZIP22, NAC130, and O11, indicating an important role in maize seed development and grain filling (Yang et al., 2021). Furthermore, a recent study proposed a model for O2 nuclear translocation mediated by the SnRK1-ZmRFWD3 pathway (Li et al., 2020). At high sucrose levels, the sucrose-responsive protein kinase SnRK1 phosphorylates ZmRFWD3, an E3 ubiquitin ligase, leading to ZmRFWD3 degradation. At low sucrose levels, SnRK1 is inhibited, and ZmRFWD3 is released to ubiquitinate O2, facilitating O2 localization into the nucleus. This model links sucrose signaling dynamics with storage protein biosynthesis during grain filling.

A striking point is that many of the known regulators function in multiple cell types and despite advances in our understanding of gene networks, it is still unclear at the GRN level what determines the different cell fate decisions during endosperm development. O2 and PBF are well known TFs important in SE (Zhang et al., 2015; Gontarek et al., 2016) but the *o2* gene is expressed in maize aleurone (Zhan et al., 2018) and a double knockdown of the rice *o2* and *pbf* homologs, *RICE SEED*

b-ZIPPER 1 (*RISBZ1*) and *RICE PROLAMIN BOX BINDING FACTOR* (*RPBF*), caused multiple layers of disordered aleurone (Kawakatsu et al., 2009). The *o11* mutant, with striking effects on SE size and decreased starch and protein accumulation, also shows multiple layers of irregular aleurone cells (Feng et al., 2018). Similar phenotypes were also observed upon RNA interference of maize *dof3*, which also caused decreased starch accumulation as well as aleurone irregularities (Qi et al., 2017). Conversely, the *nkd* mutant was first recognized for its effect on aleurone development but further analysis showed the *nkd* genes also regulate key functions in the SE (Zhang et al., 2015; Gontarek et al., 2016). Thus, there are complex networks of regulatory interactions amongst TF genes that control both SE and aleurone development (**Figure 3**). The specific features of these networks that lead to the different cell identities during development remain elusive at this time.

ENDOSPERM DEVELOPMENT AND APPLICATIONS TO IMPROVE GRAIN QUALITY

"Grain quality" encompasses a variety of traits that vary depending on the specific end use of the grain. They include traits such as grain size, composition, hardness, nutritional value, pathogen resistance, and so on. Knowledge on the regulation of grain development can be used to improve grain properties in two basic ways, either to alter metabolic pathways within the existing cellular context or to alter cellular development. Both cellular development and metabolic pathways were altered during the domestication process without the benefit of understanding the underlying biology. In modern times, the latter approach has received much more attention with significant efforts to understand and manipulate the amount and properties of stored starch, protein and lipids. However, altering cellular development may offer the potential to manipulate grain properties in other ways. Examples of key genes that may be of value for grain improvement are listed in **Table 2**.

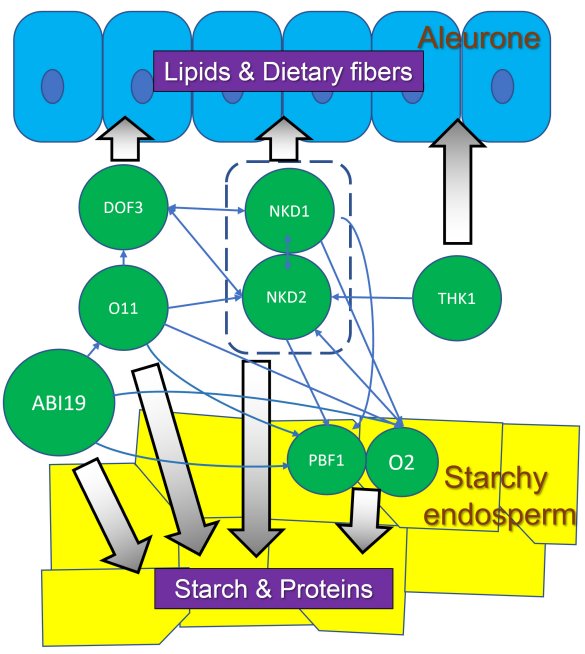

FIGURE 3 | Regulatory interactions among TFs in aleurone and SE, and their potential association with corresponding nutrient compounds. These TFs and associated pathways could be targets for bioengineering to optimize maize seed quality.

Maize Domestication Altered Grain Development

Maize was domesticated around 9,000 years ago from *Zea mays* ssp. *parviglumis*, a grassy teosinte plant native to Mesoamerica

TABLE 2 | Examples of key genes associated with maize kernel quality.

Gene	Gene model	Functional description	How is it associated with kernel quality?
O2	Zm00001d018971	BZIP family transcription factor	High lysine content
ZP27	Zm00001d020592	γ-zein protein	Potential *o2*-modifier, improved kernel hardness and high lysine content
DGAT1-2	Zm00001d036982	Acyl-CoA:diacylglycerol acyltransferase	High oil content
WRINKLED1	Zm00001d005016	HAP3 subunit of the CCAAT-binding transcription factor	High oil content Low starch content
PBF1	Zm00001d005100	Prolamin-box binding factor	Affect storage protein content
MADS47	Zm00001d046053	MADS-box transcription factor	Affect storage protein content
BZIP22	Zm00001d021191	BZIP family transcription factor	Affect storage protein content
NAC128	Zm00001d040189	NAC family transcription factor	Affect storage protein and starch fine structure
NAC130	Zm00001d008403	NAC family transcription factor	Affect storage protein and starch fine structure
NKD1	Zm00001d002654	IDD family zinc finger transcription factor	Affect content of oil, fiber and vitamin in aleurone
NKD2	Zm00001d026113	IDD family zinc finger transcription factor	Affect content of oil, fiber and vitamin in aleurone
THK1	Zm00001d027278	Scaffolding protein of CCR4-NOT complex	Affect content of oil, fiber and vitamin in aleurone

(Piperno et al., 2009). Maize and teosinte have striking morphological differences, including kernel characteristics. As reviewed by Flint-Garcia (2017), teosinte grains are small and encased in a hard fruitcase, whereas, modern maize grains are naked and typically about 10 times larger than teosinte. Increased grain size is accompanied by changes in composition, notably an increase in starch content. Elimination of the fruitcase was a critical step in domestication, making the collection and processing of grains for food much easier. Elimination of the fruitcase also removed a physical restriction, which allowed for the dramatic increase in grain size. Modification of this trait was accomplished by mutations and selection of the *teosinte glume architecture1* (*tga1*) gene (Wang et al., 2015). Signatures of selection are also found in the starch biosynthesis genes, *su1, ae1,* and *bt2* (Whitt et al., 2002). For other grain traits, the genetic basis is less clear. Signatures of selection are found in over 1,000 genes indicating that domestication involved the accumulation of many small effects (Wright et al., 2005).

Grain Improvement Based on Regulation of Metabolic Pathways

There are myriad metabolites in the endosperm that contribute to kernel quality and it is beyond the scope of a single review to cover them all. Here we will mention notable examples for the major classes of storage compounds: starch, protein and oils.

Starch

Starch is a deceptively complex molecule and structural variations can lead to variation in quality properties such as gelling temperature and digestibility. Starch metabolism is an example of a system where simple genetic changes can have profound impacts on grain quality and end use. Three examples will be mentioned here:

Sweet corn is the most familiar example of altered starch impacting grain characteristics. Mutations in enzymes of the starch biosynthetic pathway impede the incorporation of glucose subunits into starch and thereby cause an accumulation of free sugars in the endosperm. Such grain would not be suitable as feed or most other uses but is valued for human consumption. The *sugary1* (*su1*), *shrunken2* (*sh2*) and *brittle1* (*bt1*) genes are examples of loci where single gene mutations can confer the sweet corn character and form the basis of cultivar breeding programs (Lertrat and Pulam, 2007).

Waxy starch is deficient in amylose content. Normal maize endosperm starch is a mixture of amylopectin and amylose in about a 75%:25% ratio. The amylose content influences many starch properties such as gelatinization temperature, pasting and retrogradation, all important for cooking, sizing and other applications (Jane, 2004). Amylose is produced by the granule-bound starch synthase I (GBSSI) protein, encoded by the *waxy1* (*wx1*) gene. Loss-of-function *wx1* mutations produce "waxy" starch nearly devoid of amylose, whereas GWAS identified an allele of *wx1* associated with high amylose content (Li et al., 2018).

ADPglucose pyrophosphorylase (*AGPase*) is a rate limiting enzyme that catalyzes the first committed step in starch biosynthesis. Overexpression or enhanced thermostability of the AGPase enzyme can lead to increased starch production and grain yield (Li et al., 2011; Hannah et al., 2017). Interestingly, overexpression increased yield through increased seed size, while the thermostable variant increased yield through increased seed number.

Storage Proteins and Quality Protein Maize

Normal maize zeins are characterized by low content of several essential amino acids, most notably lysine, which limits the nutritional value of maize grain in human diets or livestock feed. Mutants of *o2* cause decreased α-zein content accompanied by elevated lysine levels (Mertz et al., 1964). Unfortunately, the improved nutritional composition is associated with unfavorable grain characteristics, including soft and chalky kernel texture, increased susceptibility to insects or fungi, low yields, and unappealing flour characteristics (Villegas, 1994; Habben and Larkins, 1995). To overcome these issues, breeders identified modifier loci that improve grain characteristics while maintaining high lysine content. Such modified *o2* lines are called Quality Protein Maize (QPM) (Prasanna et al., 2001).

Several genes involved in QPM have been identified through QTL mapping. A gene encoding 27 kD γ-zein was linked to the kernel texture phenotype of QPM and RNAi knockdown and genome-wide deletion of γ-zein genes resulted in an opaque and soft kernel phenotypes suggesting that soft kernel texture caused by α-zein deficiency could be compensated by γ-zeins (Lopes et al., 1995; Wu et al., 2010; Yuan et al., 2014). Another QTL mapped to *wx1* (BABU et al., 2015). This is consistent with a proteomic study that found elevated GBSSI activity and altered starch structure in QPM endosperm (Gibbon et al., 2003). These studies suggest that kernel texture derives from complex interactions among proteins, starches and possibly other molecules, and that deficiencies in one molecule can sometimes be compensated by another. These and other QTLs have facilitated marker assisted breeding programs for improved amino acid balance (Gupta et al., 2013; Hossain et al., 2018). Continued study might provide insights for additional strategies to produce improved protein maize lines.

Improving Oil Content

Maize oil (corn oil) is mainly used in cooking. Its high smoking point and low saturated fatty acid content make it favorable for frying and human consumption. Also, it may help reduce cholesterol absorption, which could increase the percentage of beneficial high-density lipoproteins (HDL) in blood (Singh et al., 2013). Corn oil is primarily derived from the embryo and the primary determinant of oil percentage is the weight ratio of embryo to endosperm (Yang et al., 2010). Within the endosperm, aleurone cells have the highest oil content. Oil quality is determined by the relative amounts of various fatty acids with different physical characteristics and flavors. Oil quantity (yield) and composition are both of interest for grain improvement. As such, kernel oil content is a complex trait influenced by many factors (Yang et al., 2012; Fang et al., 2021).

QTL-mapping studies identified numerous loci for kernel oil concentration and fatty acid composition. Significantly, many are enzymes involved in the oil metabolic pathway (Yang et al., 2012; Li et al., 2013; Fang et al., 2021). These represent targets for

marker assisted breeding or metabolic engineering, and several of them have been utilized to enhance oil content.

A high-oil QTL (qHO6) was associated with an 18.7% increase in oil concentration (in the embryo) as well as altered oil composition with 61.3% more oleic acid and 24.4% less linoleic acid (Zheng et al., 2008). This QTL mapped to a gene encoding acyl-CoA: diacylglycerol acyltransferase (DGAT1-2), a rate limiting enzyme in triacylglycerol synthesis. Transgenic expression of a "normal-oil" *DGAT1-2* allele increased embryo grain oil by 9.3%, while transgenics containing the "high-oil" allele with a phenylalanine inserted at position 469 dramatically increased oil content by 27.9% (Zheng et al., 2008).

Key TFs could also be promising targets for oil improvement. The maize *wrinkled1* gene encodes a HAP3 subunit of the CCAAT-binding factor, and regulates carbon flux between starch and oil biosynthesis during kernel development. Overexpression increased kernel oil content by up to 46% and decreased starch content by approximately 60% (Shen et al., 2010). As knowledge of the molecular basis of oil production accumulates, it is reasonable to expect new strategies to improve maize kernel oil content.

Grain Improvement Based on Regulation of Cellular Development

Different cell types have varying functions and biochemical compositions. As such, altering the cellular content of a grain has the potential to substantially impact grain characteristics. By and large, this strategy has not been extensively pursued. Here we consider 2 cell types with considerable potential for impacting grain quality, BETL and aleurone.

Basal Endosperm Transfer Layer

As the cell type responsible for transporting metabolites from maternal tissues into the endosperm for incorporation into storage products, virtually all grain yield depends on BETL function. As described earlier, expanded expression of *MEG1* caused expanded differentiation of the BETL and resulted in larger kernels (Costa et al., 2012). BETL cells contain an assortment of transporters, including sugars, amino acids, ions and hormones (Thiel, 2014), expressed as part of a BETL gene co-expression module (Zhan et al., 2015). Sugar transport is perhaps the most critical function of the BETL (Cheng et al., 1996; Kang et al., 2009; Sosso et al., 2015). Sugar translocation during grain filling has been subject to selection pressure during domestication. The *sweet4c* gene shows signatures of selection (Sosso et al., 2015). Furthermore, *mn1* is more highly expressed in maize than in teosinte, and in rice, the *mn1* homolog underwent selection during domestication and produced increased grain size and yield upon transgenic overexpression (Wang et al., 2008).

These results support the potential for improving grain size or composition by manipulating BETL development or function. Expanding BETL formation could increase overall solute import and enhance kernel size. Modulating the relative expression levels of various classes of transporters could enhance grain filling or shift grain composition. More complete understanding of the MRP1 transcriptional network will be instrumental in achieving these goals (Dai et al., 2021).

Aleurone

As reviewed, the aleurone has many important properties including storage compound remobilization during germination, dietary benefits, mineral storage and pathogen defense (Becraft and Yi, 2011; Gontarek and Becraft, 2017). Commercial maize has a single layer of aleurone and increasing the number of layers could potentially improve certain grain characteristics. Mutants such as *thk1* (Yi et al., 2011) and the multiple aleurone layer (MAL) trait present in the Coroico landrace (Wolf et al., 1972) suggest it should be possible to develop maize cultivars with multiple layers. Transcriptomic analysis of *thk1* endosperm indicated elevated levels of gene expression for pathways associated with aleurone cells, including lipid metabolism, starch degradation, cell wall formation (Wu et al., 2020). Thus, desirable compounds of normal aleurone are likely present at elevated levels in the mutant raising the possibility for enhanced dietary value. The multiple layers of aleurone in barley contributes to the high level of amylase that catalyzes the rapid conversion of starch to fermentable sugars during the malting process. Multiple aleurone layers might potentially lead to new uses for maize grains in malting.

Conversely, eliminating aleurone may be advantageous in certain situations. White rice has the lipid-rich aleurone layer milled off to prevent the grain from going rancid under storage. Similar benefit could potentially be realized from aleurone-free maize grains. Also, phytic acid in aleurone is a major source of phosphate pollution associated with manure runoff which could potentially be alleviated by aleurone-free grain. Such kernels are conferred by the *dek1* mutant (Becraft et al., 2002; Lid et al., 2002).

Existing single gene mutants with the desired aleurone traits combine unfavorable kernel characteristics, including embryo and endosperm defects. To be of practical value, these undesirable effects must be uncoupled from the target traits, similar to what was accomplished with QPM. Further studies on the regulation of endosperm gene expression and GRNs may help facilitate this goal.

Perspectives

This review summarized studies of maize endosperm development at tissue, cellular and molecular levels, discussed how maize seed development was influenced by domestication, and introduced some current and potential applications to improve maize seed quality based on this knowledge. For future directions, some of the key regulators influencing endosperm development summarized in this article (**Table 2**) could potentially be utilized for breeding to improve seed quality. Recently, gene network analyses have been applied to maize endosperm development studies (Zhan et al., 2015), providing a powerful tool to predict central regulators of gene expression modules. These regulators could play important roles in biological processes or metabolic pathways of interest, or could act as modifiers or co-factors to interact with known regulators. Based on the predicted information and modern genetic approaches, we may enhance target phenotypes or suppress undesirable side effects more efficiently than conventional breeding approaches.

AUTHOR CONTRIBUTIONS

All authors listed have made a substantial, direct, and intellectual contribution to the work, and approved it for publication.

FUNDING

The United States National Science Foundation award number 1444568 supported the research, writing and publication costs.

REFERENCES

Abendroth, L. J., Elmore, R. W., Boyer, M. J., and Marlay, S. K. (2011). *Corn Growth and Development*. Ames, IA: Iowa State University Cooperative Extension Service.

Arcalis, E., Stadlmann, J., Marcel, S., Drakakaki, G., Winter, V., Rodriguez, J., et al. (2010). The changing fate of a secretory glycoprotein in developing maize endosperm. *Plant Physiol.* 153, 693–702. doi: 10.1104/pp.109.152363

BABU, B. K., Agrawal, P. K., Saha, S., and Gupta, H. S. (2015). Mapping QTLs for opaque2 modifiers influencing the tryptophan content in quality protein maize using genomic and candidate gene-based SSRs of lysine and tryptophan metabolic pathway. *Plant Cell Rep.* 34, 37–45. doi: 10.1007/s00299-014-1685-5

Barrero, C., Muniz, L. M., Gomez, E., Hueros, G., and Royo, J. (2006). Molecular dissection of the interaction between the transcriptional activator ZmMRP-1 and the promoter of BETL-1. *Plant Mol. Biol.* 62, 655–668. doi: 10.1007/s11103-006-9047-5

Barrero, C., Royo, J., Grijota-Martinez, C., Faye, C., Paul, W., Sanz, S., et al. (2009). The promoter of ZmMRP-1, a maize transfer cell-specific transcriptional activator, is induced at solute exchange surfaces and responds to transport demands. *Planta* 229, 235–247. doi: 10.1007/s00425-008-0823-0

Becraft, P. W., and Asuncion-Crabb, Y. T. (2000). Positional cues specify and maintain aleurone cell fate in maize endosperm development. *Development* 127, 4039–4048. doi: 10.1242/dev.127.18.4039

Becraft, P. W., and Yi, G. (2011). Regulation of aleurone development in cereal grains. *J. Exp. Bot.* 62, 1669–1675. doi: 10.1093/jxb/erq372

Becraft, P. W., Brown, R. C., Lemmon, B. E., Opsahl-Ferstad, H. G., and Olsen, O.-A. (2001). "Endosperm development," in *Current Trends In The Embryology Of Angiosperms*, ed. S. S. Bhojwani (Dordrecht: Kluwer), 353–374. doi: 10.1007/978-94-017-1203-3_14

Becraft, P. W., Li, K., Dey, N., and Asuncion-Crabb, Y. T. (2002). The maize *dek*1 gene functions in embryonic pattern formation and in cell fate specification. *Development* 129, 5217–5225. doi: 10.1242/dev.129.22.5217

Becraft, P. W., Stinard, P. S., and Mccarty, D. R. (1996). CRINKLY4: a TNFR-like receptor kinase involved in maize epidermal differentiation. *Science (New York, N.Y.)* 273, 1406–1409. doi: 10.1126/science.273.5280.1406

Bhave, M. R., Lawrence, S., Barton, C., and Hannah, C. (1990). Identification and molecular characterization of *shrunken*-2 cDNA clones of maize. *Plant Cell* 2, 581–588. doi: 10.1105/tpc.2.6.581

Bonello, J. F., Opsahl-Ferstad, H. G., Perez, P., Dumas, C., and Rogowsky, P. M. (2000). *Esr* genes show different levels of expression in the same region of maize endosperm. *Gene* 246, 219–227. doi: 10.1016/s0378-1119(00)00088-3

Brink, R. A., and Cooper, D. C. (1947). Effect of the *De*17 allele on development of the maize caryopsis. *Genetics* 32, 350–368. doi: 10.1093/genetics/32.4.350

Brown, R. C., and Lemmon, B. E. (2007). "The developmental biology of cereal endosperm," in *Endosperm, Developmental, and Molecular Biology* ed. O. A. Olsen (Berlin: Springer-Verlag).

Brown, R. C., Lemmon, B. E., and Olsen, O. A. (1996). Polarization predicts the pattern of cellularization in cereal endosperm. *Protoplasma* 192, 168–177. doi: 10.1007/bf01273889

Brugiere, N., Humbert, S., Rizzo, N., Bohn, J., and Habben, J. E. (2008). A member of the maize isopentenyl transferase gene family, Zea mays isopentenyl transferase 2 (ZmIPT2), encodes a cytokinin biosynthetic enzyme expressed during kernel development. Cytokinin biosynthesis in maize. *Plant Mol. Biol.* 67, 215–229. doi: 10.1007/s11103-008-9312-x

Burton, R. A., and Fincher, G. B. (2014). Evolution and development of cell walls in cereal grains. *Front. Plant Sci.* 5:456. doi: 10.3389/fpls.2014.00456

Cai, G., Faleri, C., Del Casino, C., Hueros, G., Thompson, R., and Cresti, M. (2002). Subcellular localisation of BETL-1, -2 and -4 in Zea mays L. *endosperm*. *Sexual Plant Reproduction* 15, 85–98. doi: 10.1007/s00497-002-0141-9

Charlton, W. L., Keen, C. L., Merriman, C., Lynch, P., Greenland, A. J., and Dickinson, H. G. (1995). Endosperm development in Zea mays implication of gametic imprinting and paternal excess in regulation of transfer layer development. *Development* 121, 3089–3097. doi: 10.1242/dev.121.9.3089

Chen, J. Y., Lausser, A., and Dresselhaus, T. (2014). Hormonal responses during early embryogenesis in maize. *Biochem. Soc. Trans.* 42, 325–331. doi: 10.1042/BST20130260

Cheng, W. H., Taliercio, E. W., and Chourey, P. S. (1996). The *miniature1* seed locus of maize encodes a cell wall invertase required for normal development of endosperm and maternal cells in the pedicel. *Plant Cell* 8, 971–983. doi: 10.1105/tpc.8.6.971

Chourey, P. S., and Hueros, G. (2017). "The basal endosperm transfer layer (BETL): gateway to the maize kernel," in *Maize Kernel Development*, ed. B. A. Larkins (Wallingford: CABI Intl), 56–67. doi: 10.1079/9781786391216.0056

Coelho, C. M., Dante, R. A., Sabelli, P. A., Sun, Y., Dilkes, B. P., Gordon-Kamm, W. J., et al. (2005). Cyclin-dependent kinase inhibitors in maize endosperm and their potential role in endoreduplication. *Plant Physiol.* 138, 2323–2336. doi: 10.1104/pp.105.063917

Colasanti, J., Tremblay, R., Wong, A. Y., Coneva, V., Kozaki, A., and Mable, B. K. (2006). The maize INDETERMINATE1 flowering time regulator defines a highly conserved zinc finger protein family in higher plants. *BMC Genomics* 7:158. doi: 10.1186/1471-2164-7-158

Cooper, D. C. (1951). Caryopsis development following matings between diploid and tetraploid strains of Zea mays. *Am. J. Botany* 38, 702–708.

Cossegal, M., Vernoud, V., Depege, N., and Rogowsky, P. M. (2007). "The embryo surrounding region," in *Endosperm, Developmental, and Molecular Biology* ed. O. A. Olsen (Berlin: Springer-Verlag).

Costa, L. M., Yuan, J., Rouster, J., Paul, W., Dickinson, H., and Gutierrez-Marcos, J. F. (2012). Maternal control of nutrient allocation in plant seeds by genomic imprinting. *Curr. Biol.* 22, 160–165. doi: 10.1016/j.cub.2011.11.059

Dai, D., Ma, Z., and Song, R. (2021). Maize endosperm development. *J. Integr. Plant Biol.* 63, 613–627. doi: 10.1111/jipb.13069

Dante, R. A., Larkins, B. A., and Sabelli, P. A. (2014). Cell cycle control and seed development. *Front. Plant Sci.* 5:493. doi: 10.3389/fpls.2014.00493

Davis, R. W., Smith, J. D., and Cobb, B. G. (1990). A Light and electron-microscope investigation of the transfer cell region of maize caryopses. *Canadian J. Botany-Revue Canadienne De Botanique* 68, 471–479. doi: 10.1139/b90-063

Doll, N. M., Just, J., Brunaud, V., Caius, J., Grimault, A., Depege-Fargeix, N., et al. (2020). Transcriptomics at maize embryo/endosperm interfaces identifies a transcriptionally distinct endosperm subdomain adjacent to the embryo scutellum. *Plant Cell* 32, 833–852. doi: 10.1105/tpc.19.00756

Dominguez, F., and Cejudo, F. J. (2014). Programmed cell death (PCD): an essential process of cereal seed development and germination. *Front. Plant Sci.* 5:366. doi: 10.3389/fpls.2014.00366

Duvick, D. N. (1961). Protein granules of maize endosperm cells. *Cereal Chem.* 38, 374–385.

Egli, D. B. (2006). The role of seed in the determination of yield of grain crops. *Australian J. Agricultural Res.* 57, 1237–1247. doi: 10.1071/ar06133

Fang, H., Fu, X., Ge, H., Zhang, A., Shan, T., Wang, Y., et al. (2021). Genetic basis of maize kernel oil-related traits revealed by high-density SNP markers in a recombinant inbred line population. *BMC Plant Biol.* 21:344. doi: 10.1186/s12870-021-03089-0

Feng, F., Qi, W., Lv, Y., Yan, S., Xu, L., Yang, W., et al. (2018). OPAQUE11 is a central hub of the regulatory network for maize endosperm development and nutrient metabolism. *Plant Cell* 30, 375–396. doi: 10.1105/tpc.17.00616

Flint-Garcia, S. A. (2017). "Kernel evolution: from teosinte to maize," in *Maize kernel development*, ed. B. A. Larkins (Wallingford: CABI). doi: 10.1079/9781786391216.0001

Gao, R., Dong, S., Fan, J., and Hu, C. (1998). Relationship between development of endosperm transfer cells and grain mass in maize. *Biol. Plant.* 41, 539–546. doi: 10.1023/A:1001840316163

Gibbon, B. C., Wang, X., and Larkins, B. A. (2003). Altered starch structure is associated with endosperm modification in quality protein maize. *Proc. Natl. Acad. Sci. U S A.* 100, 15329–15334. doi: 10.1073/pnas.2136854100

Gómez, E., Royo, J., Guo, Y., Thompson, R., and Hueros, G. (2002). Establishment of cereal endosperm expression domains: identification and properties of a maize transfer cell-specific transcription factor, ZmMRP-1. *Plant Cell* 14, 599–610. doi: 10.1105/tpc.010365

Gómez, E., Royo, J., Muñiz, L. M., Sellam, O., Paul, W., Gerentes, D., et al. (2009). The maize transcription factor myb-related protein-1 is a key regulator of the differentiation of transfer cells. *Plant Cell* 21, 2022–2035. doi: 10.1105/tpc.108.065409

Gontarek, B. C., and Becraft, P. W. (2017). "Aleurone," in *Maize Kernel Development*, ed. B. A. Larkins (Boston: CABI), 68–80. doi: 10.1079/9781786391216.0068

Gontarek, B. C., Neelakandan, A. K., Wu, H., and Becraft, P. W. (2016). NKD transcription factors are central regulators of maize endosperm development. *Plant Cell* 28, 2916–2936. doi: 10.1105/tpc.16.00609

Grafi, G., and Larkins, B. A. (1995). Endoreduplication in Maize endosperm: involvement of m phase-promoting factor inhibition and induction of s phase-related kinases. *Science* 269, 1262–1264. doi: 10.1126/science.269.5228.1262

Gruis, D., Guo, H. N., Selinger, D., Tian, Q., and Olsen, O. A. (2006). Surface position, not signaling from surrounding maternal tissues, specifies aleurone epidermal cell fate in maize. *Plant Physiol.* 141, 898–909. doi: 10.1104/pp.106.080945

Guo, X. M., Yuan, L. L., Chen, H., Sato, S. J., Clemente, T. E., and Holding, D. R. (2013). Nonredundant function of zeins and their correct stoichiometric ratio drive protein body formation in maize endosperm. *Plant Physiol.* 162, 1359–1369. doi: 10.1104/pp.113.218941

Gupta, H. S., Raman, B., Agrawal, P. K., Mahajan, V., Hossain, F., and Thirunavukkarasu, N. (2013). Accelerated development of quality protein maize hybrid through marker-assisted introgression of *opaque-2* allele. *Plant Breed.* 132, 77–82.

Gutierrez-Marcos, J. F., Costa, L. M., and Evans, M. M. S. (2006). maternal gametophytic *baseless1* is required for development of the central cell and early endosperm patterning in Maize (Zea mays). *Genetics* 174, 317–329. doi: 10.1534/genetics.106.059709

Gutiérrez-Marcos, J. F., Costa, L. M., Biderre-Petit, C., Khbaya, B., O'sullivan, D. M., Wormald, M., et al. (2004). *maternally expressed gene*1 is a novel maize endosperm transfer cell-specific gene with a maternal parent-of-origin pattern of expression. *Plant Cell* 16, 1288–1301. doi: 10.1105/tpc.019778

Habben, J. E., and Larkins, B. A. (1995). "Improving protein quality in seeds," in *Seed Development and Germination*, eds J. Kijel and G. Galili (New York, NY: Marcel Dekker, Inc.).

Hannah, L. C. (2007). "Starch formation in the cereal endosperm," in *Endosperm: Developmental and Molecular Biology*, ed. O. A. Olsen (Berlin: Springer-Verlag).

Hannah, L. C., Shaw, J. R., Clancy, M. A., Georgelis, N., and Boehlein, S. K. (2017). A *brittle-2* transgene increases maize yield by acting in maternal tissues to increase seed number. *Plant Direct* 1, 1–9. doi: 10.1002/pld3.29

He, Y., Yang, Q., Yang, J., Wang, Y. F., Sun, X., Wang, S., et al. (2021). *shrunken*4 is a mutant allele of ZmYSL2 that affects aleurone development and starch synthesis in maize. *Genetics* 218:iyab070. doi: 10.1093/genetics/iyab070

Holding, D. R. (2014). Recent advances in the study of prolamin storage protein organization and function. *Front. Plant Sci.* 5:276. doi: 10.3389/fpls.2014.00276

Hossain, F., Muthusamy, V., Pandey, N., Vishwakarma, A. K., Baveja, A., Zunjare, R. U., et al. (2018). Marker-assisted introgression of *opaque*2 allele for rapid conversion of elite hybrids into quality protein maize. *J. Genet.* 97, 287–298. doi: 10.1007/s12041-018-0914-z

Hu, M., Zhao, H., Yang, B., Yang, S., Liu, H., Tian, H., et al. (2021). ZmCTLP1 is required for the maintenance of lipid homeostasis and the basal endosperm transfer layer in maize kernels. *New Phytol.* 232, 2384–2399. doi: 10.1111/nph.17754

Hueros, G., Royo, J., Maitz, M., Salamini, F., and Thompson, R. D. (1999). Evidence for factors regulating transfer cell-specific expression in maize endosperm. *Plant Mol. Biol.* 41, 403–414. doi: 10.1023/a:1006331707605

Jane, J.-L. (2004). "Starch: structure and properties," in *J Chemical Functional Properties of Food Saccharides*, ed. P. Tomasik (Boca Raton, FL: CRC Press), 82–96.

Ji, C., Xu, L., Li, Y., Fu, Y., Li, S., Wang, Q., et al. (2021). The O2-ZmGRAS11 transcriptional regulatory network orchestrates the coordination of endosperm cell expansion and grain filling in maize. *Mol. Plant.* In press. doi: 10.1016/j.molp.2021.11.013

Jia, M., Wu, H., Clay, K. L., Jung, R., Larkins, B. A., and Gibbon, B. C. (2013). Identification and characterization of lysine-rich proteins and starch biosynthesis genes in the *opaque2* mutant by transcriptional and proteomic analysis. *BMC Plant Biol.* 13:60. doi: 10.1186/1471-2229-13-60

Jin, P., Guo, T., and Becraft, P. W. (2000). The maize CR4 receptor-like kinase mediates a growth factor-like differentiation response. *Genesis* 27, 104–116.

Kang, B. H., Xiong, Y., Williams, D. S., Pozueta-Romero, D., and Chourey, P. S. (2009). *Miniature*1-encoded cell wall invertase is essential for assembly and function of wall-in-growth in the maize endosperm transfer cell. *Plant Physiol.* 151, 1366–1376. doi: 10.1104/pp.109.142331

Kawakatsu, T., Yamamoto, M. P., Touno, S. M., Yasuda, H., and Takaiwa, F. (2009). Compensation and interaction between RISBZ1 and RPBF during grain filling in rice. *Plant J.* 59, 908–920. doi: 10.1111/j.1365-313X.2009.03925.x

Khoo, U., and Wolf, M. J. (1970). Origin and development of protein granules in maize endosperm. *Am. J. Botany* 57, 1042–1050. doi: 10.1002/j.1537-2197.1970.tb09907.x

Kiesselbach, T. A. (1949). The structure and reproduction of corn. *Univ. Nebraska Agric. Stat. Res. Bull.* 161, 1–96.

Kiesselbach, T. A., and Walker, E. R. (1952). Structure of certain specialized tissues in the kernel of corn. *Am. J. Botany* 39, 561–569. doi: 10.1002/j.1537-2197.1952.tb13069.x

Kowles, R. V., and Phillips, R. L. (1985). DNA amplification patterns in maize endosperm nuclei during kernel development. *Proc. Natl. Acad. Sci. U S A.* 82, 7010–7014. doi: 10.1073/pnas.82.20.7010

Kowles, R. V., and Phillips, R. L. (1988). Endosperm development in maize. *Int. Rev. Cytol.* 112, 97–136. doi: 10.1016/S0074-7696(08)62007-0

Kumar, S. B., Venkateswaran, K., and Kundu, S. (2010). Alternative conformational model of a seed protein *DEK*1 for better understanding of structure-function relationship. *J. Proteins Proteom.* 1, 77–90.

Kyle, D. J., and Styles, E. D. (1977). Development of aleurone and sub-aleurone-layers in maize. *Planta* 137, 185–193. doi: 10.1007/BF00388149

Larkins, B. A., Dilkes, B. P., Dante, R. A., Coelho, C. M., Woo, Y. M., and Liu, Y. (2001). Investigating the hows and whys of DNA endoreduplication. *J. Exp. Bot.* 52, 183–192. doi: 10.1093/jexbot/52.355.183

Lending, C. R., and Larkins, B. A. (1989). Changes in the zein composition of protein bodies during maize endosperm development. *Plant Cell* 1, 1011–1023. doi: 10.1105/tpc.1.10.1011

Leroux, B. M., Goodyke, A. J., Schumacher, K. I., Abbott, C. P., Clore, A. M., Yadegari, R., et al. (2014). Maize early endosperm growth and development: from fertilization through cell type differentiation. *Am. J. Botany* 101, 1259–1274. doi: 10.3732/ajb.1400083

Lertrat, K., and Pulam, T. (2007). Breeding for increased sweetness in sweet corn. *Int. J. Plant Breeding* 1, 27–30.

Li, C., and Song, R. (2020). The regulation of zein biosynthesis in maize endosperm. *Theor. Appl. Genet.* 133, 1443–1453. doi: 10.1007/s00122-019-03520-z

Li, C., Huang, Y., Huang, R., Wu, Y., and Wang, W. (2018). The genetic architecture of amylose biosynthesis in maize kernel. *Plant Biotechnol. J.* 16, 688–695. doi: 10.1111/pbi.12821

Li, C., Qi, W., Liang, Z., Yang, X., Ma, Z., and Song, R. (2020). A SNRK1-ZMRFWD3-OPAQUE2 signaling axis regulates diurnal nitrogen accumulation in maize seeds. *Plant Cell* 32, 2823–2841. doi: 10.1105/tpc.20.00352

Li, C., Qiao, Z., Qi, W., Wang, Q., Yuan, Y., Yang, X., et al. (2015). Genome-wide characterization of cis-acting DNA targets reveals the transcriptional regulatory framework of *Opaque*2 in maize. *Plant Cell* 27, 532–545. doi: 10.1105/tpc.114.134858

Li, G. S., Wang, D. F., Yang, R. L., Logan, K., Chen, H., Zhang, S. S., et al. (2014). Temporal patterns of gene expression in developing maize endosperm identified through transcriptome sequencing. *Proc. Natl. Acad. Sci. U S A.* 111, 7582–7587. doi: 10.1073/pnas.1406383111

Li, H., Peng, Z., Yang, X., Wang, W., Fu, J., Wang, J., et al. (2013). Genome-wide association study dissects the genetic architecture of oil biosynthesis in maize kernels. *Nat. Genet.* 45, 43–50. doi: 10.1038/ng.2484

Li, N., Zhang, S., Zhao, Y., Li, B., and Zhang, J. (2011). Over-expression of AGPase genes enhances seed weight and starch content in transgenic maize. *Planta* 233, 241–250. doi: 10.1007/s00425-010-1296-5

Lid, S. E., Gruis, D., Jung, R., Lorentzen, J. A., Ananiev, E., Chamberlin, M., et al. (2002). The *defective kernel* 1 (*dek*1) gene required for aleurone cell development in the endosperm of maize grains encodes a membrane protein of the calpain gene superfamily. *Proc. Natl. Acad. Sci. U S A.* 99, 5460–5465. doi: 10.1073/pnas.042098799

Lopes, M. A., Takasaki, K., Bostwick, D. E., Helentjaris, T., and Larkins, B. A. (1995). Identification of two opaque2 modifier loci in quality protein maize. *Mol. Gen. Genet.* 247, 603–613. doi: 10.1007/BF00290352

Lowe, J., and Nelson, O. E., Jr. (1946). Miniature seed-a study in the development of a defective caryopsis in maize. *Genetics* 31, 525–533. doi: 10.1093/genetics/31.5.525

McClintock, B. (1978). "Development of the maize endosperm as revealed by clones," in *The Clonal Basis of Development*, eds S. Subtelny and I. M. Sussex (New York, NY: Academic Press), 217–237.

McCurdy, D. W. (2015). *Transfer Cells: Novel Cell Types with Unique Wall Ingrowth Architecture Designed for Optimized Nutrient Transport*. Hoboken, NJ: Blackwell-Wiley.

Mertz, E. T., Bates, L. S., and Nelson, O. E. (1964). Mutant gene that changes protein composition and increases lysine content of maize endosperm. *Science* 145, 279–280. doi: 10.1126/science.145.3629.279

Miller, M. E., and Chourey, P. S. (1992). The maize invertase-deficient *miniature*-1 seed mutation is associated with aberrant pedicel and endosperm development. *Plant Cell* 4, 297–305. doi: 10.1105/tpc.4.3.297

Mimura, M., Kudo, T., Wu, S., Mccarty, D. R., and Suzuki, M. (2018). Autonomous and non-autonomous functions of the maize *Shohai*1 gene, encoding a RWP-RK putative transcription factor, in regulation of embryo and endosperm development. *Plant J.* 95, 892–908. doi: 10.1111/tpj.13996

Mol, R., Matthys-Rochon, E., and Dumas, C. (1994). The kinetics of cytological events during double fertilization in *Zea mays* L. *Plant J.* 5, 197–206. doi: 10.1046/j.1365-313X.1994.05020197.x

Monjardino, P., Machado, J., Gil, F. S., Fernandes, R., and Salema, R. (2007). Structural and ultrastructural characterization of maize coenocyte and endosperm cellularization. *Canadian J. Botany-Revue Canadienne De Botanique* 85, 216–223. doi: 10.1139/b06-156

Monjardino, P., Rocha, S., Tavares, A. C., Fernandes, R., Sampaio, P., Salema, R., et al. (2013). Development of flange and reticulate wall ingrowths in maize (*Zea mays* L.) endosperm transfer cells. *Protoplasma* 250, 495–503. doi: 10.1007/s00709-012-0432-4

Muniz, L. M., Royo, J., Gomez, E., Barrero, C., Bergareche, D., and Hueros, G. (2006). The maize transfer cell-specific type-A response regulator ZmTCRR-1 appears to be involved in intercellular signalling. *Plant J.* 48, 17–27. doi: 10.1111/j.1365-313X.2006.02848.x

Muniz, L. M., Royo, J., Gomez, E., Baudot, G., Paul, W., and Hueros, G. (2010). Atypical response regulators expressed in the maize endosperm transfer cells link canonical two component systems and seed biology. *BMC Plant Biol.* 10:84. doi: 10.1186/1471-2229-10-84

Olsen, O. A. (2001). Endosperm development: cellularization and cell fate specification. *Annu. Rev. Plant Physiol. Plant Mol. Biol.* 52, 233–267. doi: 10.1146/annurev.arplant.52.1.233

Olsen, O. A. (2020). The modular control of cereal endosperm development. *Trends Plant Sci.* 25, 279–290. doi: 10.1016/j.tplants.2019.12.003

Olsen, O. A., and Becraft, P. W. (2013). "Endosperm development," in *Seed Gemonics*, ed. P. W. Becraft (New York, NY: John Wiley & Sons), 43–63.

Olsen, O.-A., Brown, R. C., and Lemmon, B. E. (1995). Pattern and process of wall formation in developing endosperm. *BioEssays* 17, 803–812. doi: 10.1002/bies.950170910

Opsahl-Ferstad, H. G., Ledeunff, E., Dumas, C., and Rogowsky, P. M. (1997). ZmEsr, a novel endosperm-specific gene expressed in a restricted region around the maize embryo. *Plant J.* 12, 235–246. doi: 10.1046/j.1365-313x.1997.12010235.x

Piperno, D. R., Ranere, A. J., Holst, I., Iriarte, J., and Dickau, R. (2009). Starch grain and phytolith evidence for early ninth millennium B.P. maize from the Central Balsas River Valley, Mexico. *Proc. Natl. Acad. Sci. U S A.* 106, 5019–5024. doi: 10.1073/pnas.0812525106

Prasanna, B. M., Vasal, S. K., Kassahun, B., and Singh, N. N. (2001). Quality protein maize. *Curr. Sci.* 81, 1308–1319.

Qi, X., Li, S., Zhu, Y., Zhao, Q., Zhu, D., and Yu, J. (2017). ZmDof3, a maize endosperm-specific Dof protein gene, regulates starch accumulation and aleurone development in maize endosperm. *Plant Mol. Biol.* 93, 7–20. doi: 10.1007/s11103-016-0543-y

Randolph, L. F. (1936). Developmental morphology of the caryopsis in maize. *J. Agric. Res.* 53, 881–916.

Reyes, F. C., Chung, T., Holding, D., Jung, R., Vierstra, R., and Otegui, M. S. (2011). Delivery of prolamins to the protein storage vacuole in maize aleurone cells. *Plant Cell* 23, 769–784. doi: 10.1105/tpc.110.082156

Rocha, S., Monjardino, P., Mendonca, D., Machado, A. D., Fernandes, R., Sampaio, P., et al. (2014). Lignification of developing maize (*Zea mays* L.) endosperm transfer cells and starchy endosperm cells. *Front. Plant Sci.* 5:102. doi: 10.3389/fpls.2014.00102

Rodrigues, J. A., and Zilberman, D. (2015). Evolution and function of genomic imprinting in plants. *Genes Dev.* 29, 2517–2531. doi: 10.1101/gad.269902.115

Sabelli, P. A. (2012). Replicate and die for your own good: endoreduplication and cell death in the cereal endosperm. *J. Cereal Sci.* 56, 9–20. doi: 10.1016/j.jcs.2011.09.006

Sabelli, P. A., and Larkins, B. A. (2009). The contribution of cell cycle regulation to endosperm development. *Sexual Plant Reproduction* 22, 207–219. doi: 10.1007/s00497-009-0105-4

Sabelli, P. A., Liu, Y., Dante, R. A., Lizarraga, L. E., Nguyen, H. N., Brown, S. W., et al. (2013). Control of cell proliferation, endoreduplication, cell size, and cell death by the retinoblastoma-related pathway in maize endosperm. *Proc. Natl. Acad. Sci. U S A.* 110, E1827–E1836. doi: 10.1073/pnas.1304903110

Schel, J. H. N., Kieft, H., and Vanlammeren, A. A. M. (1984). Interactions between embryo and endosperm during early developmental stages of maize caryopses (*Zea mays*). *Canadian J. Botany-Revue Canadienne De Botanique* 62, 2842–2853. doi: 10.1139/b84-379

Schmidt, R. J., Burr, F. A., Aukerman, M. J., and Burr, B. (1990). Maize regulatory gene *opaque*-2 encodes a protein with a "leucine-zipper" motif that binds to zein DNA. *Proc. Natl. Acad. Sci. U S A.* 87, 46–50. doi: 10.1073/pnas.87.1.46

Schmidt, R. J., Ketudat, M., Aukerman, M. J., and Hoschek, G. (1992). Opaque-2 is a transcriptional activator that recognizes a specific target site in 22-kD zein genes. *Plant Cell* 4, 689–700. doi: 10.1105/tpc.4.6.689

Shen, B., Allen, W. B., Zheng, P., Li, C., Glassman, K., Ranch, J., et al. (2010). Expression of *zmlec*1 and *zmwri*1 increases seed oil production in maize. *Plant Physiol.* 153, 980–987. doi: 10.1104/pp.110.157537

Shen, B., Li, C., Min, Z., Meeley, R. B., Tarczynski, M. C., and Olsen, O. A. (2003). *sal*1 determines the number of aleurone cell layers in maize endosperm and encodes a class E vacuolar sorting protein. *Proc. Natl. Acad. Sci. U S A.* 100, 6552–6557. doi: 10.1073/pnas.0732023100

Sheridan, W. F., and Clark, J. K. (2017). "Embryo development," in *Maize kernel Development*, ed. B. A. Larkins (Oxfordshire: CABI). doi: 10.1079/9781786391216.0081

Singh, N., Vasudev, S., Yadava, D. K., Chaudhary, D. P., and Prabhu, K. V. (2013). "Oil improvement in maize: potential and prospects," in *Maize: Nutrition Dynamics and Novel Uses*. (eds) D. P. Chuadhary, S. Kumar and S. Langyan (New Delhi: Springer-Verlag) doi: 10.1007/978-81-322-1623-0_6

Sosso, D., Luo, D., Li, Q.-B., Sasse, J., Yang, J., Gendrot, G., et al. (2015). Seed filling in domesticated maize and rice depends on SWEET-mediated hexose transport. *Nat. Genet.* 47, 1489–1493. doi: 10.1038/ng.3422

Spitzer, C., Reyes, F. C., Buono, R., Sliwinski, M. K., Haas, T. J., and Otegui, M. S. (2009). The ESCRT-related CHMP1A and B proteins mediate multivesicular body sorting of auxin carriers in Arabidopsis and are required for plant development. *Plant Cell* 21, 749–766. doi: 10.1105/tpc.108.064865

Talbot, M. J., Offler, C. E., and Mccurdy, D. W. (2002). Transfer cell wall architecture: a contribution towards understanding localized wall deposition. *Protoplasma* 219, 197–209. doi: 10.1007/s007090200021

Thiel, J. (2014). Development of endosperm transfer cells in barley. *Front. Plant Sci.* 5:108. doi: 10.3389/fpls.2014.00108

Tian, Q., Olsen, L., Sun, B., Lid, S. E., Brown, R. C., Lemmon, B. E., et al. (2007). Subcellular localization and functional domain studies of DEFECTIVE KERNEL1 in maize and *Arabidopsis* suggest a model for aleurone cell fate specification involving CRINKLY4 and SUPERNUMERARY ALEURONE LAYER1. *Plant Cell* 19, 3127–3145. doi: 10.1105/tpc.106.048868

To, T., Estrabillo, E., Wang, C., and Cicutto, L. (2008). Examining intra-rater and inter-rater response agreement: a medical chart abstraction study of a community-based asthma care program. *BMC Med. Res. Methodol.* 8:29. doi: 10.1186/1471-2288-8-29

Tran, D., Galletti, R., Neumann, E. D., Dubois, A., Sharif-Naeini, R., Geitmann, A., et al. (2017). A mechanosensitive Ca2+ channel activity is dependent on the developmental regulator DEK1. *Nat. Commun.* 8:1009.

Vilhar, B., Kladnik, A., Blejec, A., Chourey, P. S., and Dermastia, M. (2002). Cytometrical evidence that the loss of seed weight in the *miniature1* seed mutant of maize is associated with reduced mitotic activity in the developing endosperm. *Plant Physiol.* 129, 23–30.

Villegas, E. (1994). "Factors limiting quality protein maize (QPM) development and utilization," in *Quality Protein Maize 1964-1994*, eds B. A. Larkins and E. T. Mertz (Sete Lahoas: EMBRAPA/CNPMS).

Wang, C., Barry, J. K., Min, Z., Tordsen, G., Rao, A. G., and Olsen, O.-A. (2003). The calpain domain of the maize DEK1 protein contains the conserved catalytic triad and functions as a cysteine proteinase. *J. Biol. Chem.* 278, 34467–34474.

Wang, E., Wang, J., Zhu, X., Hao, W., Wang, L., Li, Q., et al. (2008). Control of rice grain-filling and yield by a gene with a potential signature of domestication. *Nat. Genet.* 40, 1370–1374.

Wang, H., Studer, A. J., Zhao, Q., Meeley, R., and Doebley, J. F. (2015). Evidence that the origin of naked kernels during maize domestication was caused by a single amino acid substitution in *tga1*. *Genetics* 200, 965–974.

Wang, Z., Ueda, T., and Messing, J. (1998). Characterization of the maize prolamin box-binding factor-1 (PBF-1) and its role in the developmental regulation of the zein multigene family. *Gene* 223, 321–332.

Whitt, S. R., Wilson, L. M., Tenaillon, M. I., Gaut, B. S., and Buckler, E. S. T. (2002). Genetic diversity and selection in the maize starch pathway. *Proc. Natl. Acad. Sci. U S A.* 99, 12959–12962.

Wolf, M. J., Cutler, H. C., Zuber, M. S., and Khoo, U. (1972). Maize with multilayer aleurone of high protein content. *Crop Sci.* 12, 440–442.

Woo, Y. M., Hu, D. W. N., Larkins, B. A., and Jung, R. (2001). Genomics analysis of genes expressed in maize endosperm identifies novel seed proteins and clarifies patterns of zein gene expression. *Plant Cell* 13, 2297–2317.

Wright, S. I., Bi, I. V., Schroeder, S. G., Yamasaki, M., Doebley, J. F., Mcmullen, M. D., et al. (2005). The effects of artificial selection on the maize genome. *Science* 308, 1310–1314.

Wu, H., and Becraft, P. W. (2021). Comparative transcriptomics and network analysis define gene coexpression modules that control maize aleurone development and auxin signaling. *Plant Genome* 14:e20126.

Wu, H., Gontarek, B. C., Yi, G., Beall, B. D., Neelakandan, A. K., Adhikari, B., et al. (2020). The *thick aleurone*1 gene encodes a NOT1 subunit of the CCR4-NOT complex and regulates cell patterning in endosperm. *Plant Physiol.* 184, 960–972.

Wu, Y., Holding, D. R., and Messing, J. (2010). γ-Zeins are essential for endosperm modification in quality protein maize. *Proc. Natl. Acad. Sci. U.S.A.* 107, 12810–12815. doi: 10.1073/pnas.1004721107

Yang, T., Guo, L., Ji, C., Wang, H., Wang, J., Zheng, X., et al. (2021). The B3 domain-containing transcription factor ZmABI19 coordinates expression of key factors required for maize seed development and grain filling. *Plant Cell* 33, 104–128.

Yang, X., Guo, Y., Yan, J., Zhang, J., Song, T., Rocheford, T., et al. (2010). Major and minor QTL and epistasis contribute to fatty acid compositions and oil concentration in high-oil maize. *Theor. Appl. Genet.* 120, 665–678.

Yang, X., Ma, H., Zhang, P., Yan, J., Guo, Y., Song, T., et al. (2012). Characterization of QTL for oil content in maize kernel. *Theor. Appl. Genet.* 125, 1169–1179.

Yi, G., Lauter, A. M., Scott, M. P., and Becraft, P. W. (2011). The *thick aleurone*1 mutant defines a negative regulation of maize aleurone cell fate that functions downstream of defective kernel1. *Plant Physiol.* 156, 1826–1836.

Yi, G., Neelakandan, A. K., Gontarek, B. C., Vollbrecht, E., and Becraft, P. W. (2015). The *naked endosperm* genes encode duplicate INDETERMINATE domain transcription factors required for maize endosperm cell patterning and differentiation. *Plant Physiol.* 167, 443–456.

Young, T. E., and Gallie, D. R. (2000). Regulation of programmed cell death in maize endosperm by abscisic acid. *Plant Mol. Biol.* 42, 397–414.

Young, T. E., Gallie, D. R., and Demason, D. A. (1997). Ethylene-mediated programmed cell death during maize endosperm development of wild-type and *shrunken*2 genotypes. *Plant Physiol.* 115, 737–751.

Yuan, L., Dou, Y., Kianian, S. F., Zhang, C., and Holding, D. R. (2014). Deletion mutagenesis identifies a haploinsufficient role for γ-Zein in opaque2 endosperm modification. *Plant Physiol.* 164, 119–130. doi: 10.1104/pp.113.230961

Zhan, J., Li, G., Ryu, C. H., Ma, C., Zhang, S., Lloyd, A., et al. (2018). Opaque-2 regulates a complex gene network associated with cell differentiation and storage functions of maize endosperm. *Plant Cell* 30, 2425–2446.

Zhan, J., Thakare, D., Ma, C., Lloyd, A., Nixon, N. M., Arakaki, A. M., et al. (2015). RNA sequencing of laser-capture microdissected compartments of the maize kernel identifies regulatory modules associated with endosperm cell differentiation. *Plant Cell* 27, 513–531.

Zhang, Z., Dong, J., Ji, C., Wu, Y., and Messing, J. (2019). NAC-type transcription factors regulate accumulation of starch and protein in maize seeds. *Proc. Natl. Acad. Sci. U S A.* 116, 11223–11228.

Zhang, Z., Qu, J., Li, F., Li, S., Xu, S., Zhang, R., et al. (2020). Genome-wide evolutionary characterization and expression analysis of SIAMESE-RELATED family genes in maize. *BMC Evol. Biol.* 20:91. doi: 10.1186/s12862-020-01619-2

Zhang, Z., Yang, J., and Wu, Y. (2015). Transcriptional regulation of zein gene expression in maize through the additive and synergistic action of *opaque*2, prolamine-box binding factor, and O2 heterodimerizing proteins. *Plant Cell* 27, 1162–1172.

Zhang, Z., Zheng, X., Yang, J., Messing, J., and Wu, Y. (2016). Maize endosperm-specific transcription factors O2 and PBF network the regulation of protein and starch synthesis. *Proc. Natl. Acad. Sci. U S A.* 113, 10842–10847.

Zheng, P., Allen, W. B., Roesler, K., Williams, M. E., Zhang, S., Li, J., et al. (2008). A phenylalanine in DGAT is a key determinant of oil content and composition in maize. *Nat. Genet.* 40, 367–372.

Zheng, Y. K., and Wang, Z. (2010). Current opinions on endosperm transfer cells in maize. *Plant Cell Rep.* 29, 935–942.

Zheng, Y. K., Wang, Z., and Gu, Y. J. (2014). Development and function of caryopsis transport tissues in maize, sorghum and wheat. *Plant Cell Rep.* 33, 1023–1031.

Conflict of Interest: The authors declare that the research was conducted in the absence of any commercial or financial relationships that could be construed as a potential conflict of interest.

Publisher's Note: All claims expressed in this article are solely those of the authors and do not necessarily represent those of their affiliated organizations, or those of the publisher, the editors and the reviewers. Any product that may be evaluated in this article, or claim that may be made by its manufacturer, is not guaranteed or endorsed by the publisher.

frontiers in Plant Science

ORIGINAL RESEARCH
published: 16 March 2022
doi: 10.3389/fpls.2022.840614

High Resolution Genome Wide Association Studies Reveal Rich Genetic Architectures of Grain Zinc and Iron in Common Wheat (*Triticum aestivum* L.)

Jingyang Tong[1], Cong Zhao[1], Mengjing Sun[1], Luping Fu[1], Jie Song[1], Dan Liu[1], Yelun Zhang[2], Jianmin Zheng[3], Zongjun Pu[3], Lianzheng Liu[4], Awais Rasheed[5,6], Ming Li[1], Xianchun Xia[1], Zhonghu He[1,5] and Yuanfeng Hao[1]**

[1] Institute of Crop Sciences, Chinese Academy of Agricultural Sciences, Beijing, China, [2] The Key Laboratory of Crop Genetics and Breeding of Hebei Province, Institute of Cereal and Oil Crops, Hebei Academy of Agricultural and Forestry Sciences, Shijiazhuang, China, [3] Crop Research Institute, Sichuan Academy of Agricultural Sciences, Chengdu, China, [4] Research Institute of Grain Crops, Xinjiang Academy of Agricultural Sciences, Urumqi, China, [5] International Maize and Wheat Improvement Center (CIMMYT) China Office, Beijing, China, [6] Department of Plant Sciences, Quaid-i-Azam University, Islamabad, Pakistan

OPEN ACCESS

Edited by:
Yingyin Yao,
China Agricultural University, China

Reviewed by:
Wricha Tyagi,
Central Agricultural University, India
Jian Ma,
Sichuan Agricultural University, China

***Correspondence:**
Zhonghu He
hezhonghu02@caas.cn
Yuanfeng Hao
haoyuanfeng@caas.cn

Specialty section:
This article was submitted to Crop and Product Physiology, a section of the journal Frontiers in Plant Science

Received: *21 December 2021*
Accepted: *28 January 2022*
Published: *16 March 2022*

Citation:
Tong J, Zhao C, Sun M, Fu L, Song J, Liu D, Zhang Y, Zheng J, Pu Z, Liu L, Rasheed A, Li M, Xia X, He Z and Hao Y (2022) High Resolution Genome Wide Association Studies Reveal Rich Genetic Architectures of Grain Zinc and Iron in Common Wheat (Triticum aestivum L.). Front. Plant Sci. 13:840614. doi: 10.3389/fpls.2022.840614

Biofortification is a sustainable strategy to alleviate micronutrient deficiency in humans. It is necessary to improve grain zinc (GZnC) and iron concentrations (GFeC) in wheat based on genetic knowledge. However, the precise dissection of the genetic architecture underlying GZnC and GFeC remains challenging. In this study, high-resolution genome-wide association studies were conducted for GZnC and GFeC by three different models using 166 wheat cultivars and 373,106 polymorphic markers from the wheat 660K and 90K single nucleotide polymorphism (SNP) arrays. Totally, 25 and 16 stable loci were detected for GZnC and GFeC, respectively. Among them, 17 loci for GZnC and 8 for GFeC are likely to be new quantitative trait locus/loci (QTL). Based on gene annotations and expression profiles, 28 promising candidate genes were identified for Zn/Fe uptake (8), transport (11), storage (3), and regulations (6). Of them, 11 genes were putative wheat orthologs of known *Arabidopsis* and rice genes related to Zn/Fe homeostasis. A brief model, such as genes related to Zn/Fe homeostasis from root uptake, xylem transport to the final seed storage was proposed in wheat. Kompetitive allele-specific PCR (KASP) markers were successfully developed for two major QTL of GZnC on chromosome arms 3AL and 7AL, respectively, which were independent of thousand kernel weight and plant height. The 3AL QTL was further validated in a bi-parental population under multi-environments. A wheat multidrug and toxic compound extrusion (MATE) transporter *TraesCS3A01G499300*, the ortholog of rice gene *OsPEZ2*, was identified as a potential candidate gene. This study has advanced our knowledge of the genetic basis underlying GZnC and GFeC in wheat and provides valuable markers and candidate genes for wheat biofortification.

Keywords: biofortification, candidate genes, GWAS, iron, zinc

INTRODUCTION

Zinc (Zn) and iron (Fe), serving as co-factors for a multitude of enzymes and regulatory peptides in critical metabolic processes, are essential micronutrients for the plant growth and human health (Hänsch and Mendel, 2009). Due to monotonous diet and heavy relying on cereal edible parts with suboptimal micronutrient levels, Zn and Fe deficiencies have become the most common public health problem in the world, especially for pregnant women and young children due to their increased demands for micronutrients (Bhati et al., 2016; Vasconcelos et al., 2017). Increasing intrinsic micronutrients in the edible parts of crops, known as biofortification, is regarded as the most cost-effective and sustainable intervention to alleviate Zn and Fe malnutrition in humans (Gómez-Galera et al., 2010). Common wheat (*Triticum aestivum* L.) as a staple food crop, supplying approximately 20% of daily calories and protein, and main source of essential micronutrients, such as Zn and Fe, is recognized as an attractive crop for biofortification (Ludwig and Slamet-Loedin, 2019). For nutritionally sufficient wheat Zn and Fe biofortification, the concentrations of Fe and Zn in whole grains have to, respectively, reach 37 and 59 mg/kg, about 50% higher than the average concentrations of popular wheat cultivars (Bouis et al., 2011). However, breeding elite cultivars with enhanced Zn/Fe content is quite challenging due to the obscurity of genetic architecture and molecular processes regulating the Zn/Fe homeostasis in wheat, which greatly hampers the implements of modern breeding technologies, such as marker-assisted selection (MAS) and genomic selection (GS) (Gupta et al., 2021).

To improve our understanding of the genetic basis of wheat grain Zn and Fe, identification of as many causal loci as possible is imperative (Tong et al., 2020). In recent years, diverse bi-parental populations have been used to identify quantitative trait locus/loci (QTL) associated with grain Zn (GZnC) and Fe concentrations (GFeC) in common wheat and its relative species (Tong et al., 2020; Gupta et al., 2021). These QTL from different studies have been integrated into a consensus map according to the physical positions of their linked markers, and provide a valuable resource for dissection of the genetic architecture underlying GZnC and GFeC (Tong et al., 2020). Nevertheless, the family based bi-parental populations usually have limited number of recombination events and low genetic diversity, thus low-mapping resolution and may be unable to provide a full genome-wide genetic landscape of complex traits (Korte and Farlow, 2013; Platten et al., 2019). As a complementary strategy to QTL mapping, a genome-wide association study (GWAS) is a powerful tool to detect the genetic regions underlying complex traits using the historical abundant crossovers and genetic variations accumulated in natural wheat germplasms (Hamblin et al., 2011). A number of genetic loci associated with GZnC and GFeC have been identified by GWAS in wheat recently (Tong et al., 2020; Gupta et al., 2021). However, large gaps in the genetic map due to low marker number and density were generally found, which greatly hindered precision in the dissection of the GZnC and GFeC traits (Korte and Farlow, 2013).

With the rapid development of next-generation sequencing (NGS) technology, high-density single nucleotide polymorphism (SNP) genotyping arrays have been developed in wheat (reviewed in Rasheed et al., 2017). For example, the Wheat Axiom 660K SNP array with more than half a million markers enables high marker resolution, large genome coverage, and low heterozygosity (Sun et al., 2020). GWAS using such high density SNPs will make it possible to obtain a large number of associated loci within very small intervals and consequently facilitate the candidate gene discovery and genetic dissection of complex traits (Yano et al., 2016; Pang et al., 2020). The mixed linear model (MLM), the fixed and random model circulating probability unification (FarmCPU), and the multiple loci mixed linear model (MLMM) in different strengths for each have been adopted to effectively control the population structure and to ensure the accuracy and reliability of significantly associated loci. It is appropriate to adopt multiple models simultaneously to conduct the GWAS for genetic dissection of complex traits (Peng et al., 2018; Alqudah et al., 2020).

In the current study, a diverse panel of 166 representative wheat accessions was chosen from elite germplasm and was genotyped with the wheat 660K and 90K SNP arrays. GWASs were carried out using three different models for GZnC and GFeC across multiple environments. Furthermore, plant height (PH), thousand kernel weight (TKW), and grain areas (GA) were investigated to study their associations with GZnC/GFeC and identify pleiotropic loci. The study aimed to (1) dissect the genetic architecture of GZnC and GFeC, (2) identify associated markers, loci, and candidate genes, and (3) develop high-throughput kompetitive allele-specific PCR (KASP) markers and validate the major QTL for wheat biofortification.

MATERIALS AND METHODS

Plant Material and Field Trials

The association panel consists of 166 representative wheat cultivars, such as 144 accessions from Yellow and Huai Valley, the major wheat zone in China, and 22 from five other countries (**Supplementary Table 1**). The panel was used in our previous studies on black point (Liu et al., 2017), flour color and polyphenol oxidase (PPO) activity (Zhai et al., 2018, 2020), grain yield related traits (Li et al., 2019), and water-soluble carbohydrate contents (Fu et al., 2020). In this study, the panel was grown in randomized complete blocks with two replications in four environments comprising Beijing (39°56′N, 116°20′E), Gaoyi (37°33′N, 114°26′E), and Shijiazhuang (37°27′N, 113°30′E) in Hebei province, and Urumqi (42°45′N, 86°37′E) in Xinjiang province during the 2019–2020 cropping season. These environments were designated as 20BJ, 20GY, 20SJZ, and 20XJ hereafter, respectively. Each entry with approximately 40–50 grains was grown in 1.0 m long row with an inter-row spacing of 20.0 cm. Standard agronomic practices were performed at each location, along with soil application of 25 kg/ha $ZnSO_4.7H_2O$ granular fertilizer (Sinochem Group Co., Ltd., Beijing, China) in 20GY and 20SJZ over three crop cycles prior to this experiment to enrich the available soil Zn and minimize heterogeneity. The green manure returning was routinely practiced in Beijing and field soil held

sufficient Zn intrinsically, so that additional Zn fertilizer was not applied in 20BJ. To investigate GZnC and GFeC in a low-Zn environment, 20XJ was set without soil Zn fertilizer application.

Phenotype Determination and Statistical Analyses

Plant materials were hand-harvested in the field and completely dried grains were hand-threshed and cleaned carefully to avoid the potential contamination of mineral element. Approximately 15 g of each sample was subjected to GZnC and GFeC analyses with an X-ray fluorescence spectrometry (EDXRF) instrument (model X-Supreme 8000, Oxford Instruments plc.), following the protocol of high-throughput screening of micronutrients in whole-wheat grain (Paltridge et al., 2012). PH, TKW, and GA in all environments were investigated following Xu et al. (2019).

ANOVA, Pearson's correlation analysis, and Student's *t*-test were conducted using the SAS 9.4 software (SAS institute, Cary, NC, United States). Broad-sense heritabilities (H^2) were calculated using the following equation (Holland et al., 2003):

$$H^2 = \sigma_g^2/(\sigma_g^2 + \sigma_{ge}^2/e + \sigma_\varepsilon^2/(re))$$

where $\sigma^2{}_g$ indicates the variance of genotypes, $\sigma^2{}_{ge}$ and $\sigma^2{}_\varepsilon$ represent the variances of genotype × environment interaction and errors, and e and r are the numbers of environments and replicates in each environment, respectively. For each trait, a best linear unbiased estimation (BLUE) using a linear model for each accession was calculated across environments by the QTL IciMapping v4.1 software (Yin et al., 2015).

Genotyping and Physical Map Construction

Genomic DNA was extracted following the CTAB method (Murray and Thompson, 1980) and the population was genotyped by the Illumina wheat 90K (such as, 81,587 SNPs) and Affymetrix wheat 660K (such as, 630,517 SNPs) SNP arrays by CapitalBio Technology Co., Ltd, Beijing, China.[1] Markers with minor allele frequency (MAF) < 5.0% and missing data containing heterozygous genotypes > 20.0% were filtered out and the same final 373,106 high-quality polymorphic SNPs were obtained (Fu et al., 2020). These markers included 359,760 (96.4%) from the 660K and 13,346 (3.6%) from 90K SNP array, indicating SNPs in wheat 90K array have relatively low polymorphisms in Chinese cultivars. Flanking sequences of SNP markers were used for BLAST analysis against IWGSC RefSeq v.1.0,[2] to obtain physical positions in accordance with the best BLAST hit results. Eventually these markers were integrated into one consensus map, covering a total physical distance of 13.7 Gb, accounting for about 95% of wheat whole genome sequences, and were further utilized for GWAS. Relevant information is available in our previous studies (Liu et al., 2017; Fu et al., 2020).

Genome-Wide Association Study

The 166 accessions were classified into three subpopulations by the population structure using Structure v2.3.4 (Liu et al., 2017). The average linkage disequilibrium (LD) decay distances for A, B, D, and whole genomes were approximately 6, 4, 11, and 8 Mb, respectively (Liu et al., 2017). In this study, GWAS was conducted for each environment and BLUE values of GZnC across 20GY, 20SJZ, and 20BJ. The site 20XJ was excluded from the analysis owning to relatively low Pearson's correlation coefficients with other environments (data not shown). The low Pearson's correlation was possibly attributed to soil Zn content heterogeneity in 20XJ with null Zn fertilizer application (Velu et al., 2018). As for GFeC, GWAS was carried out across all four environments and BLUE values. Three models, MLM ($Q + K$), FarmCPU, and MLMM, were employed for the GWAS in GAPIT a software package operating in R v3.5.1[3] (Tang et al., 2016). To maximize chances of identifying all possible QTL, a threshold of $p = 1.0 \times 10^{-3}$ ($-\log_{10}(p) = 3.0$) was set for the significance of marker-trait associations (MTAs). To control the false discovery rate (FDR) at an appropriate level, those detected in three or more environments (BLUE value was regarded as one environment hereafter) by any of the three models were considered as reliable MTAs (Fu et al., 2020). MTAs detected in the same LD block or physically closely linked were grouped into a single QTL, and the distance between the two very far flanking markers was seen as the QTL interval. The most significant MTA with the lowest value of p across environments in this interval was selected as the representative marker, and its R^2 output by MLM was used to reflect the proportion of phenotypic variance explained (Fu et al., 2020). Manhattan and quantile–quantile (*Q*–*Q*) plots were generated using the CMplot package in R v3.5.1 software.[4]

Candidate Gene Identification

According to the gene annotations from IWGSC RefSeq v.1.0 and putative homologs in the UniProt database,[5] the genes located in or adjacent to the physical intervals of QTL identified in this study were subjected to be screened as follows. (1) Those related to the molecular processes in Zn/Fe homeostasis, such as metal uptake in the root, transport in the xylem and phloem, storage in seeds, and regulatory factors, were predicted to be potential candidates; (2) analysis of orthologs between wheat and model plants was carried out to obtain candidate genes in Triticeae-Gene Tribe browser[6] (Chen et al., 2020) with most of the genes collected in Tong et al. (2020); (3) haplotype analysis was performed within Wheat SnpHub Portal[7] for 641 accessions with known genome sequences (Hao et al., 2020; Wang et al., 2020), and the genes without sequence variation were removed from candidacy. The most promising candidate genes were eventually selected. The database expVIP[8] was used to investigate spatio-temporal transcriptional dynamics of candidate genes, providing expression profiles of these genes across tissues and developmental stages (Ramírez-González et al., 2018).

[1] http://www.capitalbiotech.com/

[2] http://www.wheatgenome.org/

[3] http://zzlab.net/GAPIT

[4] https://github.com/YinLiLin/R-CMplot

[5] http://www.uniprot.org/

[6] http://wheat.cau.edu.cn/TGT/

[7] http://wheat.cau.edu.cn/Wheat_SnpHub_Portal/

[8] http://wheat-expression.com/

Kompetitive Allele-Specific PCR Marker Development and Quantitative Trait Locus/Loci Validation

The representative markers for 3AL and 7AL QTL were chosen and converted to KASP markers. Chromosome-specific primers were designed using Polymarker[9] (Ramirez-Gonzalez et al., 2015) and KASP assays were performed following Xu et al. (2020). The KASP markers were successfully converted when their genotypic results were the same as the original SNP arrays. The 146 F_6 recombinant inbred lines (RILs) developed from a cross between two modern wheat cultivars Zhongmai 175 and Lunxuan 987 (shorten as ZM175/LX987) with significantly different GZnC were used as validation population for the target QTL. GZnC was determined in the bi-parental population in the same way as mentioned earlier in the natural population. Student's *t*-tests were conducted to verify allelic effects based on the phenotypic data from the bi-parental population. For the candidate gene of QTL, its variations between ZM175 and LX987 were extracted from the genome resequencing database at Wheat SnpHub Portal (see text footnote 7; Hao et al., 2020; Wang et al., 2020).

RESULTS

Phenotypic Variations

A wide range of continuous variations of GZnC and GFeC were observed for the 166 accessions across all environments with near-normal distributions (**Supplementary Figures 1, 2**). The BLUE values for GZnC and GFeC were 29.25–50.98 mg/kg and 39.86–54.66 mg/kg with mean values of 38.03 and 45.97 mg/kg, respectively (**Table 1**). In all the accessions, six cultivars with the highest values for GZnC and GFeC were selected with the BLUE values greater than 50 mg/kg and stable performance across the environments (**Supplementary Figure 3**). Yumai2 and Xinong1376 were the cultivars with both high GZnC and GFeC. Significant correlations (r) between environments were observed for both GZnC and GFeC (**Supplementary Figure 4**). The results of ANOVA revealed that the factors of genotypes, environments, and G × E interactions markedly affect the GZnC and GFeC (**Supplementary Table 2**). Broad sense heritabilities (H^2) of GZnC and GFeC were 0.71 and 0.72, respectively, indicating a determinant role of genetic factors for phenotypic variations (**Table 1**). A significant and positive correlation was found between GZnC and GFeC based on BLUE values ($r = 0.45$, $p < 0.0001$). GFeC was positively correlated with PH ($r = 0.35$, $p < 0.0001$), whereas GZnC was not (**Supplementary Figure 4**). TKW was positively correlated with GA and negatively correlated with PH, and appeared not to be correlated with either GZnC or GFeC.

Marker-Trait Associations and Pleiotropic Loci

The significant associations were identified between SNPs and GZnC and GFeC using MLM, FarmCPU, and MLMM based on the BLUE values (**Figure 1**) and the values in each environment (**Supplementary Figures 5A, 6A**). The *Q*–*Q* plots showed that the observed values of p were close to the expected distributions indicating the proper control of false positive in GWAS (**Supplementary Figures 5B, 6B**). Among the 2,214 and 1,340 significant MTAs for GZnC and GFeC, respectively, 154 and 72 corresponding to 25 and 16 different loci were identified in at least three environments. These 41 loci were considered as stable QTL and are summarized in **Table 2**. In total, 9, 11, and 8 QTL were only detected by MLM, MLMM, and FarmCPU, respectively; five QTL were identified by two models; eight were simultaneously detected through all the three models (**Supplementary Figure 7**), indicating the complementarity and reliability of the three models we employed.

For GZnC, 25 stable loci located on chromosomes 1A (2), 2A, 3A (4), 3B (2), 5A, 5D, 6A (2), 6B, 6D (3), 7A, 7B (4), and 7D (3) explained the phenotypic variation (R^2-value) ranging from 7.73 to 13.57% (**Table 2**). Among these, six loci on chromosomal arms 3AS (*AX_111528452*, 19.89 Mb), 6AS (*AX_111556928*, 30.88 Mb), 7BL (*Tdurum_contig65979_289*, 539.22 Mb; *BS00022045_51*, 626.07 Mb; *AX_11046452*, 687.84 Mb), and 7DL (*AX_108866365*, 605.17 Mb) were the most stable and identified in all environments. The most significant marker was *AX_111528452* on 3AS with a p at 1.5×10^{-5} and R^2-value at 13.57%. For GFeC, we detected 16 stable QTL on chromosomes 1A, 1B (5), 5A, 5B (4), 7A, 7B, and 7D (3) with R^2-values ranging from 7.56 to 14.49% (**Table 2**). One stable locus on the long arm of chromosome 7D (*AX_95151824*, 614.54 Mb) was detected in all five environments comprising BLUE values. The most significant QTL was identified on 1BS (*AX_111633663*) with a p at 1.1×10^{-5} in the genomic region of 26.17–26.37 Mb.

Four pleiotropic loci were identified by comparing their physical positions of stable MTAs for GZnC, GFeC, and PH (**Table 2** and **Supplementary Table 3**). One locus on 7AL (*AX_94741862*, 706.91 Mb) was simultaneously associated with GZnC and GFeC while independent of PH and TKW, indicating its potential value in breeding for high grain zinc and

TABLE 1 | The phenotypic variation and H^2 of GZnC and GFeC in 166 wheat cultivars across different environments[a].

Trait	Environment	Min (mg/kg)	Max (mg/kg)	Mean (mg/kg)	SD (mg/kg)	H^2
GZnC	20BJ	28.60	54.30	37.38	4.07	0.71
	202GY	31.80	58.90	43.68	5.92	
	20SJZ	21.80	52.00	33.02	5.53	
	BLUE	29.25	50.98	38.03	3.95	
GFeC	20BJ	32.50	57.70	41.51	4.39	0.72
	20GY	35.20	60.95	45.96	4.80	
	20SJZ	36.00	57.50	43.82	4.27	
	20XJ	39.70	74.60	52.60	5.79	
	BLUE	39.86	54.66	45.97	3.56	

[a]*GZnC, grain zinc concentration; GFeC, grain iron concentration; 20BJ, 20GY, 20SJZ, 20XJ: Beijing, Gaoyi, Shijiazhuang, and Xinjiang locations, respectively, 2019–2020; BLUE: best linear unbiased estimation; SD, standard derivation; H^2, broad-sense heritability.*

[9]http://www.polymarker.info/

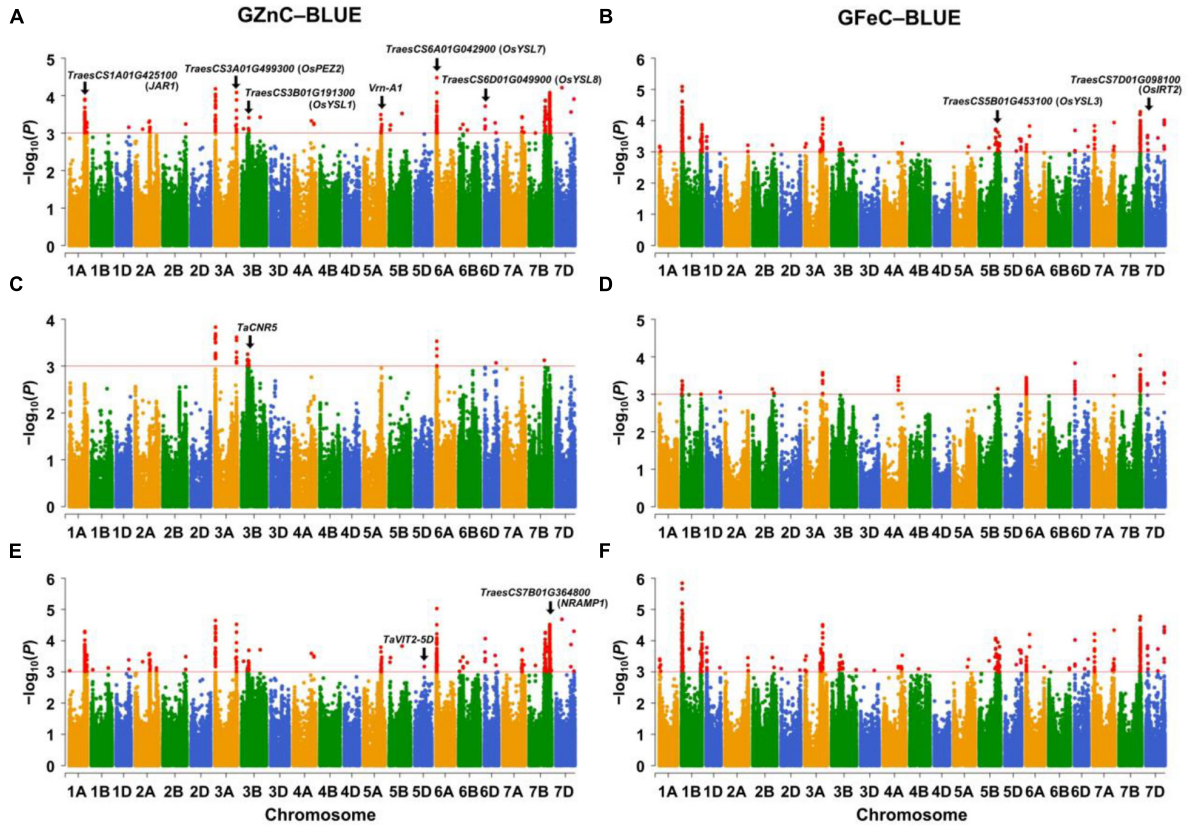

FIGURE 1 | Manhattan plots for GZnC and GFeC analyzed by **(A,B)** the mixed linear model (MLM), **(C,D)** the fixed and random model circulating probability unification (FarmCPU), and **(E,F)** the multiple loci mixed linear model (MLMM). The threshold of $p = 1.0 \times 10^{-3}$ ($-\log_{10}(p) = 3.0$) was used for calling significant marker-trait associations (MTAs). GZnC and GFeC indicate grain zinc and iron concentrations, respectively. BLUE indicates the best linear unbiased estimations across environments. The wheat gene ID indicates cloned wheat genes or wheat orthologs of known Zn/Fe-related genes in model plants.

iron. Two loci on 5AL (*AX_109311262*, 495.92 Mb) and 7BL (*Tdurum_contig61856_900*, 706.45 Mb) significantly increased GFeC and PH, suggesting that they might be useful when plant height is not an issue. The fourth pleiotropic locus located on 3AS (*AX_111528452*, 20.33 Mb) increased the GZnC but decreased the TKW. All the other 37 MTAs identified have no obvious pleiotropic effects and can be easily used in breeding for genetic improvement of either GZnC or GFeC (**Table 2**).

Candidate Genes Underlying Stable Loci

Twenty-eight promising candidate genes, located in or adjacent to the physical intervals of the QTL, were identified to be potentially involved in Zn/Fe uptake, transport, storage, and regulations (**Table 3**). They showed polymorphisms in 641 cultivars which were re-sequenced (data now shown). Among them, 17 genes were located within 2 Mb proximity of the representative markers, and nine genes were located less than 1 Mb from the marker (**Table 3**). The remaining 11 genes, mainly cloned wheat genes or wheat orthologs of known genes in model plants (7 out of 11), were likely to be causal genes for Zn/Fe homeostasis.

For Zn/Fe uptake, generally proton ATPases, nicotianamine synthases, and phenolic compound transporter played key roles. At least eight candidate genes were identified, and two of them, *TraesCS3A01G499300* and *TraesCS7D01G098100*, were wheat orthologs of rice genes *OsPEZ2* (Bashir et al., 2011; Ishimaru et al., 2011) and *OsIRT2* (Ishimaru et al., 2006) with known functions for Zn/Fe homeostasis. The expression profiles showed that all the above genes expressed at high levels in roots, further supporting their potential roles in Zn/Fe acquisition (**Supplementary Figure 8**). For Zn/Fe translocation, key transporters, such as citrate efflux transporter, yellow stripe-like (*YSL*) transporter, zinc-regulated transporter, and iron-regulated transporter-like protein (*ZIP*) transporter, were predominantly responsible for this process, and 11 putative genes were identified accordingly. Four genes were wheat orthologs of *YSL* genes (*OsYSL1*, *OsYSL3*, *OsYSL7*, and *OsYSL8*) in rice (Waters et al., 2006; Chu et al., 2010; Grillet and Schmidt, 2019), one was cloned gene (*TaCNR5*) in wheat (Qiao et al., 2019) related to zinc homeostasis, and the remaining six were possible wheat specific or yet to be discovered in model plants. These genes showed diverse expression patterns in different tissues and ages (**Supplementary Figure 8**). None or very little expression was detected in wheat grain, which partially supported their Zn/Fe transport roles in vegetative tissues (Kobayashi and Nishizawa, 2012).

TABLE 2 | Significant loci associated with GZnC and GFeC in at least three environments in 166 wheat accessions using three models in GAPIT.

Trait[a]	Environment[b]	Chr[c]	Physical interval (Mb)[d]	Representative SNP[e]	Allele[f,g]	MAF[f,h]	*P*-value ($\times 10^{-4}$)[f]	R^2 (%)[f,i]	Effect[f]	*P*-value for PH[j]	*P*-value for TKW[k]	Reported QTL[l]
GZnC	E1, E2, BLUE	1A	515.79–516.03	*AX_108845138*	C/T	0.11	1.11	11.88	2.58	0.439	0.765	*QGZn.cimmyt-1A*
	E2, E3, BLUE	1A	580.42–586.13	*AX_109976007*	C/G	0.44	2.36	9.62	2.25	0.935	0.461	*QGZn.cau-1A*
	E2, E3, BLUE	2A	246.51	*AX_109885783*	C/G	0.13	5.87	8.55	2.87	0.883	0.867	
	E2, E3, BLUE	3A	10.22	*AX_111534768*	G/A	0.18	1.91	9.91	3.19	0.964	0.164	
	E1, E2, E3, BLUE	3A	19.89–22.61	*AX_111528452*	T/G	0.31	0.15	13.57	3.06	0.377	0.001	
	E2, E3, BLUE	3A	696.23	*AX_108843516*	C/A	0.44	4.82	8.62	2.19	0.489	0.585	*QGZn.cimmyt-3A.1*
	E2, E3, BLUE	3A	721.64–724.58	*AX_109875082*	T/A	0.46	0.20	13.53	2.63	0.061	0.850	*QGZn.cimmyt-3A.2*
	E2, E3, BLUE	3B	202.41	*AX_110479767*	A/G	0.19	5.69	8.39	5.73	0.482	0.698	
	E2, E3, BLUE	3B	242.66	*AX_109384871*	G/A	0.17	7.35	8.04	6.80	0.177	0.527	
	E2, E3, BLUE	5A	591.28–592.63	*AX_94729189*	G/C	0.24	1.96	10.11	2.46	0.075	0.063	
	E2, E3, BLUE	5D	319.22	*AX_94388289*	C/G	0.20	4.21	8.81	2.82	0.284	0.599	
	E2, E3, BLUE	6A	17.77	*AX_110365398*	A/G	0.36	6.80	8.20	1.76	0.831	0.872	
	E1, E2, E3, BLUE	6A	28.31–31.37	*AX_111556928*	A/G	0.16	0.18	10.03	2.67	0.813	0.397	
	E2, E3, BLUE	6B	142.73	*AX_110935664*	A/G	0.39	0.79	11.44	2.41	0.391	0.830	*QGZn.uh-6B*
	E1, E2, BLUE	6D	16.8–16.81	*AX_108846745*	T/C	0.49	4.32	8.83	1.75	0.602	0.507	
	E2, E3, BLUE	6D	27.52	*AX_95220141*	G/A	0.20	1.45	10.55	3.19	0.554	0.422	
	E2, E3, BLUE	6D	357.01	*AX_110431664*	T/C	0.25	2.78	9.38	2.81	0.008	0.706	
	E1, E2, BLUE	7A	706.91	*AX_94741862*	T/G	0.35	9.57	7.73	1.64	0.205	0.343	*QGZn.ua-7A*
	E1, E2, E3, BLUE	7B	533.78–540.78	*Tdurum_contig65979_289*	A/G	0.39	1.34	10.48	1.97	0.920	0.974	
	E1, E2, E3, BLUE	7B	626.06–626.07	*BS00022045_51*	A/G	0.48	0.52	13.09	1.66	0.091	0.524	*QGZn.cimmyt-7B.5*
	E1, E2, E3, BLUE	7B	687.32–689.92	*AX_110464521*	G/A	0.26	0.76	12.48	1.75	0.708	0.491	
	E1, E2, BLUE	7B	708.11	*AX_95000860*	T/C	0.49	1.97	10.98	1.51	0.716	0.918	*GZn-IWA4150*
	E2, E3, BLUE	7D	203.16	*AX_110717434*	C/T	0.14	0.19	13.24	3.83	0.231	0.891	
	E1, E3, BLUE	7D	506.11	*GENE_3452_1116*	G/A	0.38	2.74	9.47	1.86	0.485	0.399	
	E1, E2, E3, BLUE	7D	605.17	*AX_108866365*	C/G	0.19	1.24	10.60	2.16	0.697	0.812	
GFeC	E2, E3, BLUE	1A	15.43	*AX_95081354*	C/T	0.20	5.43	8.37	2.07	0.047	0.102	
	E1, E2, BLUE	1B	15.65–15.74	*AX_86185361*	C/G	0.30	2.03	9.12	1.72	0.222	0.182	
	E2, E4, BLUE	1B	26.17–26.37	*AX_111633663*	A/C	0.45	0.11	13.03	2.01	0.007	0.246	
	E1, E4, BLUE	1B	38.63–38.83	*AX_109837760*	T/G	0.48	0.45	11.13	1.71	0.002	0.742	*QGFe.cimmyt-1B*
	E2, E3, BLUE	1B	660.01	*Tdurum_contig68980_448*	A/G	0.29	4.96	7.97	1.43	0.202	0.018	
	E1, E4, BLUE	1B	688.28–689.27	*AX_110457631*	C/T	0.36	1.37	9.64	1.42	0.087	0.618	
	E1, E4, BLUE	5A	495.92	*AX_109311262*	G/A	0.09	6.82	7.56	2.01	0.000	0.331	*QGFe.sau-5A.1*
	E2, E3, BLUE	5B	531.58	*AX_94967094*	C/T	0.39	5.82	7.76	1.39	0.668	0.480	*QGFe.cimmyt-5B.2*
	E2, E3, BLUE	5B	548.33	*AX_111484713*	G/A	0.20	1.89	9.22	1.68	0.404	0.002	
	E2, E3, BLUE	5B	622.54	*AX_111033847*	C/T	0.32	2.38	8.92	1.50	0.097	0.176	*QGFe.cimmyt-5B.3*
	E3, E4, BLUE	5B	679.03	*AX_109412899*	G/A	0.18	3.13	8.56	1.69	0.696	0.163	*QGFe.cimmyt-5B.4*
	E3, E4, BLUE	7A	706.91	*AX_94741862*	T/G	0.35	1.19	9.82	1.38	0.196	0.165	*QGFe.iari-7A*
	E3, E4, BLUE	7B	706.37–706.86	*Tdurum_contig61856_900*	A/C	0.36	0.52	10.93	1.42	0.001	0.035	*QGFe.cimmyt-7B*
	E2, E3, BLUE	7D	54.99	*AX_108920250*	C/T	0.44	0.14	14.49	2.27	0.989	0.005	
	E2, E3, BLUE	7D	69.31	*AX_111359934*	G/A	0.40	4.67	8.58	1.65	0.937	0.142	
	E1, E2, E3, E4, BLUE	7D	614.51–614.92	*AX_95151824*	T/G	0.32	0.96	10.12	1.43	0.122	0.101	*QGFe.sau-7D*

[a] *GZnC, grain zinc concentration; GFeC, grain iron concentration.*

[b] *E1, E2, E3, E4: Beijing, Gaoyi, Shijiazhuang, and Xinjiang locations, respectively, 2019–2020; BLUE, best linear unbiased estimation; BLUE-value was also used to conduct GWAS and was regarded as one environment.*

[c] *Chr, chromosome.*

[d] *Physical positions of single nucleotide polymorphism (SNP) markers were based on IWGSC RefSeq v.1.0 (http://www.wheatgenome.org/).*

[e] *The most significant SNP with the lowest p across environments for the corresponding locus was regarded as a representative.*

[f] *The information in corresponding columns are based on the representative SNP.*

[g] *"_" indicates the favorable allele with the increasing effect on GZnC or GFeC.*

[h] *MAF: minor allele frequency.*

[i] *R^2 indicates the percentage of phenotypic variance explained by the SNP marker.*

[j] *PH, plant height. The values of p for association between the representative markers of GZnC/GFeC QTL and plant height were calculated by GAPIT using the MLM model.*

[k] *TKW, thousand kernel weight. The p for association between the representative markers of GZnC/GFeC QTL and thousand kernel weight were calculated by GAPIT using the MLM model.*

[l] *The closest linked markers or mid-points of previous reported QTL intervals are present in Tong et al. (2020). Those loci with physical distances smaller than or approximate to one LD block away from reported QTL were considered as the same with the previous QTL.*

TABLE 3 | Putative candidate genes underlying the loci associated with GZnC and GFeC.

Trait[a]	Chr[b]	Physical interval of identified QTL (Mb)[c]	Candidate gene[d]	Physical position[c]	Distance[d] (Mb)	Ortholog/Putative functionality[e]	Putative involved process[f]
GZnC	1A	515.79–516.03	*TraesCS1A01G326700*	516.73	0.70	Citrate-binding protein	Transport
	1A	580.42–586.13	*TraesCS1A01G425100*	580.18	5.95	*JAR1* (Kobayashi, 2019)	Regulations
	3A	19.89–22.61	*TraesCS3A01G036400*	19.98	0.09	*ABC* transporter G family member	Uptake
	3A	721.64–724.58	*TraesCS3A01G499300*	724.49	0.09	*OsPEZ2* (Bashir et al., 2011; Ishimaru et al., 2011)	Uptake
	3B	202.41	*TraesCS3B01G191300*	204.28	1.88	*OsYSL1* (Chu et al., 2010)	Transport
	3B	242.66	*TraesCS3B01G214000*	253.90	11.24	*TaCNR5* (Qiao et al., 2019)	Transport
	5A	591.28–592.63	*TraesCS5A01G391700*	587.40	5.24	*Vrn-A1* (Jobson et al., 2018)	Regulations
	5D	319.22	*TraesCS5D01G209900*	318.10	1.12	*TaVIT2-5D* (Connorton et al., 2017)	Storage
	6A	17.77	*TraesCS6A01G042900*	22.54	4.76	*OsYSL7* (Chu et al., 2010)	Transport
	6A	28.31–31.37	*TraesCS6A01G051700*	26.93	1.95	*NAC* domain-containing protein	Regulations
	6B	142.73	*TraesCS6B01G145600*	145.88	3.14	*ABC* transporter B family protein	Uptake
	6D	27.52	*TraesCS6D01G049900*	24.19	3.33	*OsYSL8* (Grillet and Schmidt, 2019)	Transport
	7A	706.91	*TraesCS7A01G527900*	708.67	1.76	Magnesium transporter	Uptake
	7B	533.78–540.78	*TraesCS7B01G299200*	536.01	3.21	*BZIP* transcription factor	Regulations
	7B	626.06–626.07	*TraesCS7B01G364800*	627.98	1.91	*NRAMP1* (Segond et al., 2009)	Storage
	7B	687.32–689.92	*TraesCS7B01G429600*	698.14	9.30	Zinc ion binding protein	Storage
	7B	708.11	*TraesCS7B01G444600*	708.95	0.83	Magnesium transporter	Transport
	7D	203.16	*TraesCS7D01G237500*	201.88	1.29	Copper-transporting ATPase	Uptake
	7D	506.11	*TraesCS7D01G392800*	507.81	1.70	*BZIP* transcription factor	Regulations
	7D	605.17	*TraesCS7D01G504400*	610.53	5.36	Heavy metal transport	Transport
GFeC	1B	15.65–15.74	*TraesCS1B01G030800*	15.16	0.28	*ABC* transporter ATP-binding protein	Uptake
	1B	660.01	*TraesCS1B01G437100*	659.98	0.03	Calcium-transporting ATPase	Uptake
	5B	531.58	*TraesCS5B01G349500*	530.78	0.80	Fe^{2+} transporter	Transport
	5B	548.33	*TraesCS5B01G370100*	548.81	0.47	ATP-dependent zinc metalloprotease	Transport
	5B	622.54	*TraesCS5B01G453100*	626.01	3.46	*OsYSL3* (Waters et al., 2006)	Transport
	7D	54.99	*TraesCS7D01G098100*	58.90	3.90	*OsIRT2* (Ishimaru et al., 2006)	Uptake
	7D	69.31	*TraesCS7D01G113100*	69.26	0.06	*BHLH* family transcription factor	Regulations
	7D	614.51–614.92	*TraesCS7D01G515800*	615.91	1.37	Magnesium transporter	Transport

[a] *GZnC, grain zinc concentration; GFeC, grain iron concentration.*
[b] *Chr, chromosome.*
[c] *Physical positions of SNP markers and annotated genes were based on IWGSC RefSeq v.1.0.*
[d] *The distances between representative markers and candidate genes.*
[e] *Gene ID and functional annotations were based on IWGSC RefSeq v.1.0. The underlined genes indicated the cloned Zn/Fe-related genes in common wheat.*
[f] *Putative involved processes were based on the regulatory mechanisms of corresponding orthologous gene in Arabidopsis and rice, as well as gene annotations from IWGSC RefSeq v.1.0.*

The storage of metal into vacuoles in seeds was mainly mediated by vacuolar iron transporter (*VIT*) family members (Zhang et al., 2012), and the efflux of metal from the vacuolar to cytosol was mainly controlled by *NRAMP* family (Segond et al., 2009), which made *TraesCS5D01G209900* (*TaVIT2-5D*) and *TraesCS7B01G364800* (ortholog of *AtNRAMP1*) promising candidate genes responsible for the Zn/Fe storage in seeds (Segond et al., 2009; Connorton et al., 2017). *TraesCS7B01G429600* encoding a zinc binding protein showed high expression in wheat grain and was also considered as a promising candidate gene involved in the Zn/Fe storage (**Supplementary Figure 8**). Additionally, six regulator genes, such as *Vrn-A1,* mainly known as transcriptional factors (TFs) regulating the plant development, were identified. *TraesCS7B01G299200* and *TraesCS7D01G392800*, the *bZIP* TFs, *TraesCS7D01G113100*, the *bHLH* TF, *TraesCS6A01G0517000*, the NAC domain protein, and *TraesCS1A01G425100*, the wheat ortholog of jasmonic acid-amido synthetase (*JAR1*), were all putatively related to Zn/Fe homeostasis in wheat. Their spatio-temporal expression profiles are provided in **Supplementary Figure 8**.

Validation of 3AL Quantitative Trait Locus/Loci and the Underlying Gene

Among all the MTAs, we chose the major QTL on 3AL for GZnC (*AX_109875082*, 724.58 Mb) with high R^2-value (13.53%) and the pleiotropic locus on 7AL for GZnC and GFeC (*AX_94741862*, 706.91 Mb) to develop high-throughput KASP markers (**Table 2** and **Supplementary Table 4**). Both QTL were independent

of TKW and PH (**Table 2**). Their representative SNPs were successfully converted to KASP assays after genotyping the association panel and the same genotypic data were obtained from the wheat 660K SNP array (data not shown). The marker information was presented in **Supplementary Table 4**. The two KASP markers were further used to test the ZM175/LX987 bi-parental population. For *K_AX_109875082* on 3AL, a *t*-test showed a significant difference of GZnC between lines carrying favorable allele and lines with opposite allele across environments (**Figure 2B**). No polymorphism was detected for *K_AX_94741862* on 7AL in this population. Those markers closely linked to these QTL could be further detected in the ZM175/LX987 bi-parental population.

For the 3AL QTL, the most significant markers were located in the physical interval of 724,305,362–724,582,163 bp, where nine genes were annotated (**Figures 2A,C**). Sequence similarity analysis showed that *TraesCS3A01G499300*, annotated as a multidrug and toxic compound extrusion (MATE) family gene responsible for protein detoxification, had high amino acid sequence identity (87%) with OsPEZ2 (Tong et al., 2020). The gene *OsPEZ2* played an important role in metal uptake and translocation in rice and *pez2* mutant showed significantly reduced Fe concentration in root tips and xylem sap (Bashir et al., 2011; Ishimaru et al., 2011). *TraesCS3A01G499300* is 5,562 bp long and consists of seven exons in coding region (**Figure 2C**). Further sequence analysis revealed that *TraesCS3A01G499300* had abundant SNPs in its flanking and coding regions between ZM175 and LX987 (**Supplementary Table 5**), especially four missense SNPs within exons (**Figure 2C**), indicating *TraesCS3A01G499300* is likely to be the causal gene underlying 3AL QTL. Gene expression data indicate that the gene is constitutively expressed and is uniformly highly expressed in wheat root throughout developmental stages, which further supports its candidacy (**Figure 2C**).

DISCUSSION

Effects of Marker Density and Linear Models on Wheat Genome-Wide Association Study

In previous GWAS studies on wheat Zn/Fe, large gaps in the genetic map were generally found due to the low marker number and density as well as relatively long LD decays. In this study, GWAS was conducted using high-density markers, such as 373,106 SNPs, making it possible to change the LD pattern, thereby resulting in efficient identification of MTAs in many low-recombination regions on wheat chromosomes (Kim and Yoo, 2016). Forty-one loci for GZnC/GFeC were detected, and the number is much higher than the QTL detected in previous literature (Gupta et al., 2021). Out of the 41 representative significant MTAs, only five markers came from the 90K SNP array, and 36 were from the 660K array, indicating that high-resolution GWAS was achieved by high density markers (Fu et al., 2020; Pang et al., 2020).

In terms of population size, a relatively small collection was used in this study. Nevertheless, the 166 core accessions were selected from over 400 elite cultivars and represented much diverse wheat accessions in China's major wheat growing regions. The same population has been used to conduct GWAS on many yield or quality-related traits and performed highly informative in our previous studies (Liu et al., 2017; Zhai et al., 2018, 2020; Li et al., 2019; Fu et al., 2020). MLM using $Q + K$ as covariant might be over-fitted possibly due to the strict control of population structure and kinship, leading to false negatives (Korte and Farlow, 2013). The multiple testing corrections tended to be too stringent to detect sufficient both major and minor MTAs. Whereas, the model FarmCPU as a complement, could avoid over-corrected population structure to some extent by utilizing fixed and random effect models iteratively (Kusmec and Schnable, 2018). Using three models together, reliable loci for GZnC and GFeC detected were almost doubled than using an MLM alone in the present research.

Genetic Architecture Dissection by Comparing Current Loci With Known Quantitative Trait Locus/Loci

To date, hundreds of Fe/Zn-related QTL have been mapped on all wheat chromosomes except 6D by bi-parental linkage mapping and GWAS (Tong et al., 2020). For the 25 loci associated with GZnC in this study, eight have similar physical positions with known Zn-related QTL on 1AL (2), 3AL (2), 6BS, 7AL, and 7BL (2), respectively (**Table 2** and **Figure 3**). As for GFeC, half of the 16 loci were identified to coincide with the documented QTL on 1BS, 5AL, 5BL (3), 7AL, 7BL, and 7DL, respectively. Major overlapping regions were observed on 5BL, where previous literatures reported a large number of Fe-related QTL by bi-parental mapping, confirming its importance for the gene discovery (Tong et al., 2020).

For the other 25 loci, comprising 17 loci for GZnC and 8 for GFeC, they were located in the chromosomal regions that were different from the QTL previously reported and are probably new loci (**Table 2** and **Figure 3**). For example, three QTL on 6D (*AX_108846745*, 16.81 Mb; *AX_95220141*, 27.52 Mb; *AX_110431664*, 357.01 Mb) are highly likely to be novel since no Zn/Fe-related QTL has been previously mapped on this chromosome (Tong et al., 2020). Similarly, on chromosome 7D, there were only two Fe related QTL reported at 13.9 Mb and 616.6 Mb, so the three loci for GZnC (*AX_110717434*, 203.16 Mb; *GENE_3452_1116*, 506.11 Mb; and *AX_108866365*, 605.17 Mb) and two loci for GFeC (*AX_108920250*, 54.99 and *AX_111359934*, 69.31 Mb) were likely to be new. The new loci identified in this research have significantly enriched our understanding of the genetic basis of the complicated Zn and Fe traits in wheat.

Promising Candidate Genes Related to Grain Zinc Concentration and Grain Iron Concentration

To date, numerous genes involved in Zn and Fe homeostasis in model plants have been extensively studied (Tong et al., 2020;

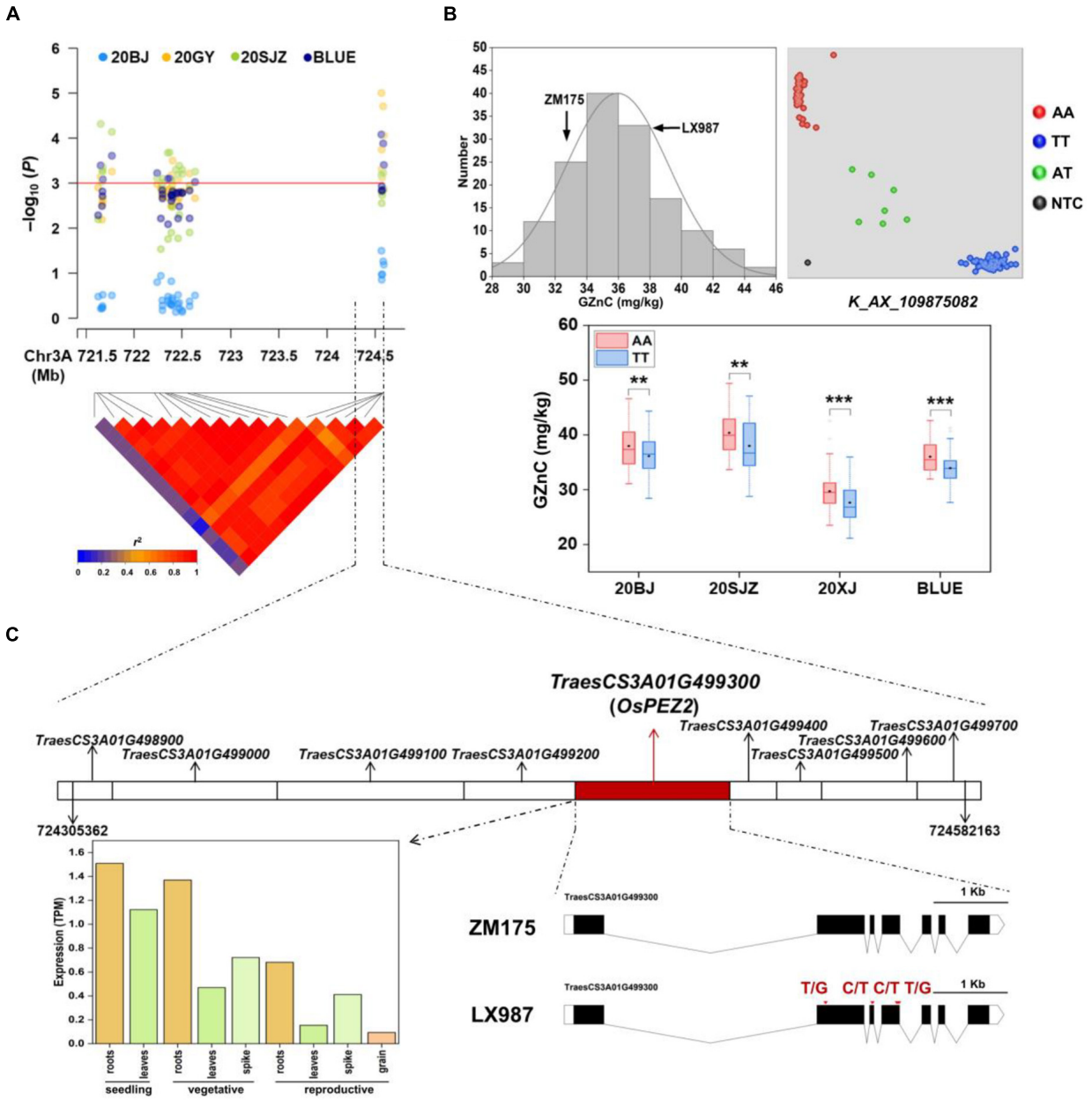

FIGURE 2 | (A) Local Manhattan plot and linkage disequilibrium (LD) heatmap of single nucleotide polymorphisms (SNPs) within the 3AL quantitative trait loci (QTL) identified for grain zinc concentration (GZnC). 20BJ, 20GY, and 20SJZ: Beijing, Gaoyi, and Shijiazhuang locations, respectively, 2019–2020. BLUE: best linear unbiased estimations. **(B)** The validation of 3AL QTL in ZM175/LX987 RIL population. Histograms for GZnC in the population using BLUE values across three environments (top and left); genotype calling result of the kompetitive allele-specific PCR (KASP) markers for *K_AX_109875082* in the population (top and right); allelic effects of *K_AX_109875082* on GZnC in the population across 20BJ, 20SJZ, 20XJ, and BLUE (bottom). AA and TT indicate two homozygous genotypes for this marker from LX987 and ZM175, respectively. AT indicates the heterozygous genotype, and NTC represents no template control. 20XJ: Xinjiang location in during 2019–2020. The black diamond in each box indicates the mean. $^{*}p < 0.05$; $^{**}p < 0.01$; $^{***}p < 0.001$; ns: not significant. **(C)** The nine annotated genes identified close to *AX_109875082* with the highest *p* in the 3AL QTL region (top); the spatio-temporal expression profiles of the candidate gene *TraesCS3A01G499300* (bottom and left); the gene structure of *TraesCS3A01G499300* containing four exons with missense variants between ZM175 and LX987 (bottom and right), and red arrows indicate the positions of the exon missense variants between ZM175 and LX987.

Gupta et al., 2021). Wheat gene annotations from the IWGSC RefSeq v.1.0 provided a useful tool to further investigate the candidate genes located in or adjacent to the QTL identified. In the current study, 28 candidate genes were identified for Zn/Fe homeostasis, such as uptake, transport, storage, and regulations (**Figure 4**). The spatio-temporal expression profiles were highly consistent with their putative functions, indicating their possible roles in wheat Zn/Fe homeostasis. Of them, 11

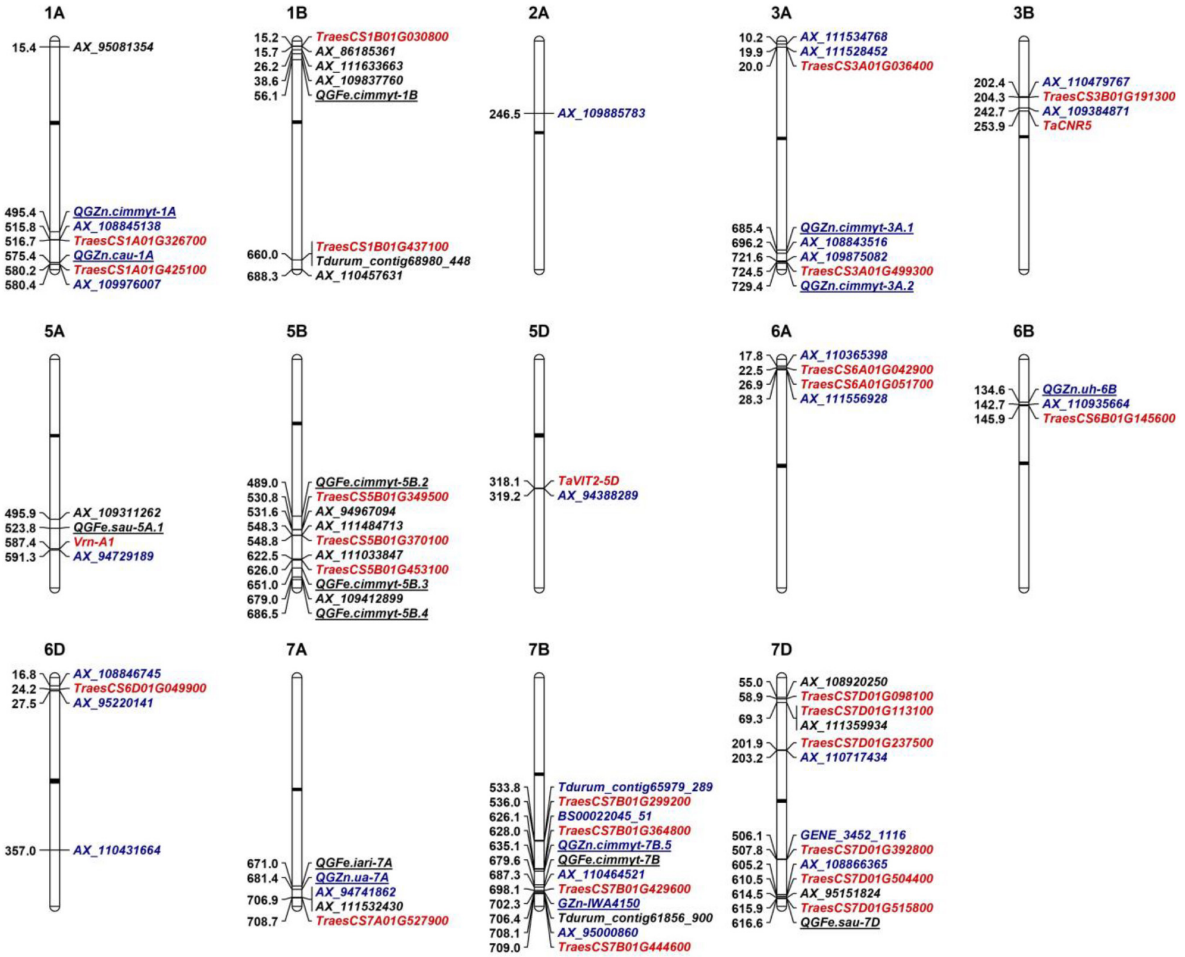

FIGURE 3 | Genetic architectures of grain zinc and iron in wheat. The top of each graph indicates the chromosome number in wheat and the left shows the physical positions based on IWGSC RefSeq v.1.0. The loci identified to associate with GZnC and GFeC are shown with black and blue fonts, respectively. The representative markers (noted in **Table 2**) identified in this study were used to be compared with previous reported QTL that are underlined. The closest linked markers or mid-points of previous reported QTL intervals were from Tong et al. (2020). Promising candidate genes are highlighted as red color. Black bars indicate the locations of centromeres.

genes were putative wheat orthologs of known *Arabidopsis* and rice genes related to Zn/Fe homeostasis, partially supporting the authenticity of the detected loci.

TraesCS3A01G499300, the candidate gene for 3AL QTL, was an ortholog of *OsPEZ2*, an efflux transporter for phenolics that served as chelators to facilitate metal uptake by root in rice (Bashir et al., 2011; Ishimaru et al., 2011). A very recent study demonstrated the pivotal roles of MATE family genes of protein detoxification for metal uptake and transport in rice roots and stems, further supporting the potential role of *TraesCS3A01G499300* on Zn/Fe homeostasis (Ren et al., 2021). Abundant sequence variations of the gene between ZM175 and LX987 were observed and provided strong evidence that it is possibly the causal gene and deserves further studies. In addition, we successfully developed KASP markers for the 7AL QTL but unfortunately it returned monomorphic in ZM175/LX987 RILs. However, it was interesting to find that the candidate gene *TraesCS7A01G527900* (706.91 Mb) underlying 7AL QTL was homologous with *TraesCS7B01G444600* (708.11 Mb) on 7BL and *TraesCS7D01G515800* (615.91 Mb) on 7DL for the three QTL identified in this study. The three candidate genes annotated as magnesium transporters were exactly the three homeologs for the same gene in each sub-genome. These loci are potentially important and we are now developing KASP markers for 7BL and 7DL QTL for validation. If any loci are validated in ZM175/LX987 or other mapping populations, the roles of all three loci in metal homeostasis can be presumed. The candidate genes identified in this study provided genetic bases for further elucidating the mechanisms of Zn and Fe homeostasis in wheat.

Applications in Wheat Breeding for Biofortification

Since most common wheat had suboptimal GZnC and GFeC, it is imperative to identify Zn/Fe-related QTL or genes as many as possible and to re-introduce or to pyramid them into

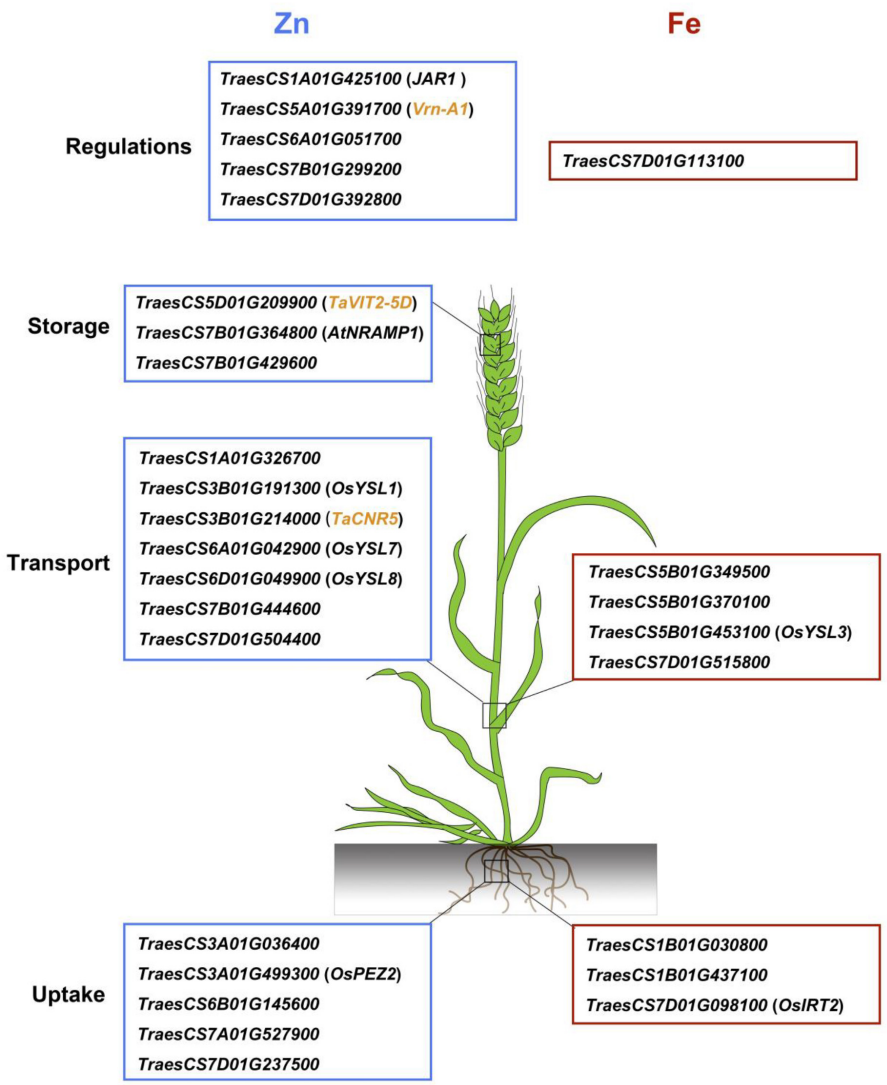

FIGURE 4 | A brief model proposed for grain zinc and iron accumulation in common wheat based on the promising candidate genes identified. The wheat gene ID framed with blue and red boxes indicates zinc and iron genes, respectively, and the genes in the small brackets indicate known Zn/Fe related genes in model plants. The cloned zinc related genes in wheat are highlighted as yellow.

current wheat gene pools. In this study, 12 accessions with stable high GZnC or GFeC were identified with BLUE values over 50 mg/kg (**Supplementary Figure 3**). The elite germplasm, such as Xiaoyan54 and Xinong1376 are currently cultivars in wheat production and can be used immediately as donor parents for wheat biofortification.

Although no significant correlation was observed between TKW and GZnC/GFeC in the present study, one pleiotropic locus on 3AS (*AX_111528452*, 20.33 Mb) was identified to increase GZnC but decrease TKW in all four environments. This QTL may be useful in certain crosses for biofortification when TKW is high enough. In addition, when plant height does not significantly affect the overall performance, pleiotropic loci on 5AL (*AX_109311262*, 495.92 Mb) and 7BL (*Tdurum_contig61856_900*, 706.45 Mb) could exert effects on Zn/Fe enrichment. It should be noted that favorable allele frequencies for the above three representative markers were 0.31, 0.09, and 0.36, respectively, indicating quite low frequency in our association panel (**Supplementary Table 3**). Considering only very few GZnC/GFeC loci had negative pleiotropic effects on agronomic traits such as TKW and PH, we speculated that there were still high chances for the improvement of GZnC/GFeC without yield penalty (Velu et al., 2018).

The fast release of wheat reference genome sequences and pan-genomes will undoubtedly speed up the process of marker development and gene discovery for wheat biofortification. Cloning important genes involved in Zn/Fe uptake, transport, storage, and regulations and pyramiding favorable alleles are promising avenues to increase the GZnC and GFeC in wheat cultivars. The 3AL locus was validated using a bi-parental

population and its candidate gene was proposed as an uptake related gene, highlighting its potential use in wheat breeding. High-throughput and breeder-friendly KASP markers will pave the way for MAS in breeding and accelerate the release of biofortified wheat.

CONCLUSION

A GWAS using multiple models is demonstrated as a powerful approach for genetic dissection of micronutrient traits in wheat based on a high-resolution physical map. Sixteen loci were identified in the similar regions of known QTL related to Zn/Fe, and 25 loci were new. Twenty-eight promising candidate genes were identified based on bioinformatics analyses and gene expression data and are worthy of further investigation. The effect of one major QTL on 3AL was validated in a bi-parental population, highlighting its potential application for wheat biofortification.

DATA AVAILABILITY STATEMENT

The original contributions presented in the study are included in the article/**Supplementary Material**, further inquiries can be directed to the corresponding author/s.

AUTHOR CONTRIBUTIONS

YH and ZH conceived this work. YH and JT designed the experiments and wrote the manuscript. JT, CZ, MS, JS, DL, YZ, JZ, ZP, and LL completed the field work and data investigation. JT, CZ, and LF analyzed and interpreted the data. YH, ZH, AR, ML, and XX critically reviewed and revised the manuscript. All authors have read and approved the final manuscript.

FUNDING

This research was financially supported by the National Key Research and Development Program of China (2021YFF1000204 and 2020YFE0202300), the National Natural Science Foundation of China (31950410563 and 31961143007), the Agricultural Science and Technology Innovation Program of CAAS (CAAS-ZDRW202109), and the Fundamental Research Funds for Central Non-Profit of Institute of Crop Sciences, CAAS.

SUPPLEMENTARY MATERIAL

The Supplementary Material for this article can be found online at: https://www.frontiersin.org/articles/10.3389/fpls.2022.840614/full#supplementary-material

REFERENCES

Alqudah, A. M., Sallam, A., Stephen Baenziger, P., and Börner, A. (2020). GWAS: Fast-forwarding gene identification and characterization in temperate cereals: lessons from Barley – A review. *J. Adv. Res.* 22, 119–135. doi: 10.1016/j.jare.2019.10.013

Bashir, K., Ishimaru, Y., Shimo, H., Kakei, Y., Senoura, T., Takahashi, R., et al. (2011). Rice phenolics efflux transporter 2 (PEZ2) plays an important role in solubilizing apoplasmic iron. *Soil Sci. Plant Nutr.* 57, 803–812. doi: 10.1080/00380768.2011.637305

Bhati, K. K., Alok, A., Kumar, A., Kaur, J., Tiwari, S., and Pandey, A. K. (2016). Silencing of ABCC13 transporter in wheat reveals its involvement in grain development, phytic acid accumulation and lateral root formation. *J. Exp. Bot.* 67, 4379–4389. doi: 10.1093/jxb/erw224

Bouis, H. E., Hotz, C., McClafferty, B., Meenakshi, J. V., and Pfeiffer, W. H. (2011). Biofortification: A new tool to reduce micronutrient malnutrition. *Food Nutr. Bull.* 32, S31–S40. doi: 10.1177/15648265110321S105

Chen, Y., Song, W., Xie, X., Wang, Z., Guan, P., Peng, H., et al. (2020). A collinearity-incorporating homology inference strategy for connecting emerging assemblies in Triticeae Tribe as a pilot practice in the plant pangenomic era. *Mol. Plant* 13, 1694–1708. doi: 10.1016/j.molp.2020.09.019

Chu, H., Chiecko, J., Punshon, T., Lanzirotti, A., Lahner, B., Salt, D. E., et al. (2010). Successful reproduction requires the function of Arabidopsis YELLOW STRIPE-LIKE1 and YELLOW STRIPE-LIKE3 metal-nicotianamine transporters in both vegetative and reproductive structures. *Plant Physiol.* 154, 197–210. doi: 10.1104/pp.110.159103

Connorton, J. M., Jones, E. R., Rodríguez-Ramiro, I., Fairweather-Tait, S., Uauy, C., and Balk, J. (2017). Wheat vacuolar iron transporter TaVIT2 transports Fe and Mn and is effective for biofortification. *Plant Physiol.* 174, 2434–2444. doi: 10.1104/pp.17.00672

Fu, L., Wu, J., Yang, S., Jin, Y., Liu, J., Yang, M., et al. (2020). Genome-wide association analysis of stem water-soluble carbohydrate content in bread wheat. *Theor. Appl. Genet.* 133, 2897–2914. doi: 10.1007/s00122-020-03640-x

Gómez-Galera, S., Rojas, E., Sudhakar, D., Zhu, C., Pelacho, A. M., Capell, T., et al. (2010). Critical evaluation of strategies for mineral fortification of staple food crops. *Transgenic Res.* 19, 165–180. doi: 10.1007/s11248-009-9311-y

Grillet, L., and Schmidt, W. (2019). Iron acquisition strategies in land plants: not so different after all. *New Phytol.* 224, 11–18. doi: 10.1111/nph.16005

Gupta, P. K., Balyan, H. S., Sharma, S., and Kumar, R. (2021). Biofortification and bioavailability of Zn, Fe and Se in wheat: present status and future prospects. *Theor. Appl. Genet.* 134, 1–35. doi: 10.1007/s00122-020-03709-7

Hamblin, M. T., Buckler, E. S., and Jannink, J. L. (2011). Population genetics of genomics-based crop improvement methods. *Trends Genet.* 27, 98–106. doi: 10.1016/j.tig.2010.12.003

Hänsch, R., and Mendel, R. R. (2009). Physiological functions of mineral micronutrients (Cu, Zn, Mn, Fe, Ni, Mo, B, Cl). *Curr. Opin. Plant Biol.* 12, 259–266. doi: 10.1016/j.pbi.2009.05.006

Hao, C., Jiao, C., Hou, J., Li, T., Liu, H., Wang, Y., et al. (2020). Resequencing of 145 landmark cultivars reveals asymmetric sub-genome selection and strong founder genotype effects on wheat breeding in China. *Mol. Plant.* 13, 1733–1751. doi: 10.1016/j.molp.2020.09.001

Holland, J. B., Carolina, N., Nyquist, W. E., and Lafayette, W. (2003). Estimating and interpreting heritability for plant breeding: an update. *Plant Breed. Rev.* 22, 11–112. doi: 10.1002/9780470650202.ch2

Ishimaru, Y., Kakei, Y., Shimo, H., Bashir, K., Sato, Y., Sato, Y., et al. (2011). A rice phenolic efflux transporter is essential for solubilizing precipitated apoplasmic iron in the plant stele. *J. Biol. Chem.* 286, 24649–24655. doi: 10.1074/jbc.M111.221168

Ishimaru, Y., Suzuki, M., Tsukamoto, T., Suzuki, K., Nakazono, M., Kobayashi, T., et al. (2006). Rice plants take up iron as an Fe^{3+} -phytosiderophore and as Fe^{2+}. *Plant J.* 45, 335–346. doi: 10.1111/j.1365-313X.2005.02624.x

Jobson, E. M., Martin, J. M., Schneider, T. M., and Giroux, M. J. (2018). The impact of the *Rht-B1b*, *Rht-D1b*, and *Rht-8* wheat semi-dwarfing genes on flour milling, baking, and micronutrients. *Cereal Chem.* 95, 770–778. doi: 10.1002/cche.10091

Kim, S. A., and Yoo, Y. J. (2016). Effects of single nucleotide polymorphism marker denstity on haplotype block partition. *Genomics Inform.* 14, 196–204. doi: 10.5808/GI.2016.14.4.196

Kobayashi, T. (2019). Understanding the Complexity of Iron Sensing and Signaling Cascades in Plants. *Plant Cell Physiol.* 60, 1440–1446. doi: 10.1093/pcp/pcz038

Kobayashi, T., and Nishizawa, N. K. (2012). Iron uptake, translocation, and regulation in higher plants. *Annu. Rev. Plant Biol.* 63, 131–152. doi: 10.1146/annurev-arplant-042811-105522

Korte, A., and Farlow, A. (2013). The advantages and limitations of trait analysis with GWAS: a review. *Plant Methods* 9:29. doi: 10.1186/1746-4811-9-29

Kusmec, A., and Schnable, P. S. (2018). FarmCPUpp: Efficient large-scale genomewide association studies. *Plant Direct* 2, 1–6. doi: 10.1002/pld3.53

Li, F., Wen, W., Liu, J., Zhang, Y., Cao, S., He, Z., et al. (2019). Genetic architecture of grain yield in bread wheat based on genome-wide association studies. *BMC Plant Biol.* 19:168. doi: 10.1186/s12870-019-1781-3

Liu, J., He, Z., Rasheed, A., Wen, W., Yan, J., Zhang, P., et al. (2017). Genome-wide association mapping of black point reaction in common wheat (*Triticum aestivum* L.). *BMC Plant Biol.* 17:220. doi: 10.1186/s12870-017-1167-3

Ludwig, Y., and Slamet-Loedin, I. H. (2019). Genetic biofortification to enrich rice and wheat grain iron: From genes to product. *Front. Plant Sci.* 10:833. doi: 10.3389/fpls.2019.00833

Murray, M. G., and Thompson, W. F. (1980). Rapid isolation of high molecular weight plant DNA. *Nucleic Acids Res.* 8, 4321–4326. doi: 10.1093/nar/8.19.4321

Paltridge, N. G., Milham, P. J., Ortiz-Monasterio, J. I., Velu, G., Yasmin, Z., Palmer, L. J., et al. (2012). Energy-dispersive X-ray fluorescence spectrometry as a tool for zinc, iron and selenium analysis in whole grain wheat. *Plant Soil* 361, 261–269. doi: 10.1007/s11104-012-1423-0

Pang, Y., Liu, C., Wang, D., Amand, P., Bernardo, A., Li, W., et al. (2020). High-resolution genome-wide association study identifies genomic regions and candidate genes for important agronomic traits in wheat. *Mol. Plant* 13, 1311–1327. doi: 10.1016/j.molp.2020.07.008

Peng, Y., Liu, H., Chen, J., Shi, T., Zhang, C., Sun, D., et al. (2018). Genome-wide association studies of free amino acid levels by six multi-locus models in bread wheat. *Front. Plant Sci.* 9:1196. doi: 10.3389/fpls.2018.01196

Platten, J. D., Cobb, J. N., and Zantua, R. E. (2019). Criteria for evaluating molecular markers: Comprehensive quality metrics to improve marker-assisted selection. *PLoS One* 14:e0210529. doi: 10.1371/journal.pone.0210529

Qiao, K., Wang, F., Liang, S., Wang, H., Hu, Z., and Chai, T. (2019). New biofortification tool: wheat TaCNR5 enhances zinc and manganese tolerance and increases zinc and manganese accumulation in rice grains. *J. Agric. Food Chem.* 67, 9877–9884. doi: 10.1021/acs.jafc.9b04210

Ramírez-González, R. H., Borrill, P., Lang, D., Harrington, S. A., Brinton, J., Venturini, L., et al. (2018). The transcriptional landscape of polyploid wheat. *Science* 361:eaar6089. doi: 10.1126/science.aar6089

Ramirez-Gonzalez, R. H., Uauy, C., and Caccamo, M. (2015). PolyMarker: A fast polyploid primer design pipeline: Fig. 1. *Bioinformatics* 31, 2038–2039. doi: 10.1093/bioinformatics/btv069

Rasheed, A., Hao, Y., Xia, X., Khan, A., Xu, Y., Varshney, R. K., et al. (2017). Crop breeding chips and genotyping platforms: Progress, challenges, and perspectives. *Mol. Plant* 10, 1047–1064. doi: 10.1016/j.molp.2017.06.008

Ren, Z., Bai, F., Xu, J., Wang, L., Wang, X., Zhang, Q., et al. (2021). A chloride efflux transporter *OsBIRG1* regulates grain size and salt tolerance in rice. *BioRxiv* [Preprint]. doi: 10.1101/2021.03.07.434240

Segond, D., Dellagi, A., Lanquar, V., Rigault, M., Patrit, O., Thomine, S., et al. (2009). *NRAMP* genes function in *Arabidopsis thaliana* resistance to *Erwinia chrysanthemi* infection. *Plant J.* 58, 195–207. doi: 10.1111/j.1365-313X.2008.03775.x

Sun, C., Dong, Z., Zhao, L., Ren, Y., Zhang, N., and Chen, F. (2020). The Wheat 660K SNP array demonstrates great potential for marker-assisted selection in polyploid wheat. *Plant Biotechnol. J.* 18, 1354–1360. doi: 10.1111/pbi.13361

Tang, Y., Liu, X., Wang, J., Li, M., Wang, Q., Tian, F., et al. (2016). GAPIT Version 2: An enhanced integrated tool for genomic association and prediction. *Plant Genome* 9:0120. doi: 10.3835/plantgenome2015.11.0120

Tong, J., Sun, M., Wang, Y., Zhang, Y., Rasheed, A., Li, M., et al. (2020). Dissection of molecular processes and genetic architecture underlying iron and zinc homeostasis for biofortification: From model plants to common wheat. *Int. J. Mol. Sci.* 21:9280. doi: 10.3390/ijms21239280

Vasconcelos, M. W., Gruissem, W., and Bhullar, N. K. (2017). Iron biofortification in the 21st century: setting realistic targets, overcoming obstacles, and new strategies for healthy nutrition. *Curr. Opin. Biotechnol.* 44, 8–15. doi: 10.1016/j.copbio.2016.10.001

Velu, G., Singh, R. P., Crespo-Herrera, L., Juliana, P., Dreisigacker, S., Valluru, R., et al. (2018). Genetic dissection of grain zinc concentration in spring wheat for mainstreaming biofortification in CIMMYT wheat breeding. *Sci. Rep.* 8:13526. doi: 10.1038/s41598-018-31951-z

Wang, W., Wang, Z., Li, X., Ni, Z., Hu, Z., Xin, M., et al. (2020). SnpHub: an easy-to-set-up web server framework for exploring large-scale genomic variation data in the post-genomic era with applications in wheat. *GigaScience* 9, 1–8. doi: 10.1093/gigascience/giaa060

Waters, B. M., Chu, H., DiDonato, R. J., Roberts, L. A., Eisley, R. B., Lahner, B., et al. (2006). Mutations in Arabidopsis Yellow Stripe-Like1 and Yellow Stripe-Like3 reveal their roles in metal ion homeostasis and loading of metal ions in seeds. *Plant Physiol.* 141, 1446–1458. doi: 10.1104/pp.106.082586

Xu, D., Wen, W., Fu, L., Li, F., Li, J., Xie, L., et al. (2019). Genetic dissection of a major QTL for kernel weight spanning the *Rht-B1* locus in bread wheat. *Theor. Appl. Genet.* 132, 3191–3200. doi: 10.1007/s00122-019-03418-w

Xu, X., Zhu, Z., Jia, A., Wang, F., Wang, J., Zhang, Y., et al. (2020). Mapping of QTL for partial resistance to powdery mildew in two Chinese common wheat cultivars. *Euphytica* 216:3. doi: 10.1007/s10681-019-2537-8

Yano, K., Yamamoto, E., Aya, K., Takeuchi, H., Lo, P., Hu, L., et al. (2016). Genome-wide association study using whole-genome sequencing rapidly identifies new genes influencing agronomic traits in rice. *Nat. Genet.* 48, 927–934. doi: 10.1038/ng.3596

Yin, C., Li, H., Li, S., Xu, L., Zhao, Z., and Wang, J. (2015). Genetic dissection on rice grain shape by the two-dimensional image analysis in one *japonica* × *indica* population consisting of recombinant inbred lines. *Theor. Appl. Genet.* 128, 1969–1986. doi: 10.1007/s00122-015-2560-7

Zhai, S., He, Z., Wen, W., Liu, J., Jin, H., Yan, J., et al. (2020). Genetic architecture of polyphenol oxidase activity in wheat flour by genome-wide association study. *Crop Sci.* 60, 1281–1293. doi: 10.1002/csc2.20038

Zhai, S., Liu, J., Xu, D., Wen, W., Yan, J., Zhang, P., et al. (2018). A genome-wide association study reveals a rich genetic architecture of flour color-related traits in bread wheat. *Front. Plant. Sci.* 9:1136. doi: 10.3389/fpls.2018.01136

Zhang, Y., Xu, Y., Yi, H., and Gong, J. (2012). Vacuolar membrane transporters OsVIT1 and OsVIT2 modulate iron translocation between flag leaves and seeds in rice. *Plant J.* 72, 400–410. doi: 10.1111/j.1365-313X.2012.05088.x

Conflict of Interest: The authors declare that the research was conducted in the absence of any commercial or financial relationships that could be construed as a potential conflict of interest.

Publisher's Note: All claims expressed in this article are solely those of the authors and do not necessarily represent those of their affiliated organizations, or those of the publisher, the editors and the reviewers. Any product that may be evaluated in this article, or claim that may be made by its manufacturer, is not guaranteed or endorsed by the publisher.

frontiers in Plant Science

ORIGINAL RESEARCH
published: 28 March 2022
doi: 10.3389/fpls.2022.829229

Relationship of Starch Pasting Properties and Dough Rheology, and the Role of Starch in Determining Quality of Short Biscuit

Liang Liu, Tao Yang, Jianting Yang, Qin Zhou, Xiao Wang, Jian Cai, Mei Huang, Tingbo Dai, Weixing Cao and Dong Jiang**

College of Agriculture, Nanjing Agricultural University, Nanjing, China

OPEN ACCESS

Edited by:
Vincenzo Rossi, Research Centre for Cereal and Industrial Crops, Council for Agricultural and Economics Research (CREA), Italy

Reviewed by:
Min Zhu, Yangzhou University, China
Gengjun Chen, Kansas State University, United States
Măăălina Ungureanu-Iuga, Ştefan cel Mare University of Suceava, Romania

***Correspondence:**
Qin Zhou
qinzhou@njau.edu.cn
Dong Jiang
jiangd@njau.edu.cn

Specialty section:
This article was submitted to Crop and Product Physiology, a section of the journal Frontiers in Plant Science

Received: *05 December 2021*
Accepted: *22 February 2022*
Published: *28 March 2022*

Citation:
Liu L, Yang T, Yang J, Zhou Q, Wang X, Cai J, Huang M, Dai T, Cao W and Jiang D (2022) Relationship of Starch Pasting Properties and Dough Rheology, and the Role of Starch in Determining Quality of Short Biscuit. Front. Plant Sci. 13:829229. doi: 10.3389/fpls.2022.829229

Starch plays an important role in food industry. In this study, three wheat cultivars with different protein contents were used to investigate the different ratios of starch addition on starch pasting properties, starch thermal performance, dough rheology, biscuit quality, and their relationships. Results showed that with the increase in starch content, gluten, protein and glutenin macropolymer (GMP), lactic acid solvent retention capacity (SRC), sucrose SRC, and onset temperature (To) decreased, while most pasting parameters and gelatinization enthalpy (ΔH) increased. Viscosity parameters were significantly negatively correlated with dough stability time, farinograph quality number (FQN), and sucrose SRC. Biscuit quality was improved by starch addition, indicated by lower thickness and hardness, higher diameter, spread ratio, and sensory score. Viscosity parameters were positively correlated to diameter, spread ratio, and sensory score of biscuit, while negatively correlated to hardness and thickness of biscuit. Image analysis showed that the crumbs of biscuit were improved as shown by bigger pores in the bottom side. The results provide useful information for the clarification of the role of starch in determining biscuit quality and the inter-relationships of flour, dough, and biscuit.

Keywords: gelatinization, quality, short biscuit, starch, wheat

INTRODUCTION

Biscuits are one of the most popular wheat products due to their ready to-eat, long shelf-time, and wide-variety (Moriano et al., 2018). The biscuit production had increased from 1.05 to 12.5 million tons with an annual growth rate of 18.0% from 2004 to 2019 in China (Yang et al., 2022). Wheat flour with low content of protein and gluten is believed an ideal material for biscuits, cookies, and other bakery foods (Manley, 2011). However, most of the commercial wheat grains in China had medium to high protein content due to higher N fertilizer input. Xu et al. (2016) analyzed 7,561 samples of 742 varieties from the main production region of wheat in China from 2006 to 2015 and found that the ratio of weak gluten wheat was lower than 1%. It is thus of importance to produce wheat flour with low-protein content for the biscuit industry in China.

It is believed that biscuit quality is closely related to flour protein content. The hardness of biscuits are suggested to increase gradually with elevated protein and gluten levels (Fustier et al., 2008; Pauly et al., 2013). Good quality soft wheat flour produces large spread cookies with a large diameter and low thickness. However, Moiraghi et al. (2011) found that protein and gluten contents

were not related to cookie diameter. The protein content in flour for biscuit baking varied greatly among different flours. In the U.S., the protein content of five popular brands of self-rising flours applied in biscuit-baking varied widely, with protein contents of 6.7, 8.5, 9.4, 9.7, and 10.0%, respectively (Ma and Baik, 2018). The wide variation in the protein content of commercial self-rising flours indicates that flour protein content may not be a critical wheat characteristic for biscuit production (Ma and Baik, 2018). During the dough formation, gluten proteins in the flour are hydrated to form gluten networks. The gluten network is important in bread and other soft products, whereas it does not play a fundamental role in biscuits (Schober et al., 2003). Actually, the gluten network has to be only slightly developed to obtain a cohesive but not a very elastic dough. It is also reported that biscuits can be produced without gluten. Reasonable textural quality biscuits can be made from flours of many different types of gluten-free grains, including sorghum, pseudocereals, and legumes to meet the demand of population affected by the celiac disease (Di Cairano et al., 2020; Adedara and Taylor, 2021). So gluten may play a secondary role in the production and end-product quality of biscuit (Engleson and Atwell, 2008).

Although starch is the most abundant component of wheat grain (about 70–75%), its role in biscuit baking has not been paid enough attention. Our previous studies showed that the characteristics of starch are strongly related to biscuit quality (Zhou et al., 2018; Yang et al., 2022). The texture of biscuits does not depend on protein/starch structure, but primarily on starch gelatinization and super-cooled sugars (Thejasri et al., 2017). Adedara and Taylor (2021) reported that the increased proportion of pre-gelatinized flour starch in the dough reduced the breaking strength of biscuits. Ma and Baik (2018) reported that biscuit-specific volume exhibited positive correlations with the peak viscosity of starch. In biscuit structure, gas cells with various sizes and shapes are embedded in the matrix of gelatinized starch, fat, and sugar. The gelatinization of starch contributes to the formation of the biscuit matrix (Pauly et al., 2013).

Weak gluten wheat was less supplied because it is usually associated with low yield due to low N input. Starch addition is an effective way to produce flour with low protein and gluten content to meet the requirement for biscuit baking. However, the functionality of starch on the processing quality during biscuit making is far less understood than protein. In this work, recombined flour of different starch gradients were produced to probe and clarify the influence of different incorporation levels of starch addition on starch pasting properties, starch thermal performance, dough rheology, biscuit quality, and their inter-relationships. This work will be attempted to disclose how starch addition may regulate the properties of flour, dough, and biscuits and provide guidance for the improvement in biscuit quality.

MATERIALS AND METHODS

Materials

Three widely grown winter wheat cultivars (*Triticum aestivum* L.) in Jiangsu province and surrounding areas were taken in the present experiment. The three cultivars contain different grain protein content (GPC), such as Ningmai 13 (NM13, low GPC), Yangmai 16 (YM16, medium GPC), and Zhengmai 9023 (ZM9023, high GPC). Wheat grain was tempered to 14% moisture prior to milling for 12 h with a laboratory Miller (ZS70-II, grain and oil foodstuff machine factory, Zhuozhou, China). The flour yield was about 70%. The starch contents of NM13, YM16, and ZM9023 were 78.81, 78.30, and 77.61%, respectively.

Preparation of Flour Varied With Starch Content

Starch from flour of each cultivar of wheat was isolated with the method of Gujral et al. (2013). Briefly, wheat flour was mixed with a moderate quantity of water to form dough. The dough was washed thoroughly with 0.2 M NaCl solution. The slurry was filtrated through a sieve, followed by being centrifugation at 3,000g for 10 min. After isolation, the purified starch was freeze-dried using an Alpha 1-4 LD plus freeze dryer (Christ, Germany). The purified starch obtained from the above-mentioned process was returned to the native flour of the corresponding cultivars to obtain flour with different starch contents. For each cultivar, the additive amount of starch was set at 5, 10, 15, 20, and 25 g, respectively, to make a final amount of 100 g for each recombined flour. The samples without addition of starch were used as control (0). Three biological replicates were used for further analysis.

Contents of Protein, Gluten, Glutenin Macropolymer, and Starch Components

Flour N content was determined using the micro-Kjeldahl distillation method of AACC 46-11A (2000), and the protein content was calculated as N content multiplied by 5.7. Gluten content was determined according to AACC 38-12.02 procedure (AACC, 2000) with a gluten instrument (Perten instruments AB, Stockholm, Sweden). The GMP content was determined by the method described by Weegels et al. (1994). Briefly, 50 mg of flour sample was suspended in 1 ml of SDS (1.5%) solution and then centrifuged at 15,500 g at 20°C for 30 min. The sediment was washed twice with SDS solution (1.5%). Then the sediment was dissolved in 2 ml NaOH (0.2%) for 30 min, and the N content in the sediment was recorded as GMP content. Contents of amylose and amylopectin were determined using dual-wavelength spectrophotometric assay following the method of Zhang et al. (2010).

Solvent Retention Capacity

Solvent retention capacity tests of flour were determined according to AACC 56-11 (AACC, 2000). Briefly, SRC is the weight of solvent held by flour after centrifugation. It is expressed as a percent of flour weight. Four solvents are independently used to produce four SRC values: water SRC, 50% sucrose SRC, 5% sodium carbonate SRC, and 5% lactic acid SRC.

Pasting and Thermal Properties

Pasting properties were analyzed with a Rapid Viscosity Analyzer 130 (RVA-3D super-type, Newport Scientific, Australia) according to AACC 76-21 (2000). Thermal properties were

measured by differential scanning calorimetry 8,000 (DSC) (PerkinElmer, USA) according to the method described in our previous study (Yang et al., 2022). The gelatinization temperature (To, onset temperature; Tp, peak of gelatinization temperature; Tc, conclusion temperature) and gelatinization enthalpy (ΔH) were calculated by Pyris software.

Rheology and Texture Profile of Dough

Dough rheology was determined using Brabender Farinograph-E (Duisburg, Germany) following the method of Chinese national standards GB/T 14614-2006 (Committee, 2006). Dough texture profile (adhesiveness and cohesiveness) was determined by the texture analyzer (TA. XT2i, Stable Micro Systems, Surrey, United Kingdom) using a 25 mm Perspex cylinder probe (P/25P) with 5-kg load cell. The conditions for TPA were kept at: pre-test speed of 0.5 mm/s, test speed of 0.5 mm/s, post-test speed of 10 mm/s with a force of 40 g.

Biscuit-Making Procedure

The biscuit-baking procedure was carried out according to the Commercial Industry Standard SB/T10141-93 (China, 1993). The formula included flour (300 g, 14% moisture basis), sugar (85.5 g), maltose (13.8 g), shortening (45 g), cream(6 g), sodium chloride (0.9 g), sodium bicarbonate (0.21 g), ammonium bicarbonate (0.9 g), non-fat dry milk(13.8 g), and egg (50 g). The dough was developed using a Hobart N5 mixer (Hobart Corporation, Troy, OH, United States) and then sheeted to a thickness of 2.5–3 mm, followed by being cut using a rotary mold with 40 mm in diameter, and finally being baked at 200°C for 10 min. Biscuits were cooled for 30 min after removing from the oven and then the baking-quality-related parameters were analyzed.

Biscuit Quality Test

Width, thickness, and spread ratio of biscuit were measured according to the method of Kaur et al. (2015). Biscuit width (W) was measured by laying six biscuits edge to edge and rotating the biscuits 90° and rearranging them to get the average width. Biscuit thickness (T) was measured by stacking six biscuits on top of each other and restacking them in different orders to get the average thickness. The spread ratio (SR) was calculated as follows: SR = W/T.

The color of biscuit was determined using a Chroma Meter (CS-10, Caipu company, Hangzhou, China). Five replicates of each biscuit type were measured from five different points. The color parameters determined were L^* (0, black; 100, white), a^* (−100, green; + 100, red), and b^* (−100, blue; + 100, yellow).

Biscuit hardness was determined by a texture analyzer (TA. XT, Stable Micro Systems, Surrey, United Kingdom) using a sharping P/5 probe according to our previous method (Zhou et al., 2018).

Image analysis of the bottom side of the biscuit was carried out according to Wilderjans et al. (2008). The biscuits were placed on a flatbed scanner (Epson Perfection V30, Seiko Epson Corporation, Japan), and images of the bottom side of the biscuit were captured. The images were processed using Image J version 1.49 software (NIH, Bethesda, United States), and two features, namely, mean cell area and cell to total area ratio were selected to reflect the collapse condition of the biscuits. The bottom side cells detection was conducted on the binary images based on the Otsu thresholding algorithm (Ohtsu, 1979).

Sensory evaluation of biscuits was evaluated by a panel of ten trained judges from the laboratory according to the method of Commercial Industry Standard SB/T10141-93 (China, 1993). Biscuits were coded with different numbers and presented to the evaluator at a random order to evaluate the appearance, mouth feel, texture, crispness, and general acceptability.

Statistical Analysis

All data were subjected to one-way ANOVA using the SPSS Version 10.0. ANOVA mean comparisons were performed in terms of the least significant difference (LSD), at the significance level of $p < 0.05$. Correlation regression was analyzed using Sigmaplot 12.5. All the tests were performed with three technical repetitions.

RESULTS

Flour Protein, Glutenin Macropolymer, Wet Gluten, Damaged Starch, and Starch Components

Protein content in native flour was significantly different among the three cultivars (**Figure 1A**), and that of NM 13, YM 16, and ZM 9023 was 10.7, 11.25, and 12.2%, respectively. The addition of starch linearly decreased protein content in the recombined flour. The final protein content in the recombined flour still followed the pattern as in native flour among three cultivars. Increasing starch addition up to15%, the corresponding protein content decreased to 9.1, 9.5, and 10.4% of NM 13, YM 16, and ZM 9023, respectively. Consistent with protein, contents of gluten and GMP in the recombined flours also linearly decreased with the increase of starch addition in the three cultivars (**Figures 1B,D**), and at the same starch addition, ZM 9023 had the highest value, and NM 13 the lowest. The addition of starch linearly increased contents of damaged starch, amylose, and amylopectin in the recombined flours (**Figures 1C,E,F**).

Solvent Retention Capacity

Lactic acid SRC (LASRC) and sucrose SRC (SUCSRC) linearly decreased with the increasing starch addition in the recombined flour of the three cultivars (**Figures 1G,H**), while Na_2CO_3 SRC (SODSRC) increased with the increasing addition of starch (**Figure 1I**). The highest LASRC and SUCSRC were found in ZM9023 and the lowest in NM13. Water SRC (WSRC) first increased and then decreased with increasing starch addition (**Figure 1J**), and it reached the maximum at 15% of starch addition for NM13 and ZM9023, and at 10% of addition for YM 16.

Pasting and Thermal Properties

NM13 had the highest value of most pasting parameters, with an exception of the pasting temperature, followed by YM 16 and ZM9023 (**Table 1**). Starch addition increased the peak viscosity,

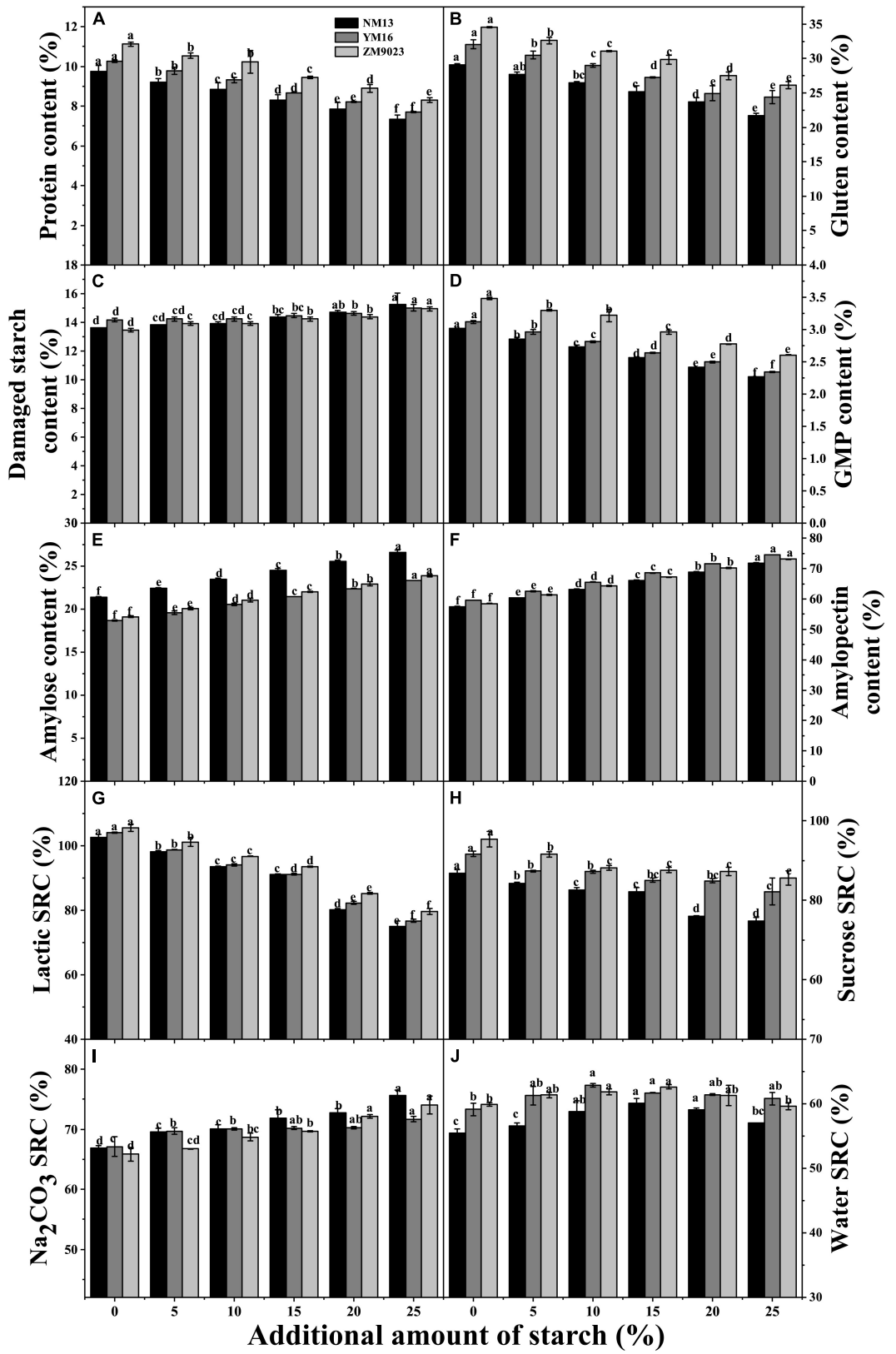

FIGURE 1 | Effects of the addition amount of starch on contents of protein **(A)**, gluten **(B)**, GMP **(D)**, damaged starch **(C)**, starch components (**E**, amylose content; **F** amylopection content) and SRC in the recombined flour (**G**, Latic SRC; **H**, Sucrose SRC; **I**, Na_2CO_3 SRC; **J**, Water SRC). NM13, YM16, and ZM9023 indicate Ningmai 13, Yangmai 16, and Zhengmai 9023, respectively.

TABLE 1 | Effect of additional amount of starch on starch component, pasting, and thermal properties of wheat.

Cultivar	Treatment	Viscosity properties							Thermal properties			
		Peak V/cP	Trough V/cP	Breakdown/cP	Final V/cP	Setback/cP	Peak time/min	Pasting T/°C	To(°C)	Tp(°C)	Tc(°C)	ΔH(J/g)
NM 13	0	3288 ± 5.65f	1803 ± 2.82f	1485 ± 2.82f	3344 ± 8.48f	1541 ± 5.65f	6.50 ± 0.04c	68.45 ± 0.00a	60.58 ± 0.29a	66.02 ± 0.11a	71.15 ± 0.21a	7.76 ± 0.31e
	5%	3432 ± 2.82e	1911 ± 7.07e	1521 ± 4.24e	3540 ± 7.07e	1629 ± 0.00e	6.60 ± 0.00b	68.38 ± 0.03a	60.59 ± 0.29a	65.84 ± 0.15b	70.99 ± 0.31ab	7.88 ± 0.06de
	10%	3552 ± 14.84d	2013 ± 5.65d	1539 ± 9.19d	3682 ± 5.65d	1669 ± 0.00d	6.60 ± 0.00b	68.10 ± 0.07b	58.38 ± 0.17b	66.00 ± 0.26a	71.20 ± 0.31a	8.23 ± 0.16d
	15%	3600 ± 9.89c	2031 ± 8.48c	1569 ± 1.41c	3730 ± 5.65c	1699 ± 2.82c	6.60 ± 0.00b	67.40 ± 0.07c	57.72 ± 0.14c	65.90 ± 0.26ab	71.13 ± 0.21a	9.51 ± 0.11c
	20%	3758 ± 5.65b	2163 ± 5.65b	1595 ± 0.00b	3870 ± 4.24b	1707 ± 1.41b	6.67 ± 0.00a	67.43 ± 0.03c	56.10 ± 0.25d	66.01 ± 0.15a	70.76 ± 0.39b	10.32 ± 0.39b
	25%	3926 ± 4.94a	2256 ± 6.36a	1670 ± 1.41a	3969 ± 3.53a	1713 ± 2.82a	6.66 ± 0.00a	66.40 ± 0.00d	55.12 ± 0.16e	66.00 ± 0.15a	71.13 ± 0.23a	11.09 ± 0.34a
YM 16	0	3019 ± 3.53f	1688 ± 9.19f	1331 ± 5.65f	3038 ± 7.77f	1350 ± 1.41d	6.27 ± 0.00c	68.90 ± 0.07a	61.55 ± 0.35a	66.00 ± 0.21a	70.31 ± 0.28a	6.59 ± 0.27f
	5%	3131 ± 2.82e	1721 ± 9.89e	1410 ± 7.07e	3101 ± 2.12e	1380 ± 12.02d	6.33 ± 0.00b	68.75 ± 0.07b	61.33 ± 0.31a	65.79 ± 0.11a	70.67 ± 0.37a	7.09 ± 0.34e
	10%	3248 ± 6.36d	1779 ± 7.77d	1469 ± 1.41d	3240 ± 3.53d	1461 ± 4.24c	6.33 ± 0.00b	68.18 ± 0.03c	59.88 ± 0.36b	65.80 ± 0.15a	70.46 ± 0.12a	8.09 ± 0.16d
	15%	3351 ± 7.77c	1843 ± 18.38c	1508 ± 10.61c	3339 ± 4.24c	1496 ± 22.62bc	6.33 ± 0.00b	68.15 ± 0.00cd	58.80 ± 0.25c	65.17 ± 0.14b	70.26 ± 0.01a	9.21 ± 0.39c
	20%	3411 ± 7.07b	1887 ± 14.14b	1524 ± 7.07b	3416 ± 7.77b	1529 ± 21.92b	6.46 ± 0.01a	68.10 ± 0.07cd	57.50 ± 0.38d	66.00 ± 0.18a	70.66 ± 0.34a	10.09 ± 0.11b
	25%	3470 ± 4.24a	1915 ± 8.48a	1555 ± 4.24a	3520 ± 16.26a	1605 ± 24.74a	6.47 ± 0.00a	68.03 ± 0.02d	56.00 ± 0.34e	65.20 ± 0.22b	70.82 ± 0.34a	10.89 ± 0.34a
ZM 9023	0	2040 ± 6.33f	1238 ± 9.19e	802 ± 2.82e	2409 ± 4.24f	1170 ± 4.94f	6.07 ± 0.00d	68.75 ± 0.00bc	63.50 ± 0.21a	65.33 ± 0.29a	69.87 ± 0.31a	5.55 ± 0.11e
	5%	2088 ± 9.19e	1239 ± 5.65e	849 ± 3.53d	2425 ± 9.19e	1186 ± 3.53e	6.20 ± 0.00c	69.22 ± 0.67ab	63.33 ± 0.47a	65.32 ± 0.34a	69.80 ± 0.31a	5.61 ± 0.26e
	10%	2162 ± 2.82d	1285 ± 4.24d	877 ± 1.41c	2486 ± 6.36d	1201 ± 2.12d	6.23 ± 0.04c	68.55 ± 0.21bc	62.33 ± 0.45b	64.96 ± 0.31a	70.00 ± 0.41a	7.32 ± 0.28d
	15%	2217 ± 8.48c	1320 ± 4.24c	897 ± 4.24b	2538 ± 3.53c	1218 ± 0.71c	6.30 ± 0.04b	69.68 ± 0.03a	60.50 ± 0.68c	65.00 ± 0.23a	69.80 ± 0.52a	8.16 ± 0.19c
	20%	2339 ± 7.77b	1403 ± 8.48b	936 ± 0.71a	2639 ± 9.89b	1236 ± 1.41b	6.40 ± 0.00a	68.32 ± 0.03c	60.23 ± 0.23c	65.29 ± 0.53a	70.02 ± 0.43a	9.08 ± 0.15b
	25%	2373 ± 7.77a	1430 ± 4.94a	944 ± 2.82a	2705 ± 7.77a	1276 ± 2.82a	6.40 ± 0.00a	66.47 ± 0.03d	58.90 ± 0.21d	65.30 ± 0.29a	69.88 ± 0.29a	10.00 ± 0.33a

NM13, YM16, and ZM9023 indicate Ningmai 13, Yangmai 16 and Zhengmai 9023, respectively. Peak V means peak viscosity, Trough V means trough viscosity, Final V means final viscosity, Pasting T means pasting temperature, To, Tp, Tc, and ΔH represent the onset temperature, peak temperature, conclusion temperature, and enthalpy, Softening D means softening degree, FQN means Farinograph quality number. Data are means of three replicates. Different small letters in the same column with the same cultivar are significantly different at the 0.05 probability level.

TABLE 2 | Effect of additional amount of starch on dough rheology of wheat.

Cultivar	Treatment	Farinograph properties				Dough texture properties	
		Stability time/min	Softening D/FU	FQN	Absorption/%	Cohesiveness (g)	Adhesiveness (g·sec)
NM13	0	3.00 ± 0.14a	77.5 ± 6.36d	39.5 ± 2.12a	0.632 ± 0.00d	31.94 ± 0.58a	5.01 ± 0.09a
	5%	2.75 ± 0.07b	89.5 ± 3.53d	35.5 ± 0.71b	0.644 ± 0.00c	30.26 ± 0.52b	4.79 ± 0.18a
	10%	2.65 ± 0.07bc	106 ± 1.41c	32.0 ± 1.41c	0.645 ± 0.00bc	29.45 ± 0.91bc	4.06 ± 0.18b
	15%	2.45 ± 0.07cd	118 ± 2.82c	27.5 ± 0.71d	0.6465 ± 0.00abc	28.67 ± 0.97c	4.12 ± 0.26b
	20%	2.30 ± 0.14de	132 ± 4.24b	24.5 ± 0.71e	0.647 ± 0.00ab	26.34 ± 0.32d	3.9 ± 0.11bc
	25%	2.20 ± 0.14e	149 ± 5.65a	21.0 ± 1.41f	0.6485 ± 0.00a	26.02 ± 2.41d	3.77 ± 0.23c
YM16	0	4.80 ± 0.14a	54.0 ± 4.24f	58.5 ± 2.12a	0.634 ± 0.00c	35.14 ± 0.61a	6.01 ± 0.07a
	5%	4.55 ± 0.07a	67.0 ± 2.82e	50.5 ± 0.71b	0.648 ± 0.00ab	33.66 ± 0.34b	5.52 ± 0.14b
	10%	4.25 ± 0.07b	84.0 ± 4.24d	45.0 ± 1.41c	0.6495 ± 0.00a	31.04 ± 0.75c	4.98 ± 0.17c
	15%	3.95 ± 0.07c	100 ± 1.41c	39.5 ± 2.12d	0.645 ± 0.00b	29.83 ± 0.53d	4.22 ± 0.29d
	20%	3.75 ± 0.07cd	110 ± 2.12b	35.5 ± 2.12de	0.647 ± 0.00ab	28.4 ± 0.73e	4.05 ± 0.23de
	25%	3.60 ± 0.14d	120 ± 2.12a	31.5 ± 2.12e	0.645 ± 0.00b	28.02 ± 0.38e	3.98 ± 0.11e
ZM9023	0	8.40 ± 0.42a	26.5 ± 2.12f	106 ± 0.00a	0.645 ± 0.00a	40.63 ± 0.37a	7.64 ± 0.09a
	5%	8.15 ± 0.21ab	33.5 ± 0.71e	99.5 ± 0.71b	0.649 ± 0.00a	38.58 ± 0.43b	7.08 ± 0.18b
	10%	8.00 ± 0.14ab	41.5 ± 0.71d	94.0 ± 1.41c	0.6485 ± 0.00a	36.39 ± 0.31c	6.46 ± 0.06c
	15%	7.60 ± 0.14bc	46.5 ± 0.71c	89.5 ± 0.71c	0.6485 ± 0.00a	34.59 ± 0.26d	5.64 ± 0.12d
	20%	7.25 ± 0.07cd	51.5 ± 2.12b	80.5 ± 2.12d	0.6485 ± 0.00a	33.49 ± 0.31e	5.26 ± 0.19e
	25%	6.85 ± 0.35d	57.5 ± 2.12a	76.0 ± 2.82d	0.648 ± 0.00a	32.93 ± 0.39f	5.03 ± 0.15f

NM13, YM16, and ZM9023 indicate Ningmai 13, Yangmai 16 and Zhengmai 9023, respectively. Softening D means softening degree, FQN means Farinograph quality number. Data are means of three replicates. Different small letters in the same column with the same cultivar are significantly different at the 0.05 probability level.

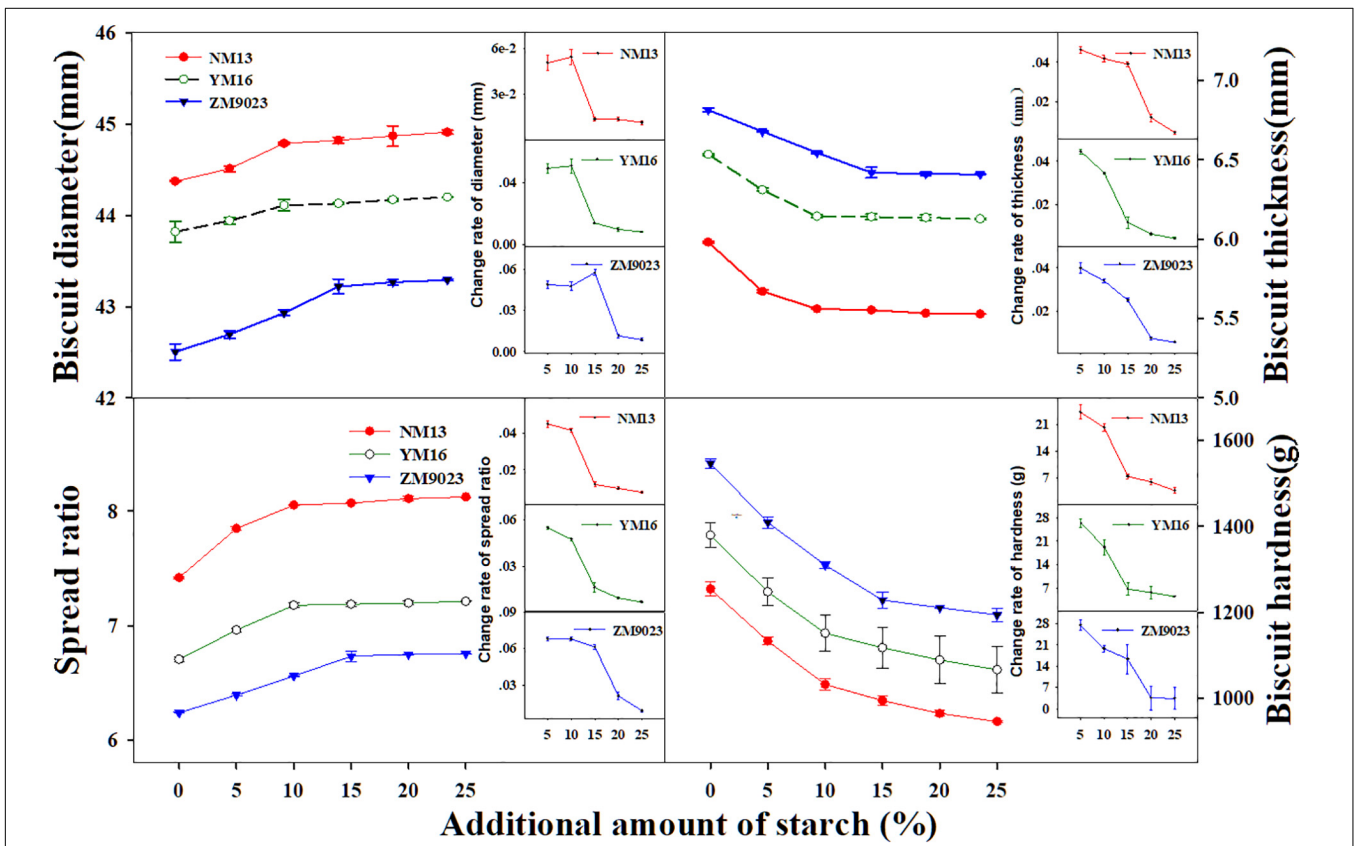

FIGURE 2 | Effect of the addition amount of starch on diameter, thickness, spread ratio, and hardness of short biscuits. NM13, YM16, and ZM9023 indicate Ningmai 13, Yangmai 16 and Zhengmai 9023, respectively. Small figures in the corner of big Figs are rate of change of biscuit traits.

TABLE 3 | Effect of additional amount of starch on the sensory evaluation, colors, and cracks on the biscuit.

Cultivar	Treatment	Sensory evaluation							Biscuit colors			IABSB	
		Appearance	Clearness	Gumminess	Crispness	Mouth feel	Texture	Total score	L*	a*	b*	CA (mm2)	RCA(%)
NM13	0	9.67 ± 0.06c	10.00 ± 0.00a	9.67 ± 0.14c	43.5 ± 0.86b	8.83 ± 0.28c	10.00 ± 0.00a	91.66 ± 0.84c	65.6 ± 0.24d	5.68 ± 1.21a	28.08 ± 1.61a	0.50 ± 0.01c	52.05 ± 1.19a
	5%	9.73 ± 0.06bc	10.00 ± 0.00a	9.75 ± 0.00bc	44.0 ± 0.86ab	9.00 ± 0.00c	10.00 ± 0.00a	92.48 ± 0.89b	66.22 ± 0.19d	4.46 ± 1.56a	25.31 ± 0.12ab	0.51 ± 0.01bc	51.64 ± 0.96ab
	10%	9.97 ± 0.06a	10.00 ± 0.00a	9.83 ± 0.14abc	44.6 ± 0.287a	9.67 ± 0.28b	10.00 ± 0.00a	94.13 ± 0.34a	68.99 ± 1.73c	3.67 ± 0.16a	25.25 ± 2.78ab	0.50 ± 0.02c	50.74 ± 0.46abc
	15%	9.87 ± 0.15ab	10.00 ± 0.00a	9.83 ± 0.14abc	44.8 ± 0.283a	10.00 ± 0.00a	10.00 ± 0.00a	94.53 ± 0.11a	71.15 ± 0.01b	3.66 ± 0.13a	24.12 ± 0.55ab	0.55 ± 0.02a	48.67 ± 2.22c
	20%	9.77 ± 0.06bc	10.00 ± 0.00a	9.92 ± 0.14ab	44.8 ± 0.283a	10.00 ± 0.00a	10.00 ± 0.00a	94.51 ± 0.25a	71.32 ± 0.05b	3.45 ± 0.19a	24.52 ± 0.58ab	0.55 ± 0.02ab	49.44 ± 1.21bc
	25%	9.67 ± 0.06c	10.00 ± 0.00a	10.00 ± 0.00a	44.8 ± 0.283a	10.00 ± 0.00a	10.00 ± 0.00a	94.5 ± 0.26a	74.19 ± 0.09a	3.42 ± 0.52a	22.28 ± 1.58b	0.54 ± 0.02abc	48.95 ± 0.95c
YM16	0	9.63 ± 0.06b	10.00 ± 0.00a	9.58 ± 0.14c	43.0 ± 0.00b	8.67 ± 0.28d	10.00 ± 0.00a	90.88 ± 0.21d	69.71 ± 0.21d	4.88 ± 0.78a	25.59 ± 0.94a	0.46 ± 0.00c	56.6 ± 4.72a
	5%	9.73 ± 0.06ab	10.00 ± 0.00a	9.67 ± 0.14bc	43.5 ± 0.86b	9.00 ± 0.00c	10.00 ± 0.00a	91.9 ± 0.77c	70.02 ± 0.14d	4.67 ± 0.11a	24.61 ± 0.71ab	0.46 ± 0.02c	56.48 ± 0.68a
	10%	9.83 ± 0.06a	10.00 ± 0.00a	9.83 ± 0.14ab	44.5 ± 0.00a	9.50 ± 0.00b	10.00 ± 0.00a	93.66 ± 0.21b	72.56 ± 0.02c	4.44 ± 0.55ab	24.27 ± 0.35bc	0.48 ± 0.02c	53.57 ± 0.93a
	15%	9.77 ± 0.11a	10.00 ± 0.00a	9.92 ± 0.14a	44.6 ± 0.287a	9.83 ± 0.28a	10.00 ± 0.00a	94.18 ± 0.02ab	72.86 ± 0.47c	3.99 ± 0.13ab	23.73 ± 1.08bc	0.55 ± 0.01b	52.05 ± 0.46a
	20%	9.73 ± 0.06ab	10.00 ± 0.00a	9.92 ± 0.14a	44.8 ± 0.283a	10.00 ± 0.00a	10.00 ± 0.00a	94.48 ± 0.25a	74.42 ± 0.45b	3.42 ± 0.46ab	23.43 ± 0.81c	0.58 ± 0.01a	54.96 ± 4.14a
	25%	9.63 ± 0.06b	10.00 ± 0.00a	10.00 ± 0.00a	44.8 ± 0.283a	10.00 ± 0.00a	10.00 ± 0.00a	94.46 ± 0.23a	76.7 ± 0.38a	3.16 ± 0.96b	22.4 ± 1.41d	0.57 ± 0.00ab	53.24 ± 1.68a
ZM9023	0	9.6 ± 0.00c	10.00 ± 0.00a	9.5 ± 0.00d	43.0 ± 0.00b	8.67 ± 0.28c	10.00 ± 0.00a	90.76 ± 0.28d	71.25 ± 0.25a	5.93 ± 3.69a	26.67 ± 0.79a	0.45 ± 0.00c	58.34 ± 0.64a
	5%	9.67 ± 0.06bc	10.00 ± 0.00a	9.67 ± 0.14cd	43.5 ± 0.86ab	8.83 ± 0.28bc	10.00 ± 0.00a	91.66 ± 0.71c	71.91 ± 0.77de	5.97 ± 4.07a	26.07 ± 0.85a	0.46 ± 0.01c	56.87 ± 0.76ab
	10%	9.73 ± 0.06ab	10.00 ± 0.00a	9.75 ± 0.00bc	43.5 ± 0.86ab	9.33 ± 0.57b	10.00 ± 0.00a	92.31 ± 0.71b	72.53 ± 0.01cd	3.03 ± 0.77ab	23.38 ± 0.02b	0.48 ± 0.01b	56.95 ± 0.85ab
	15%	9.8 ± 0.00a	10.00 ± 0.00a	9.83 ± 0.14abc	44.5 ± 0.00a	10.00 ± 0.00a	10.00 ± 0.00a	94.13 ± 0.14a	73.43 ± 0.43bc	3.03 ± 0.77ab	23.38 ± 0.02b	0.51 ± 0.01a	57.04 ± 1.47ab
	20%	9.77 ± 0.06a	10.00 ± 0.00a	9.92 ± 0.14ab	44.5 ± 0.00a	10.00 ± 0.00a	10.00 ± 0.00a	94.18 ± 0.12a	74.43 ± 0.43b	1.55 ± 0.15ab	22.49 ± 0.64b	0.51 ± 0.02a	54.58 ± 2.14bc
	25%	9.63 ± 0.06c	10.00 ± 0.00a	10.00 ± 0.00a	44.5 ± 0.00a	10.00 ± 0.00a	10.00 ± 0.00a	94.13 ± 0.05a	76.49 ± 0.29a	0.77 ± 0.17b	20.89 ± 0.06c	0.51 ± 0.01a	53.01 ± 0.44c

NM13, YM16, and ZM9023 indicate Ningmai 13, Yangmai 16 and Zhengmai 9023, respectively. IABSB means image analysis of bottom side of biscuit, CA is mean cell area, RCA is ratio of cell to total area. Data are means of three replicates. Different small letters in the same column with the same cultivar are significantly different at the 0.05 probability level.

trough viscosity, breakdown, final viscosity, and setback and peak time of the three cultivars. As compared with native flour, the peak viscosity of the recombined flour with 25% starch addition increased by 19.4, 14.9, and 16.3% for NM13, YM16, and ZM9023, respectively. In addition, increasing starch addition decreased pasting temperature in NM 13, while it showed little effect on YM16 and ZM9023.

NM13 had the highest value of Tp, Tc, and ΔH, followed by YM16 and ZM9023, while ZM9023 had the highest To value (**Table 1**). Starch addition decreased the value of To and increased the value of ΔH of the three cultivars, while it had little effect on the value of Tp and Tc. As compared with native flour, the To value of the recombined flour with 25% starch addition decreased by 9.01, 9.02, and 7.24%, respectively while the ΔH of the recombined flour increased by 42.91, 65.25, and 32.46%, respectively.

Dough Rheology and Texture Profile

The addition of starch dramatically decreased dough development time, stability time, farinograph quality number (FQN), cohesiveness, and adhesiveness, while it increased softening degree in all the three cultivars (**Table 2**). However, starch addition had no significant influence on water absorption in ZM9023, while it slightly increased in NM13 and YM16 when starch addition was less than 15%. ZM9023 had the highest values of dough development time, stability time, FQN, cohesiveness, and adhesiveness, and the lowest softening degree among the three cultivars (**Table 2**). It was contrary for NM13 when compared to ZM9023.

Biscuit Properties

The lowest protein content cultivar, NM 13, showed the largest biscuit diameter and spread ratio, while the highest protein content cultivar ZM9023 showed the lowest biscuit diameter and spread ratio (**Figure 2**). Biscuit thickness and hardness showed opposite patterns to diameter and spread ratio among the three cultivars. The starch addition increased biscuit diameter and spread ratio, while it decreased biscuit thickness and hardness. Biscuit diameter and spread ratio increased very fast with starch addition at a rate lower than 10% for NM 13 and YM 16, 15% for ZM 9023, and with further starch addition the increase rate leveled off (**Figure 2**). Similarly, biscuit thickness and hardness decreased rapidly at a starch addition rate lower than 10% for NM 13 and YM 16, and 15% for ZM9023 (**Figure 2**). The turning point of the change rate of diameter, spread ratio, thickness, and hardness was at 10% of starch addition for NM 13 and YM 16, and 15% for ZM 9023, the corresponding protein content was 9.70, 10.22, and 10.37%.

The lightness (L*) of biscuit and dough was the lowest for NM13 and the highest for ZM9023 (**Table 3**). The addition of starch gradually increased the values of L* of biscuit along with the addition amount for all cultivars, whereas it decreased the redness (a*) and yellowness (b*) of the biscuit and the dough. With too much starch addition, the short biscuits were light in color and undesirable. Starch addition increased scores of biscuit appearance, which reached a maximum at the starch addition rate of ca. 10–15% (**Table 3**). But there were some cracks that

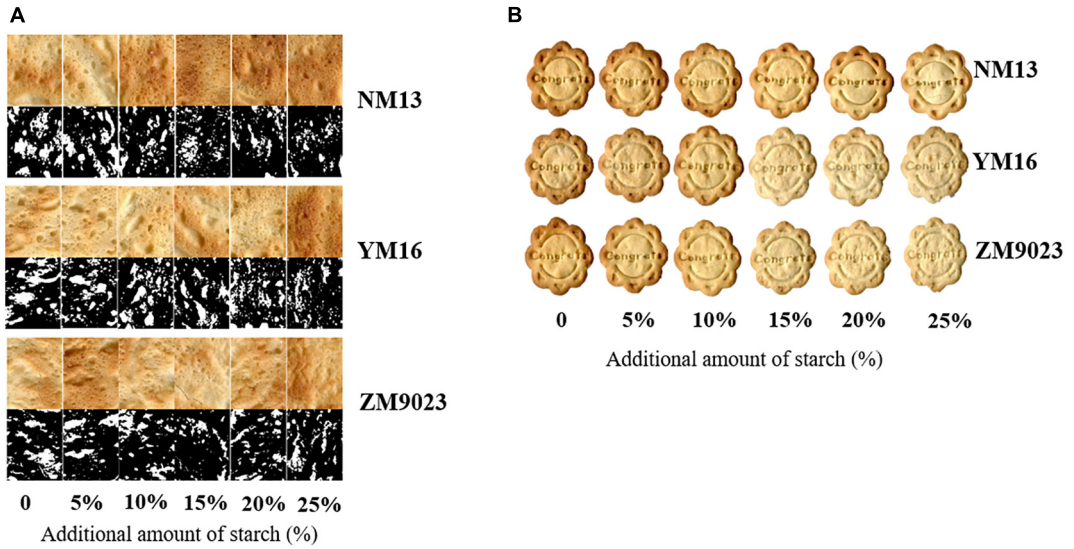

FIGURE 3 | Appearance of short biscuits **(A)** and image of the bottom side of biscuit **(B)**. NM13, YM16, and ZM9023 indicate Ningmai 13, Yangmai 16, and Zhengmai 9023, respectively. In left figure **(B)**, the first, third and fifth lines were view of bottom side of biscuit, and second, fourth and sixth lines were binary images of biscuit.

appeared in the biscuit when starch addition amount exceeded 10% for NM13 and YM16, and 15% for ZM9023. The sensory evaluation score increased faster at starch addition from 0 to 10% than from 15 to 25%.

Image analysis of the biscuits indicated the effect of starch on texture and appearance (**Figure 3**). The mean cell area increased first and reached the maximum at 20% starch addition and then decreased (**Table 3**). The ratio of cell to total area showed a decreased trend with the addition of starch in three cultivars. Crumbs of biscuit baked with higher starch content had larger pores but with a lower ratio of cell to total area in the bottom side.

Relationship of Biscuit Quality With SRC, Pasting, and Thermal Properties and Dough Rheology

Sucrose SRC was significantly negatively correlated with peak viscosity, trough viscosity, breakdown, final viscosity, setback, peak time, Tc and ΔH, while positively with To and pasting temperature (**Table 4**, r = −0.775, −0.83, −0.705, −0.832, −0.823, −0.898, −0.661, −0.845, 0.911, 0.713, respectively, $p \leq 0.01$). SODSRC was significantly positively related with final viscosity, setback, peak T, and ΔH, while negatively with To and pasting temperature (r = 0.504, 0.475, 0.657, 0.8838, −0.817, −0.817, respectively, $p \leq 0.05$). Consistent with SUCSRC, dough stability time, FQN, cohesiveness, and adhesiveness were significantly negatively correlated with peak viscosity, trough viscosity, breakdown, final viscosity, setback, and peak time, while positively with pasting temperature (**Table 4**, $p \leq 0.01$). The softening degree was on the contrary to stability time and FQN.

Hardness and thickness of biscuit significantly positively correlated with flour protein, gluten, GMP, and SUCSRC, but negatively related with amylopectin and SODSRC (**Table 5**). Diameter, spread ratio, and sensory scores of biscuit showed significantly negative correlation with protein, gluten GMP, SUCSRC, and WSRC, but a positive relation with amylopectin and SODSRC. There was no significant correlation between LASRC and thickness, diameter and spread ratio of biscuit.

Pasting and thermal properties were closely associated with biscuit quality. Peak viscosity, trough viscosity, breakdown, final viscosity, setback, peak time, Tp, Tc, and ΔH were significantly positively correlated to diameter, spread ratio, and sensory score of biscuit, but negatively correlated to hardness and thickness of the biscuit (**Table 5**). As for dough rheological and texture properties, stability time, FQN, cohesiveness, and adhesiveness showed strong significant positive correlation with the hardness and thickness of biscuit, and negative with diameter and spread ratio ($p < 0.01$). Water absorption had no relation with hardness, thickness, diameter, and spread ratio.

Protein content was closely related to biscuit sensory score (**Figure 4**). There was a quadratic non-linear relationship between protein content and appearance score. When the appearance score reached the highest value, the corresponding protein content was about 9%. Protein content was negatively correlated with the scores of gumminess, clearness of patter, and mouthfeel of biscuit.

DISCUSSION

Wheat flour with low content of protein and gluten is believed to be an ideal material for biscuits, cookies, and other baking foods (Manley, 2011). Starch is widely applied in food industry due to its unique chemical characteristics of gelling, thickening, and stabilization (Gerits et al., 2015), which provides the possibility to produce flour for biscuit baking by starch addition. In the

TABLE 4 | Linear correlation coefficients between SRC, farinograph, dough texture profile, pasting, and thermal properties.

	Peak V	Trough V	Breakdown	Final V	Setback	Peak T	Pasting T	To	Tp	Tc	ΔH
WSRC	−0.439	−0.4645	−0.406	−0.483*	−0.507*	−0.563*	0.359	0.201	−0.586*	−0.619**	−0.101
SUCSRC	−0.775**	−0.830**	−0.705**	−0.832**	−0.823**	−0.898**	0.713**	0.911**	−0.400	−0.661**	−0.845**
SODSRC	0.448	0.516*	0.370	0.504*	0.475*	0.657**	-0.817**	-0.817**	0.106	0.286	0.884**
LASRC	−0.408	−0.466	−0.341	−0.457	−0.437	−0.574*	0.728**	0.869**	−0.009	−0.216	−0.941**
Stability time	−0.987**	−0.977**	−0.982**	−0.981**	−0.973**	−0.848**	0.480*	0.723**	−0.766**	−0.933**	−0.553*
Softening D	0.934**	0.956**	0.896**	0.957**	0.945**	0.857**	−0.648**	−0.926**	0.553*	0.801**	0.798**
FQN	−0.991**	−0.980**	−0.987**	−0.979**	−0.964**	−0.845**	0.525*	0.796**	−0.703**	−0.896**	−0.652**
Absorption	−0.193	−0.146	−0.2393	−0.148	−0.149	−0.041	−0.186	−0.151	−0.389	−0.307	0.235
Cohesiveness	−0.901**	−0.918**	−0.869**	−0.919**	−0.907**	−0.894**	0.640**	0.937**	−0.510*	−0.756**	−0.865**
Adhesiveness	−0.859**	−0.871**	−0.832**	−0.873**	−0.865**	−0.871**	0.623**	0.924**	−0.455	−0.722**	−0.874**

*Peak V means peak viscosity, Trough V means Trough viscosity, Peak T means Peak Time, Pasting T means Pasting temperature, To, Tp, Tc, and ΔH represent the onset temperature, peak temperature, conclusion temperature, and enthalpy; WSRC means water SRC, SUCSRC means sucrose SRC, LASRC means Lactic acid SRC, SODSRC means Na_2CO_3 SRC, Softening D means softening degree, FQN means Farinograph. * and ** indicate significance at the levels of 0.05 and 0.01, respectively.*

TABLE 5 | Linear correlation coefficients between mixed flour characteristics and quality attributes of baking biscuit.

	Quality traits	Hardness	Thickness	Diameter	Spread ratio	Sensory scores
Flour	Protein	0.924**	0.711**	−0.702**	−0.701**	-0.889**
	Gluten	0.938**	0.775**	−0.764**	−0.766**	-0.842**
	GMP	0.927**	0.713**	−0.737**	−0.707**	-0.869**
	Amylopectin	−0.855**	−0.755**	0.612**	0.739**	0.814**
	Amylose	−0.607**	−0.200	0.193	0.183	0.849**
SRC	WSRC	0.189	0.517*	−0.484*	−0.528*	0.190
	SUSRC	0.942**	0.869**	−0.811**	−0.863**	-0.747**
	SODSRC	−0.793**	−0.554*	0.489*	0.540*	0.826**
	LASRC	0.746**	0.435	−0.400	−0.42	-0.857**
Pasting	Peak V	−0.8137**	−0.8772**	0.975**	0.893**	0.446
Properties	Trough V	−0.8468**	−0.9089**	0.9775**	0.9241**	0.4910*
	Breakdown	−0.7662**	−0.8300**	0.9558**	0.8461**	0.393
	Final V	−0.8538**	−0.9288**	0.9812**	0.9417**	0.4981*
	Setback	−0.8530**	−0.9477**	0.9729**	0.9567**	0.5029*
	Peak T	−0.8957**	−0.9514**	0.8969**	0.9451**	0.6165**
	Pasting T	0.6501**	0.5643*	−0.5136*	−0.5632*	-0.5623*
Thermal	To	0.9207**	0.7520**	−0.7702**	−0.7517**	-0.8324**
Properties	Tp	−0.4089	−0.6426**	0.7367**	0.6702**	0.0022
	Tc	−0.6891**	−0.8718**	0.9165**	0.8830**	0.2685
	ΔH	−0.8638**	−0.6122**	0.6110**	0.5993**	0.8836**
Farinographic	Stability time	0.7894**	0.8998**	−0.9855**	-0.9132**	-0.3981
Properties	Softening D	−0.9219**	−0.8827**	0.9124**	0.8896**	0.6746**
	FQN	0.8431**	0.8789**	−0.9780**	-0.8897**	-0.4998*
	Absorption	−0.2309	0.0231	−0.1929	-0.0484	0.4927*
Dough texture properties	Cohesiveness	0.9661**	0.8766**	−0.9113**	-0.8738**	-0.7619**
	Adhesiveness	0.9593**	0.8420**	−0.8835**	−0.8356**	−0.8031**

*WSRC means water SRC, SUCSRC means sucrose SRC, LASRC means Lactic acid SRC, SODSRC means Na_2CO_3 SRC, Peak V means peak viscosity, Trough V means Trough viscosity, Peak T means Peak Time, Pasting T means Pasting temperature, To, Tp, Tc, and ΔH represent the onset temperature, peak temperature, conclusion temperature, and enthalpy, Softening D means softening degree, FQN means Farinograph quality number. * and ** indicate significance at the levels of 0.05 and 0.01, respectively.*

present study, we add starch to flours of different wheat cultivars differing in grain protein content to produce recombined flour. We observed that the addition of starch improved biscuit-baking quality, as exemplified with the improved diameter and spread ratio of biscuit, and with reduced biscuit thickness and hardness due to the increased addition of starch (**Figure 3**).

Protein and gluten contents are important factors affecting biscuit-baking quality. Gluten is an essential structure-building protein, which is hydrated to form gluten networks providing viscoelasticity of dough (Lindsay and Skerritt, 1999). Dough development time and stability time are indicators of dough strength, and longer development time and stability time

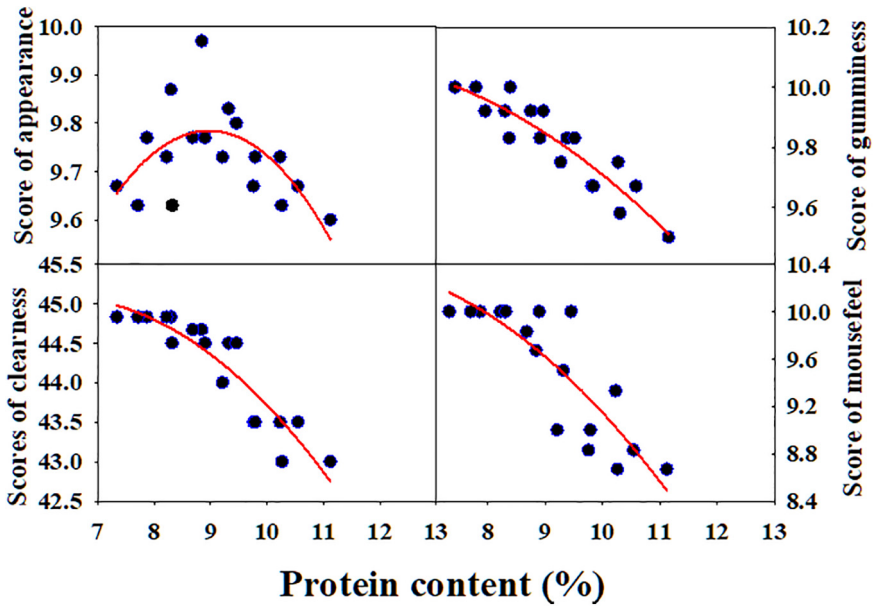

FIGURE 4 | Correlation of protein content with sensory scores of short biscuit. NM13, YM16, and ZM9023 indicate Ningmai 13, Yangmai 16, and Zhengmai 9023, respectively.

indicates better viscoelastic properties (Panghal et al., 2019). Plenty of gluten networks are necessary for bread making, but it is undesired for biscuit making since gluten network tends to increase biscuit hardness. Protein level, especially when exceeds 10 g/100 g, profoundly affects biscuit hardness and dimensions (Pauly et al., 2013). Our results also showed that protein content was positively related to hardness and thickness of biscuit, which was agreed with other reports (Pauly et al., 2013; Ma and Baik, 2018). Here, contents of protein, gluten and GMP, dough stability time, cohesiveness, and adhesiveness declined rapidly with increasing starch addition (**Figure 1** and **Table 2**). The decrease in protein content and dough strength should be related to the filling of starch granules, resulting in poor gluten network. At an addition rate of 10%, contents of protein of NM13 in the recombined flour of the three cultivars decreased to 9.7%, which may well fit the requirement for biscuit making.

A good quality biscuit is expected to have both a desirable appearance and a tender crumb texture (Ma and Baik, 2018). Our study showed that protein content is quadratic non-linearly related with the appearance of the biscuit (**Figure 4**). Although less gluten network formation is required in biscuit baking, gluten formation is still very critical in influencing the volume, texture, and appearance of the final baking product. Lack of gluten often gives biscuits of lower quality, both in terms of technological properties and sensory quality (Di Cairano et al., 2018). Here, when starch addition higher than 10 to 15% it caused some cracks on the biscuit surface, which decreased the scores of the appearance of the biscuit. Ma and Baik (2018) evaluated quality characteristics of 15 soft wheat varieties in United States and found that protein content of 7.9–9.7% was suitable for making desirable quality biscuits (Ma and Baik, 2018).

Since gluten free biscuit can be produced, starch may play a more important role in biscuit baking. Viscosity indicates the propensity of starch to gelation, and high starch content in wheat flour is responsible for high peak and final viscosity (Panghal et al., 2019). Starch gelatinization contributes to the biscuit matrix formation (Pauly et al., 2013). Our study showed that most starch pasting and thermal parameters (except for pasting temperature) were positively related to diameter, spread ratio, and sensory scores of biscuit, while negatively related with hardness and thickness of biscuit (**Table 5**). The starch weak network is formed after the swelling of granules and leaching of starch chains during heat treatment. The short-dough biscuit can be described as a matrix of starch in which gas bubbles of various sizes and shapes were incorporated (Baldino et al., 2014; Sozer et al., 2014). Good biscuits facilitate expansion with a weak functional network formation (Laguna et al., 2011). A firm crumb is an undesirable quality for biscuits (Ma and Baik, 2018). Crumbs of biscuit baked with higher starch content had larger pores, but a lower ratio of cell to total area in the bottom side (**Table 3**), which might be related to three-dimensional honeycomb network of starch gel after heating (Hedayati and Niakousari, 2018). Starch addition can improve the pasting of starch and inner fill of starch granule in the gluten network. The enlargement of pores may be beneficial to reduce density and improve the crispness of the biscuit.

Solvent retention capacity can provide useful information for predicting the quality of soft wheat products (Kaur et al., 2014). LASRC is associated with glutenin characteristics, SODSRC is related to levels of damaged starch, SUCSRC is associated with pentosan and gliadin characteristics, and WSRC is influenced by all the flour constituents (Zhang et al., 2018). Here, WSRC, SSRC, and LASRC were negatively correlated to biscuit diameter,

spread ratio, and sensory scores. Reversely, SODSRC was positively correlated to biscuit diameter, spread ratio, and sensory scores. Moiraghi et al. (2011) reported a significant negative correlation between SUCSRC/WSRC and spread ratio, which is consistent with our results. Peak viscosity, trough viscosity, breakdown, final viscosity, and setback were significantly negatively correlated with SUCSRC, which might suggest that the presence of gliadin and pentosan caused interference to the swelling and rupture of the starch granule. Final viscosity and setback were significantly positively related with SODSRC, which might be due to the damaged starch granules that tend to be easier to gelatinize. It also showed that sucrose and Na_2CO_3 SRC were more important than water and lactic acid SRC in determining biscuit quality.

Meanwhile, the increased rate of diameter and spread and the decreased rate of hardness and thickness vs. starch addition amount showed a turning point at 10% starch addition for NM 13 and YM 16, and at 15% for ZM 9023 (**Figure 2**). At the turning point, the flour protein content of NM13, YM16, and ZM9023 were 8.84, 9.32, and 9.46%, respectively. Thinking about appearance scores, therefore, a criterion of flour protein content around 9% was recommended for baking high quality short biscuits.

CONCLUSION

Weak gluten wheat (with low protein and gluten) is in short supply because of low yield due to low N input. Starch addition is an effective way to produce flour with low protein and gluten content to meet the requirements of biscuit industry. Starch addition decreased the contents of protein, gluten and GMP, lactic acid SRC, sucrose SRC, and onset temperature (To), while it increased most pasting parameters and gelatinization enthalpy (ΔH). Viscosity parameters were significantly negatively correlated with dough stability time, farinograph quality number (FQN), and sucrose SRC. Biscuit quality was greatly improved by the addition of starch, as shown by higher diameter, spread ratio, and sensory score of biscuit, but lower thickness and hardness. Starch gelatinization can contribute to biscuit matrix. Viscosity parameters were negatively correlated to hardness and thickness of biscuit, but positively correlated to diameter, spread ratio, and sensory score of biscuit. Considering the effects of starch addition on the dough rheology and biscuit quality, the recombined flour with around 9% protein content after mixing with starch was more suitable for biscuit baking. The interaction between starch and protein during baking needs further investigation. This study provides guidance for the application of wheat starch in the development of high quality biscuit and discloses how starch addition may regulate the properties of flour and the inter-relationships of flour, dough, and biscuit.

DATA AVAILABILITY STATEMENT

The original contributions presented in the study are included in the article/supplementary material, further inquiries can be directed to the corresponding author/s.

AUTHOR CONTRIBUTIONS

LL analyzed the dataset and prepared the first draft. TY and JY critically reviewed the manuscript. QZ and DJ conceived the project idea. MH and JC helped the isolation of starch. WC and TD reviewed the manuscript. All authors contributed to the article and approved the submitted version.

FUNDING

This work was supported by National Natural Science Foundation of China (32030076, 32172116, and 31901458), the China Agriculture Research System (CARS-03), Collaborative Innovation Center for Modern Crop Production co-sponsored by Province and Ministry (CIC-MCP).

REFERENCES

AACC (2000). *Approved Methods of the AACC*, 10 Edn. MN, USA: St. Paul.

Adedara, O. A., and Taylor, J. R. N. (2021). Roles of protein, starch and sugar in the texture of sorghum biscuits. *LWT* 136:110323. doi: 10.1016/j.lwt.2020.110323

Baldino, N., Gabriele, D., Lupi, F. R., de Cindio, B., and Cicerelli, L. (2014). Modeling of baking behavior of semi-sweet short dough biscuits. *Innov. Food Sci. Emerg. Technol.* 25, 40–52. doi: 10.1016/j.ifset.2013.12.022

China (1993). *The Short Biscuit Baking Test*. Beijing: Standards Press of China

Committee (2006). *Wheat Flour-Physical Characteristics of Doughs-Determination of Water Absorption and Rheological Properties Using a Farinograph*. Beijing: Standards Press of China.

Di Cairano, M., Condelli, N., Caruso, M. C., Marti, A., Cela, N., and Galgano, F. (2020). Functional properties and predicted glycemic index of gluten free cereal, pseudocereal and legume flours. *LWT* 133:109860. doi: 10.1016/j.lwt.2020.109860

Di Cairano, M., Galgano, F., Tolve, R., Caruso, M. C., and Condelli, N. (2018). Focus on gluten free biscuits: ingredients and issues. *Trends Food Sci. Technol.* 81, 203–212. doi: 10.1016/j.tifs.2018.09.006

Engleson, J., and Atwell, B. (2008). Gluten-free Product Development. *Cereal Foods World* 53, 180–184. doi: 10.1094/CFW-53-4-0180

Fustier, P., Castaigne, F., Turgeon, S. L., and Biliaderis, C. G. (2008). Flour constituent interactions and their influence on dough rheology and quality of semi-sweet biscuits: a mixture design approach with reconstituted blends of gluten, water-solubles and starch fractions. *J. Cereal Sci.* 48, 144–158. doi: 10.1016/j.jcs.2007.08.015

Gerits, L. R., Pareyt, B., and Delcour, J. A. (2015). Wheat starch swelling, gelatinization and pasting: effects of enzymatic modification of wheat endogenous lipids. *LWT* 63, 361–366. doi: 10.1016/j.lwt.2015.02.035

Gujral, H. S., Sharma, P., Kaur, H., and Singh, J. (2013). Physiochemical, Pasting, and Thermal Properties of Starch Isolated from Different Barley Cultivars. *Int. J. Food Proper.* 16, 1494–1506. doi: 10.1080/10942912.2011.595863

Hedayati, S., and Niakousari, M. (2018). Microstructure, pasting and textural properties of wheat starch-corn starch citrate composites. *Food Hydrocoll.* 81, 1–5. doi: 10.1016/j.foodhyd.2018.02.024

Kaur, A., Singh, N., Kaur, S., Ahlawat, A. K., and Singh, A. M. (2014). Relationships of flour solvent retention capacity, secondary structure and rheological properties with the cookie making characteristics of wheat cultivars. *Food Chem.* 158, 48–55. doi: 10.1016/j.foodchem.2014.02.096

Kaur, M., Sandhu, K. S., Arora, A., and Sharma, A. (2015). Gluten free biscuits prepared from buckwheat flour by incorporation of various gums:

physicochemical and sensory properties. *LWT* 62, 628–632. doi: 10.1016/j.lwt.2014.02.039

Laguna, L., Salvador, A., Sanz, T., and Fiszman, S. M. (2011). Performance of a resistant starch rich ingredient in the baking and eating quality of short-dough biscuits. *LWT* 44, 737–746. doi: 10.1016/j.lwt.2010.05.034

Lindsay, M. P., and Skerritt, J. H. (1999). The glutenin macropolymer of wheat flour doughs: structure–function perspectives. *Trends Food Sci. Technol.* 10, 247–253. doi: 10.1016/S0924-2244(00)00004-2

Ma, F., and Baik, B. K. (2018). Soft wheat quality characteristics required for making baking powder biscuits. *J. Cereal Sci.* 79, 127–133. doi: 10.1016/j.jcs.2017.10.016

Manley, D. (2011). *Manley's Technology of Biscuits, Crackers and Cookies:* Fourth edition. Sawston: Woodhead Publishing.

Moiraghi, M., Vanzetti, L., Bainotti, C., Helguera, M., León, A., and Pérez, G. (2011). Relationship Between Soft Wheat Flour Physicochemical Composition and Cookie-Making Performance. *Cereal Chem.* 88, 130–136. doi: 10.1094/CCHEM-09-10-0131

Moriano, M. E., Cappa, C., and Alamprese, C. (2018). Reduced-fat soft-dough biscuits: multivariate effects of polydextrose and resistant starch on dough rheology and biscuit quality. *J. Cereal Sci.* 81, 171–178. doi: 10.1016/j.jcs.2018.04.010

Ohtsu, N. (1979). A Threshold Selection Method from Gray-Level Histograms. *IEEE Trans. Syst. Man Cybern.* 9, 62–66. doi: 10.1109/TSMC.1979.4310076

Panghal, A., Khatkar, B. S., Yadav, D. N., and Chhikara, N. (2019). Effect of finger millet on nutritional, rheological, and pasting profile of whole wheat flat bread (chapatti). *Cereal Chem.* 96, 86–94. doi: 10.1002/cche.10111

Pauly, A., Pareyt, B., Lambrecht, M. A., Fierens, E., and Delcour, J. A. (2013). Flour from wheat cultivars of varying hardness produces semi-sweet biscuits with varying textural and structural properties. *LWT* 53, 452–457. doi: 10.1016/j.lwt.2013.03.014

Schober, T., O'Brien, C., McCarthy, D., Darnedde, A., and Arendt, E. (2003). Influence of gluten-free flour mixes and fat powders on the quality of gluten-free biscuits. *Eur. Food Rese. Technol.* 216, 369–376. doi: 10.1007/s00217-003-0694-3

Sozer, N., Cicerelli, L., Heiniö, R.-L., and Poutanen, K. (2014). Effect of wheat bran addition on in vitro starch digestibility, physico-mechanical and sensory properties of biscuits. *J. Cereal Sci.* 60, 105–113. doi: 10.1016/j.jcs.2014.01.022

Thejasri, V., Hymavathi, T., Roberts, T., Anusha, B., and devi, S. (2017). Sensory, Physico-Chemical and Nutritional Properties of Gluten Free Biscuits Formulated with Quinoa (Chenopodium quinoa Willd.), Foxtail Millet (Setaria italica) and Hydrocolloids. *Int. J. Curr. Microbiol. Appl. Sci.* 6, 1710–1721. doi: 10.20546/ijcmas.2017.608.205

Weegels, P. L., Verhoek, J. A., Amgde, G., and Hamer, R. J. (1994). Effects on gluten of heating at different moisture contents. I. Changes in functional properties. *J. Cereal Sci.* 19, 31–38. doi: 10.1006/jcrs.1994.1005

Wilderjans, E., Pareyt, B., Goesaert, H., Brijs, K., and Delcour, J. A. (2008). The role of gluten in a pound cake system: a model approach based on gluten–starch blends. *Food Chem.* 110, 909–915. doi: 10.1016/j.foodchem.2008.02.079

Xu, H. X., Sun, L. J., Zhou, G. Y., Na, W. L., Wei, L. U., Xi, L. W., et al. (2016). Variations of Wheat Quality in China From 2006 to 2015. *Sci. Agricu. Sin.* 49, 3063–3072.

Yang, T., Wang, P., Wang, F., Zhou, Q., Wang, X., Cai, J., et al. (2022). Influence of starch physicochemical properties on biscuit-making quality of wheat lines with high-molecular-weight glutenin subunit (HMW-GS) absence. *LWT* 158:113166. doi: 10.1016/j.lwt.2022.113166

Zhang, C., Jiang, D., Liu, F., Cai, J., Dai, T., and Cao, W. (2010). Starch granules size distribution in superior and inferior grains of wheat is related to enzyme activities and their gene expressions during grain filling. *J. Cereal Sci.* 51, 226–233. doi: 10.1016/j.jcs.2009.12.002

Zhang, X., Zhang, B. Q., Hong-Ya, W. U., Cheng-Bin, L. U., Guo-Feng, L., Liu, D. T., et al. (2018). Effect of high-molecular-weight glutenin subunit deletion on soft wheat quality properties and sugar-snap cookie quality estimated through near-isogenic lines. *J. Integr. Agricu.* 17, 1066–1073. doi: 10.1016/S2095-3119(17)61729-5

Zhou, Q., Li, X., Yang, J., Zhou, L., Cai, J., Wang, X., et al. (2018). Spatial distribution patterns of protein and starch in wheat grain affect baking quality of bread and biscuit. *J. Cereal Sci.* 79, 362–369. doi: 10.1016/j.jcs.2017.07.017

Conflict of Interest: The authors declare that the research was conducted in the absence of any commercial or financial relationships that could be construed as a potential conflict of interest.

Publisher's Note: All claims expressed in this article are solely those of the authors and do not necessarily represent those of their affiliated organizations, or those of the publisher, the editors and the reviewers. Any product that may be evaluated in this article, or claim that may be made by its manufacturer, is not guaranteed or endorsed by the publisher.

frontiers in Plant Science

REVIEW
published: 30 March 2022
doi: 10.3389/fpls.2022.834654

Wheat Quality Formation and Its Regulatory Mechanism

*Yanchun Peng[1], Yun Zhao[2,3], Zitong Yu[3], Jianbin Zeng[2], Dengan Xu[2], Jing Dong[1] and Wujun Ma[2,3]**

[1]Hubei Key Laboratory of Food Crop Germplasm and Genetic Improvement, Food Crops Institute, Hubei Academy of Agricultural Sciences, Wuhan, China, [2]College of Agronomy, Qingdao Agricultural University, Qingdao, China, [3]Food Futures Institute and College of Science, Health, Engineering and Education, Murdoch University, Perth, WA, Australia*

Elucidation of the composition, functional characteristics, and formation mechanism of wheat quality is critical for the sustainable development of wheat industry. It is well documented that wheat processing quality is largely determined by its seed storage proteins including glutenins and gliadins, which confer wheat dough with unique rheological properties, making it possible to produce a series of foods for human consumption. The proportion of different gluten components has become an important target for wheat quality improvement. In many cases, the processing quality of wheat is closely associated with the nutritional value and healthy effect of the end-products. The components of wheat seed storage proteins can greatly influence wheat quality and some can even cause intestinal inflammatory diseases or allergy in humans. Genetic and environmental factors have great impacts on seed storage protein synthesis and accumulation, and fertilization and irrigation strategies also greatly affect the seed storage protein content and composition, which together determine the final end-use quality of wheat. This review summarizes the recent progress in research on the composition, function, biosynthesis, and regulatory mechanism of wheat storage proteins and their impacts on wheat end-product quality.

Keywords: wheat quality, fertilization, watering regime, regulatory mechanism, sulfur deficiency

OPEN ACCESS

Edited by:
Vincenzo Rossi, Council for Agricultural and Economics Research (CREA), Italy

Reviewed by:
Patricia Giraldo, Polytechnic University of Madrid, Spain
Grazia Maria Borrelli, Council for Agricultural and Economics Research (CREA), Italy
Yueming Yan, Capital Normal University, China
Fei Xiong, Yangzhou University, China

****Correspondence:***
Wujun Ma
w.ma@murdoch.edu.au

Specialty section:
This article was submitted to Crop and Product Physiology, a section of the journal Frontiers in Plant Science

Received: *13 December 2021*
Accepted: *09 March 2022*
Published: *30 March 2022*

Citation:
Peng Y, Zhao Y, Yu Z, Zeng J, Xu D, Dong J and Ma W (2022) Wheat Quality Formation and Its Regulatory Mechanism. Front. Plant Sci. 13:834654. doi: 10.3389/fpls.2022.834654

INTRODUCTION

Wheat (*Triticum aestivum*) is one of the largest grain crops in the world, and its quality mainly comprises processing and nutritional quality. The term "wheat quality" usually refers to the processing quality, which is mainly dependent on the content and characteristics of storage proteins in wheat grains (Shewry and Halford, 2002; Ma et al., 2019) and directly determines wheat's market price and end-use value. Since storage proteins contain some components that can cause human intestinal inflammatory diseases or allergy, the concept of wheat "protein quality" is often used to cover the scope of the processing and nutritional quality (Scherf et al., 2016a).

Wheat processing quality is represented by the physical and chemical characteristics of the dough, which make it possible to process wheat into a variety of food products (Payne, 1987; He et al., 2005; Don et al., 2006; Zhang et al., 2007, 2014b, 2021; Li et al., 2015; Gao et al., 2016b; Chen et al., 2019; Jiang et al., 2019). Dough properties are mainly determined by

gluten proteins, glutenins, and gliadins (Shewry and Halford, 2002). Glutenins can be subdivided into high molecular weight glutenin (HMW-GS) and low molecular weight glutenin (LMW-GS; Shewry et al., 2002; Veraverbeke and Delcour, 2002). HMW-GS is the main factor determining gluten elasticity, which is encoded by the *Glu-1* genes including *Glu-A1*, *Glu-B1,* and *Glu-D1* loci on the long arm of chromosomes 1A, 1B, and 1D, respectively. Each locus comprises two linked genes encoding two different types (X type and Y type) of HMW-GS subunits (McIntosh et al., 1991; Liu et al., 2003; Sun et al., 2006; Zheng et al., 2011; Peng et al., 2015; Yu et al., 2019). Gliadins are mainly monomer proteins, including ω-, α/β-, and γ-gliadins (Kasarda et al., 1984; Zhou et al., 2022). According to the Chinese National Standard (Wang et al., 2013), wheat can be divided into four categories based on the usage and gluten strength: (1) Strong gluten wheat: the endosperm is hard and the wheat flour produces very strong gluten, which is suitable for baking bread; (2) Medium strong gluten wheat: the endosperm is hard and the gluten is rather strong and is suitable for making instant noodles, dumplings, steamed bread, noodles, and other foods; (3) Medium gluten wheat: the endosperm is hard and the gluten strength is moderate and is suitable for making noodles, dumplings, steamed bread, and other foods; and (4) Weak gluten wheat: the endosperm is soft and the gluten is weak and is suitable for making cake, biscuit, and other foods. Strong gluten dough has high ductility resistance and can maintain stability (Ma et al., 2019). The dough can retain the gas produced during fermentation in discrete cells evenly distributed in the dough (Don et al., 2006). A lower gluten strength can cause the excessive expansion of gas cells during baking, resulting in the collapse of cell walls and aggregation of cells, and thereby a rough bread texture (Don et al., 2006). Therefore, strong gluten wheat has always been an important goal of wheat breeding programs.

Generally, the protein content in wheat grains ranges from 10 to 18% (Qi et al., 2012; Liu et al., 2018). To some extent, the protein content is positively correlated with wheat processing quality, particularly dough strength. However, the protein content and grain yield are usually negatively correlated with each other (Kibite and Evans, 1984). In real production, a large amount of nitrogen fertilizer is often applied in order to promote wheat yield and protein content, which tends to reduce the nitrogen use efficiency and cause negative impacts on the environment (Justes et al., 1994). In recent years, multiple methods have been developed with the aim to simultaneously improve wheat yield and protein content, such as the utilization of new genes and optimization of water and fertilization regimes (Alhabbar et al., 2018; Balotf et al., 2018; Roy et al., 2018, 2020, 2021; Yang et al., 2018; Yu et al., 2018a,b; Li et al., 2021a). However, the effect of protein content on wheat quality is rather complex due to the presence of gliadin components in the storage protein. Gliadins have an odd number of cysteine residues and a negative effect on wheat processing quality (Lindsay and Skerritt, 1999; Wieser, 2007; Rasheed et al., 2014). Therefore, high-quality wheat should be characterized by a higher content of glutenins and a lower content of gliadins, and wheat processing quality is not necessarily related to the grain protein content.

In Australia, researchers have been pursuing the breeding goal of wheat varieties with low-protein content but high quality since 2000, targeting at the improvement of wheat quality by optimizing the gluten composition, namely, a higher glu/gli ratio (Roy et al., 2018, 2020, 2021). In this approach, the protein content is no longer a target. Since there is a negative correlation between the grain protein content and yield, a low-protein content naturally means a higher yield without sacrificing the quality. However, considering the nutritional value of protein, the breeding goal of low-protein and high-quality wheat is not suitable for some developing countries. Therefore, "three-high wheat" (high quality, high yield, and high protein) should be the breeding goal for most countries.

GENETICS AND APPLICATIONS IN RELATION TO WHEAT QUALITY BREEDING

Wheat quality can be improved by manipulation of the main storage protein genes. As a matter of fact, many effective genes have been efficiently utilized for decades, such as *GluD1* (5 + 10) and *GluB1* (17 + 18; Payne et al., 1981, 1987; Payne, 1987; Altpeter et al., 2004; Mohan and Gupta, 2015). The common HMW-GS alleles have been assigned with quality scores to facilitate their application in breeding (Payne et al., 1987). Although there are six HMW-GS genes in the wheat genome, most hexaploid wheat varieties only have three to five HMW glutenin subunits due to the silencing of some genes (Ma et al., 2003), such as the genes encoding the Ay subunit (Yu et al., 2019). Roy et al. (2018, 2020, 2021) found that the expression of Ay subunit has positive effects on grain protein content, grain yield, and quality. A new storage protein family consisting of the avenin-like proteins has also been identified to have great breeding value for the improvement of wheat quality (Chen et al., 2016). Since the genetic control of wheat quality has been comprehensively reviewed (Shewry and Tatham, 1997; Vasila and Anderson, 1997; Gras et al., 2001; She et al., 2011; Ortolan and Steel, 2017; Ma et al., 2019; Sharma et al., 2020; Wang et al., 2020), this review will not focus on this aspect.

MANIPULATION OF FERTILIZATION AND WATERING REGIMES

Seed storage proteins can account for 40–60% of wheat processing quality (Békés et al., 2006), and those unaccounted quality variations can be attributed to environmental factors. In wheat production, fertilization and watering strategies are also often considered for quality improvement (Li et al., 2018, 2019b; Yu et al., 2018a, 2021). As nitrogen (N) is one of the most important and essential elements for wheat, N fertilizer is usually the most efficient input for simultaneously increasing grain protein content and grain yield in wheat production

(Zebarth et al., 2007; Malik et al., 2013; Zhen et al., 2018, 2020; Zhong et al., 2018, 2020; Ding et al., 2020; Xia et al., 2020; Hermans et al., 2021; Landolfi et al., 2021; Lyu et al., 2021; Dong et al., 2022; Liu et al., 2022; Ma et al., 2022). Kichey et al. (2007) demonstrated that 50–95% of nitrogen in mature grains is derived from the remobilization of nitrogen stored in the tissues before anthesis. However, nitrogen applied later in the growth period, namely, at anthesis or during grain filling, often increases grain protein content (Gooding and Davies, 1992; Sultana et al., 2017; Zhong et al., 2018, 2020). Li et al. (2018, 2019b) reported that nitrogen application during the grain filling period in winter wheat can significantly increase the uptake and accumulation of nitrogen. Yu et al. (2018a) reported that apart from the influence of genotype, grain yield and protein content have similar responses to nitrogen availability, with the former being slightly more sensitive than the latter. Furthermore, Yu et al. (2018a) proposed an N-mediated mechanism for protein polymerization in wheat grains: N promotes PPIase SUMOylation by interacting with SUMO1, facilitating the transport of PPIase into cytoplasm to support the formation of protein polymers (Yu et al., 2018a; **Figure 1**). Zhong et al. (2018, 2020) reported that at the same N application rate (240 kg ha^{-1}), N topdressing can better promote the protein content and quality of wheat grains at the emergence of the top first leaf than at the emergence of the top third leaf of the main stem. The timing of N topdressing can significantly regulate γ-gliadins and HMW-GSs, while has almost no effect on the LMW-GS level, leading to a higher HMW-GS/LMW-GS ratio (Zhong et al., 2018). Furthermore, a delay of N topdressing was found to alter the grain hardness and flour allergenicity (Zhong et al., 2019). Ding et al. (2020) found that an increase in total N provision (210–270 kg ha^{-1}) in the Yangtze River basin of China could enhance wheat grain yield, grain protein content, and nitrogen efficiency, with the appropriate topdressing timing and N application dose depending on the environment. Moreover, the biotic and abiotic stresses during wheat growth also significantly affect the quality of wheat (Duan et al., 2020). Among various stresses, drought has been identified to have a severe negative impact on wheat quality, particularly at the early grain filling stage (Gu et al., 2015). Usually, drought can cause stomatal closure, inhibit photosynthesis, increase respiration, and ultimately reduce starch biosynthesis, thereby leading to low yield of plants (Deng et al., 2018; Zhu et al., 2020). However, on the other hand, drought can enhance the content of wheat storage proteins to contribute to improved baking quality (Dong et al., 2012; Gu et al., 2015; Zhou et al., 2018). Different watering conditions were found to result in significant differences in the phosphorylation level of corresponding phosphoproteins in wheat grains (Zhang et al., 2014a). The changes in protein and starch synthesis during drought may be ascribed to post-translational protein modifications such as phosphorylation (Zhang et al., 2014a; Xia et al., 2018).

To reduce the yield loss caused by drought, moderate to high amounts of nitrogen fertilizer is often applied during wheat growth. A recent study showed that high-nitrogen fertilization under drought can increase the enzymatic protein synthesis for nitrogen and carbohydrate metabolism (Duan et al., 2020). Liu et al. (2022) reported that high-nitrogen treatments under drought conditions can either independently

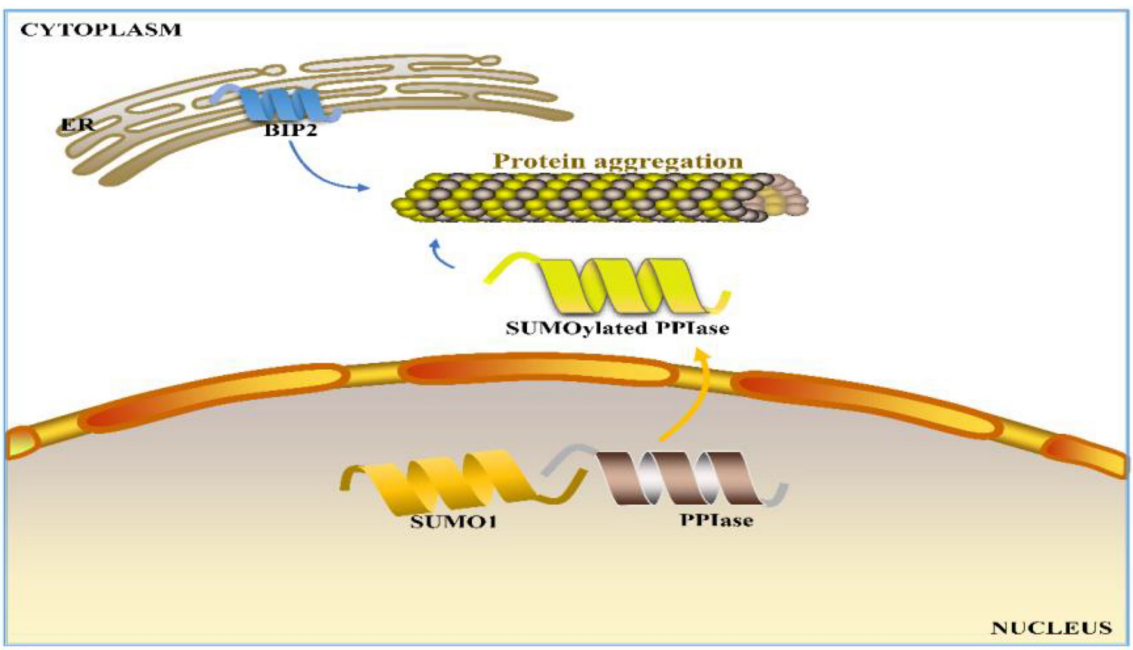

FIGURE 1 | Proposed N-regulated mechanism for wheat grain protein polymerization in the cytoplasm. ER: endoplasmic reticulum, BIP2: luminal-binding protein 2 precursor, SUMO1: small ubiquitin-related modifier 1, and PPIase: peptidyl-prolyl cis-trans isomerase.

or coordinately facilitate the accumulation of wheat storage protein and gluten macropolymer, as well as improve lipid accumulation and protein secondary structure. The content of random coils and β-sheets of gluten proteins was also increased (Liu et al., 2022). These changes can contribute to the improvement of baking quality. Moreover, irrigation strategies under drought conditions have great impacts on crop yield and quality (Flagella et al., 2010; Xu et al., 2018b; Jha et al., 2019; Li et al., 2019b, 2021a). Li et al. (2021a) proposed an irrigation method that integrates micro-sprinkling irrigation and fertilizer, which could synergistically improve the grain yield and protein content of winter wheat. Compared with conventional irrigation, this method can reduce the total amount of water use and provide water and nitrogen at later growth stages, making more water and nitrogen available to wheat plants after flowering, which can reduce the canopy temperature and significantly delay leaf senescence and finally enhance the grain yield and protein content simultaneously.

Also, studies of glutamine synthetase activity in wheat developing grains and flag leaves have demonstrated that high-nitrogen availability facilitates the participation of glutamine in biological processes (Yu et al., 2018a, 2021; Zhong et al., 2018, 2020). A number of studies have revealed that application of sulfur fertilizer can significantly improve wheat quality (Zhao et al., 1999a,b; Luo et al., 2000; Yu et al., 2021). Based on the differences in the distribution of cysteine residues among wheat gluten subunits, wheat storage proteins can be categorized into three types of subunits, including sulfur-poor subunits (ω-gliadins), sulfur-medium subunits (HMW-GS and α/β-gliadins), and sulfur-rich subunits (LMW-GS and γ-gliadins; Shewry et al., 1995). It is worth noting that this classification is based on the number of cysteine residues within each subunit instead of the total sulfur amount (Lindsay and Skerritt, 1999; Wieser, 2007; note: apart from cysteine, methionine is another sulfur containing amino acid). Since the disulfide bond is believed to be the foundation of gluten rheological properties, for a long time, it has been generally believed that sulfur's positive effects on wheat quality are implemented through mediating the gluten component ratios based on their sulfur or cysteine contents (Ma et al., 2019). However, Yu et al. (2021) recently proposed a different regulatory mechanism through proteomics, transcriptomics, metabolomics, and field experiments (**Figure 2**). It clearly demonstrated that sulfur does not mediate the gluten component ratios based on their sulfur or cysteine contents (Yu et al., 2021). Their study showed that the application of sulfur enhances the accumulation of free glycine at the beginning of grain filling and then promotes the participation of glycine in glutenin biosynthesis. Glycine belongs to aspartate acid family, and its content disparity between gliadins (1.75%) and glutenins (13.33%) marks the main difference of the two gluten components (Yu et al., 2021). A higher content of free glycine under sulfur fertilizer treatment can more significantly promote the biosynthesis of glutenins than that of gliadins, resulting in a high glu/gli ratio (Yu et al., 2021). The gene network regulating the biosynthesis and accumulation of glutenin components is mediated by S-adenosylmethionine (SAM; Yu et al., 2021). In addition, a high concentration of SAM indicates that more secondary metabolites are involved in the final development of grains. Chen et al. (2014) found that the downregulation of SAM decarboxylase genes would reduce the rice grain length, pollen viability, seed setting rate, grain yield per plant, and abiotic stress (salinity, drought, and chilling) tolerance, indicating a positive effect of SAM on rice yield.

GENE NETWORKS REGULATING STORAGE PROTEIN BIOSYNTHESIS

The wheat storage protein genes have spatiotemporal specific expression, and generally function at the middle and late stage of seed development (Diaz et al., 2002; Dong et al., 2007; Gao et al., 2021). Although wheat storage protein synthesis is regulated by many factors, it is mainly regulated at the transcriptional level (Gao et al., 2021). In recent years, important progress has been achieved in research on the regulation of wheat storage protein synthesis (**Table 1**). A series of conserved *cis*-elements in the promoter region of wheat seed storage protein genes have been identified, including the bZIP binding sites (GCN4-like motifs, ATGAG/CTCAT and G-box motif, TTACGTGG), DNA binding with one finger (DOF) binding sites (PB-box, TGTAAAG), R2R3MYB-binding sites (AACAAC), RY repeat sites (RY-box, CATGCA), and other basal promoter elements (Aryan et al., 1991; Juhasz et al., 2011; Ravel et al., 2014; Guo et al., 2015; Makai et al., 2015). Thirty conserved motifs and three conserved *cis*-regulatory modules (CCRMs) were found within the 1-kb region upstream of the start codon of *Glu-1*: CCRM3 (−950 to −750), CCRM 2 (−650 to −400), and CCRM 1 (−300 to −101; Li et al., 2019a). All three CCRMs can regulate the expression of wheat storage proteins and the 300 bp promoter (−300 to −1) can ensure the precise initiation of *Glu-1* gene expression in the endosperm at 7 days after flowing and maintain its expression pattern during seed development. Further analysis revealed that CCRM1-1 (−208 to −101) is the core region for maintaining the endosperm-specific expression of *Glu-1* genes (Li et al., 2019a). In addition, various transcription factors (TFs) involved in gluten gene regulation have been identified, such as bZIP, DOF, MYB (myeloblastosis), and B3. A bZIP transcription factor SPA (storage protein activator) can bind to the GCN4-like motif (GLM and ATGAG/CTCAT) in the promoters of HMW-GS genes to enhance their expression in common wheat (Albani et al., 1997; Conlan et al., 1999; Ravel et al., 2014). Averagely, the expression intensity of SPA-B is 10- and 7-fold that of SPA-A and SPA-D, respectively (Ravel et al., 2009). SPA markers are associated with dough viscoelasticity such as dough strength, extensibility, and tenacity (Ravel et al., 2009). As a bZIP transcription factor, the SPA Heterodimerizing Protein (SHP) prevents the binding of SPA to the *cis*-motifs and represses the synthesis of both LMW-GS and HMW-GS (Boudet et al., 2019). Thus, the glu/gli ratio is decreased in common wheat (Boudet et al., 2019). Wheat prolamin-box binding factor (WPBF), a DOF transcription factor, was first identified from wheat as a homolog of barley prolamin-box binding factor (BPBF; Dong et al., 2007). WPBF binds the prolamin box of the gliadin promoter region and interacts with TaQM (cloned from the wheat root cDNA library; *QM*, initially found as a putative

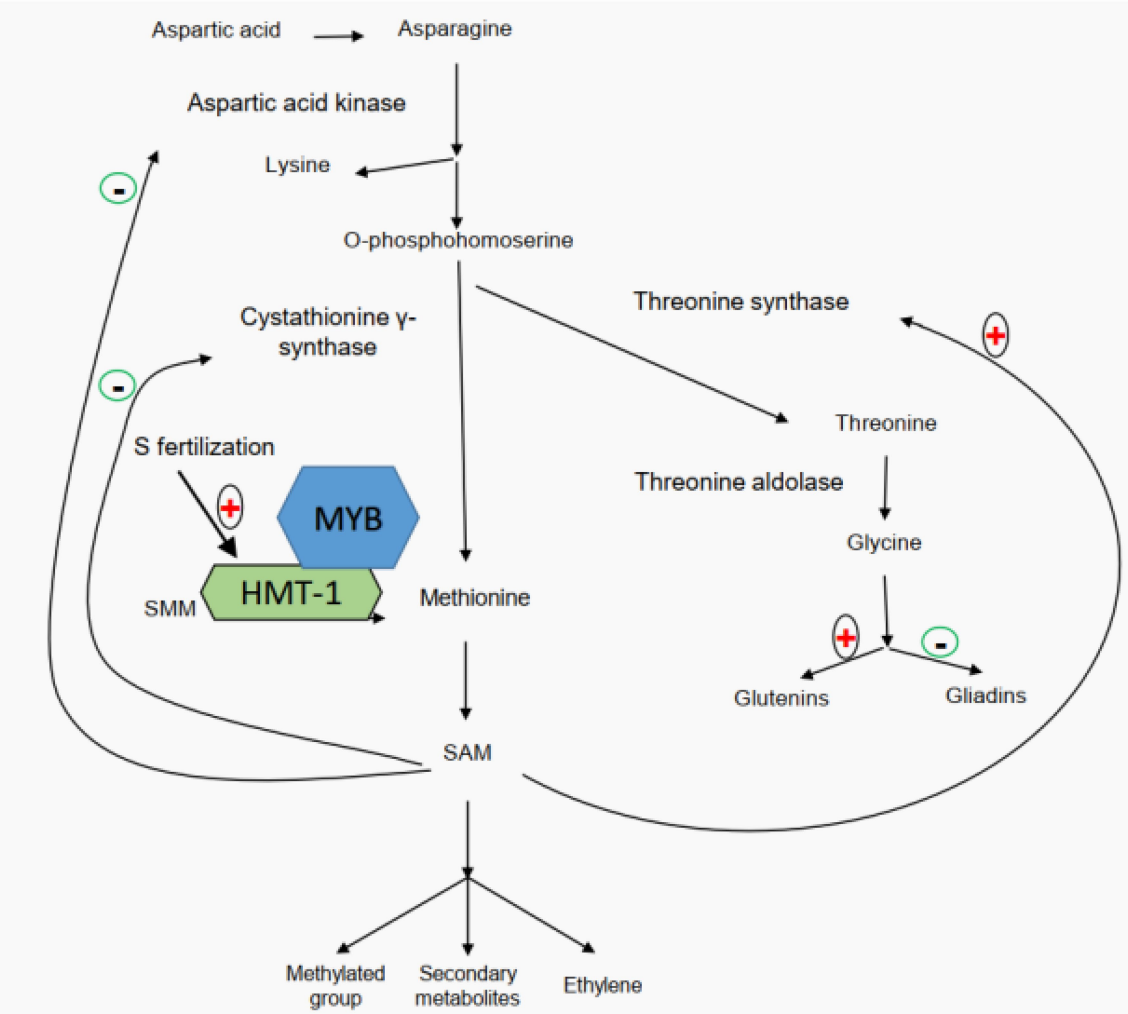

FIGURE 2 | Sulfur-mediated regulation network of wheat gluten component biosynthesis (modified from Yu et al., 2021).

TABLE 1 | The identified transcription factors regulate seed storage protein synthesis in wheat.

Transcription factor	Function	Target gene	Cis motif	Sequence	Reference
SPA	Transcriptional activation	glutenin promoters	G-box; GLM	ATGAG/CTCAT; ACGTG	Albani et al., 1997; Ravel et al., 2014
SHP	Transcriptional repression	glutenin promoters	G-box; GLM	ATGAG/CTCAT; ACGTG	Boudet et al., 2019
WPBF	Transcriptional activation	gliadin gene promoters	P-box	TGTAAAG	Mena et al., 1998; Dong et al., 2007
TaPBF-D	Transcriptional activation	HMW-GS gene promoters	P-box	TGTAAAG	Zhu et al., 2018
TaGAMyb	Transcriptional activation	HMW-GS gene promoters	unnamed	C/TAACAAA/CC	Diaz et al., 2002; Guo et al., 2015
TaFUSCA3	Transcriptional activation	HMW-GS gene promoters	RY-box	CATGCA	Sun et al., 2017
TaNAC019	Transcriptional activation	glutenin promoters	unnamed	[AT]NNNNNN[ATC][CG]A[CA]GN[ACT]A	Gao et al., 2021
TaNAC100	Transcriptional repression	HMW-GS gene promoters	unnamed	CATGT	Li et al., 2021b
TaSPR	Transcriptional repression	SSP gene promoters	unnamed	CANNTG	Shen et al., 2021

tumor suppressor gene) to activate the expression of LMW-GS and gliadin genes during wheat grain development (Dowdy et al., 1991; Mena et al., 1998; Dong et al., 2007). TaPBF-D, another DOF transcription factor, binds *in vitro* the prolamin box of *Glu-1By8* and *Glu-1Dx2* promoters and decreases their C-methylation level, and its overexpression was found to enhance HMW-GS accumulation in wheat grains (Zhu et al., 2018). TaGAMyb, a TF of the R2R3MYB family, binds to a C/TAACAAA/

CC-like motif in the HMW-GS gene promoter, recruits the histone acetyltransferase TaGCN5, and activates the expression of the *Glu-1Dy* by facilitating the acetylation of histones H3K9 and H3K14 (Diaz et al., 2002; Guo et al., 2015). TaFUSCA3 is a wheat B3-superfamily TF specifically binding to the RY motif of the *Glu-1Bx7* promoter region to activate the *Glu-1Bx7* expression (Sun et al., 2017). TF interactions between TaSPA and TaFUSCA3 were discovered (Sun et al., 2017). It is well known that NAM-ATAF-CUC (NAC) TFs participate in a series of biological processes, including abiotic and biotic stress responses and organ development (Uauy et al., 2006; Xue et al., 2011; Liang et al., 2014; Borrill et al., 2017; Guerin et al., 2019). Recently, some NAC TFs (TaNAC019, TaNAC100, and TaSPR) in wheat have been identified to regulate grain storage protein synthesis (Gao et al., 2021; Li et al., 2021b; Shen et al., 2021). TaNAC019, a wheat endosperm-specific NAC TF, binds to the motif ([AT]NNNNNN[ATC][CG]A[CA]GN[ACT]A) in the promoter region of *Glu-1* genes. In coordination with TaGAMyb, it directly activates the expression of HMW-GS genes and indirectly modulates that of TaSPA (Gao et al., 2021). In a wheat natural population, two allelic variations of TaNAC019-B, TaNAC019-BI, and TaNAC019-BII were identified (Gao et al., 2021). TaNAC019-BI can improve flour processing quality and is an important candidate gene for wheat quality improvement (Gao et al., 2021). However, two recent studies demonstrated that both TaNAC100 and TaSPR function as repressors of seed storage protein expression in common wheat, indicating that further research is needed for better utilization of such TFs in breeding (Li et al., 2021b; Shen et al., 2021). The TaDME (wheat DEMETER) gene encoding 5-methylcytosine DNA glycosylase on the long arm of group 5 chromosomes suppresses the LMW-GS and gliadin gene expression by activating the demethylation of their promoters in the endosperm (Wen et al., 2012). It is worth noting that these studies have been mainly focused on the molecular regulatory mechanism of HMW-GS, LMW-GS, gliadins, or the total seed storage protein, and future research should be targeted at the regulatory mechanism for each subtype of gluten components, including different LMW-GSs (i-, m-, s-,α-, ω-, and γ-types) and gliadin components (α/β-, ω-, and γ-gliadins), so as to fine-tune wheat processing quality and improve the quality of wheat products for human consumption (Rasheed et al., 2014; Ma et al., 2019).

HEALTH EFFECTS OF WHEAT GRAINS AND THE UNDERLYING REGULATORY MECHANISM

Gluten can cause human diseases related to digestion of wheat flour products, such as celiac disease, non-celiac gluten sensitivity, and gluten allergy (Scherf et al., 2016a). The intake of too much proline-rich gluten can reduce pepsin activity in the gastrointestinal tract, resulting in the accumulation of flour polypeptides rich in Pro and Gln in the small intestine (Scherf et al., 2016a). Previous studies have demonstrated that gliadins are the most toxic wheat protein components related to celiac disease, and glutenins are classified as non-toxic or weakly toxic (Barone and Zimmer, 2016; Scherf et al., 2016a,b). In order to reduce the toxicity of wheat gluten, a variety of flour treatment methods have been developed, including chemical, physical, and enzymatic methods (Buddrick et al., 2015; Scherf et al., 2018; Xue et al., 2019; Abedi and Pourmohammadi, 2021). In addition, some genetic methods have also been used to knock out or silence gliadin coding genes. Generally, RNAi can reduce the content of total gliadin in wheat gluten by 60–80% (Gil-Humanes et al., 2010). However, some negative effects on the processing quality were observed in RNAi wheat lines (Gil-Humanes et al., 2010, 2014). For instance, CRISPR-Cas9 editing was applied to silence the α-gliadin gene to reduce immune reactivity by 85%, but the treatment also greatly reduced the gluten content by 85% and led to an obvious decline in processing quality (Sánchez-León et al., 2018). At present, the greatest challenge is to find a technical solution to reduce wheat gliadin and increase gluten content with high yield and high total protein.

Yu et al. (2021) showed that sulfur treatment can reduce sulfur-poor ω-gliadins (the most abundant among all gliadin subtypes) by up to 31.4% in the total gluten, particularly the ω5-gliadin known to cause WDEIA (wheat-dependent exercise-induced anaphylaxis disease), which could be reduced by 83.9%. The α/β-gliadins, ω1,2-gliadins, and γ-gliadins, which are known to cause celiac disease, were also reduced by up to 25.9% under sulfur treatment. Carcinogen acrylamide is a processing contaminant usually formed from free asparagine and reducing sugars through the Maillard reaction (Mottram et al., 2002; Stadler et al., 2002; Zyzak et al., 2003). It has been discovered in a range of baked, fried, roasted, and toasted foods, including bread, pies, cakes, biscuits, batter, and breakfast cereals (Raffan and Halford, 2019). Since free asparagine is the major precursor for the formation of acrylamide during food processing especially high temperature baking, its accumulation mechanism in wheat grains has emerged as a hot research topic (Mottram et al., 2002; Stadler et al., 2002; Raffan et al., 2021). In living cells, aspartate is the substrate of asparagine, which is formed through enzymes that catalyze the ATP-dependent transfer of an amino group from glutamine (Gaufichon et al., 2010). Five asparagine synthetase genes have been found in the wheat genome, including TaASN1, TaASN2, TaASN3.1, TaASN3.2, and TaASN4 (Xu et al., 2018a; Raffan and Halford, 2021). Among these genes, TaASN2 is seed-specific with the highest expression in the embryo (Gao et al., 2016a; Curtis et al., 2019). It has been revealed that free asparagine is commonly present in wheat even under normal growth conditions (Curtis et al., 2018). Both environmental factors and agricultural practice can affect its accumulation (Zhong et al., 2018, 2020). In addition, adverse growing conditions such as sulfur deficiency and pathogen infection can increase asparagine concentration (Raffan and Halford, 2019). World Health Organization[1] has stated that acrylamide in the diet has potential cancer-causing effects. The food industry is in demand of available raw materials with lower

[1]https://www.who.int/

acrylamide-forming potential. So far, numerous studies have been carried out to reduce acrylamide in wheat products, mainly by reducing the free asparagine concentration in wheat grains. For example, Muttucumaru et al. (2006) reported that sulfur application can reduce the asparagine accumulation in mature wheat grains, making the wheat products healthier for human daily consumption. More recently, Raffan et al. (2021) successfully reduced the asparagine concentration through CRISPR-Cas9 approach to knock out the six alleles of TaASN2, a seed-specific asparagine synthetase gene in wheat.

CONCLUSION

The formation mechanism of wheat processing quality has been extensively studied *via* a broad range of biological approaches. Sulfur deficiency in soil has been reported as a global issue, which has negative impacts on wheat quality. An adequate level of sulfur fertilization is highly recommended in modern wheat farming to gain high processing quality as well as desirable nutritional value and healthy effect of the wheat end-products. Nitrogen fertilization after flowering should be considered for better processing quality. In the predicted drought season, low-protein content wheat cultivars may be selected for cultivation so that the grain starch can be allocated with more biosynthesis capacity to reduce yield loss. Molecular biological research has been mostly focused on the regulatory mechanism of the biosynthesis of various gluten components, which has led to the discovery of some key TFs that influence the quality. In future, TFs regulating specific HMW-GS subunits, LMW-GS types, and particularly the gliadin subtypes should be focused so that the relevant molecular markers can be used in breeding to meet a broad range of consumer needs.

AUTHOR CONTRIBUTIONS

YP, YZ, ZY, JZ, and DX prepared the first draft. JD and WM critically reviewed and revised the manuscript. All authors contributed to the article and approved the submitted version.

FUNDING

This work is supported by National Natural Science Foundation of China (31701506), Youth Science Fund of Hubei Academy of Agricultural Sciences (2020NKYJJ03), and Fund of Hubei Key Laboratory of Food Crop Germplasm and Genetic Improvement (2020LZJJ04).

ACKNOWLEDGMENTS

We are grateful to Jiangsheng Wu (College of Plant Science and Technology, Huazhong Agricultural University, Wuhan, China) for his critical revision of the manuscript.

REFERENCES

Abedi, E., and Pourmohammadi, K. (2021). Chemical modifications and their effects on gluten protein: An extensive review. *Food Chem.* 343:128398. doi: 10.1016/j.foodchem.2020.128398

Albani, D., HammondKosack, M. C. U., Smith, C., Conlan, S., Colot, V., Holdsworth, M., et al. (1997). The wheat transcriptional activator SPA: A seed-specific bZIP protein that recognizes the GCN4-like motif in the bifactorial endosperm box of prolamin genes. *Plant Cell* 9, 171–184. doi: 10.1105/tpc.9.2.171

Alhabbar, Z., Yang, R., Juhasz, A., Xin, H., She, M., Anwar, M., et al. (2018). NAM gene allelic composition and its relation to grain-filling duration and nitrogen utilisation efficiency of Australian wheat. *PLoS One* 13:e0205448. doi: 10.1371/journal.pone.0205448

Altpeter, F., Popelka, J. C., and Wieser, H. (2004). Stable expression of 1Dx5 and 1Dy10 high-molecular-weight glutenin subunit genes in transgenic rye drastically increases the polymeric glutelin fraction in rye flour. *Plant Mol. Biol.* 54, 783–792. doi: 10.1007/s11103-004-0122-5

Aryan, A. P., An, G., and Okita, T. W. (1991). Structural and functional analysis of promoter from gliadin, an endosperm-specific storage protein gene of *Triticum aestivum* L. *Mol. Gen. Genet.* 225, 65–71. doi: 10.1007/BF00282643

Balotf, S., Islam, S., Kavoosi, G., Kholdebarin, B., Juhasz, A., and Ma, W. (2018). How exogenous nitric oxide regulates nitrogen assimilation in wheat seedlings under different nitrogen sources and levels. *PLoS One* 13:e0190269. doi: 10.1371/journal.pone.0190269

Barone, M. V., and Zimmer, K. P. (2016). Endocytosis and transcytosis of gliadin peptides. *Mol. Cell Pediatr.* 3:8. doi: 10.1186/s40348-015-0029-z

Békés, F., Kemény, S., and Morell, M. (2006). An integrated approach to predicting end-product quality of wheat. *Eur. J. Agron.* 25, 155–162. doi: 10.1016/j.eja.2006.04.008

Borrill, P., Harrington, S. A., and Uauy, C. (2017). Genome-wide sequence and expression analysis of the NAC transcription factor family in Polyploid wheat. *G three* 7, 3019–3029. doi: 10.1534/g3.117.043679

Boudet, J., Merlino, M., Plessis, A., Gaudin, J. C., Dardevet, M., Perrochon, S., et al. (2019). The bZIP transcription factor SPA Heterodimerizing protein represses glutenin synthesis in *Triticum aestivum*. *Plant J.* 97, 858–871. doi: 10.1111/tpj.14163

Buddrick, O., Cornell, H., and Small, D. (2015). Reduction of toxic gliadin content of wholegrain bread by the enzyme caricain. *Food Chem.* 170, 343–347. doi: 10.1016/j.foodchem.2014.08.030

Chen, X. Y., Cao, X. Y., Zhang, Y. J., Islam, S., Zhang, J. J., Yang, R. C., et al. (2016). Genetic characterization of cysteine-rich type-b avenin-like protein coding genes in common wheat. *Sci. Rep.* 6:30692. doi: 10.1038/srep30692

Chen, M., Chen, J. J., Fang, J. Y., Guo, Z. F., and Lu, S. Y. (2014). Down-regulation of S-adenosylmethionine decarboxylase genes results in reduced plant length, pollen viability, and abiotic stress tolerance. *Plant Cell Tissue Organ Cult.* 116, 311–322. doi: 10.1007/s11240-013-0405-0

Chen, Q., Zhang, W. J., Gao, Y. J., Yang, C. F., Gao, X., Peng, H. R., et al. (2019). High molecular weight glutenin subunits 1Bx7 and 1By9 encoded by Glu-B1 locus affect wheat dough properties and sponge cake quality. *J. Agric. Food Chem.* 67, 11796–11804. doi: 10.1021/acs.jafc.9b05030

Conlan, R. S., Hammond-Kosack, M., and Bevan, M. (1999). Transcription activation mediated by the bZIP factor SPA on the endosperm box is modulated by ESBF-1 in vitro. *Plant J.* 19, 173–181. doi: 10.1046/j.1365-313x.1999.00522.x

Curtis, T. Y., Powers, S. J., Wang, R., and Halford, N. G. (2018). Effects of variety, year of cultivation and Sulphur supply on the accumulation of free asparagine in the grain of commercial wheat varieties. *Food Chem.* 239, 304–313. doi: 10.1016/j.foodchem.2017.06.113

Curtis, T. Y., Raffan, S., Wan, Y., King, R., Gonzalez-Uriarte, A., and Halford, N. G. (2019). Contrasting gene expression patterns in grain of high and low asparagine wheat genotypes in response to Sulphur supply. *BMC Genomics* 20:628. doi: 10.1186/s12864-019-5991-8

Deng, X., Liu, Y., Xu, X. X., Liu, D. M., Zhu, G. R., Yan, X., et al. (2018). Comparative proteome analysis of wheat flag leaves and developing grains under water deficit. *Front. Plant Sci.* 9:425. doi: 10.3389/fpls.2018.00425

Diaz, I., Vicente-Carbajosa, J., Abraham, Z., Martinez, M., Isabel-La Moneda, I., and Carbonero, P. (2002). The GAMYB protein from barley interacts with the DOF transcription factor BPBF and activates endosperm-specific genes during seed development. *Plant J.* 29, 453–464. doi: 10.1046/j.0960-7412.2001.01230.x

Ding, J., Li, F., Le, T., Wu, P., Zhu, M., Li, C., et al. (2020). Nitrogen management strategies of tillage and no-tillage wheat following rice in the Yangtze river basin, China: grain yield, grain protein, nitrogen efficiency, and economics. *Agronomy* 10:155. doi: 10.3390/agronomy10020155

Don, C., Mann, G., Bekes, F., and Hamer, R. J. (2006). HMW-GS affect the properties of glutenin particles in GMP and thus flour quality. *J. Cereal Sci.* 44, 127–136. doi: 10.1016/j.jcs.2006.02.005

Dong, F., Feng, L., Ya, J., Feng, Y., Qiu, Y., Jin, L., et al. (2022). Effect of nitrogen topdressing rate on yield and quality of black-grained wheat varieties (strains). *J. Nuc. Agric. Sci.* 36, 435–444. doi: 10.11869/j.issn.100-8551.2022.02.0435

Dong, K., Ge, P., Ma, C. Y., Wang, K., Yan, X., Gao, L. Y., et al. (2012). Albumin and globulin dynamics during grain development of elite Chinese wheat cultivar Xiaoyan 6. *J. Cereal Sci.* 56, 615–622. doi: 10.1016/j.jcs.2012.08.016

Dong, G. Q., Ni, Z. F., Yao, Y. Y., Nie, X. L., and Sun, Q. X. (2007). Wheat Dof transcription factor WPBF interacts with TaQM and activates transcription of an alpha-gliadin gene during wheat seed development. *Plant Mol. Biol.* 63, 73–84. doi: 10.1007/s11103-006-9073-3

Dowdy, S. F., Lai, K. M., Weissman, B. E., Matsui, Y., Hogan, B. L., and Stanbridge, E. J. (1991). The isolation and characterization of a novel cDNA demonstrating an altered mRNA level in nontumorigenic Wilms' microcell hybrid cells. *Nucleic Acids Res.* 19, 5763–5769. doi: 10.1093/nar/19.20.5763

Duan, W. J., Zhu, G. R., Zhu, D., and Yan, Y. M. (2020). Dynamic proteome changes of wheat developing grains in response to water deficit and high-nitrogen fertilizer conditions. *Plant Physiol. Biochem.* 156, 471–483. doi: 10.1016/j.plaphy.2020.08.022

Flagella, Z., Giuliani, M. M., Giuzio, L., Volpi, C., and Masci, S. (2010). Influence of water deficit on durum wheat storage protein composition and technological quality. *Eur. J. Agron.* 33, 197–207. doi: 10.1016/j.eja.2010.05.006

Gao, Y. J., An, K. X., Guo, W. W., Chen, Y. M., Zhang, R. J., Zhang, X., et al. (2021). The endosperm-specific transcription factor TaNAC019 regulates glutenin and starch accumulation and its elite allele improves wheat grain quality. *Plant Cell* 33, 603–622. doi: 10.1093/plcell/koaa040

Gao, R., Curtis, T. Y., Powers, S. J., Xu, H., Huang, J., and Halford, N. G. (2016a). Food safety: structure and expression of the asparagine synthetase gene family of wheat. *J. Cereal Sci.* 68, 122–131. doi: 10.1016/j.jcs.2016.01.010

Gao, X., Liu, T., Yu, J., Li, L., Feng, Y., and Li, X. (2016b). Influence of high-molecular-weight glutenin subunit composition at Glu-B1 locus on secondary and micro structures of gluten in wheat (*Triticum aestivum* L.). *Food Chem.* 197, 1184–1190. doi: 10.1016/j.foodchem.2015.11.085

Gaufichon, L., Reisdorf-Cren, M., Rothstein, S. J., Chardon, F., and Suzuki, A. (2010). Biological functions of asparagine synthetase in plants. *Plant Sci.* 179, 141–153. doi: 10.1016/j.plantsci.2010.04.010

Gil-Humanes, J., Piston, F., Barro, F., and Rosell, C. M. (2014). The shutdown of celiac disease-related gliadin epitopes in bread wheat by RNAi provides flours with increased stability and better tolerance to over-mixing. *PLoS One* 9:e91931. doi: 10.1371/journal.pone.0091931

Gil-Humanes, J., Piston, F., Tollefsen, S., Sollid, L. M., and Barro, F. (2010). Effective shutdown in the expression of celiac disease-related wheat gliadin T-cell epitopes by RNA interference. *Proc. Natl. Acad. Sci. U. S. A.* 107, 17023–17028. doi: 10.1073/pnas.1007773107

Gooding, M. J., and Davies, W. P. (1992). Foliar urea fertilization of cereals - a review. *Fert. Res.* 32, 209–222. doi: 10.1007/Bf01048783

Gras, P. W., Anderssen, R. S., Keentok, M., Békés, F., and Appels, R. (2001). Gluten protein functionality in wheat flour processing: a review. *Aust. J. Agric. Res.* 52, 1311–1323. doi: 10.1071/AR01068

Gu, A. Q., Hao, P. C., Lv, D. W., Zhen, S. M., Bian, Y. W., Ma, C. Y., et al. (2015). Integrated proteome analysis of the wheat embryo and endosperm reveals central metabolic changes involved in the water deficit response during grain development. *J. Agric. Food Chem.* 63, 8478–8487. doi: 10.1021/acs.jafc.5b00575

Guerin, C., Roche, J., Allard, V., Ravel, C., Mouzeyar, S., and Bouzidi, M. F. (2019). Genome-wide analysis, expansion and expression of the NAC family under drought and heat stresses in bread wheat (T. aestivum L.). *PLoS One* 14:e0213390. doi: 10.1371/journal.pone.0213390

Guo, W. W., Yang, H., Liu, Y. Q., Gao, Y. J., Ni, Z. F., Peng, H. R., et al. (2015). The wheat transcription factor TaGAMyb recruits histone acetyltransferase and activates the expression of a high-molecular-weight glutenin subunit gene. *Plant J.* 84, 347–359. doi: 10.1111/tpj.13003

He, Z. H., Liu, L., Xia, X. C., Liu, J. J., and Pena, R. J. (2005). Composition of HMW and LMW glutenin subunits and their effects on dough properties, pan bread, and noodle quality of Chinese bread wheats. *Cereal Chem.* 82, 345–350. doi: 10.1094/Cc-82-0345

Hermans, W., Mutlu, S., Michalski, A., Langenaeken, N. A., and Courtin, C. M. (2021). The contribution of sub-aleurone cells to wheat endosperm orotein content and gradient is dependent on cultivar and N-fertilization level. *J. Agric. Food Chem.* 69, 6444–6454. doi: 10.1021/acs.jafc.1c01279

Jha, S. K., Ramatshaba, T. S., Wang, G. S., Liang, Y. P., Liu, H., Gao, Y., et al. (2019). Response of growth, yield and water use efficiency of winter wheat to different irrigation methods and scheduling in North China plain. *Agric. Water Manag.* 217, 292–302. doi: 10.1016/j.agwat.2019.03.011

Jiang, P., Xue, J., Duan, L., Gu, Y., Mu, J., Han, S., et al. (2019). Effects of high-molecular-weight glutenin subunit combination in common wheat on the quality of crumb structure. *J. Sci. Food Agric.* 99, 1501–1508. doi: 10.1002/jsfa.9323

Juhasz, A., Makai, S., Sebestyen, E., Tamas, L., and Balazs, E. (2011). Role of conserved non-coding regulatory elements in LMW glutenin gene expression. *PLoS One* 6:e29501. doi: 10.1371/journal.pone.0029501

Justes, E., Mary, B., Meynard, J. M., Machet, J. M., and Thelierhuche, L. (1994). Determination of a critical nitrogen dilution curve for winter-wheat crops. *Ann. Bot.* 74, 397–407. doi: 10.1006/anbo.1994.1133

Kasarda, D. D., Okita, T. W., Bernardin, J. E., Baecker, P. A., Nimmo, C. C., Lew, E. J., et al. (1984). Nucleic acid (cDNA) and amino acid sequences of alpha-type gliadins from wheat (*Triticum aestivum*). *Proc. Natl. Acad. Sci. U. S. A.* 81, 4712–4716. doi: 10.1073/pnas.81.15.4712

Kibite, S., and Evans, L. E. (1984). Causes of negative correlations between grain-yield and grain protein-concentration in common wheat. *Euphytica* 33, 801–810. doi: 10.1007/Bf00021906

Kichey, T., Hirel, B., Heumez, E., Dubois, F., and Le Gouis, J. (2007). In winter wheat (*Triticum aestivum* L.), post-anthesis nitrogen uptake and remobilisation to the grain correlates with agronomic traits and nitrogen physiological markers. *Field Crops Res.* 102, 22–32. doi: 10.1016/j.fcr.2007.01.002

Landolfi, V., Visioli, G., and Blandino, M. (2021). Effect of nitrogen fertilization and fungicide application at heading on the gluten protein composition and rheological quality of wheat. *Agronomy* 11:1687. doi: 10.3390/agronomy11091687

Li, Y. W., An, X. L., Yang, R., Guo, X. M., Yue, G. D., Fan, R. C., et al. (2015). Dissecting and enhancing the contributions of high-molecular-weight glutenin subunits to dough functionality and bread quality. *Mol. Plant* 8, 332–334. doi: 10.1016/j.molp.2014.10.002

Li, J. H., Lina, X., Xie, L., Tian, X., Liu, S. Y., Jin, H., et al. (2021b). TaNAC100 acts as an integrator of seed protein and starch synthesis conferring pleiotropic effects on agronomic traits in wheat. *Plant J.* 108, 829–840. doi: 10.1111/tpj.15485

Li, J. H., Wang, K., Li, G. Y., Li, Y. L., Zhang, Y., Liu, Z. Y., et al. (2019a). Dissecting conserved cis-regulatory modules of Glu-1 promoters which confer the highly active endosperm-specific expression via stable wheat transformation. *Crop J.* 7, 8–18. doi: 10.1016/j.cj.2018.08.003

Li, J., Wang, Z., Yao, C., Zhang, Z., Liu, Y., and Zhang, Y. (2021a). Micro-sprinkling irrigation simultaneously improves grain yield and protein concentration of winter wheat in the North China plain. *Crop J.* 9, 1397–1407. doi: 10.1016/j.cj.2020.12.009

Li, J. P., Wang, Y. Q., Zhang, M., Liu, Y., Xu, X. X., Lin, G., et al. (2019b). Optimized micro-sprinkling irrigation scheduling improves grain yield by increasing the uptake and utilization of water and nitrogen during grain filling in winter wheat. *Agric. Water Manag.* 211, 59–69. doi: 10.1016/j.agwat.2018.09.047

Li, J. P., Xu, X. X., Lin, G., Wang, Y. Q., Liu, Y., Zhang, M., et al. (2018). Micro-irrigation improves grain yield and resource use efficiency by co-locating the roots and N-fertilizer distribution of winter wheat in the North China plain. *Sci. Total Environ.* 643, 367–377. doi: 10.1016/j.scitotenv.2018.06.157

Liang, C. Z., Wang, Y. Q., Zhu, Y. N., Tang, J. Y., Hu, B., Liu, L. C., et al. (2014). OsNAP connects abscisic acid and leaf senescence by fine-tuning abscisic acid biosynthesis and directly targeting senescence-associated genes in rice. *Proc. Natl. Acad. Sci. U. S. A.* 111, 10013–10018. doi: 10.1073/pnas.1321568111

Lindsay, M. P., and Skerritt, J. H. (1999). The glutenin macropolymer of wheat flour doughs: structure-function perspectives. *Trends Food Sci. Technol.* 10, 247–253. doi: 10.1016/S0924-2244(00)00004-2

Liu, J., Feng, B., Xu, Z., Fan, X., Jiang, F., Jin, X., et al. (2018). A genome-wide association study of wheat yield and quality-related traits in Southwest China. *Mol. Breeding* 38, 1–11. doi: 10.1007/s11032-017-0759-9

Liu, Z., Yan, Z., Wan, Y., Liu, K., Zheng, Y., and Wang, D. (2003). Analysis of HMW glutenin subunits and their coding sequences in two diploid Aegilops species. *Theor. Appl. Genet.* 106, 1368–1378. doi: 10.1007/s00122-002-1175-y

Liu, J., Zhang, J., Zhu, G., Zhu, D., and Yan, Y. (2022). Effects of water deficit and high N fertilization on wheat storage protein synthesis, gluten secondary structure, and breadmaking quality. *Crop J.* 10, 216–223. doi: 10.1016/j.cj.2021.04.006

Luo, C., Branlard, G., Griffin, W. B., and McNeil, D. L. (2000). The effect of nitrogen and Sulphur fertilisation and their interaction with genotype on wheat glutenins and quality parameters. *J. Cereal Sci.* 31, 185–194. doi: 10.1006/jcrs.1999.0298

Lyu, X., Liu, Y., Li, N., Ku, L., Hou, Y., and Wen, X. (2021). Foliar applications of various nitrogen (N) forms to winter wheat affect grain protein accumulation and quality via N metabolism and remobilization. *Crop J.* doi: 10.1016/j.cj.2021.10.009 (in press).

Ma, Q., Tao, R., Ding, Y., Zhang, X., Li, F., Zhu, M., et al. (2022). Can split application of slow-release fertilizer improve wheat yield, nitrogen efficiency and their stability in different ecological regions? *Agronomy* 12:407. doi: 10.3390/agronomy12020407

Ma, W. J., Yu, Z. T., She, M. Y., Zhao, Y., and Islam, S. (2019). Wheat gluten protein and its impacts on wheat processing quality. *Front. Agr. Sci. Eng.* 6, 279–287. doi: 10.15302/J-FASE-2019267

Ma, W., Zhang, W., and Gale, K. R. (2003). Multiplex-PCR typing of high molecular weight glutenin alleles in wheat. *Euphytica* 134, 51–60. doi: 10.1023/A:1026191918704

Makai, S., Eva, C., Tamas, L., and Juhasz, A. (2015). Multiple elements controlling the expression of wheat high molecular weight glutenin paralogs. *Funct. Integr. Genomics* 15, 661–672. doi: 10.1007/s10142-015-0441-4

Malik, A. H., Kuktaite, R., and Johansson, E. (2013). Combined effect of genetic and environmental factors on the accumulation of proteins in the wheat grain and their relationship to bread-making quality. *J. Cereal Sci.* 57, 170–174. doi: 10.1016/j.jcs.2012.09.017

McIntosh, R. A., Hart, G. E., and Gale, M. D. (1991). Catalog of gene symbols for wheat - 1991 supplement. *Cereal Res. Commun.* 19, 491–508.

Mena, M., Vicente-Carbajosa, J., Schmidt, R. J., and Carbonero, P. (1998). An endosperm-specific DOF protein from barley, highly conserved in wheat, binds to and activates transcription from the prolamin-box of a native B-hordein promoter in barley endosperm. *Plant J.* 16, 53–62. doi: 10.1046/j.1365-313x.1998.00275.x

Mohan, D., and Gupta, R. K. (2015). Gluten characteristics imparting bread quality in wheats differing for high molecular weight glutenin subunits at Glu D1 locus. *Physiol. Mol. Biol. Plants* 21, 447–451. doi: 10.1007/s12298-015-0298-y

Mottram, D. S., Wedzicha, B. L., and Dodson, A. T. (2002). Acrylamide is formed in the Maillard reaction. *Nature* 419, 448–449. doi: 10.1038/419448a

Muttucumaru, N., Halford, N. G., Elmore, J. S., Dodson, A. T., Parry, M., Shewry, P. R., et al. (2006). Formation of high levels of acrylamide during the processing of flour derived from sulfate-deprived wheat. *J. Agric. Food Chem.* 54, 8951–8955. doi: 10.1021/jf0623081

Ortolan, F., and Steel, C. J. (2017). Protein characteristics that affect the quality of vital wheat gluten to be used in baking: a review. *Compr. Rev. Food Sci. Food Saf.* 16, 369–381. doi: 10.1111/1541-4337.12259

Payne, P. I. (1987). Genetics of wheat storage proteins and the effect of allelic variation on bread-making quality. *Annu. Rev. Plant Physiol. Plant Mol. Biol.* 38, 141–153. doi: 10.1146/annurev.pp.38.060187.001041

Payne, P. I., Holt, L. M., and Law, C. N. (1981). Structural and genetical studies on the high-molecular-weight subunits of wheat glutenin: part 1: allelic variation in subunits amongst varieties of wheat (*Triticum aestivum*). *Theor. Appl. Genet.* 60, 229–236. doi: 10.1007/BF02342544

Payne, P. I., Nightingale, M. A., Krattiger, A. F., and Holt, L. M. (1987). The relationship between hmw glutenin subunit composition and the bread-making quality of british-grown wheat-varieties. *J. Sci. Food Agric.* 40, 51–65. doi: 10.1002/jsfa.2740400108

Peng, Y., Yu, K., Zhang, Y., Islam, S., Sun, D., and Ma, W. (2015). Two novel y-type high molecular weight glutenin genes in chinese wheat landraces of the yangtze-river region. *PLoS One* 10:e0142348. doi: 10.1371/journal.pone.0142348

Qi, L. J., Hu, X. X., Zhou, G. Y., Wang, S., Li, J. M., Lu, W., et al. (2012). Analysis of wheat protein quality in main wheat producing areas of China from 2004 to 2011. *Sci. Agric. Sin.* 45, 4242–4251. doi: 10.3864/j.issn.0578-1752.2012.20.014

Raffan, S., and Halford, N. G. (2019). Acrylamide in food: Progress in and prospects for genetic and agronomic solutions. *Ann. Appl. Biol.* 175, 259–281. doi: 10.1111/aab.12536

Raffan, S., and Halford, N. G. (2021). Cereal asparagine synthetase genes. *Ann. Appl. Biol.* 178, 6–22. doi: 10.1111/aab.12632

Raffan, S., Sparks, C., Huttly, A., Hyde, L., Martignago, D., Mead, A., et al. (2021). Wheat with greatly reduced accumulation of free asparagine in the grain, produced by CRISPR/Cas9 editing of asparagine synthetase gene TaASN2. *Plant Biotechnol. J.* 19, 1602–1613. doi: 10.1111/pbi.13573

Rasheed, A., Xia, X. C., Yan, Y. M., Appels, R., Mahmood, T., and He, Z. H. (2014). Wheat seed storage proteins: advances in molecular genetics, diversity and breeding applications. *J. Cereal Sci.* 60, 11–24. doi: 10.1016/j.jcs.2014.01.020

Ravel, C., Fiquet, S., Boudet, J., Dardevet, M., Vincent, J., Merlino, M., et al. (2014). Conserved cis-regulatory modules in promoters of genes encoding wheat high-molecular-weight glutenin subunits. *Front. Plant Sci.* 5:621. doi: 10.3389/fpls.2014.00621

Ravel, C., Martre, P., Romeuf, I., Dardevet, M., El-Malki, R., Bordes, J., et al. (2009). Nucleotide polymorphism in the wheat transcriptional activator spa influences its pattern of expression and has pleiotropic effects on grain protein composition, dough viscoelasticity, and grain hardness. *Plant Physiol.* 151, 2133–2144. doi: 10.1104/pp.109.146076

Roy, N., Islam, S., Al-Habbar, Z., Yu, Z., Liu, H., Lafiandra, D., et al. (2021). Contribution to breadmaking performance of two different HMW glutenin 1Ay alleles expressed in hexaploid wheat. *J. Agr. Food Chem.* 69, 36–44. doi: 10.1021/acs.jafc.0c03880

Roy, N., Islam, S., Ma, J. H., Lu, M. Q., Torok, K., Tomoskozi, S., et al. (2018). Expressed ay HMW glutenin subunit in Australian wheat cultivars indicates a positive effect on wheat quality. *J. Cereal Sci.* 79, 494–500. doi: 10.1016/j.jcs.2017.12.009

Roy, N., Islam, S., Yu, Z. T., Lu, M. Q., Lafiandra, D., Zhao, Y., et al. (2020). Introgression of an expressed HMW 1Ay glutenin subunit allele into bread wheat cv. Lincoln increases grain protein content and breadmaking quality without yield penalty. *Theor. Appl. Genet.* 133, 517–528. doi: 10.1007/s00122-019-03483-1

Sánchez-León, S., Gil-Humanes, J., Ozuna, C. V., Gimenez, M. J., Sousa, C., Voytas, D. F., et al. (2018). Low-gluten, nontransgenic wheat engineered with CRISPR/Cas9. *Plant Biotechnol. J.* 16, 902–910. doi: 10.1111/pbi.12837

Scherf, K. A., Ciccocioppo, R., Pohanka, M., Rimarova, K., Opatrilova, R., Rodrigo, L., et al. (2016a). Biosensors for the diagnosis of celiac disease: current status and future perspectives. *Mol. Biotechnol.* 58, 381–392. doi: 10.1007/s12033-016-9940-3

Scherf, K. A., Koehler, P., and Wieser, H. (2016b). Gluten and wheat sensitivities - An overview. *J. Cereal Sci.* 67, 2–11. doi: 10.1016/j.jcs.2015.07.008

Scherf, K. A., Wieser, H., and Koehler, P. (2018). Novel approaches for enzymatic gluten degradation to create high-quality gluten-free products. *Food Res. Int.* 110, 62–72. doi: 10.1016/j.foodres.2016.11.021

Sharma, A., Garg, S., Sheikh, I., Vyas, P., and Dhaliwal, H. S. (2020). Effect of wheat grain protein composition on end-use quality. *J. Food Sci. Technol.* 57, 2771–2785. doi: 10.1007/s13197-019-04222-6

She, M., Ye, X., Yan, Y., Howit, C., Belgard, M., and Ma, W. (2011). Gene networks in the synthesis and deposition of protein polymers during grain

development of wheat. *Funct. Integr. Genomics* 11, 23–35. doi: 10.1007/s10142-010-0196-x

Shen, L. S., Luo, G. B., Song, Y. H., Xu, J. Y., Ji, J. J., Zhang, C., et al. (2021). A novel NAC family transcription factor SPR suppresses seed storage protein synthesis in wheat. *Plant Biotechnol. J.* 19, 992–1007. doi: 10.1111/pbi.13524

Shewry, P. R., and Halford, N. G. (2002). Cereal seed storage proteins: structures, properties and role in grain utilization. *J. Exp. Bot.* 53, 947–958. doi: 10.1093/jexbot/53.370.947

Shewry, P. R., Halford, N. G., Belton, P. S., and Tatham, A. S. (2002). The structure and properties of gluten: an elastic protein from wheat grain. *Philos. Trans. R. Soc. Lond. Ser. B Biol. Sci.* 357, 133–142. doi: 10.1098/rstb.2001.1024

Shewry, P. R., Napier, J. A., and Tatham, A. S. (1995). Seed storage proteins: structures and biosynthesis. *Plant Cell* 7, 945–956. doi: 10.1105/tpc.7.7.945

Shewry, P. R., and Tatham, A. S. (1997). Disulphide bonds in wheat gluten proteins. *J. Cereal Sci.* 25, 207–227. doi: 10.1006/jcrs.1996.0100

Stadler, R. H., Blank, I., Varga, N., Robert, F., Hau, J., Guy, P. A., et al. (2002). Acrylamide from maillard reaction products. *Nature* 419, 449–450. doi: 10.1038/419449a

Sultana, H., Armstrong, R., Suter, H., Chen, D. L., and Nicolas, M. E. (2017). A short-term study of wheat grain protein response to post-anthesis foliar nitrogen application under elevated CO2 and supplementary irrigation. *J. Cereal Sci.* 75, 135–137. doi: 10.1016/j.jcs.2017.03.031

Sun, X., Hu, S., Liu, X., Qian, W., Hao, S., Zhang, A., et al. (2006). Characterization of the HMW glutenin subunits from Aegilops searsii and identification of a novel variant HMW glutenin subunit. *Theor. Appl. Genet.* 113, 631–641. doi: 10.1007/s00122-006-0327-x

Sun, F. S., Liu, X. Y., Wei, Q. H., Liu, J. N., Yang, T. X., Jia, L. Y., et al. (2017). Functional characterization of TaFUSCA3, a B3-superfamily transcription factor gene in the wheat. *Front. Plant Sci.* 8:1133. doi: 10.3389/fpls.2017.01133

Uauy, C., Distelfeld, A., Fahima, T., Blechl, A., and Dubcovsky, J. (2006). A NAC gene regulating senescence improves grain protein, zinc, and iron content in wheat. *Science* 314, 1298–1301. doi: 10.1126/science.1133649

Vasila, I. K., and Anderson, O. D. (1997). Genetic engineering of wheat gluten. *Trends Plant Sci.* 2, 292–297. doi: 10.1016/S1360-1385(97)89950-5

Veraverbeke, W. S., and Delcour, J. A. (2002). Wheat protein composition and properties of wheat glutenin in relation to breadmaking functionality. *Crit. Rev. Food Sci. Nutr.* 42, 179–208. doi: 10.1080/10408690290825510

Wang, L., Chen, A., Lin, Z., Zhao, R., Lan, J., and Dai, C (2013). GB/T 17320–2013: Quality Classification of Wheat Varieties; General Administration of Quality Supervision, Inspection and Quarantine of P.R.C: Beijing, China.

Wang, D., Li, F., Cao, S., and Zhang, K. (2020). Genomic and functional genomics analyses of gluten proteins and prospect for simultaneous improvement of end-use and health-related traits in wheat. *Theor. Appl. Genet.* 133, 1521–1539. doi: 10.1007/s00122-020-03557-5

Wen, S. S., Wen, N. A., Pang, J. S., Langen, G., Brew-Appiah, R. A. T., Mejias, J. H., et al. (2012). Structural genes of wheat and barley 5-methylcytosine DNA glycosylases and their potential applications for human health. *Proc. Natl. Acad. Sci. U. S. A.* 109, 20543–20548. doi: 10.1073/pnas.1217927109

Wieser, H. (2007). Chemistry of gluten proteins. *Food Microbiol.* 24, 115–119. doi: 10.1016/j.fm.2006.07.004

Xia, J., Zhu, D., Chang, H., Yan, X., and Yan, Y. (2020). Effects of water-deficit and high-nitrogen treatments on wheat resistant starch crystalline structure and physicochemical properties. *Carbohydr. Polym.* 234:115905. doi: 10.1016/j.carbpol.2020.115905

Xia, J., Zhu, D., Wang, R. M., Cui, Y., and Yan, Y. M. (2018). Crop resistant starch and genetic improvement: a review of recent advances. *Theor. Appl. Genet.* 131, 2495–2511. doi: 10.1007/s00122-018-3221-4

Xu, H. W., Curtis, T. Y., Powers, S. J., Raffan, S., Gao, R. H., Huang, J. H., et al. (2018a). Genomic, biochemical, and modeling analyses of asparagine synthetases from wheat. *Front. Plant Sci.* 8:2237. doi: 10.3389/fpls.2017.02237

Xu, X. X., Zhang, M., Li, J. P., Liu, Z. Q., Zhao, Z. G., Zhang, Y. H., et al. (2018b). Improving water use efficiency and grain yield of winter wheat by optimizing irrigations in the North China plain. *Field Crops Res.* 221, 219–227. doi: 10.1016/j.fcr.2018.02.011

Xue, L., Li, Y., Li, T., Pan, H., Liu, J., Fan, M., et al. (2019). Phosphorylation and enzymatic hydrolysis with alcalase and papain effectively reduce allergic reactions to gliadins in normal mice. *J. Agric. Food Chem.* 67, 6313–6323. doi: 10.1021/acs.jafc.9b00569

Xue, G. P., Way, H. M., Richardson, T., Drenth, J., Joyce, P. A., and McIntyre, C. L. (2011). Overexpression of TaNAC69 leads to enhanced transcript levels of stress up-regulated genes and dehydration tolerance in bread wheat. *Mol. Plant* 4, 697–712. doi: 10.1093/mp/ssr013

Yang, R. C., Juhasz, A., Zhang, Y. J., Chen, X. Y., Zhang, Y. J., She, M. Y., et al. (2018). Molecular characterisation of the NAM-1 genes in bread wheat in Australia. *Crop Pasture Sci.* 69, 1173–1181. doi: 10.1071/Cp18273

Yu, Z., Islam, S., She, M., Diepeveen, D., Zhang, Y., Tang, G., et al. (2018a). Wheat grain protein accumulation and polymerization mechanisms driven by nitrogen fertilization. *Plant J.* 96, 1160–1177. doi: 10.1111/tpj.14096

Yu, Z., Juhasz, A., Islam, S., Diepeveen, D., Zhang, J., Wang, P., et al. (2018b). Impact of mid-season Sulphur deficiency on wheat nitrogen metabolism and biosynthesis of grain protein. *Sci. Rep.* 8:2499. doi: 10.1038/s41598-018-20935-8

Yu, Z. T., Peng, Y. C., Islam, M. S., She, M. Y., Lu, M. Q., Lafiandra, D., et al. (2019). Molecular characterization and phylogenetic analysis of active y-type high molecular weight glutenin subunit genes at Glu-A1 locus in wheat. *J. Cereal Sci.* 86, 9–14. doi: 10.1016/j.jcs.2019.01.003

Yu, Z., She, M., Zheng, T., Diepeveen, D., Islam, S., Zhao, Y., et al. (2021). Impact and mechanism of Sulphur-deficiency on modern wheat farming nitrogen-related sustainability and gliadin content. *Commun. Biol.* 4:945. doi: 10.1038/s42003-021-02458-7

Zebarth, B. J., Botha, E. J., and Rees, H. (2007). Rate and time of fertilizer nitrogen application on yield, protein and apparent efficiency of fertilizer nitrogen use of spring wheat. *Can. J. Plant Sci.* 87, 709–718. doi: 10.4141/Cjps06001

Zhang, P. P., He, Z. H., Chen, D. S., Zhang, Y., Larroque, O. R., and Xia, X. C. (2007). Contribution of common wheat protein fractions to dough properties and quality of northern-style Chinese steamed bread. *J. Cereal Sci.* 46, 1–10. doi: 10.1016/j.jcs.2006.10.007

Zhang, P. P., Jondiko, T. O., Tilley, M., and Awika, J. M. (2014b). Effect of high molecular weight glutenin subunit composition in common wheat on dough properties and steamed bread quality. *J. Sci. Food Agric.* 94, 2801–2806. doi: 10.1002/jsfa.6635

Zhang, M., Ma, C. Y., Lv, D. W., Zhen, S. M., Li, X. H., and Yan, Y. M. (2014a). Comparative phosphoproteome analysis of the developing grains in bread wheat (*Triticum aestivum* L.) under well-watered and water-deficit conditions. *J. Proteome Res.* 13, 4281–4297. doi: 10.1021/pr500400t

Zhang, F. L., Wang, C. M., and Li, D. (2021). Study on the quality evaluation of steamed bread and the physical and chemical properties of wheat. *Agricul. Biotechnol.* 10, 125–127. doi: 10.19759/j.cnki.2164-4993.2021.02.029

Zhao, F., Hawkesford, M., and McGrath, S. (1999a). Sulphur assimilation and effects on yield and quality of wheat. *J. Cereal Sci.* 30, 1–17. doi: 10.1006/jcrs.1998.0241

Zhao, F. J., Salmon, S. E., Withers, P. J. A., Monaghan, J. M., Evans, E. J., Shewry, P. R., et al. (1999b). Variation in the breadmaking quality and rheological properties of wheat in relation to Sulphur nutrition under field conditions. *J. Cereal Sci.* 30, 19–31. doi: 10.1006/jcrs.1998.0244

Zhen, S. M., Deng, X., Li, M. F., Zhu, D., and Yan, Y. M. (2018). 2D-DIGE comparative proteomic analysis of developing wheat grains under high-nitrogen fertilization revealed key differentially accumulated proteins that promote storage protein and starch biosyntheses. *Anal. Bioanal. Chem.* 410, 6219–6235. doi: 10.1007/s00216-018-1230-4

Zhen, S. M., Deng, X., Xu, X. X., Liu, N. N., Zhu, D., Wang, Z. M., et al. (2020). Effect of high-nitrogen fertilizer on gliadin and glutenin subproteomes during kernel development in wheat (*Triticum aestivum* L.). *Crop J.* 8, 38–52. doi: 10.1016/j.cj.2019.06.002

Zheng, W., Peng, Y. C., Ma, J. H., Appels, R., Sun, D. F., and Ma, W. J. (2011). High frequency of abnormal high molecular weight glutenin alleles in Chinese wheat landraces of the Yangtze-River region. *J. Cereal Sci.* 54, 401–408. doi: 10.1016/j.jcs.2011.08.004

Zhong, Y., Vidkjær, N. H., Massange-Sanchez, J. A., Laursen, B. B., Gislum, R., Borg, S., et al. (2020). Changes in spatiotemporal protein and amino acid gradients in wheat caryopsis after N-topdressing. *Plant Sci.* 291:110336. doi: 10.1016/j.plantsci.2019.110336

Zhong, Y., Wang, W., Huang, X., Liu, M., Hebelstrup, K., Yang, D., et al. (2019). Nitrogen topdressing timing modifies the gluten quality and grain hardness related protein levels as revealed by iTRAQ. *Food Chem.* 277, 135–144. doi: 10.1016/j.foodchem.2018.10.071

Zhong, Y., Xu, D., Hebelstrup, K. H., Yang, D., Cai, J., Wang, X., et al. (2018). Nitrogen topdressing timing modifies free amino acids profiles and storage protein gene expression in wheat grain. *BMC Plant Biol.* 18:353. doi: 10.1186/s12870-018-1563-3.doi:10.1186/s12870-018-1563-3

Zhou, J. X., Liu, D. M., Deng, X., Zhen, S. M., Wang, Z. M., and Yan, Y. M. (2018). Effects of water deficit on breadmaking quality and storage protein compositions in bread wheat (*Triticum aestivum* L.). *J. Sci. Food Agric.* 98, 4357–4368. doi: 10.1002/jsfa.8968

Zhou, Z., Liu, C., Qin, M., Li, W., Hou, J., Shi, X., et al. (2022). Promoter DNA hypermethylation of *TaGli-γ-2.1* positively regulates gluten strength in bread wheat. *J. Adv. Res.* 36, 163–173. doi: 10.1016/j.jare.2021.06.021

Zhu, J. T., Fang, L. L., Yu, J. Q., Zhao, Y., Chen, F. G., and Xia, G. M. (2018). 5-Azacytidine treatment and TaPBF-D over-expression increases glutenin accumulation within the wheat grain by hypomethylating the Glu-1 promoters. *Theor. Appl. Genet.* 131, 735–746. doi: 10.1007/s00122-017-3032-z

Zhu, D., Zhu, G. R., Zhang, Z., Wang, Z. M., Yan, X., and Yan, Y. M. (2020). Effects of independent and combined water-deficit and high-nitrogen treatments on flag leaf proteomes during wheat grain development. *Int. J. Mol. Sci.* 21:2098. doi: 10.3390/ijms21062098

Zyzak, D. V., Sanders, R. A., Stojanovic, M., Tallmadge, D. H., Eberhart, B. L., Ewald, D. K., et al. (2003). Acrylamide formation mechanism in heated foods. *J. Agric. Food Chem.* 51, 4782–4787. doi: 10.1021/jf034180i

Conflict of Interest: The authors declare that the research was conducted in the absence of any commercial or financial relationships that could be construed as a potential conflict of interest.

Publisher's Note: All claims expressed in this article are solely those of the authors and do not necessarily represent those of their affiliated organizations, or those of the publisher, the editors and the reviewers. Any product that may be evaluated in this article, or claim that may be made by its manufacturer, is not guaranteed or endorsed by the publisher.

frontiers | Frontiers in Plant Science

ORIGINAL RESEARCH
published: 12 May 2022
doi: 10.3389/fpls.2022.835164

Premature Termination Codon of *1Dy12* Gene Improves Cookie Quality in Ningmai9 Wheat

Guangxiao Liu[1†], Yujiao Gao[1†], Huadun Wang[2], Yonggang Wang[1], Jianmin Chen[1], Pingping Zhang[2] and Hongxiang Ma[1*]*

[1] Jiangsu Co-innovation Center for Modern Production Technology of Grain Crops/Jiangsu Key Lab of Crop Genomics and Molecular Breeding, Yangzhou University, Yangzhou, China, [2] Co-innovation Center for Modern Crop Production Co-sponsored by Province and Ministry, Jiangsu Academy of Agricultural Sciences, Nanjing, China

The area between middle and lower reaches of the Yangtze River is the largest region for soft wheat production in China. In soft wheat breeding, the lack of germplasm with desirable quality for end-use products is a barrier. Ningmai9 is the main variety of soft wheat planted in this area. To create germplasm with better quality and yield potential than Ningmai9, mutants of HMW-GSs in Ningmai9 induced by ethylmethanesulfonate (EMS) were obtained. SDS-PAGE showed that two mutants, md10 and md11, were HMW-GS 1Dy deletions. DNA sequencing confirmed that one mutation was caused by a C/T substitution, resulting in the change of CAA encoding glutamine into the termination codon TAA, and another mutation was due to a G/A substitution in the central repetitive domain of the coding region, causing TGG encoding tryptophan to become the termination codon TGA. The premature termination codon of the *1Dy12* gene affected the expression of *1Dy12* and kept the mRNA at a lower transcription level during the kernel development stage in comparison with the wild type. HMW-GS 1Dy12 deletion mutants decreased the content of HMW-GSs and glutenin macropolymers, mixograph envelope peak time and TIMEX width, water solvent retention capacity (WSRC), and lactic acid solvent retention capacity (LASRC). In the HMW-GS 1Dy12 deletion lines, the sugar-snap cookie diameter was 8.70–8.74 cm, which was significantly larger than that in the wild type of 8.0 cm. There were no significant differences in spike number, kernel number, thousand kernel weight, and yield between the deletion lines and wild type. Overall, the study indicated that the knockout of the *HMW-GS* gene induced by EMS is an effective way to improve wheat quality, and deletion mutants of HMW-GS 1Dy12 decrease gluten strength and increase sugar snap cookie diameter without yield penalty in Ningmai9 wheat.

Keywords: wheat, quality, mutant, HMW-GS, cookie

OPEN ACCESS

Edited by:
Awais Rasheed,
Quaid-i-Azam University, Pakistan

Reviewed by:
Zhengqiang Ma,
Nanjing Agricultural University, China
Satinder Kaur,
Punjab Agricultural University, India

****Correspondence:***
Hongxiang Ma
mahx@yzu.edu.cn
Pingping Zhang
pp_zh@126.com

[†]These authors have contributed equally to this work

Specialty section:
This article was submitted to Crop and Product Physiology, a section of the journal Frontiers in Plant Science

Received: *14 December 2021*
Accepted: *12 April 2022*
Published: *12 May 2022*

Citation:
Liu G, Gao Y, Wang H, Wang Y, Chen J, Zhang P and Ma H (2022) Premature Termination Codon of 1Dy12 Gene Improves Cookie Quality in Ningmai9 Wheat. Front. Plant Sci. 13:835164. doi: 10.3389/fpls.2022.835164

INTRODUCTION

Wheat is a primary staple food crop worldwide and has specific quality requirements for particular end uses, such as bread, cake, biscuit, and noodle. Improving processing quality is one of the major targets in wheat breeding. Hard and soft wheat are two basic market classes of wheat. Hard wheat flour usually has high protein content, strong gluten strength, and high water absorption,

which enhances yeast growth and increases bread volume, whereas soft wheat flour has low protein content, less water absorption, and a small particle size distribution, which improves dough flow and product texture associated with cookie, cake, and cracker (Souza et al., 2002).

Wheat grain protein is divided into gluten and non-gluten fractions, and the wheat processing quality mainly depends on the gluten fractions (Ma W. et al., 2019). Wheat gluten is regarded as the major determinant of dough elasticity and viscosity, largely affecting the processing properties of wheat flour suitable for leavened bread and other bakery products (Shewry, 2019). Wheat gluten is comprised of many types of proteins, which are traditionally categorized into two groups, namely, glutenins and gliadins, in approximately equal amounts. Glutenins are assembled into polymers stabilized by interchain disulfide bonds, whereas gliadins are present as single polypeptide chains (Shewry and Halford, 2002; Lambourne et al., 2010). The polymeric glutenins include high molecular weight glutenin subunits (HMW-GSs) and low molecular weight glutenin subunits (LMW-GSs) (Rasheed et al., 2014). HMW-GSs are at relatively low levels in wheat grains, accounting for 5–10% of the storage proteins (Branlard and Dardevet, 1985; He et al., 2005); however, they provide disulfide-bonded backbones in the gluten network and are recognized as the most important components in determining the strength and elasticity of wheat gluten (Shewry et al., 2003; Li et al., 2021). Three homoeologous alleles *Glu-A1*, *Glu-B1*, and *Glu-D1* encode HMW-GSs at the *Glu-1* loci on the long arms of group 1 chromosomes in wheat (Payne et al., 1981). There are two tightly linked genes at each HMW-GS locus, encoding an x-type (80–88 kDa) and a y-type (67–73 kDa) subunits. Theoretically, six different HMW-GSs are involved in wheat, but in fact, there are only three to five HMW-GSs in most wheat cultivars (Payne, 1987). The genes of *1Bx*, *1Dx*, and *1Dy* are present in most cases, whereas the genes of *1Ay* are usually silenced (Roy et al., 2018; Yu et al., 2019). Each *HMW-GS* gene has multiple alleles, which constructs different composition among different varieties of wheat and other species of *Triticeae* (Liu et al., 2005). So far, more than 30 alleles of *HMW-GS* genes have been isolated, and the sequences of HMW-GSs are highly conserved and share the same primary structure composed of a signal peptide, an N-terminal domain, a central repetitive domain, and a C-terminal domain. The majority of x-type subunits possess four conserved cysteine residues, and the y-type subunits generally contain seven conserved cysteine residues. Different subunits possess different numbers of cysteines (Rasheed et al., 2014; Ma W. et al., 2019). The cysteine residues in both x-type and y-type subunits form glutenin macropolymers (GMPs) in the gluten complex in dough by intermolecular disulfide bonding. Based on SDS extractability, the GMP complexes are divided into SDS-unextractable polymeric protein (UPP) and SDS-extractable polymeric protein (EPP) (Ma W. et al., 2019). UPP contains larger GMP complexes, while EPP is composed of smaller GMP complexes. The ratio of UPP% is positively correlated with gluten and dough strength (Shewry and Tatham, 1997).

High molecular weight glutenin subunits and their combinations affect the physical and physicochemical properties of dough. Some subunit combinations, such as 1Dx5 + 1Dy10, 1Bx7 + 1By8, and 1Bx17 + 1By18, are desirable subunits for bread-making quality by contributing to superior dough strength and elasticity, whereas other subunit combinations, such as 1Dx2 + 1Dy12, 1Bx20, and 1Bx7 + 1By9, decrease dough strength (Shewry et al., 1992; Yan et al., 2009; Liu et al., 2016; Guo et al., 2019; Jiang et al., 2019).

The main biological function of storage protein is to provide nutrition and energy sources for seed germination and seedling growth in wheat. Mutations of *HMW-GS* gene silencing are not fatal for the plant, so the selection pressure on these genes has less effect on the growth and development of wheat than that on functional genes (Liu et al., 2008). As a result, these genes can be modified to create more mutations to improve the processing quality of wheat breeding. However, as shown in previous reports, the effect of silencing HWM-GSs on end-use products, especially in soft wheat, was not consistent. The deletion of all HMW-GSs significantly reduced the dough strength, GMP content, and bread-backing quality (Zhang Y. et al., 2018). The loaf volumes of the five knockout mutants with the deletion of one or two HMW-GS genes in *1Ax1*, *1Bx14*, *1By15*, *1Dx2*, and *1Dy12* were significantly smaller than those of the wild-type Xiaoyan54 (Li et al., 2015). Wang et al. (2017) found that the *Glu-D1* locus had a greater effect on bread-processing quality than the loci of Glu-A1 and Glu-B1, and 1Dx2 had a stronger function than 1Dy12 in promoting functional glutenin macropolymers by comparing two series of genetic mutants. The contribution of each of the HMW-GS to the bread-processing quality of deletion lines missing the loci *Glu-A1*, *Glu-B1*, and *Glu-D1* created by the ion beam methods showed that the genetic effects of the *Glu-1* locus on gluten functionality were *Glu-D1* > *Glu-B1* > *Glu-A1* (Yang et al., 2014). Ram et al. (2007) reported that double nulls of x-type and y-type subunits at the *Glu-D1* locus were associated with reduced gluten strength and suitable for biscuit making in the Indian wheat landrace Nap Hal, which might be useful in soft wheat breeding. Two lines containing Glu-Bx17 and By18 HMW-GSs and lacking *Glu-A1* and *Glu-D1* significantly increased tortilla diameters (Mondal et al., 2008). The deletion lines decreased UPP, HMW/LMW, and dough extensibility compared with non-deletion lines (Zhang P. et al., 2014). Gao et al. (2018) found that the dough development and stability time were significantly reduced in near-isogenic lines with the deletion of 1Ax1 or 1Dx2, but the uniformity of the microstructure in wheat was increased. Knocking-out 1Bx7 or 1By9 significantly decreased the accumulation of gluten proteins and weakened dough strength, which led to an inferior sponge cake quality (Chen et al., 2019). Recent research showed that 1Dy missing had a negative impact on the quality of bread, sponge cake, and biscuit (Chen et al., 2021).

China is one of the world's largest wheat producers, with output reaching more than 130 million tons in 2020, according to the statistics of Ministry of Agriculture and Rural Affairs of the People's Republic of China. To meet the market demand, Chinese scientists began focusing on wheat quality improvement in the last 30 years (Wang et al., 2018). Many hard white wheat cultivars with good end-use quality were released in northern China (Zhang et al., 2007; Li et al., 2019). However, the improvement in soft wheat quality was less than that in hard wheat (Yao et al., 2014). Soft wheat consumption has significantly

increased, reaching more than six million metric tons annually in China. Soft wheat quality improvement is highlighted of great importance in production, especially in the middle to lower reaches of the Yangtze River for winter wheat growing. This is the best region for soft red winter wheat production in China (Zhang et al., 2012).

A lack of germplasm with desirable quality for end-use products is a barrier to soft wheat breeding in China. Most soft wheat varieties with good quality from the United States or Australia are hard to use in direct wheat breeding and production in China as the yield potential and the resistance to biotic or abiotic stress are not adapted to the local ecological regions in China. Zhang et al. (2007) evaluated the quality of soft wheat varieties in China and found that only three varieties were considered good soft wheat with acceptable cookie-making qualities. Ningmai9 is the major variety used in the middle and lower reaches of the Yangtze River, which has desirable agronomic traits and has had stable soft wheat quality across variable regions for many years. In addition, Ningmai9 is a founder parent in wheat breeding and has derived 23 released varieties for wheat production so far (Ma H. et al., 2019).

Soft wheat flour is suitable for producing cookie, cake, and cracker. It usually needs smaller flour particles, higher amylose content, and fewer gluten proteins than hard wheat. The variation of gluten protein in soft wheat weakens the gluten network in dough. There were significant positive correlations between high molecular weight polymeric protein fractions and single kernel hardness index as well as mixograph water absorption/tolerance, but a negative correlation with break flour yield, cookie diameter, and cake volume in soft wheat (Ohm et al., 2009). To meet the urgent demand for soft wheat breeding in China, we developed a set of deletion mutants of HMW-GSs in Ningmai9 (Zhang J. et al., 2014). This research is expected to identify the molecular mechanisms and functions of HMW-GS deletion mutants and their effects on cookie quality, so as to evaluate their yield potential and provide useful materials in the breeding and production of soft wheat.

MATERIALS AND METHODS

Plant Materials and Field Experiment Design

Wheat seeds were treated by 0.4% EMS and sowed in the experiment station of Jiangsu Academy of Agricultural Sciences (Zhang J. et al., 2014). M_2 and M_3 seeds of EMS-mutagenized population were harvested and screened for the variation of HMW-GS. The wild type is a soft wheat variety, Ningmai9, which was released by the Jiangsu Academy of Agricultural Sciences using an intervarietal cross of Yangmai 6/Xifeng. The HMW-GS composition of Ningmai9 consists of 1Ax, 1Bx7, 1By8, 1Dx2, and 1Dy12. After three generations of self-pollination and selection, we planted M_7 seeds of mutant lines and the wild type at the experimental station. The field experiment was designed as a randomized complete block experiment for one factor. Each treatment had a plot size of 5 m^2, with a seed density of 2.4×10^6 ha^{-1} and a row spacing of 25 cm. There were three replications in each treatment. The spike number was measured at the maturity stage. The yield in each plot was calculated after harvest. Other agronomic traits, including plant height, kernel number per spike, and thousand kernel weight, were examined using an average of 10 plants randomly collected from each plot. The seeds were harvested and mixed up for a grain quality test in each plot.

Five immature kernels were collected from mutants and wild types in the middle part of the selected spikes at 7, 11, 14, and 21 days after anthesis. The collected samples were immediately frozen in liquid nitrogen and then used to extract RNA for gene expression analysis.

SDS-Polyacrylamide Gel Electrophoresis Assay for Seed Storage Proteins

High molecular weight glutenin subunits were separated by SDS-PAGE according to the method described previously (Khan et al., 1989). In brief, a 40 mg grain was ground and defatted with chloroform in a 2 ml Eppendorf tube. The tube with sample was subsequently mixed with 1 ml of extraction buffer, which contained 62.5 mmol l^{-1} Tris–HCl (pH6.8), 10% glycerol, 2% SDS, and 5% β-mercaptoethanol. The mixture was incubated at room temperature for 30 min with unremitting shaking, and then incubated at 90°C for 5 min. Thereafter, the sample was centrifuged at 8,000 × *g* for 15 min. The supernatant was used for SDS-PAGE.

The acrylamide concentration was 10 and 4% in the resolving gel and stacking gel, respectively. In total, 25 ml of glutenin extract was loaded in each lane for 10 h of electrophoresis. The resolving gel was then stained with 0.05% Coomassie Brilliant Blue R250 for 24 h, followed by destaining in distilled water for 48 h until the bands were clearly distinguished. The destained gel was then scanned using VersaDoc Model 5000 Imaging Systems and analyzed for the preliminary content of each HMW-GS with Quantity 1-D Analysis Software (Bio-Rad Laboratories, Irvine, CA, United States). Afterward, each band was cut separately from the gel and placed in an Eppendorf tube. A 500–1,000 ml mixture of 50% isopropyl alcohol containing 3% SDS was added to the tube according to the content of each band, and then the tube was placed for incubation at 37°C for 24 h until the gel cleared. The extraction was then detected at a wavelength of 595 nm using a UV-2401 Shimadzu spectrophotometer.

The standard protein (116 kD, Sigma) was dissolved in 20, 30, and 40 ml volumes and loaded in three lanes on the same gel, and the standard curve was obtained according to the content of the standard protein extracted and measured following the above steps for quantification. Each HMW-GS of collected samples was then quantified based on the standard curve.

DNA Extraction and PCR Amplification

Genomic DNA was extracted from the leaves of a 3-week-old seedling using the cetyl trimethyl ammonium bromide (CTAB) method. The forward primer (5′-GGCTAACAGACACCCAAAC-3′) and reverse primer (5′-TGTGAACACGCATCACGT-3′) for specific detection of 1Dy12 were designed according to published DNA sequences

to amplify the complete coding sequence in mutants and wild type. TksGflex DNA polymerase (TaKaRa, Shanghai, China) was used for the amplification. In each reaction, 500 ng of genomic DNA, 1× Gflex buffer, 1 μl of Tkspolymerase, and a concentration of 0.2 μM of each primer were added to the tube in a volume of 50 μl of double-distilled water. The PCR was run in a Bio-rad T100 thermal cycler starting with 2 min at 94°C, followed by 35 cycles of denaturing at 98°C for 10 s, annealing for 15 s at 60°C, and extension at 68°C for 90 s, with a final extension of 5 min at 68°C. The PCR products were separated on 1.0% agarose gels at 170 V for 10 min.

1Dy Gene Cloning and Sequencing

The target DNA fragments were cut from the agarose gel and purified using the TIAN gel Midi Purification Kit (TIANGEN BIOTECH, Beijing, China). Purified regenerants were then ligated into the pEASY-Blunt Simple Cloning Kit (TransGen Biotech, Beijing, China) and transformed into *Escherichia coli* Trans1-T1 Phage Resistant Chemically Competent Cells (TransGen Biotech, Beijing, China). The transformed cells were tiled on ampicillin LB medium containing IPTG and X-Gal for culturing at 37°C for 12–16 h. The positive clones were amplified to test for the target fragment, which was then sent to Takara Bio (Shanghai, China) for sequencing. DNAMAN version 6.0 software (Lynnon Biosoft, San Ramon, United States) and BioEdit version 7.1.3 software were used for assembling and aligning the gene sequences.

RNA Extraction and Quantitative Reverse Transcription-PCR

Wheat kernels from all spikelets of spike were collected from mutants and wild types at different grain development stages from anthesis to harvest. The total RNAs of collected kernels were extracted using the Promega (Madison, WI, United States) SV total RNA isolation system (Promega, United States). The RNA PCR Kit (AMV) version 3.0 (Takara Bio, Shanghai, China) was used for synthesizing the first-strand cDNAs. In addition, 10 μl 2× RealStar Green Fast Mixture with ROXII, 0.6 μl primer mix (10 μM) each for 1Dy12, 1 μl first-strand cDNA, and 8.2 μl ddH_2O were added to a 20 μl reaction volume for qRT-PCR. The reactants were amplified using an ABI PRISM 7500 Real-Time PCR System (ABI, Redwood City, CA, United States) starting with 2 min at 94°C, followed by 50 cycles of denaturing at 95°C for 20 s, annealing for 20 s at 55°C, and extension at 72°C for 20 s. The tubulin gene was used as an endogenous control gene. Data from individual runs were collated using the $2^{-\Delta\Delta CT}$ method (Livak and Schmittgen, 2001).

Polymeric Protein Examined by High-Performance Liquid Chromatography

The SDS extractable and unextractable proteins were extracted, and HPLC analysis was conducted according to the method described previously (Larroque et al., 2000). A total of 10 mg of flour sample in a 1.5-ml microfuge tube was mixed with 1 ml of 0.5% SDS in 0.05 M of phosphate extraction buffer (PEB). The mixture was subjected to a 1 min vortex and centrifuged at 14,000 rpm for 15 min. After centrifugation, the SDS-soluble fraction was separated on supernatant and subsequently decanted into a clean 1.5-ml microfuge tube. The remaining pellet in the microfuge tube was mixed with 1 ml of PEB for resuspending and subjected to a 30 s sonication. The sample was then subjected to centrifugation for 15 min at 14,000 rpm. The supernatant was an SDS-insoluble fraction. The SDS-insoluble fraction was transferred to a clean 1.5-ml microfuge tube. Both SDS-soluble and insoluble fractions were subjected to an 80°C water bath for 2 min to inactivate proteases and then filtered into 2 ml glass vials for HPLC. The percentage of SDS-unextractable polymeric protein in total polymeric protein (UPP/UPP + EPP) was calculated based on the ratio of the peak area for unextractable polymeric protein relative to the total area of both the extractable and unextractable polymeric protein.

Quality Testing of Grain, Flour, and Sugar Snap Cookie

Grain protein content (GPC) was determined using a near-infrared reflectance spectroscopy analyzer (NIR) (Perten DA 7200, Perten Instruments, Huddinge, Sweden) following AACC method 39-10 (AACC 2000). Wet gluten content was examined based on the National Standards of China (GB/T5506.2-2008 and GB/T5506.4-2008). The results were expressed on a 14% moisture basis.

Hardness and diameter of the grain were tested using the Single Kernel Characterization System (SKCS 4100, Perten Instruments Co., Ltd., Stockholm, Sweden) of AACC method 55-31.03 (AACC 2000).

For milling, grain samples were cleaned and adjusted to 14.5% moisture for 18 h. Grain samples were then roller-milled to straight-grade flours according to AACC 26-31 using a Buhler Experimental Mill [MLU-202, Buhler Equipment Engineering (Wuxi) Co., Ltd., Jiangsu, China]. The yield of straight-grade flour was about 70%.

Solvent retention capacity (SRC) of flour, including water solvent retention capacity (WSRC), sodium carbonate solvent retention capacity (SCSRC), lactic acid solvent retention capacity (LASRC), and sucrose solvent retention capacity (SUSRC), were measured according to AACC method 56-11 (AACC 2000). Dough rheological properties were determined using mixograph according to AACC 54-40.02. Sugar snap cookie was processed according to AACC 10-52, and the cookie diameter was noted.

Statistical Analysis

A significant difference in the tested characters between deletion mutants and wild type was determined using analysis of variance (ANOVA) and Student's *t*-test. The criterion for statistical significance was set at $P < 0.01$ and $P < 0.05$.

RESULTS

Identification of 1Dy12 Mutants

SDS-PAGE analysis showed that the composition of HMW-GSs in the soft wheat Ningmai9 was 1Ax1, 1Bx7, 1By8, 1Dx2, and

1Dy12. In total, 3,781 lines mutagenized from the Ningmai9 by EMS were used to screen for mutants lacking the HMW-GSs. Two independent mutants (md10 and md11) with 1Dy12 deletion were identified, but the patterns of LMW-GSs and other HMW-GSs were unchanged when compared with the wild type (**Figure 1**).

Sequencing of *1Dy12* Gene in Wild Type and Mutants

A pair of specific primers designed outside the coding region of the *1Dy12* gene was amplified, and a target band of approximately 2.5 kbp was amplified in mutants and wild type (**Supplementary Figure 1**). The sequences of coding regions of *1Dy12* in mutants and wild type were analyzed. The open reading frames of *1Dy12* in wild type were 1,980 bp in length with the initiation codon and two duplicate termination codons, encoding 658 amino acid residues (**Supplementary File 1**). The sequence comparison between the mutants and wild types indicated that each mutant has single base substitutions, respectively. The mutation site of md10 occurred at 1,663 bp with a substitution of C/T, which changed the codon CAA of glutamine to the termination codon TAA, substitution located on the fifth amino acid residue of the central repetitive domain (TGQAQQ) (**Figures 2A,B**). A G/A substitution occurred at 798 bp in mutant md11, causing the tryptophan codon TGG to become the termination codon TGA; this substitution occurred at the W position of the PGQWQQ in the central repetitive domain (**Figures 2C,D**).

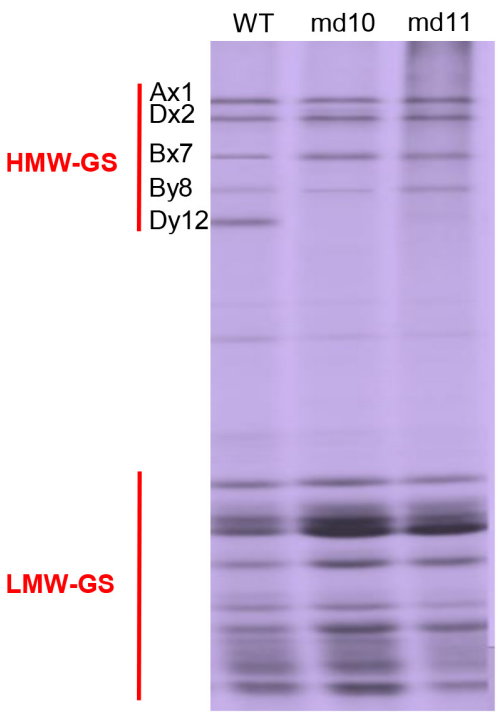

FIGURE 1 | SDS-PAGE pattern of HMW-GSs and LMW-GSs in the wild type and mutants, md10 and md11.

Expression of *1Dy12* Gene in Grain Development Stages

Total RNA was extracted and reverse transcribed to cDNA from the grains of mutants and wild type at different days after anthesis (DPA) and used for gene expression analysis to clarify if the *1Dy12* gene at the *Glu-D1* locus was normally expressed at transcriptional and translational levels in mutants during the course of grain development. The expression profiles of the *1Dy12* gene in mutants and Ningmai9 were determined using qRT-PCR. The gene expression of *1Dy12* at least started at 7 DPA, reached its highest level with the relative expression of 11.3 at 14 DPA, and then declined as grain-filling progressed in the wild type of Ningmai9. The expression of *1Dy12* decreased across all developmental stages in both mutants of md10 and md11 in comparison with wild type; the values of relative expression ranged from 0.03 to 0.72 and from 0.07 to 0.55 in md10 and md11, respectively, which implied that the expression of *1Dy12* in mutants was significantly suppressed and resulted from a premature termination codon (**Figure 3**).

Grain Characters and Storage Protein in Wild Type and Mutants

Grain hardness and diameter were detected by SKCS. There was minimal difference between wild type and 1Dy12 deletion mutants in both characters. The grain hardness and diameter of 1Dy12 deletion mutants were ranged from 38.97 to 40.23 and from 2.65 to 2.68 mm, respectively, while those of the wild type were ranged between 39.85 and 2.71 mm (**Figures 4A,B**). Test weight in mutants was not significantly different from that in wild type, too (**Figure 4C**). Similarly, no significant differences were detected in grain protein content and wet gluten content. The grain protein content and wet gluten in 1Dy12 deletion mutants ranged from 14.13 to 14.26% and from 25.88 to 27.40%, respectively, while those of the wild type were 13.77 and 25.53% (**Figures 4D,E**). In comparison with the wild type, the total amount of HMW-GSs in mutant md10 and md11 was decreased by 19.6 and 21.8% (**Figure 4F**). The comparison of storage protein components showed that Glu/Gli in md10 and md11 was 1.17–1.18. It was significantly lower than that in the wild type (1.6) (**Figure 4G**). UPP% in mutants and wild type were tested by high-performance liquid chromatography (HPLC). Compared with the wild type (24.07%), a significant decrease was observed in md10 (15.36%) and md11 (14.93%) (**Figure 4H**). The results indicated that the deletion of *1Dy12* has a negative impact on total HWM-GSs content, Glu/Gli, and UPP accumulation level, though other grain characters remain unchanged.

Effect of the Lack of 1Dy12 on Solvent Retention Capacity

The SRC test can describe the intrinsic characteristics of flour components and is widely used in soft wheat breeding. The comparison of SRC value between *1Dy12* deletion mutants and wild type showed that the effect varied among different SRC components. The WSRC in md10 and md11 was 59.48 and 54.72%, respectively, a significant decrease in comparison with that in wild type (63.68%) (**Figure 5A**). LASRC in *1Dy12* deletion

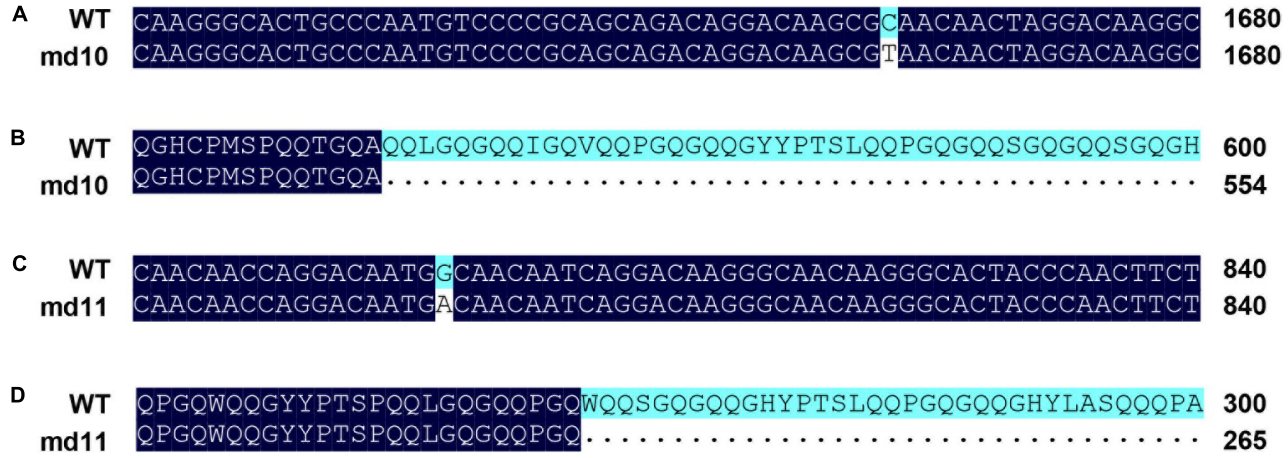

FIGURE 2 | Alignment analysis of the *1Dy12* sequences in mutant md10, md11, and wild type. **(A)** Partial DNA sequence alignment of *1Dy12* of md10 and wild type, **(B)** partial protein sequence alignment of 1Dy12 of md10 and wild type, **(C)** partial DNA sequence alignment of *1Dy12* of md11 and wild type, and **(D)** partial protein sequence alignment of 1Dy12 of md11 and wild type.

mutants was ranged from 98.41 to 98.65%, and significantly lower than that in wild type (121.85%) (**Figure 5C**). There was a small difference between wild type and *1Dy12* deletion mutants in SCSRC and SUSRC, and the variation ranged from 68.79 to 72.76% and from 101.46 to 103.58%, respectively (**Figures 5B,D**).

Effect of the Lack of 1Dy12 on Processing Quality

Processing quality parameters related to dough rheological properties were characterized, and comparisons between 1Dy12 deletion mutants and wild type were made. Dough rheological properties were detected using mixograph. There were significant differences in peak time and TIMEX width between 1Dy12 deletion mutants and wild type. The peak time and TIMEX width were 1.73 min and 4.57% in wild type and decreased to 1.15–1.22 min and 3.54–3.58% in deletion mutants, respectively (**Figures 6A,E**). No significant differences in peak value, peak width, and right slope were found between deletion mutants and wild type (**Figures 6B–D**). Sugar snap cookies with flours of *1Dy12* deletion mutants and wild type were made, and their diameter is shown in **Figure 6F**. The wild type had a cookie diameter of 8.00 cm, and the deletion mutants had an increased spreading ability and more width compared with those of the wild type, which had a cookie diameter of 8.70–8.74 cm. The result suggested that 1Dy12 deletion in Ningmai9 demonstrated the superior quality of sugar snap cookies (**Figure 6G**).

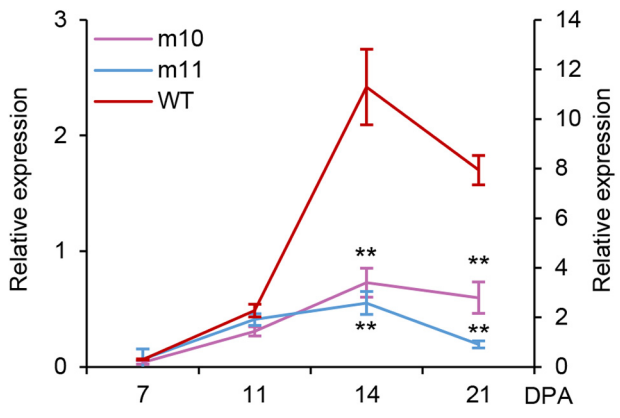

FIGURE 3 | Expression profiling of the *1Dy12* gene at a different developmental stage in mutants md10, md11 (y-axis on the left), and wild type (y-axis on the right) by qRT-PCR. The double asterisks represent significant differences determined by Student's *t*-test at $P < 0.01$.

Yield Related Traits in Wild Type and Mutants

The 1Dy12 deletion mutants, md10 and md11, and wild type were sown in the field at the end of October 2017 and harvested in early June in 2018. Morphological traits were studied in mutants and wild type. The 1Dy12 deletion mutants md10 and md11 had similar performance to wild type. The plant height, spike number per ha, kernel number per spike, thousand kernel weight, and yield per ha of 1Dy12 deletion mutant were 80.33–80.50 cm, 563.0–580.3 $\times$ 10^4, 57.83–59.17, 35.08–35.22 g, and 6,520–6,770 kg ha^{-1}, respectively, while those of wile type were 80.67 cm, 572.7 $\times$ 10^4, 57.83, 35.16 g, and 6,573 kg ha^{-1} (**Figures 7A–E**). The results indicated that 1Dy12 deletion mutants possessed the same yield potential as wild type.

DISCUSSION

The quality of end-use products is affected by different subunits of wheat HMW-GSs both individually and cooperatively (Delcour et al., 2012). Generally, the absence of an individual or combination of HMW-GSs decreases the gluten strength and elasticity and has negative effects on bread-processing quality (Li et al., 2015; Liu et al., 2016; Wang et al., 2017; Gao et al., 2018; Zhang Y. et al., 2018). However, for the end-use of soft wheat, the effect of the deletion of HMW-GSs was inconsistent

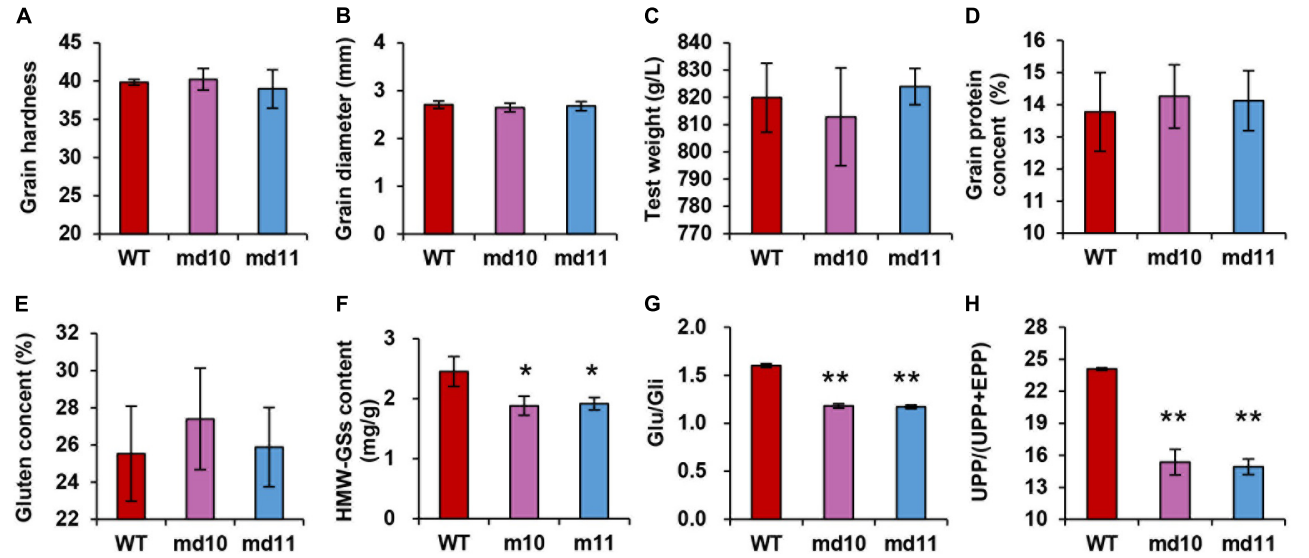

FIGURE 4 | Values of **(A)** grain hardness, **(B)** grain diameter (mm), **(C)** test weight, **(D)** grain protein content (%), **(E)** grain gluten content (%), **(F)** HMW-GS content (mg g^{-1}), and **(G)** Glu/Gli and **(H)** UPP/(UPP + EPP) in wild type and mutants (md10 and md11). Data represent mean ± standard deviation. Single and double asterisks show significant differences at $P < 0.05$ and $P < 0.01$ using Student's *t*-test, respectively.

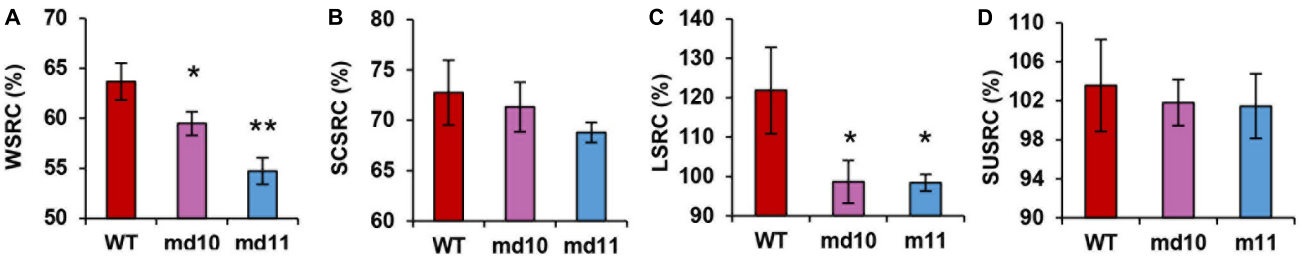

FIGURE 5 | Solvent retention capacity, **(A)** WSRC, **(B)** SCSRC, **(C)** LASRC (%), and **(D)** SUSRC (%) of flour in wild type and mutants (md10 and md11). Data represent mean ± standard deviation. Single and double asterisks show significant differences at $P < 0.05$ and $P < 0.01$ using Student's *t*-test, respectively.

with the previous studies. Tuncil et al. (2016) reported that the presence of 1Bx7 and 1By9 at Glu-B1 and the absence of Glu-A1 and Glu-D1 consistently enlarged the diameter and kept favorable flexibility during storage for tortillas. Significantly higher cookie diameter and lower cookie height were found in near-isogenic lines of double null in Glu-A1 and Glu-D1 and single null in Glu-D1 compared with their recurrent parent Yangmai18 (Zhang X. et al., 2018). However, Chen et al. (2019) found that 1Bx7 and 1By9 make important contributions to gluten functionality, and the deletion of 1Bx7 or 1By9 in mutants resulted in weaker dough strength and inferior sponge cake performance. It was also reported that a wheat somatic variation of the 1Dy12 deletion line showed an inferior sponge cake and biscuit in KN199 (Chen et al., 2021). The results show that the effects on the quality of end-use products are not only dependent on the function of different HMW-GSs but also related to the genetic backgrounds of wheat varieties. Clarifying the contributions of HMW-GSs in flour-processing quality is important in commercial varieties so that the effects of HMW-GSs can be efficiently utilized in wheat breeding. To improve soft wheat processing quality, we created deletion mutants of HMW-GSs from Ningmai9, a major soft wheat variety in the reaches of the middle to lower Yangtze River, using the EMS mutagenized method (Zhang J. et al., 2014). We found that the absence of 1Dy12 in both mutants, md10 and md11, had a positive effect on the quality of sugar snap cookies compared with the wild type, Ningmai9 (**Figure 6**). Yield-related traits in both mutants were similar to those in Ningmai9 in this study (**Figure 7**), which was similar to the report of Zhang X. et al. (2018), but not consistent with the result of the somatic mutant in KN199 (Chen et al., 2021). We speculated that different methods of mutant induction and the genetic background of the experimental materials might be responsible for such differences. Somatic variation may produce more variation loci than EMS; meanwhile, KL199 is hard winter wheat and Ningmai9 is soft spring wheat. However, md10 and md11 in this study could be useful for soft wheat production and breeding.

Deletion of HMW-GSs results from gene silencing. The gene silencing of HMW-GSs could be caused by the deletion of small chromosomal fragments and the alteration of promoter regions

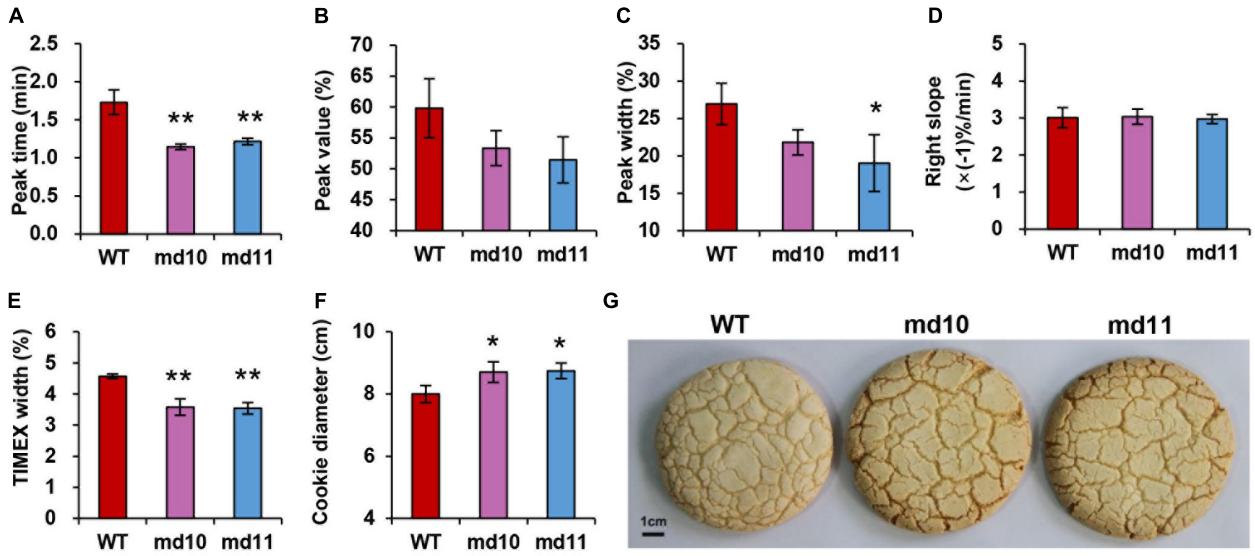

FIGURE 6 | Dough rheological properties, **(A)** peak time (min), **(B)** peak value (%), **(C)** peak width (%), **(D)** right slope (% min^{-1}), **(E)** TIMEX (%) using mixograph, **(F)** cookie diameter in wild type and mutants (md10 and md11), and **(G)** top view of sugar snap cookie of wild type (middle) and mutants, md10 (left) and md11 (right). Data represent mean ± standard deviation. Single and double asterisks show significant differences at $P < 0.05$ and $P < 0.01$ using Student's *t*-test, respectively.

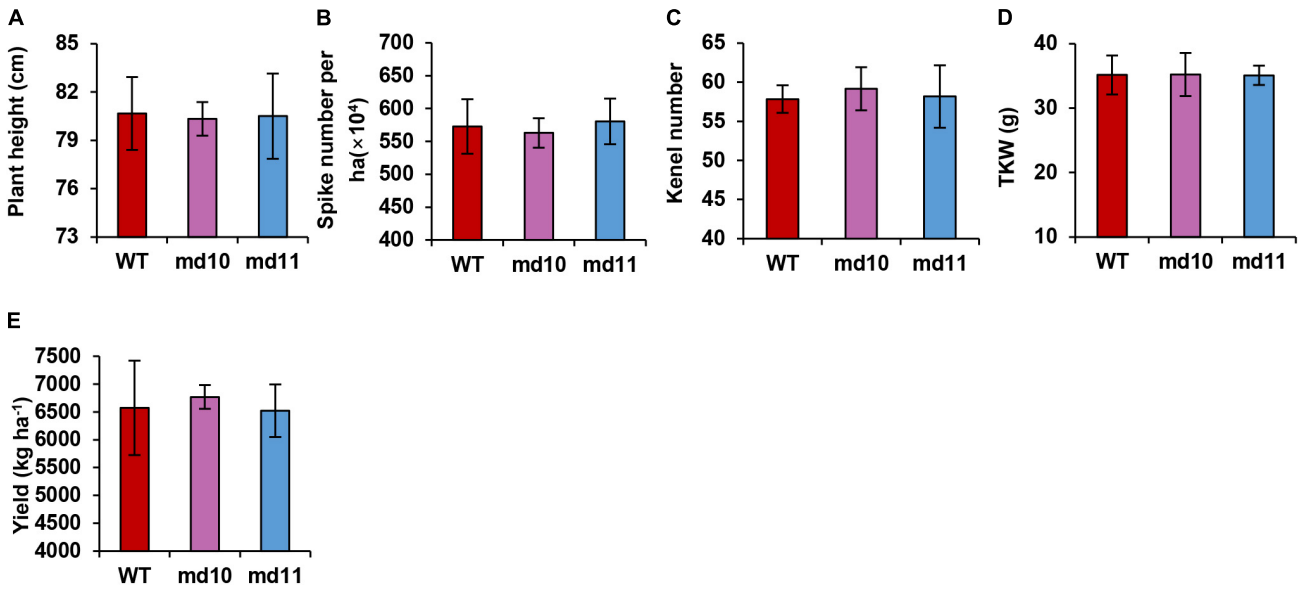

FIGURE 7 | Yield related characters, **(A)** plant height (cm), **(B)** spike number per ha, **(C)** kernel number per spike, **(D)** TKW (g), and **(E)** yield (kg ha^{-1}).

(Upelniek et al., 1995; Beshkova et al., 1998; Liu et al., 2016). Single base substitutions in the coding region sequences also cause gene silencing in the deletion of HMW-GSs in wheat, which usually results from premature termination codons (Chen et al., 2019, 2021). The gene silencing of *Glu-1Ay* in wheat is largely attributed to premature termination codons (Luo et al., 2018). There are two major mechanistic classes inducing gene silence, post-transcriptional gene silencing (PTGS), and transcriptional gene silencing (TGS) (Hammond et al., 2001). Chen et al. (2021) found that the gene silencing of *1Dy12* in the somatic mutant derived from KL199 was caused by PTGS, as RT-PCR and qRT-PCR results of *1Dy12* gene expression implied that this gene was normally expressed in the mutant through all grain developmental stages. In this study, DNA sequencing confirmed that one mutation caused by a C/T substitution in md10 would result in the change of CAA encoding glutamine into termination codon TAA, and the mutation of md11 is due to a G/A substitution within the coding region repeat sequence, making the tryptophan encoding TGG become the termination codon TGA (**Figure 2**). The gene expression of *1Dy12* in deletion

mutants is different from that reported by Chen et al. (2021). In the research, the relative expression of *1Dy12* significantly decreased across all developmental stages in both mutants of md10 and md11 in comparison with the wild type (**Figure 3**). Therefore, we speculated that the gene silencing in md10 and md11 was caused by TGS. The result is similar to the research by Gao et al. (2021), in which a premature stop codon of *TaNAC019* affected not only its protein biosynthesis but also its mRNA production.

High molecular weight glutenin subunits are associated with the formation of intramolecular and intermolecular disulfide bonds, which largely determine gluten structure and network (Shewry et al., 1997). Glutenin protein usually exists in gluten as polymers. According to the solubility in SDS solution, glutenin polymers were divided into SDS-unextractable polymeric protein (UPP) and SDS-extractable polymeric protein (EPP). The percentage of UPP in total glutenin polymer (UPP%) was strongly related to optimal mixing time of dough rheological property and thimble-loaf height (Don et al., 2006). We found that gene silencing of *1Dy12* in Ningmai9 decreased the total HMW-GSs content and led to a decrease in UPP% (**Figure 4**). It is speculated that this phenomenon results from the inefficient formation of disulfide bonds. The decrease of UPP% reduced the peak time and TIMEX width in dough rheological properties using mixograph, which reflected a decrease in gluten strength.

Solvent retention capacity (SRC) is a solvation examination for wheat flour that is widely applied for evaluating flour functionality in soft wheat breeding in the United States. The functional contributions of different polymeric components in SRC are predicted on the basis of their swelling properties in different diagnostic solvents (Guttieri et al., 2004). LASRC reflected glutenin network and gluten strength, WSRC is associated with all the assessed polymers water-holding capacity (Meera et al., 2011). A low WSRC would be required to make flour for cookies. With the small amount of water needed for a processable dough for cookies, water therefore could be easier to remove during the baking process, leading to a lower-moisture cookie with a prolonged shelf life. Low LASRC value prevents the formation of networks during dough mixing and baking, which resulted in promoting the collapse of cookie structure, yielding cookies with larger diameter and thinner height (Slade et al., 1993). In this study, SRC tests showed that WSRC and LASRC in 1Dy12 deletion mutants were lower than those in the wild type (**Figure 5**), which improved the snap-cookie quality.

DATA AVAILABILITY STATEMENT

The original contributions presented in the study are included in the article/**Supplementary Material**, further inquiries can be directed to the corresponding authors.

AUTHOR CONTRIBUTIONS

HM conceived the experiments. PZ developed the mutants. GL performed major experiments. YG supplemented experiments and analyzed the data. HW performed field experiments. HM and YG wrote the manuscript. JC and YW modified the manuscript. All authors have read and agreed on the published version of the manuscript.

FUNDING

This research was funded by the Jiangsu Key Project for the Research and Development (BE2021335), the Seed Industry Revitalization Project of Jiangsu Province (JBGS2021006), Jiangsu Agriculture Science and Technology Innovation Fund (CX (20) 3034), and the National Key Project for the Research and Development of China (2017YFD010086).

SUPPLEMENTARY MATERIAL

The Supplementary Material for this article can be found online at: https://www.frontiersin.org/articles/10.3389/fpls.2022.835164/full#supplementary-material

Supplementary Figure 1 | Amplified fragment of *1Dy12*.

Supplementary Table 1 | Values of grain hardness, grain diameter (mm), test weight, grain protein content (%), grain gluten content (%), HMW-GS content (mg g^{-1}), Glu/Gli, and UPP/(UPP + EPP) in the wild type and mutants (md10 and md10).

Supplementary Table 2 | Solvent retention capacity, WSRC, SCSRC, LASRC (%), and SUSRC (%) of flour in the wild type and mutants (md10 and md10).

Supplementary Table 3 | Dough rheological properties, peak time (min), peak value (%), peak width (%), right slope (% min^{-1}), TIMEX (%) using mixograph, and cookie diameter in wild type and mutants (md10 and md10).

Supplementary Table 4 | Yield-related characters, plant height (cm), spike number ha^{-1}, kernel number $spike^{-1}$, TKW (g), and yield (kg ha^{-1}).

Supplementary File 1 | Sequence of DNA and deduced amino acid sequence of *1Dy12* in Ningmai9.

REFERENCES

Beshkova, N., Ivanov, P., and Ivanova, I. (1998). Further evidence for glutenin modifications in winter wheat (*Triticum aestivum* L.) induced by somaclonal variation. *Biotechnol. Biotechnol. Equip.* 12, 53–57. doi: 10.1080/13102818.1998.10818988

Branlard, G., and Dardevet, M. (1985). Diversity of grain protein and bread wheat quality: II. Correlation between high molecular weight subunits of glutenin and flour quality characteristics. *J. Cereal Sci.* 3, 345–354.

Chen, H., Li, S., Liu, Y., Liu, J., Ma, X., Du, L., et al. (2021). Effects of 1Dy12 subunit silencing on seed storage protein accumulation and flour-processing quality in a common wheat somatic variation line. *Food Chem.* 335:127663. doi: 10.1016/j.foodchem.2020.127663

Chen, Q., Zhang, W., Gao, Y., Yang, C., Gao, X., Peng, H., et al. (2019). High molecular weight glutenin subunits 1Bx7 and 1By9 encoded by Glu-B1 locus affect wheat dough properties and sponge cake quality. *J. Agric. Food Chem.* 67, 11796–11804. doi: 10.1021/acs.jafc.9b05030

Delcour, J., Joye, I., Pareyt, B., Wilderjans, E., Brijs, K., and Lagrain, B. (2012). Wheat gluten functionality as a quality determinant in cereal-based food products. *Annu. Rev. Food Sci. Technol.* 3, 469–492. doi: 10.1146/annurev-food-022811-101303

Don, C., Mann, G., Bekes, F., and Hamer, R. (2006). HMW-GS affect the properties of glutenin particles in GMP and thus flour quality. *J. Cereal Sci.* 44, 127–136. doi: 10.1016/j.jcs.2006.02.005

Gao, X., Liu, T., Ding, M., Wang, J., Li, C., Wang, Z., et al. (2018). Effects of HMW-GS Ax1 or Dx2 absence on the glutenin polymerization and gluten micro structure of wheat (*Triticum aestivum* L.). *Food Chem.* 240, 626–633. doi: 10.1016/j.foodchem.2017.07.165

Gao, Y., An, K., Guo, W., Chen, Y., Zhang, R., Zhang, X., et al. (2021). The endosperm-specific transcription factor TaNAC19 regulates glutenin and starch accumulation and its elite improves wheat grain quality. *Plant Cell* 33, 603–622. doi: 10.1093/plcell/koaa040

Guo, H., Wu, J., Lu, Y., and Yan, Y. (2019). High-molecular-weight glutenin 1Bx17 and 1By18 subunits Encoded by Glu-B1i enhance rheological properties and breadmaking quality of wheat dough. *J. Food Qual.* 2019:1958747.

Guttieri, M. J., Becker, C., and Souza, E. (2004). Application of wheat meal solvent retention capacity tests within soft wheat breeding population. *Cereal Chem.* 81, 261–266. doi: 10.1094/cchem.2004.81.2.261

Hammond, S. M., Caudy, A. A., and Hannon, G. J. (2001). Post-transcriptional gene silencing by double-stranded RNA. *Nat. Rev. Genet.* 2, 110–119. doi: 10.1038/35052556

He, Z., Liu, L., Xia, X., Liu, J., and Pena, R. J. (2005). Composition of HMW and LMW glutenin subunits and their effects on dough properties, pan bread, and noodle quality of Chinese bread wheats. *Cereal Chem.* 82, 345–350. doi: 10.1094/cc-82-0345

Jiang, P., Xue, J., Duan, L., Gu, Y., Mu, J., Han, S., et al. (2019). Effects of high-molecular weight glutenin subunit combination in common wheat on the quality of crumb structure. *J. Sci. Food and Agric.* 99, 1501–1508. doi: 10.1002/jsfa.9323

Khan, K., Frohberg, R., Olson, T., and Huckle, L. (1989). Inheritance of gluten protein components of high-protein hard red spring wheat lines derived from *Triticum turgidum* var. dicoccoides. *Cereal Chem.* 66, 397–401.

Lambourne, J., Tosi, P., Marsh, J., Bhandari, D., Green, R., Frazier, R., et al. (2010). Characterisation of an s-type low molecular weight glutenin subunit of wheat and its proline and glutamine-rich repetitive domain. *J. Cereal Sci.* 51, 96–104. doi: 10.1016/j.jcs.2009.10.003

Larroque, O., Gianibelli, M., Gomez-Sanchez, M., and MacRitchie, F. (2000). Procedure for obtaining stable protein extracts of cereal flour and whole meal for size-exclusion HPLC analysis. *Cereal Chem.* 77, 448–450. doi: 10.1094/cchem.2000.77.4.448

Li, H., Zhou, Y., Xin, W., Wei, Y., Zhang, J., and Guo, L. (2019). Wheat breeding in northern China: achievments and technical advances. *Crop J.* 7, 718–729. doi: 10.1016/j.cj.2019.09.003

Li, Y., An, X., Yang, R., Guo, X., Yue, G., Fan, R., et al. (2015). Dissecting and enhancing the contributions of high-molecular-weight glutenin subunits to dough functionality and bread quality. *Mol. Plant* 8, 332–334. doi: 10.1016/j.molp.2014.10.002

Li, Y., Fu, J., Shen, Q., and Yang, D. (2021). High molecular glutenin subunits: genetics, structures, and relation to end use qualities. *Int. J. Mol. Sci.* 22:184. doi: 10.3390/ijms22010184

Liu, H., Wang, K., Xiao, L., Wang, S., Du, L., Cao, X., et al. (2016). Comprehensive identification and bread-making quality evaluation of common wheat somatic variation line AS208 on glutenin composition. *PLoS One* 11:e146933. doi: 10.1371/journal.pone.0146933

Liu, L., He, Z., Yan, J., Zhang, Y., Xia, X., and Peña, R. (2005). Allelic variation at the Glu-1 and Glu-3 loci, presence of the 1B.1R translocation, and their effects on mixographic properties in Chinese bread wheats. *Euphytica* 142, 197–204. doi: 10.1007/s10681-005-1682-4

Liu, S., Gao, X., and Xia, G. (2008). Chracterizing HMW-GS alleles of decaploid *Agropyron elonggatum* in relation to evolution and wheat breeding. *Theor. Appl. Genet.* 116, 325–334. doi: 10.1007/s00122-007-0669-z

Livak, K., and Schmittgen, T. (2001). Analysis of relative gene expression data using real-time quantitative pcr and the $2-\Delta\Delta$ct method. *Methods* 25, 402–408. doi: 10.1006/meth.2001.1262

Luo, G., Song, S., Zhao, L., Shen, L., Song, Y., Wang, X., et al. (2018). Mechanisms, origin and heredity of Glu-1Ay silencing in wheat evolution and domestication. *Theor. Appl. Genet.* 131, 1561–1575. doi: 10.1007/s00122-018-3098-2

Ma, H., Zhang, X., Yao, J., and Cheng, S. (2019). Breeding for the resistance to *Fusarium* head blight of wheat in China. *Front. Agric. Sci. Eng.* 6:251–264. doi: 10.15302/J-FASE-2019262

Ma, W., Yu, Z., She, M., Zhao, Y., and Islam, S. (2019). Wheat gluten protein and its impacts on wheat processing quality. *Front. Agric. Sci. Eng.* 6:279–287. doi: 10.15302/j-fase-2019267

Meera, K., Louise, S., and Harry, L. (2011). Solvent retention capacity (SRC) testing of wheat flour: principles and value in predicting flour functionality in different wheat-based food processes and in wheat breeding—a review. *Cereal Chem.* 88, 537–552. doi: 10.1094/cchem-07-11-0092

Mondal, S., Tilley, M., Alviola, J., Waniska, R., Bean, S., and Glover, K. (2008). Use of near-isogenic wheat lines to determine the glutenin composition and functionality requirements for flour tortillas. *J. Agric. Food Chem.* 56, 179–184. doi: 10.1021/jf071831s

Ohm, J., Ross, A., Peterson, C., and Morris, C. (2009). Relationship of quality characteristics with size exclusion HPLC chromatogram of protein extract in soft white winter wheats. *Cereal Chem.* 86, 197–203. doi: 10.1094/cchem-86-2-0197

Payne, P. (1987). Genetics of wheat storage proteins and the effect of allelic variation on breadmaking quality. *Ann. Rev. Plant Physiol.* 38, 141–153. doi: 10.1146/annurev.pp.38.060187.001041

Payne, P., Holt, L., and Law, C. (1981). Structural and genetical studies on the highmolecular-weight subunits of wheat glutenin. *Theor. Appl. Genet.* 60, 229–236. doi: 10.1007/bf02342544

Ram, S., Shoran, J., and Mishra, B. (2007). Nap Hal, an Indian landrace of wheat, contains unique genes for better biscuit making quality. *J. Plant Biochem. Biotechnol.* 16, 83–86. doi: 10.1007/bf03321979

Rasheed, A., Xia, X., Yan, Y., Appels, R., Mahmood, T., and He, Z. (2014). Wheat seed storage proteins: advances in molecular genetics, diversity and breeding applications. *J. Cereal Sci.* 60, 11–24. doi: 10.1016/j.jcs.2014.01.020

Roy, N., Islam, S., Ma, J., Lu, M., Torok, K., Tomoskozi, S., et al. (2018). Expressed Ay HMW glutenin subunit in Australian wheat cultivars indicates a positive effect on wheat quality. *J. Cereal Sci.* 79, 494–500. doi: 10.1007/s00122-019-03483-1

Shewry, P. (2019). What is gluten—why is it special? *Front. Nutr.* 6:101. doi: 10.3389/fnut.2019.00101

Shewry, P., and Halford, N. (2002). Cereal seed storage proteins: structures, properties and role in grain utilization. *J. Exp. Bot.* 53, 947–958. doi: 10.1093/jexbot/53.370.947

Shewry, P., and Tatham, A. (1997). Disulphide bonds in wheat gluten proteins. *J. Cereal Sci.* 25, 207–227. doi: 10.1006/jcrs.1996.0100

Shewry, P., Halford, N., and Tatham, A. (1992). High molecular weight subunits of wheat glutenin. *J. Cereal Sci.* 15, 105–120. doi: 10.1094/cchem.2000.77.2.105

Shewry, P. R., Halford, N. G., and Lafiandra, D. (2003). Genetics of wheat gluten proteins. *Adv. Genet.* 49, 111–184. doi: 10.1016/s0065-2660(03)01003-4

Shewry, P. R., Tatham, A. S., and Lazzeri, P. (1997). Biotechnology of wheat quality. *Trends Food Sci. Technol.* 73, 397–406.

Slade, L., Levine, H., Ievolella, J., and Wang, M. (1993). The glassy state phenomenon in applications for the food industry: application of the food polymer science approach to structure-function relationships of sucrose in cookie and cracker systems. *J. Sci. Food Agric.* 63, 133–176.

Souza, E., Graybosch, R., and Guttieri, M. (2002). Breeding wheat for improved milling and baking quality. *J. Crop Prod.* 5, 39–74. doi: 10.1300/j144v05n01_03

Tuncil, Y., Jondiko, T., Tilley, M., Hays, D., and Awika, J. (2016). Combination of null alleles with 7 + 9 allelic pair at Glu-B1 locus on the long arm of group 1 chromosome improves wheat dough functionality for tortillas. *LWT Food Sci. Technol.* 65, 683–688. doi: 10.1016/j.lwt.2015.08.074

Upelniek, V., Novoselskaya, A., Sutka, J., Galiba, G., and Metakovsky, E. (1995). Genetic variation at storage protein-coding loci of common wheat (cv'Chinese Spring') induced by nitrosoethylurea and by the cultivation of immature embryos in vitro. *Theor. Appl. Genet.* 90, 372–379. doi: 10.1007/BF00221979

Wang, D., Zhang, K., Dong, L., Dong, Z., Li, Y., Hussain, A., et al. (2018). Molecular genetic and genomic analysis of wheat milling and end-use traits in China: progress and perspectives. *Crop J.* 6, 68–81. doi: 10.1016/j.cj.2017.10.001

Wang, Z., Li, Y., Yang, Y., Liu, X., Qin, H., Dong, Z., et al. (2017). New insight into the function of wheat glutenin proteins as investigated with two series of genetic mutants. *Sci. Rep.* 7:3428. doi: 10.1038/s41598-017-03393-6

Yan, Y., Jiang, Y., An, X., Pei, Y., Li, X., Zhang, Y., et al. (2009). Cloning, expression and functional analysis of HMW glutenin subunit 1By8 gene from Italy pasta

wheat (*Triticum turgidum* L. ssp. durum). *J. Cereal Sci.* 50, 398–406. doi: 10.1016/j.jcs.2009.08.004

Yang, Y., Li, S., Zhang, K., Dong, Z., Li, Y., An, X., et al. (2014). Efficient isolation of ion beam-induced mutants for homoeologous loci in common wheat and comparison of the contributions of Glu-1 loci to gluten functionality. *Theor. Appl. Genet.* 127, 359–372. doi: 10.1007/s00122-013-2224-4

Yao, J., Ma, H., Yang, X., Zhou, M., and Yang, D. (2014). Gentic analysis of the grain protein content in soft red winter wheat. *Turkish J.Field Crops* 19, 246–251.

Yu, Z., Peng, Y., Islam, S., She, M., Lu, M., Lafiandra, D., et al. (2019). Molecular characterization and phylogenetic analysis of active y-type high molecular weight glutenin subunit genes at Glu-A1 locus in wheat. *J. Cereal Sci.* 86, 9–14. doi: 10.1016/j.jcs.2019.01.003

Zhang, J., Zhang, P., Yao, J., Yang, D., Yang, X., and Ma, H. (2014). EMS induced HMW-GS mutants from soft wheat ningmai9. *Acta Agron. Sin.* 40, 1579–1584. doi: 10.3724/sp.j.1006.2014.01579

Zhang, P., He, Z., Zhang, Y., Xia, X., Liu, J., Yan, J., et al. (2007). Pan bread and Chinese white salted noodle qualities of Chinese winter wheat cultivars and their relationship with gluten protein fractions. *Cereal Chem.* 84, 370–378. doi: 10.1094/cchem-84-4-0370

Zhang, P., Jondiko, T., Tilley, M., and Awika, J. (2014). Effect of high molecular weight glutenin subunit composition in common wheat on dough properties and steamed bread quality. *J. Sci. Food Agric.* 94, 2801–2806. doi: 10.1002/jsfa.6635

Zhang, X., Zhang, B., Wu, H., Lu, C., Lü, G., Liu, D., et al. (2018). Effect of high-molecular-weight glutenin subunit deletion on soft wheat quality properties and sugar-snap cookie quality estimated through near-isogenic lines. *J. Integr. Agric.* 17, 1066–1073. doi: 10.1016/s2095-3119(17)61729-5

Zhang, X., Zhang, Y., Gao, D., Bie, T., and Zhang, B. (2012). The development of weak gluten wheat breeding and present situation of its production. *J. Triticeae Crops* 32, 184–189.

Zhang, Y., Hu, M., Liu, Q., Sun, L., Chen, X., Lv, L., et al. (2018). Deletion of high-molecular-weight glutenin subunits in wheat significantly reduced dough strength and bread-baking quality. *BMC Plant Biol.* 18:319. doi: 10.1186/s12870-018-1530-z

Conflict of Interest: The authors declare that the research was conducted in the absence of any commercial or financial relationships that could be construed as a potential conflict of interest.

Publisher's Note: All claims expressed in this article are solely those of the authors and do not necessarily represent those of their affiliated organizations, or those of the publisher, the editors and the reviewers. Any product that may be evaluated in this article, or claim that may be made by its manufacturer, is not guaranteed or endorsed by the publisher.

Advantages of publishing in Frontiers

OPEN ACCESS
Articles are free to read for greatest visibility and readership

FAST PUBLICATION
Around 90 days from submission to decision

HIGH QUALITY PEER-REVIEW
Rigorous, collaborative, and constructive peer-review

TRANSPARENT PEER-REVIEW
Editors and reviewers acknowledged by name on published articles

Frontiers
Avenue du Tribunal-Fédéral 34
1005 Lausanne | Switzerland

Visit us: www.frontiersin.org
Contact us: frontiersin.org/about/contact

REPRODUCIBILITY OF RESEARCH
Support open data and methods to enhance research reproducibility

DIGITAL PUBLISHING
Articles designed for optimal readership across devices

FOLLOW US
@frontiersin

IMPACT METRICS
Advanced article metrics track visibility across digital media

EXTENSIVE PROMOTION
Marketing and promotion of impactful research

LOOP RESEARCH NETWORK
Our network increases your article's readership